Protocols for Multi-Antenna Ad-Hoc Wireless Networking in Interference Environments

by

Danielle A. Hinton

SB, Massachusetts Institute of Technology (2000)
MEng, Massachusetts Institute of Technology (2002)
BA, University of Cambridge (2004)
MA, University of Cambridge (2007)

Submitted to the Department of Electrical Engineering and Computer Science
in partial fulfillment of the requirements for the degree of
Doctor of Philosophy in Electrical Engineering
at the
MASSACHUSETTS INSTITUTE OF TECHNOLOGY
September 2010

Author .....
Department of Electrical Engineering and Computer Science
August 2, 2010

Certified by .....
David H. Staelin
Professor of Electrical Engineering
Thesis Supervisor

Certified by .....
Dr. Daniel W Bliss, Jr.
Senior Staff, MIT Lincoln Laboratory
Thesis Supervisor

Accepted by .....
Terry P. Orlando
Chairman, Department Committee on Graduate Theses

Protocols for Multi-Antenna Ad-Hoc Wireless Networking in Interference Environments

by

Danielle A. Hinton

Submitted to the Department of Electrical Engineering and Computer Science
on August 2, 2010, in partial fulfillment of the
requirements for the degree of
Doctor of Philosophy in Electrical Engineering

Abstract

A fundamental question for the design of future wireless networks concerns the nature of spectrum management and the protocols that govern use of the spectrum. In the oligopoly model, spectrum is owned and centrally managed, and the protocols tend to reflect this centralized nature. In the common's model, spectrum is a public good, and protocols must support ad hoc communication.

This work presents the design, tradeoffs and parameter optimization for a new protocol (Simultaneous Transmissions in Interference (STI-MAC)) for ad hoc wireless networks. The key idea behind the STI-MAC protocol is 'channel stuffing,' that is, allowing network nodes to more efficiently use spatial, time and frequency degrees of freedom. This is achieved in three key ways. First, 'channel stuffing' is achieved through multiple antennas that are used at the receiver to mitigate interference using Minimum-Mean-Squared-Error (MMSE) receivers, allowing network nodes to transmit simultaneously in interference limited environments. The protocol also supports the use of multiple transmit antennas to beamform to the target receiver. Secondly, 'channel stuffing' is achieved through the use of a control channel that is orthogonal in time to the data channel, where nodes contend in order to participate on the data channel. And thirdly, 'channel stuffing' is achieved through a protest scheme that prevents data channel overloading.

The STI-MAC protocol is analyzed via Monte-Carlo simulations in which transmitter nodes are uniformly distributed in a plane, each at a fixed distance from their target receiver; and as a function of network parameters including the number of transmit and receive antennas, the distance between a transmitter-receiver pair (link-length), the average number of transmitters whose received signal is stronger at a given receiver than its target transmitter (link-rank), number of transmitter-receiver pairs, the distribution on the requested rate, the offered load, and the transmit scheme. The STI-MAC protocol is benchmarked relative to simulations of the 802.11(n) (Wi-Fi) protocol. The key results of this work show a 3X

gain in throughput relative to 802.11(n) in typical multi-antenna wireless networks that have 20 transmitter-receiver pairs, a link-length of 10 meters, four receive antennas and a single transmit antenna. We also show a reduction in delay by a factor of two when the networks are heavily loaded. We find that the link-rank is a key parameter affecting STI-MAC gains over Wi-Fi. In simulations of networks with 40 transmit-receiver pairs, link-rank of three, a link-length of 10 meters, and eight transmit and receive antennas in which the transmitter beamforms to its target receiver in its strongest target channel mode, we find gains in throughput of at least 5X over the 802.11(n) protocol.

Thesis Supervisor: David H. Staelin
Title: Professor of Electrical Engineering

Thesis Supervisor: Dr. Daniel W. Bliss, Jr.
Title: Senior Staff, MIT Lincoln Laboratory

Acknowledgments

Philippians 1:6.

I should first thank Prof Staelin for allowing me to be in RSEG, for use of the very powerful computer resources in the group, and for his advising during my stay in RLE. At several challenging and important moments in this process, Prof Staelin provided encouragement and guidance, particularly in the final month of producing this work, that enabled this process to come to a successful end. I would also like to thank Prof. Hari Balakrishnan for his very helpful guidance as a member of my thesis committee, and for welcoming me in several of his group meetings. I am immensely grateful to Bell Laboratories, and to the EECS Department for financial support. Prof Terry Orlando, Prof George Verghese, Marilyn Pierce, Janet Fischer and Lisa Bella were amazingly helpful in navigating the graduate process, and in finding and providing support. I would also like to thank Seth for providing me with access to the RSEG machines, and for his quick responses to many emails at odd hours with various questions I had throughout this process. I would also very much like to thank Laura Von Bosau for her scheduling and proof-reading prowess, and for her patience, kindness and understanding over the years, particularly in dealing with those aspects of life at MIT, that still must be delt with, but that I am sure we would both rather forget about.

There have been two key colleagues to whom I am very grateful for their exceedingly helpful academic and professional support. First, Prof Siddhartan Govindasamy who was first my office mate, and now a Professor at Olin College, and a member of my thesis committee. I am immensely grateful to Siddhartan who very generously came back to be on my thesis committee, welcomed me in visits to Olin, and for the crucial and stunning level of support and kindness he and his wonderful family offered to me just before multiple critical stages in this process. It was definitely because of his guidance and support as a friend and colleague through out this graduate experience that I was able to get to this point. My work grew out of conversations I had with him, and the many contributions he made in his own

graduate work. Key bits of progress came through discussing and clarifying ideas with him. And his friendship and support have meant the world to me. In the eleventh hour of all major steps in this experience, Siddharthan has been there for and with me. This day truly would not have come without his support. Secondly, I would like to thank Dr. Dan Bliss, a supervisor, advisor and mentor who has the rare mix of practical experience and academic and theoretical rigor – and over a breadth of topics – that made him the key source of guidance throughout this process. Dan's stunning capacity to inspire and motivate, and his amazing generosity with his time and his truly impressive level of expertise are qualities that I greatly appreciated, and that I greatly admire. I only wish that I had realized all of this about him earlier in my graduate experience, because he is definitely what I was looking for. This day would have been impossible without the guidance and supervision of Dr. Dan Bliss.

I have had many friends and colleagues who have been great supporters, and to whom I owe a debt of gratitude. A few who have stuck with me from the beginning of this process till the end deserve special mention: Jovonne, my sister, you have all of my love, gratitude and admiration for too many reasons to even count; Bhuvana, her wonderful husband Hyder and beautiful little girl Maya – Bhuv, weve been close friends since the first day of 3.091 – your friendship and support throughout all of this time back in Boston has meant so much to me; my dear friend Guy Weichenberg, who has been such an amazingly supportive friend and co-laborer in EECS, and with whom I share a deep weakness for political distractions (particularly those involving President Obama); and Aisha and Reginald, co-laborers in the struggle, wonderful friends, and a source of great inspiration and support! Carol Frederick and Toni Robinson were my aunties away from home – a rich and loving presence in my life since my days as an undergraduate.

I am always grateful to my family and extended family for their love and support – Maurice, Brenda, Debbie, Robin, Diondre, Ty, Carole, Fletcher; Uncle James, Vanessa, Pat, Jack, Linda, Shirley, Leroy, Betty, Bernie, I love you more than you know. And of course, my dear

Mother: I am not sure what words can express my deep love, admiration and gratitude to the blessed woman whose truly remarkable love, patience, support, and stunning generosity to me, her daughter, have enabled all of this. Mother, thank you so very much. I love you endlessly, and I thank God every day for you.

Psalms 63.

Contents

List of Figures

List of Tables

Chapter 1

Introduction

The rate of increase in the number and diversity of wireless networked devices offers exciting prospects for creativity and innovation in the design of future networks. Many future wireless networks, and the ones focused on in this research, will be ad hoc. That is, they will have no predefined structure or members, and no central organizing or regulating terminal – features that greatly reduce their cost and and rate of deployment compared to traditional networks with significant infrastructure. The forecasts for wireless traffic are also growing at a high rate, demanding that the spectrum is used more efficiently. According to ABI Research, the 802.11(n)[1] – IEEE's high throughput medium access control and physical layer standard for wireless local area networks – access point market is expected to reach 14 million units by 2014, growing with a compound-annual-growth-rate (CAGR) of more than 105% – a CAGR even larger than that of annual global IP Traffic (CAGR of 40 %) which will exceed two-thirds of a zettabyte by 2012 [1].

Many also foresee at least parts of the wireless spectrum moving towards a (unlicensed) Common's Model, which would require greater research and innovation into technologies and protocols for sharing the wireless medium [2], [3]. Steps toward this model have already

[1]The IEEE Standard for information technology – Telecommunications and information exchange between systems – Local and metropolitan area networks – Specific requirements; Part 11: Wireless LAN Medium Access Control (MAC) and Physical Layer (PHY) Specifications, Amendment 5: Enhancements for Higher Throughput.

been taken, for instance, in Verizon Wireless' 'Any Apps, Any Device' initiative in C-Block of the 700MHz band (698 - 806 MHz)[2], which will allow devices meeting their minimal technical standard to participate in the network. These new challenges require new physical layer (PHY) and medium access control layer (MAC) protocols that provide mechanisms for sharing the wireless resource in a decentralized environment, and increase spectral efficiency over today's most common wireless network protocols.

The majority of today's wireless local area network (WLAN) protocols use orthogonal multiple access schemes that require each user to communicate in noise, without interference, [4], [5], [6], [7]. The 802.11 protocols, for instance, use Carrier Sense Multiple Access with Collision Avoidance (CSMA/CA),[3] Time Division Multiple Access (TDMA)[4] and Frequency Division Multiple Access (FDMA) schemes[8], [9].[5] Allocating a full degree of freedom to each link by requiring that no other link in the network be transmitting at the same time (for TDMA) or in the same frequency band (FDMA) at a power level that causes interference above the clear-channel-assesment level at an unintended receiving terminal may be wasteful in networks where nodes are spread spatially as there is no spectral reuse.

The information theoretic bounds on communication in interference environments are unknown; but recent results on the expected Signal-to-Interference-plus-Noise (SINR) and the expected spectral efficiency of communications in interference environments have shown a supra-linear gain in SINR as a function of the number of degrees of freedom when receivers use interference-mitigating decoding techniques such as Minimum-Mean-Squared-Error (MMSE) receive beamforming techniques [10, 11]. We build off of these results, and distinguish ourselves by investigating the design of protocols in interference environments. We focus on protocol schemes that require minimal cooperation between nodes, and that are governed

[2]http://news.vzw.com/news/2007/11/pr2007-11-27.html

[3]802.11(a, b, n) in Ad Hoc Mode

[4]802.11 in Infrastructure mode

[5]5 GHz U-NII band offers 8 non-overlapping channels, 2.4GHz ISM frequency band offers 3 non-overlapping channels.

by a few simple rules, but that are flexible enough to adapt to the needs of nodes with different quality-of-service requirements. Possible applications of this work include WLAN on the scale of 802.11, a PHY-MAC to underlie MESH networking[6], and a low complexity sensor-network.

The key idea behind the protocol is channel stuffing; that is, enabling transmitting and receiving node pairs in a wireless network to more efficiently use time, frequency and spatial degrees of freedom relative to today's protocol structures. Channel stuffing is facilitated by using spatial and frequency degrees of freedom for interference mitigation. Protocols like Wi-Fi require that transmit-receive-node pair transmissions to be nearly orthogonal to other transmit-receive-node pair transmissions in time and frequency, and use spatial degrees of freedom for power gain and diversity gain. The requirement of orthogonal transmissions is very wasteful of degrees of freedom. The protocols developed in this work allow nodes to transmit simultaneously in interference, sharing the same time and frequency space, and also use spatial degrees of freedom for power gain diversity gain, and also use spatial degrees of freedom and frequency space for interference mitigation.

The key contributions of this work are the following:

1. The development of a joint PHY and MAC layer protocol that allows multiple transmiter-receiver pairs to communicate simultaneously in an interference environment, taking advantage of the spectral efficiency gains available under non-orthogonal communication schemes where MMSE receivers, multiple antennas and CDMA with random spreading codes are employed to achieve the optimal nulling of interferers and beaming towards the target transmitter.

2. We benchmark our results relative to the 802.11(n) protocol in a slow fading environment.

[6]MESH Networking is a type of networking wherein each node in the network may act as an independent router. We outline the IEEE version of MESH network in chapter 3

3. An analysis of the overall cost in terms of spectral efficiency and delay in our protocol relative to the maximum spectral efficiency for a given network when there is perfect knowledge of the channel and network, and compare these costs to today's most common ad hoc networking protocols.

In chapter 2 we begin with a review of the theoretical and engineering context of our work. In chapter 3 we summarize the prior work in the area of wireless networking. In chapter 4 we discuss the Simultaneous Transmissions in Interference (STI-MAC) joint MAC and PHY layer designs we developed. In chapter 5 we discuss the parameter space in which we seek to operate. In chapter 6 we discuss the optimization of the design parameters contained within the STI-MAC protocols. In chapter 7 we discuss simulation results for the STI-MAC protocol and compare them to simulation results for 802.11(n). We conclude in chapter 8 with a summary of our results and suggestions for future work.

Chapter 2

Background

In this section, we begin by framing our problem within the larger context of wireless communications and networking, and wireless networking protocols. Then we briefly review the fundamentals of Information-theoretic channel capacity, Antenna Arrays, MMSE Receivers, and Multi-Carrier Code-Division-Multiple-Access (MC-CDMA) that underly our work.

2.1 Wireless Networking

In this work we are concerned primarily with the interaction of wireless devices at distances up to 50 meters, which are the distances typically associated with wireless local area networks (WLAN). The traditional Open System Interconnection (OSI) model breaks up the software and firmware aspects of a computer network in to the functional layers shown in table 2.1.

The details of the implementation at each layer are unknown to other layers. And interaction between the network layers are carried out via an interface with pre-defined variables. In traditional layered networks that operate according to a collision-detection or collision-avoidance MAC scheme, a boolean can be fed from the physical layer (PHY) to the Medium-Access-Control (MAC) with the results of an assessment of the channel usage. In this work

Table 2.1: Open System Interconnection (OSI) Model

Application Layer	The application layer supports all network functionality for end-user processes. These functions include indentifying communicating nodes, quality of service requirements, and user authentication.
Presentation Layer	The presentation layer handles the delivery, syntax formatting and interpretation of information to the application layer.
Session	The session layer facilitates connections between applications by managing the set up procedure, termination, and packet exchanges.
Transport	The transport layer ensures reliable end-to-end communication, flow control, and error control between two nodes on a network.
Network Layer	At the network layer, routing, flow control, packet fragmentation and reassembly functionality are handled. The network layer aims to achieve the quality of service level requested by higher layers.
Data Link	The data link layer governs communications between individual nodes, and ensures that packet transmissions are error free. This layer is subdivided into the (1) Logical Link Control sublayer and the (2) Medium Access Control (MAC) sublayer. (1) The Logical Link Control sublayer is the interface between the MAC layer and the Network layer, enabling several network protocols to coexist, and providing flow and error control. (2) The Medium Access Control (MAC) sublayer governs the control and management mechanisms by which a collection of nodes access the physical medium to exchange data packets.
Physical Layer (PHY)	The physical layer defines the format and methods by which an individual node encodes, modulates, and electrically transmits signals over a given medium (copper fiber, optical fiber, wireless medium, etc.).

we define a joint PHY-MAC protocol in which transmission decisions traditionally in the MAC layer, and encoding decisions traditionally in the PHY layer, are made jointly in a cross-layer design based on measurements of the interference environment. This allows us to exploit the richness of scattering environments with multiple antennas and interference mitigation techniques, allowing more users to transmit simultaneously.

2.2 Channel Model

The literature that investigates experimental measurements and analytic modeling of wireless channels is vast, and the subject of many theses [12] and books [13, 14]. In our work we will use a fairly common and straight forward characterization of the channel that encompasses the key parameters that affect the performance of the protocol. These include (1) the small-scale effects of multiple reflections and refraction on the signal amplitude which is known as the channel fade, (2) the large-scale effect of multiple reflections and refraction on the received power which is known as the path-loss, (3) a characterization of the nature of the variation of the channel in the frequency domain and (4) a characterization of the nature of the variation of the channel over time.

2.2.1 Channel Fading Model

We assume that many statistically independent scattering paths arrive at each node within the duration of a sample, as well as a line-of-sight (LOS) component, where we vary the ratio in power of these two components (K-factor) to model different environmental conditions [12]. The sum of these multipath signals is represented as a channel coefficient modeling small-scale channel fading. For the non-line-of-sight components, we assume that these random amplitude and phase components are independent, and by the central limit theorem we model these channel coefficients (taps) as complex Gaussian random variables with zero mean and unit variance. The magnitude of a tap is then a Rayleigh random variable, and the squared magnitude is an exponential random variable. When we assume the presence of

a LOS component, the magnitude of a tap is modeled as a Ricean random variable parameterized by K, the ratio of the energy in the LOS path to the energy in the scattering paths.

2.2.2 Path Loss Model

Path-loss models describe the large scale power attenuation of a transmit signal as a function of distance. This power attenuation, which is above the r^2 loss due to propagation, is caused by the energy lost when signals reflect from objects in the environment. When channels are modeled stochastically, the exponential power decay with distance can be inferred from the data. In accordance with experimental results, [12],[15] we will model the path loss as $r^{-\alpha}$, where $\alpha = 3.8$.

2.2.3 Additive White Gaussian Noise

Each node contends with thermal noise as well as with an interference component from each of the transmitting nodes in the local area. The thermal noise power is modeled classically as kTB, where k is the Boltzmann constant, T is the system noise temperature in Kelvin, and B is the reception bandwidth.

2.2.4 Delay Spread & Coherence Bandwidth

The delay spread of the channel τ_{ds} is a measure of the duration of time between the arrival time of the multipath component with the strongest power, and the arrival of the last multipath component whose power is above a particular threshold C:

$$\tau_{ds}(C) = \max_{i,j \in S} |t_j - t_i| \tag{2.1}$$

With the duality of time and frequency, the coherence bandwidth W_c is inversely proportional to the delay spread. The coherence bandwidth characterizes the bandwidth over which the

frequency domain channel can be considered 'flat', with constant magnitude and minimal change in phase. This relationship is given by $W_c = \frac{1}{\tau_{ds}}$.

2.2.5 Channel Coherence Time

The channel coherence time is a statistical measure of the length of the interval over which the channel maintains relatively constant time and frequency domain response. The coherence time is inversely proportional to the Doppler spread. Doppler spread is a measure of the extent to which the signal bandwidth increases due to the relative velocity between transmitter and receiver. When a pure sine wave with frequency f is transmitted, the received signal spectrum, will be spread over $[f - f_d, f + f_d]$,where f_d is the Doppler shift.[1] A channel is described as fast fading when the coherence time is much shorter than the delay requirement of the application, and slow fading if the coherence time is longer than the delay requirements of the channel.

2.3 Evolution of the Channel in Time and Frequency

The variation of the channel with time will be an important factor in the performance of any wireless system, as the rate at which the channel changes will affect the reliability of the channel and the rate at which decoding weights must be updated. The coherence time of the channel is understood to be the interval over which the channel changes significantly [16]. Based on the PHY architecture we have chosen, we operate in a slow fading channel, which is defined here as a channel having a coherence time that exceeds the delay requirements of applications. This allows us to use a single set of decoding weights over several symbol intervals.

To evolve the channel in time we consider the simple model below. We partition the time access into intervals of length d, where d is the average coherence time of the channel. On the y axis we model the frequency response, and partition the axis into K points, where each

[1] Amplitude modulation independent of path length can also decrease coherence times.

point represents the frequency response on tone k. In figure 2-1, this is illustrated for $K = 3$.

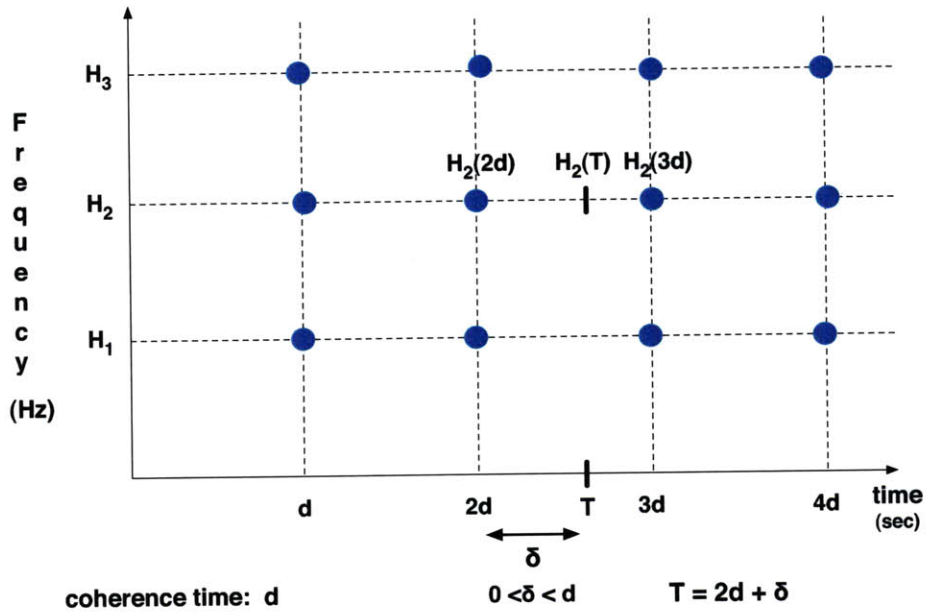

Figure 2-1: Channel Evolution in Time

Since the channel response is independent at instances in time that are larger than the coherence time d, the frequency response at time instances { 0, d, 2d, 3d, ... } are generated independently and randomly. These responses are created by generating a complex Gaussian, length L delay response, and performing the DFT to obtain the frequency domain coefficients. To determine the frequency response at time $T = 2d + \delta$ where $0 \leq \delta/d < 1$ and $md \leq T < (m+1)d$, we use the following relationship:

$$H_k(T) = \sqrt{(\delta/d)}H_k(md) + \sqrt{1-(\delta/d)}H_k((m+1)d) \tag{2.2}$$

Since $H_k(md)$ and $H_k((m+1)d)$ are Gaussian, $H_k(T)$ is also Gaussian. This simple model, which aims just to capture the non-static nature of the channel, is based on the Gauss-Markov model [17, 18]. Other more complicated models that consider the evolution of the

channel in time include the well-known Jakes' fading model [19, 20], in which a random phase is introduced to the N oscillators located in a ring around the target receiver, resulting in a received signal with correlation function approximately equal to the zeroth order Bessel function for large N. In the frequency domain, this corresponds to the Doppler Spectrum which is often used to filter received signal to model time-correlations [21, 22].

Experimental results [12] have reported a statistical relationship between the channel magnitude and phase and the duration with which that given level of stability persists, and have reported a stability of the magnitude of the channel on the order of seconds. In [16], a stability of the phase of the channel is reported to be on the order of milliseconds. Here and throughout this thesis we exclusively consider stationary nodes.

2.4 Multiple-Input-Multiple-Output (MIMO) Channels

When nodes transmit and receive using multiple transmit antennas and multiple receive antennas[2], the channel between any pair of these nodes is called a MIMO channel. The use of multiple antennas is a method to take advantage of the variability of the multipath environment available when the antennas are at different locations in space. This enables the use of signal processing techniques which can increase the reliability of the channel, the power gain, and in some cases, the number of degrees of freedom for multiplexing different streams of data in a wireless system. When multiple paths are available between transmitter and receiver, the likelihood that at least one of the paths has a favorable channel is increased, increasing the reliability of the channel. The power gain can be improved by coherently summing received copies of the transmitted signal. A multiplexing gain can be achieved when the scattering environment is sufficiently rich. This spatial diversity can be achieved in a rich multipath environment when multiple antenna elements at a particular node are placed far enough apart that the channel fade observed at each antenna is independent from

[2]Each antenna must have their own radio frequency chain for MIMO gains to be achieved.

the channel fade observed at the other antenna elements. Experimental results have shown that antenna elements greater than 1/2 wavelength apart see approximately independent channel fades [23] in rich scattering environments.

There is a dense literature on propagation models for MIMO wireless channels [24, 25]. The channel between any pair of antennas at different terminals is accounted for by the modeling techniques described above. The additional concern in MIMO channels is the degree of correlation between antennas at the same terminal. When the distance between any two antennas is greater than 1/2 wavelength – which is $\sim$ 3cm for 5GHz signals – the fades associated with different antenna elements are typically modeled as effectively independent [26]. This model is well known to over-optimistically predict the mutual information of the channel [15]. Several studies – both theoretical analyses and experimental results – have shown that the capacity of a MIMO channel degrades when there is correlation between the channel fades at the transmitter and / or correlation between the channel fades at the receiver [26, 27, 23]. Although the Kronecker model [28] is the most frequently used – and the model used in the development of 802.11(n) – to capture this correlation, many studies have reported that this model underestimates the channel's mutual information, and is not necessarily realistic in its partition of the transmit side and receive side correlations [29, 12]. For the sake of simplicity, in this work we will model co-located antennas as having an inter-element spacing of 1/2 wavelength, and independent.

2.5 Mathematical Channel Model

We assume the channel is quasi-static and thus fixed over the duration of a block (n) for a given flat-frequency bandwidth B, yielding this matrix representation of the channel[3]

[3]Matrices will be represented in bold and capitalized text ($\mathbf{X}$). Vectors will be represented in bold and lower case text ($\mathbf{x}$). Scalar quantities will be represented in italicized text (x).

$$\mathbf{Y} = \frac{P^{1/2}}{r^{\alpha/2}}\mathbf{H}\mathbf{X}^{\mathbf{T}} + \mathbf{N} \tag{2.3}$$

where $\mathbf{H}$ is an n_r by n_t matrix of channel coefficients, $\mathbf{X}$ is an n by n_t matrix of transmit signals, $\mathbf{Y}$ is an n_r by n matrix of received signals, and $\mathbf{N}$ is an n_r by n matrix of additive white gaussian noise. The distance between transmitter and receiver is r, the pathloss-exponent is α, and the transmit power constraint is $P = E[\text{trace}(\mathbf{X}^\dagger\mathbf{X})]$.

2.6 Beamforming

Beamforming is a method to electronically steer the energy radiated from a collection of antennas in order to maximize the energy received from or directed to a particular source, while minimizing the interference and noise seen at the receiver. If we consider, for example, a linear antenna array in free space receiving a line-of-sight transmission from a single transmitter, the receive beamformer corresponds to steering the main beam of the antenna array pattern towards a target angle and with a specified phase. In order to produce the desired antenna pattern with the main beam aimed at the target, the antenna-arrays are phased so that their signals add constructively in the particular target direction. As shown in figure 2-2, this corresponds to phasing the receive array to account for the delay that ensues due to the longer propagation distance to the ith receiver, where $r_i = r + (i-1)\lambda/2\cos\theta$ and where λ is the wavelength corresponding to the transmit frequency f ($\lambda = \frac{c}{f}$):

The channel can be modeled as introducing a phase at different receive antennas:

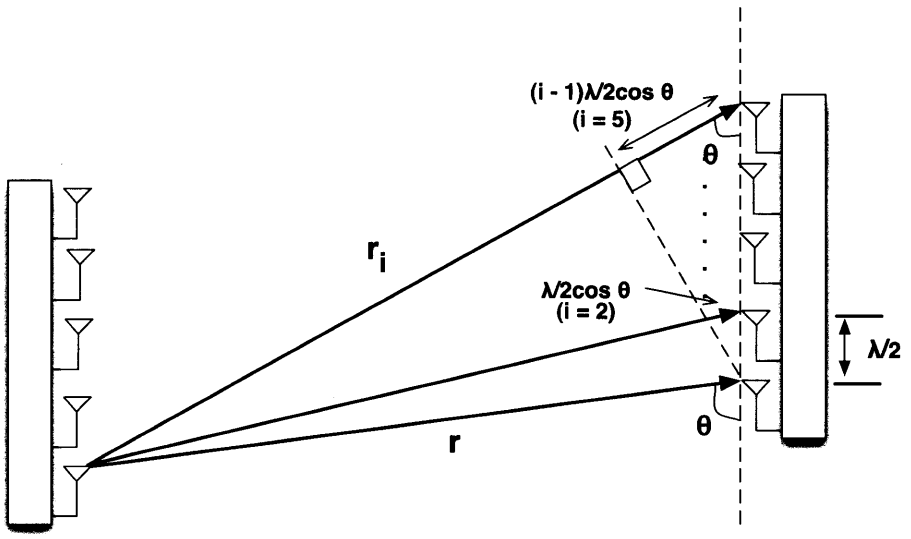

Figure 2-2: Line of Sight Beamformer

$$\mathbf{h} = a \exp\left(\frac{-j2\pi r}{\lambda}\right) \begin{bmatrix} 1 \\ \exp\left(-j2\pi \cdot 1\frac{\cos\theta}{2}\right) \\ \exp\left(-j2\pi \cdot 2\frac{\cos\theta}{2}\right) \\ \exp\left(-j2\pi \cdot 3\frac{\cos\theta}{2}\right) \\ \exp\left(-j2\pi \cdot 4\frac{\cos\theta}{2}\right) \end{bmatrix} \tag{2.4}$$

The optimal receive beamformer multiplies the received signal at each antenna by the phase i that allows the received signal at each antenna to be summed in phase

$$\mathbf{h}^\dagger\mathbf{h} = \exp\left(\frac{-j2\pi r}{\lambda}\right) \exp\left(\frac{j2\pi r}{\lambda}\right) \sum_i^{n_r} \exp\left(-j2\pi \cdot i\frac{\cos\theta}{2}\right) \exp\left(j2\pi \cdot i\frac{\cos\theta}{2}\right) \tag{2.5}$$

$$= |a|^2 \sum_i^{n_r} 1 \tag{2.6}$$

$$= |a|^2 n_r \tag{2.7}$$

In the same manner, signals can be made to add destructively, placing a null in a given

target direction. An antenna-array with n elements can independently steer $n-1$ beams and/or nulls.

Instead consider the use of a beamformer in a scattering environment where the channel between the single target transmitter and receive antenna array is described through the vector channel $\mathbf{h}$ and additive white Gaussian noise n. In the construction of the beamformer, the principle of steering the energy towards the target remains, but in this case corresponds to the superposition of many scattering paths captured through the matched fading coefficients in the vector $\mathbf{h}^{\dagger}$. This receive beamformer, also called the Matched Filter, maximizes the receiver Signal-to-Noise ratio.

When the interference environment seen at the receiver is non-white additive noise, the SINR maximizing beamformer is the minimum mean squared error (MMSE) which first whitens the interference, and then projects the whitened received signal onto the product of whitening filter and the target channel. A rigorous derivation of the whitening filter is given in [30]. Also see [30] for a derivation of the subspace whitening filter when the covariance matrix $\mathbf{K_y}$ is not invertible.

2.7 MIMO Channel Capacity in Additive White Gaussian Noise

The capacity of a single link with multiple transmit and multiple receive antennas (MIMO system), has been studied extensively in the literature. For an exhaustive review of the capacity of multiple-input-multiple-output channels, see [31], [16], [15], [32]. Here we review several of the key results that have had a tremendous impact in the wireless research community, and in commercial products.[4]

[4]For examples, see arraycomm.com, and the recent 802.11(n) Wi-Fi protocol.

Let $\mathbf{Y}$ be the received signal at a given receiver with n_r receive antennas, and $\mathbf{X}$ be the transmit signal from its target transmitter with n_t transmit antennas. $\mathbf{H}$ is the $(n_r \times n_t)$ channel drawn from a complex gaussian channel between the receiver and the transmitter. The signal $\mathbf{Y}$ is received in additive white gaussian noise $\mathbf{N} \sim CN(0, N_o\mathbf{I})$.

$$\mathbf{Y} = \mathbf{HX} + \mathbf{N} \tag{2.8}$$

The capacity of a channel is defined as the supremum of the achievable rates which maximizes the mutual information between the received signal and the transmit signal over all input distributions on the transmit signal:

$$\begin{aligned} C &= \sup_{p(\mathbf{X})} I(\mathbf{Y};\mathbf{X}) \quad b/s/Hz & (2.9)\\ &= H(\mathbf{Y}) - H(\mathbf{Y}|\mathbf{X}) & (2.10) \end{aligned}$$

Since the Gaussian distribution maximizes entropy, when the distribution on $\mathbf{X}$ is Gaussian, $\mathbf{Y}$ is Gaussian, and distribution on $\mathbf{Y}$ is parameterized by the mean and the covariance of $\mathbf{Y}$. The covariance of $\mathbf{Y}$ is given by:

$$\begin{aligned} E[\mathbf{YY}^\dagger] &= E[(\mathbf{HX} + \mathbf{N})(\mathbf{HX} + \mathbf{N})^\dagger] & (2.11)\\ &= \mathbf{H}E[\mathbf{XX}^\dagger]\mathbf{H}^\dagger + N_o\mathbf{I} & (2.12)\\ &= \mathbf{HRH}^\dagger + N_o\mathbf{I} & (2.13) \end{aligned}$$

where we have assumed that the transmit symbols $\mathbf{X}$ are independent of the noise and also Gaussian distributed, and where $\mathbf{R}$ is the transmit covariance matrix. We always assume that the receiver has perfect knowledge of the channel $\mathbf{H}$ in forming the beamforming weights and during decoding. The capacity of the channel depends on the channel knowledge (or lack thereof) at the transmitter, and its subsequent ability to carry out transmit beamforming

(when $n_t > 1$). We discuss these two cases separately below.

2.7.1 Uninformed Transmitter

When $\mathbf{H}$ is unknown at the transmitter (i.e., no channel-state-information (CSI) at the transmitter), we are solving the problem described above where we maximize the mutual information:

$$C = \sup_{p(\mathbf{X})} I(\mathbf{Y};\mathbf{X}) \tag{2.14}$$

$$= H(\mathbf{Y}) - H(\mathbf{Y}|\mathbf{X}) \quad b/s/Hz \tag{2.15}$$

The capacity is given by:

$$\log_2 \left| I + \frac{1}{N_o}\mathbf{H}\mathbf{R}\mathbf{H}^\dagger \right| \quad b/s/Hz \tag{2.16}$$

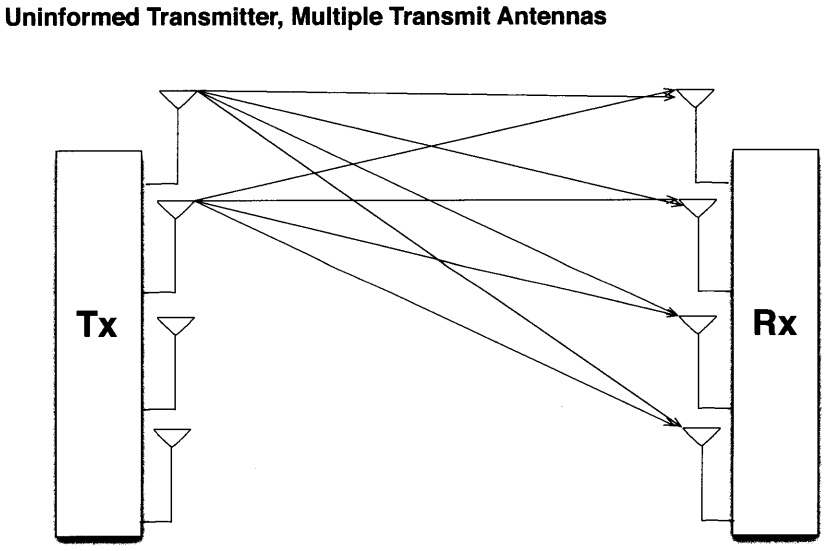

Figure 2-3: Uninformed Transmitter

When the rank of the transmit covariance matrix is 1 ($n_t = 1$), this corresponds to a single-

input-multiple-output (SIMO) channel, and is called receiver beamforming:

$$C = \log_2 \left(1 + ||\mathbf{h}||^2 \frac{P}{N_o} \right) \quad b/s/Hz \tag{2.17}$$

where the channel $\mathbf{H}$ is a $n_t \times 1$ vector $\mathbf{h}$. When $n_t > 1$ and $n_r = 1$, this corresponds to a multiple-input-single-output (MISO) channel. Since the transmitter does not have channel-state-information (knowledge of $\mathbf{h}$), it radiates equal power P/n_t on each transmit antenna.

$$C = \log_2 \left(1 + ||\mathbf{h}||^2 \frac{P/n_t}{N_o} \right) \quad b/s/Hz \tag{2.18}$$

2.7.2 Informed Transmitter

When $\mathbf{H}$ is known at the transmitter, we are trying to maximize the mutual information given perfect knowledge of the channel $\mathbf{H}$ at the transmitter:

$$C = \sup_{p(\mathbf{X})} I(\mathbf{Y}; \mathbf{X}|\mathbf{H}) \quad b/s/Hz \tag{2.19}$$

With multiple transmit antennas and perfect channel knowledge, the transmitter is able to steer its transmit beams in the eigenvectors of the channel, transforming the channel into parallel channels.

The capacity of the channel can be determined by employing the singular value decomposition (SVD) coordinate transform which decomposes $\mathbf{H}$ into the matrix product of a unitary rotation matrix $\mathbf{U}$, a scaling matrix $\mathbf{\Lambda}$ and another rotation matrix $\mathbf{V}$.

$$\mathbf{H} = \mathbf{U}\mathbf{\Lambda}\mathbf{V}^\dagger \tag{2.20}$$

The scaling matrix $\mathbf{\Lambda}$ is a diagonal matrix, containing the ordered singular values of $\mathbf{H}$, where the ordered singular values $\lambda_1 \geq \lambda_2 \geq \cdots \geq \lambda_{n_{min}}$ are the square root of the eigenvalues of $\mathbf{H}^\dagger\mathbf{H}$ (and of $\mathbf{H}\mathbf{H}^\dagger$), where n_{min} is the rank of $\mathbf{H}$, which is the number of non-zero eigen-

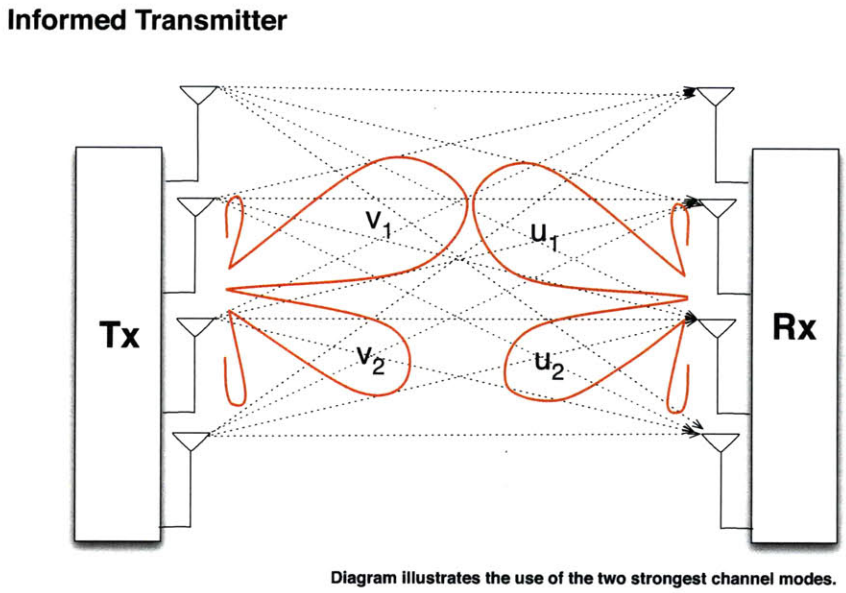

Figure 2-4: Informed Transmitter

values of $\mathbf{H}$. The columns of $\mathbf{U}$ are the eigenvectors of $\mathbf{H}\mathbf{H}^\dagger$, and the columns of $\mathbf{V}$ are the eigenvectors of $\mathbf{H}^\dagger\mathbf{H}$. When the channel $\mathbf{H}$ is known to both the transmitter and receiver, the transmission and reception can be conducted along the eigenmodes of the channel. By substituting equation (2.20) into equation (2.8), we define the linear transformation which decomposes the $n_r \times n_t$ channel into $n_{\min}$ parallel channels:

$$\begin{aligned} \tilde{\mathbf{x}} &= \mathbf{V}^\dagger \mathbf{x} \\ \tilde{\mathbf{y}} &= \mathbf{U}^\dagger \mathbf{y} \\ \tilde{\mathbf{n}} &= \mathbf{U}^\dagger \mathbf{n} \end{aligned}$$

Consequently, the effective channel between transmitter and receiver is n_{min} parallel channels, where $n_{min} = \min(n_t, n_r)$ when the channel is well conditioned:

$$\tilde{\mathbf{y}} = \mathbf{\Lambda}\tilde{\mathbf{x}} + \tilde{\mathbf{n}} \tag{2.21}$$

And the capacity of the channel is:

$$C = \sum_{i}^{n_{min}} \log_2 \left(1 + \frac{\lambda_i P_i}{N_o}\right) \quad b/s/Hz \tag{2.22}$$

where P_i are the 'water filling' power allocations $P_i = \max\left(0, \left(\mu - \frac{N_o}{\lambda_i^2}\right)\right)$ and μ is chosen such that $\sum P_i = P$.

2.8 Channel Capacity in Colored Noise

When we consider the channel capacity in a non-white channel, this interference channel is also called a 'colored noise' channel. To find the capacity of the channel, the receiver must, as we will show below, have knowledge of the covariance matrix of the interference. And similarly to the case of the additive white Gaussian channel, the capacity of the channel depends on the presence (or absence) of channel state information at the transmitter – where the channel state information includes knowledge of the target channel matrix $\mathbf{H}$ and the interference covariance matrix of the interference seen at the receiver $\mathbf{K}$.

2.8.1 Channel Capacity in Colored Noise, Uninformed Transmitter

When we add an interference component to the system above in order to model the systems we consider in this work, we let $\mathbf{H_j}$ be the $(n_r \times n_t)$ interference channel, drawn from a complex Gaussian distribution, between the given receiver and transmitter j.

$$\mathbf{Y} = \mathbf{HX} + \sum \mathbf{H_j X_j} + \mathbf{N} \tag{2.23}$$

The interference plus noise component $\sum \mathbf{H_j X} + \mathbf{N}$ together constitute 'colored noise'. The capacity of this channel is found by 'whitening' the interference plus noise by filtering the received signal with the whitening filter, which is the square root of the inverse of the interference covariance matrix $\mathbf{K^{-1/2}}$, where the interference covariance matrix is given by:

$$\begin{aligned} \mathbf{K} &= E[(\sum \mathbf{H_j X_j} + \mathbf{N})(\sum \mathbf{H_j X_j} + \mathbf{N})^\dagger] && (2.24) \\ &= \sum \mathbf{H_j H_j^\dagger} + N_o \mathbf{I} && (2.25) \end{aligned}$$

The whitened channel is given by:

$$\begin{aligned} \mathbf{K^{-1/2} Y} &= \mathbf{K^{-1/2} H X} + \mathbf{K^{-1/2}} \left(\sum \mathbf{H_j X_j} + \mathbf{N} \right) && (2.26) \\ &= \mathbf{K^{-1/2} H X} + \mathbf{N} && (2.27) \end{aligned}$$

where $\mathbf{N} \sim CN(0, \mathbf{I})$. When there is no channel state information present at the transmitter (uninformed transmitter), the capacity of the channel is given by:

$$\log_2 \left| I + \mathbf{K^{-1/2} H R H^\dagger K^{-1/2}} \right| \quad b/s/Hz \tag{2.28}$$

where $\mathbf{R}$ is the transmit covariance matrix.

2.8.2 Channel Capacity in Colored Noise, Informed Transmitter

When the transmitter has knowledge of the target channel $\mathbf{H}$, and the interference covariance matrix $\mathbf{K}$ seen at the receiver, the transmitter can beamform through the effective target channel that has been whitened by the receiver:

$$\mathbf{Y_{eff}} = \mathbf{K^{-1/2} H} + \bar{\mathbf{N}} \tag{2.29}$$

where $\bar{\mathbf{N}}$ is the whitened channel with distribution $\sim CN(0, \mathbf{I})$. The procedure is the same as the case of additive white Gaussian noise capacity, where the capacity is determined by

performing the Singular Value Decomposition (SVD) on $\mathbf{K^{-1/2}H}$:

$$\mathbf{K^{-1/2}H} = \bar{\mathbf{U}}\bar{\mathbf{\Lambda}}\bar{\mathbf{V}}^{\dagger} \tag{2.30}$$

The scaling matrix $\bar{\mathbf{\Lambda}}$ is a diagonal matrix, containing the ordered singular values of $\mathbf{K^{-1/2}H}$, where the ordered singular values $\lambda_1 \geq \lambda_2 \geq \cdots \geq \lambda_{n_{min}}$ are the square root of the eigenvalues of $\mathbf{H^{\dagger}K^{-1}H}$, where n_{min} is the rank of $\mathbf{K^{-1/2}H}$, which is the number of non-zero eigenvalues of $\mathbf{K^{-1/2}H}$.

$$\begin{aligned} \tilde{\mathbf{x}} &= \bar{\mathbf{V}}^{\dagger}\mathbf{x} \\ \tilde{\mathbf{y}} &= \bar{\mathbf{U}}^{\dagger}\mathbf{y} \\ \tilde{\mathbf{n}} &= \bar{\mathbf{U}}^{\dagger}\mathbf{n} \end{aligned}$$

Consequently, the effective channel between transmitter and receiver is n_{min} parallel channels, where $n_{min} = \min(n_t, n_r)$ when the channel is well conditioned:

$$\tilde{\mathbf{y}} = \mathbf{\Lambda}\tilde{\mathbf{x}} + \tilde{\mathbf{n}} \tag{2.31}$$

And the capacity of the channel is:

$$C = \sum_{i}^{n_{min}} \log_2 (1 + \lambda_i P_i) \quad b/s/Hz \tag{2.32}$$

where P_i are the 'water filling' power allocations $P_i = \max\left(0, \left(\mu - \frac{1}{\lambda_i^2}\right)\right)$ and μ is chosen such that $\sum P_i = P$.

2.8.3 Diversity-Multiplexing Tradeoffs

There is a fundamental tradeoff between diversity gains and multiplexing gains in slow fading MIMO systems, which was formalized by Zheng and Tse [33]. The maximum number

of diversity paths in a N_t transmit antenna and N_r receive antenna MIMO system is $N_t N_r$, and consequently the average error probability can be made to decay like $SNR^{-N_r N_t}$ when the appropriate transmit and receive schemes are used. And as explained above, a MIMO system can also be used to transmit $\min(n_t, n_r)$ independent streams through a channel whose transfer matrix is well-conditioned (with high probability), and the average data rate scales like $\min(n_t, n_r) \log_2(SNR)$ when there is perfect channel knowledge at the transmitter and receiver, and when a successive interference cancellation scheme is used at the receiver. Zheng and Tse focus on the high SNR regime and characterize the optimal trade-off curve achieveable by any transmit and receive scheme where a given scheme has spatial multiplexing gain r if the rate of the scheme scales like $r \log_2 SNR$, and a given scheme has a diversity gain d if the average probability of error decays like SNR^{-d}.

2.9 Interference Channels

The broad theoretical framework for the analysis of ad hoc networking is in the classical Interference channel problem in Network Information Theory. The problem, simply stated, seeks to determine the bounds of the multi-dimensional rate region for the transmitter-receiver pairs that make up a network. The 2x2 Gaussian interference channel problem illustrated in Figure 2-5 is not solved in general, though it has been solved in specific cases (independent channels; strong interference case) [34]. A recent result by Etkin, Tse and Wang [35] has solved the capacity of the two-user Gaussian interference channel to within one bit accuracy, extending the well known Han-Kobayashi result [36] that splits transmissions into private and public portions and enables a subset of the interference to be decoded and subtracted from the received signals. The Etkin et al. result proves that the Han-Kobayashi scheme achieves rates within 1 b/s/Hz of the capacity of the channel, and provides a method for choosing the ratio of the power for the private versus the public information.

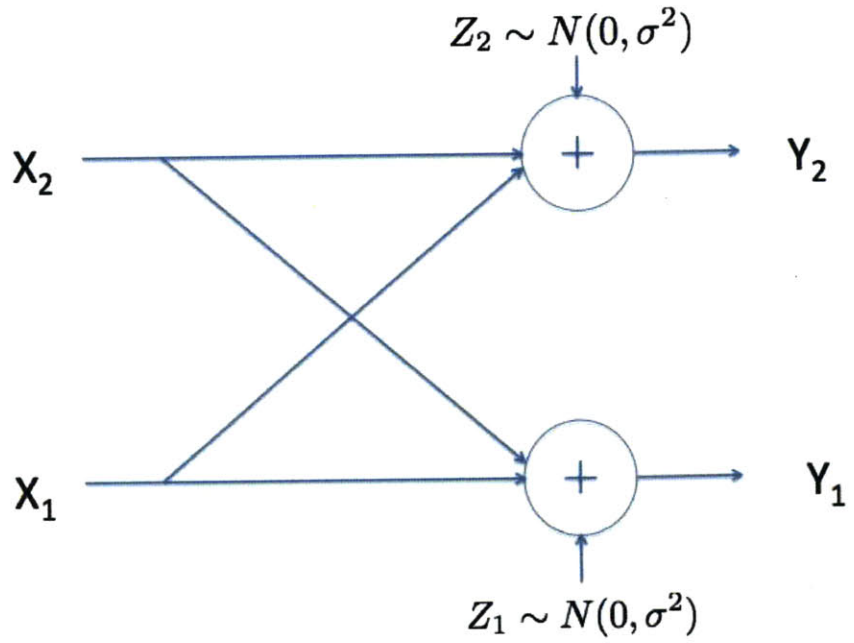

Figure 2-5: 2x2 Interference Channel where Receiver Nodes are subject to Additive White Gaussian Noise

2.10 Ad Hoc Wireless Networks

Many researchers have also sought to determine the rate at which throughput capacity scales as a function of the number of nodes in interference channels (wireless networks), in order to move beyond questions related to the many ways that nodes in a network can cooperate and the effects of these strategies on capacity. The groundbreaking results by Gupta and Kumar [37] showed that the order of growth of throughput to be $O(\frac{1}{\sqrt{n}})$ bits per second for each node in a specific network topology and traffic pattern that allow for multiple hops, and operating under protocols that treat other users as interference. They also analyzed a more general network with random topologies and traffic patterns, and found the order of growth of throughput capacity to be $O(\frac{1}{\sqrt{n \log n}})$. In [38] Xie and Kumar verify that under a multi-hop strategy in which nodes are fully decoded at each hop and employ only point-to-point coding, and where the attenuation of signal power is high as a function of distance, the order

of growth of capacity is $O(\frac{1}{\sqrt{\log n}})$. Franceschetti et al. [39] have recently proved that the order of growth of throughput $O(\frac{1}{\sqrt{n}})$ proved in the special case in Gupta and Kumar [37] holds, with high probability for nodes with random locations in a multi-hop network where interference is treated as noise. Franceschetti et al. [39] prove their order of growth result using percolation theory. With percolation theory, they demonstrate the existence of a 'data highway' – in effect a wireless backbone – through the network made up of a chain of nodes that acts as a relay for other nodes, leading to their order of growth result. Franceschetti has also recently contended in [40] that the maximum order of growth per user in a wireless network is $O(\frac{(\log n)^2}{\sqrt{n}})$ based on an electro-magnetic theory argument and using a cut-set bound on the number of degrees of freedom between nodes on the interior and exterior of a circular cut set. Results showing larger orders of growth, he contends, suffer from unrealistic channel models. Ozgur, Leveque and Tse [41] have proposed a hierarchical cooperation schemes for nodes in wireless networks in which nodes exchange their digitized transmissions with their neighbors, and then groups of nodes act like a virtual antenna array to transmit and receive data from groups of nodes in other parts of the network. With increasing levels of hierarchy, they show that this scheme allows the total network capacity to scale linearly with the number of nodes (and thus the per-node capacity to be constant).

As several authors have noted, while scaling laws are important work, the constant coefficients of the scaling laws have an enormous effect on the actual data rates achieved in the network [39], [41]. In [41] in particular, Govindasamy [11] has found that just two levels of hierarchy requires on the order of 1 billion nodes for the proposed scheme to surpass the average data rate of a TDMA network.

2.10.1 Ad Hoc Networks with Multiple Transmit and Receive Antennas

Several researchers have explored the use of Multiple antennas in Ad Hoc wireless Networks, employing different transmit and receive strategies to determine how to maximize the sum

capacity over the network when nodes transmit simultaneously causing interference to the others in the network. In [42], Blum considers the sum capacity for nodes with multiple transmit and receive antennas in a network employing single-user detection where there is no channel state information at the transmitter. He considers two strategies: (1) transmitting equal power on each antenna, and (2) transmitting from a single antenna. He shows that in the case that interference is either sufficiently weak or sufficiently strong, either strategy is optimum. Blum also identifies sum-capacity surfaces for the 2 link network that distinguish for which interference levels each of these strategies is optimal. Chen and Gans [43] consider the problem of how the system capacity scales with the number of Tx-Rx pairs when there is channel state information at the receivers, and when receivers employ single user detection in the case of channel state information at the transmitter (Tx CSI), and in the case where channel state information is not present at the transmitter. In both the cases of Tx CSI and no Tx CSI, they show that the per link spectral efficiency scales $O(\frac{1}{K})$. In the absence of channel state information at the transmitter, they show that the asymptotic spectral efficiency is proportional to the number of receive antennas and independent of the number of transmit antennas and transmit power when transmitters transmit equal power from each antenna. When CSI is present at the transmitter, they show that the asymptotic spectral efficiency is at least $t + r + 2\sqrt{tr}$ where t is the number of transmit antennas and r is the number of receive antennas, and transmitters are using a water filling strategy to allocate power to the strongest tones.

The work of Govindasamy et al. [11], [10], [44] studies the distribution of the spectral efficiency of nodes in Ad Hoc Networks with multiple antennas when nodes in the network cooperate minimally, and where the distribution of nodes in space is considered in the decoding algorithms. Govindasamy introduces the parameter 'link rank' to characterize and interference environment, and which is approximately 'the number of interferers that are stronger than the target transmitter as measured by the receiver'. Employing Minimum-Mean-Square-Error (MMSE) receivers, they show that the expected Signal-to-Interference-

plus-Noise Ratio of a link is:

$$E[SINR] \approx G_\alpha \left(\frac{N}{A}\right)^{\frac{\alpha}{2}}$$

where N is the number of receive antennas in a wireless network with nodes uniformly and randomly distributed in a plane, α is the path loss exponent in the $r^{-\alpha}$ model, G_α is gain term dependent on the value of α, A is the link rank $A = \pi r_1^2$, and r_1 is the distance to the target transmitter. This important result shows that in the interference-limited regime, MMSE receivers provide greater than linear growth in SINR, surpassing the growth of matched filter decoders. The average spectral efficiency of a representative link then grows as $\log(N)$. The authors also finds that the variance of the spectral efficiency for a representative link decays as $\frac{1}{N}$. These results are extended to the multiple transmitter case where there is no transmitter state information, and it is shown that the expected spectral efficiency per link in this case is:

$$E[C] \approx N_t \log_2 \left(1 + G_\alpha \left(\frac{N}{N_t A}\right)^{\frac{\alpha}{2}}\right) \tag{2.33}$$

Consequent of this result, Gonvindasamy [11] highlights that the network optimal number of transmit streams is fewer than the number of streams that would maximize the spectral efficiency for an individual link. Under specific densities of users, numbers of transmit and receive antennas, Govindasamy finds the number of transmit streams for each node in the network that maximize the sum spectral efficiency over the network.

2.11 Minimum-Mean-Squared-Error Receivers

The Minimum-Mean-Squared-Error (MMSE) receiver beamforming weights maximize the received SINR over all linear receivers by optimally placing degrees of freedom to attenuate interfering signals and amplify the target transmitter. Consider the case of determining receiver beamforming weights for one (of potentially several) radiated signals from the target transmitter. The derivation of the MMSE beamforming weights $\mathbf{w}$ is well known [45], and is

restated below. Let x be an unknown scalar we seek to estimate, and let x_j for $j \in [2, M]$ be unknown interfering scalars where $|x_i|^2 = P$, and $|x_j|^2 = P$. Let $\mathbf{h}$ be a vector drawn from a complex Gaussian distribution and represent our target signature, and let vectors $\mathbf{h_j}$ for $j \in [2, M]$ represent the interfering signatures. And let $\mathbf{n}$ be additive white Gaussian noise $\sim CN(0, No\mathbf{I})$.

$$\mathbf{y} = x\mathbf{h} + \sum x_j \mathbf{h_j} + \mathbf{n} \tag{2.34}$$

To find beamforming weights ($\hat{x} = \mathbf{w}^\dagger \mathbf{y}$) to minimize the mean squared error between x and the estimate $\hat{x}$, where the expectation is taken over many realizations of unknown scalars x, x_j that are independent, and equally likely to be -1 or $+1$:

$$\begin{aligned}
E[(\mathbf{w}^\dagger\mathbf{y} - x)(\mathbf{w}^\dagger\mathbf{y} - x)^\dagger] &= E[\mathbf{w}\mathbf{y}\mathbf{y}^\dagger - \mathbf{w}^\dagger\mathbf{y}x' - x\mathbf{y}^\dagger\mathbf{w} + ||x||^2] && (2.35)\\
&= \mathbf{w}^\dagger\mathbf{K_y}\mathbf{w} - \mathbf{w}^\dagger E[\mathbf{h}xx'] - \mathbf{w}^\dagger E[\mathbf{h_j}x_j x'] - && (2.36)\\
&\quad E[\mathbf{w}x'] - E[xx'\mathbf{h}^\dagger]\mathbf{w} - E[x_j x'\mathbf{h_j}]\mathbf{w} + E[|x|^2] && (2.37)\\
&= \mathbf{w}^\dagger\mathbf{K_y}\mathbf{w} - P\mathbf{w}^\dagger\mathbf{h} - P\mathbf{h}^\dagger\mathbf{w} + P && (2.38)
\end{aligned}$$

where the covariance matrix of the interference plus the target channel $\mathbf{K_y}$ is given by:

$$\begin{aligned}
\mathbf{K_y} &= \mathbf{y}\mathbf{y}^\dagger && (2.39)\\
&= P\mathbf{h}\mathbf{h}^\dagger + (\sum_j \mathbf{h_j} + \mathbf{n})(\sum_j \mathbf{h_j} + \mathbf{n})^\dagger && (2.40)\\
&= P\mathbf{h}\mathbf{h}^\dagger + \sum_j \mathbf{h_j}\mathbf{h_j}^\dagger P + No\mathbf{I} && (2.41)\\
&= P(\mathbf{h}\mathbf{h}^\dagger + \sum_j \mathbf{h_j}\mathbf{h_j}^\dagger P + \frac{No}{P}\mathbf{I}) && (2.42)
\end{aligned}$$

Differentiating equation (2.38) with respect to $\mathbf{w}$ and setting equal to zero and solving for $\mathbf{w}$:

$$\mathbf{w} = \mathbf{K_y^{-1}}\mathbf{h} \tag{2.43}$$

If we let $\mathbf{K}$ be the covariance matrix of the interference plus the noise:

$$\mathbf{K} = \sum_{j}^{M} P\mathbf{h_j}\mathbf{h_j^\dagger} + No\mathbf{I} \tag{2.44}$$

The average Signal-to-Interference-plus-Noise Ratio that is achieved when the MMSE beamforming weights are used is given by:

$$\begin{aligned} SINR &= \frac{E\left[||\mathbf{h_1^\dagger}\mathbf{K^{-1}}\mathbf{h_1}x_1||^2\right]}{E\left[||\mathbf{w}^\dagger(\sum_i^M x_i\mathbf{h_i}+\mathbf{n})||^2\right]} \\ &= \frac{P||\mathbf{h_1^\dagger}\mathbf{K^{-1}}\mathbf{h_1}||^2}{\mathbf{w}^\dagger\mathbf{K}\mathbf{w}} \\ &= \frac{P\mathbf{h_1^\dagger}\mathbf{K^{-1}}\mathbf{h_1}\mathbf{h_1^\dagger}\mathbf{K^{-1}}\mathbf{h_1}}{\mathbf{h}^\dagger\mathbf{K^{-1}}\mathbf{K}\mathbf{K^{-1}}\mathbf{h}} \qquad (2.45) \\ &= P\mathbf{h_1^\dagger}\mathbf{K^{-1}}\mathbf{h_1} \qquad (2.46) \end{aligned}$$

The expectation is again taken over the transmit symbols x. The same average Signal-to-Interference-plus-Noise Ratio can be achieved when the interference covariance matrix used to contstruct the MMSE beamforming weights contains the target channel:

$$\mathbf{K_t} = P\mathbf{h_1}\mathbf{h_1^\dagger} + \sum_{j}^{M} P\mathbf{h_j}\mathbf{h_j^\dagger} + N_o\mathbf{I} \tag{2.47}$$

Using the following identity, the expression for the beamforming weights $\mathbf{w_t} = \mathbf{K_t^{-1}}\mathbf{h_1}$ can be simplified to the original weights times a scale factor:

$$(\mathbf{a}\mathbf{a}^\dagger + \mathbf{A})^{-1}\mathbf{a} = \frac{1}{1+\mathbf{a}^\dagger\mathbf{A^{-1}}\mathbf{a}}\mathbf{A^{-1}}\mathbf{a} \tag{2.48}$$

$$\mathbf{w} = \frac{1}{1+\mathbf{h}^\dagger(\mathbf{K}+\frac{\mathbf{N_o}}{\mathbf{P}}\mathbf{I})^{-1}\mathbf{h}}(\mathbf{K}+\frac{No}{P}\mathbf{I})^{-1}\mathbf{h} \tag{2.49}$$

In the computation of the SINR, this scale factor cancels, and the SINR is unchanged.

There are several strengths to using MMSE beamformers. The first is that MMSE beam-

forming weights are linear, and as shown in chapter 6, estimates of the target channel and interference channel are easily obtained and lead to low degradation in the received SINR. Secondly, among linear receivers, the MMSE receiver maximizes the received SINR – behaving identically to the matched-filter at low SINR and like the decorrelator at high SINR [16]. Thirdly, though the capacity of the interference channel is unknown, when the MMSE receiver is used in point-to-point channel to multiplex data through an independent and identically distributed (i.i.d.) Rayleigh fading channel with multiple transmit and receive antennas, MMSE processing with individual decoding of the data streams and successive-interference-cancellation achieves capacity [16].

2.12 Orthogonal Frequency Division Multiplexing (OFDM)

In this wireless local area network protocol, we are working in environments and transmission ranges where the delay spread is much less than the coherence time of the channel, because this will allow us to model the channel as a linear and time invariant system over several symbol times up to the channel coherence time. The network itself is ad hoc and control is distributed, so we would prefer to not rely on power control or an orthogonal hopping pattern for the functionality of the network to minimize the required coordination between users. And regarding data rates, we would like the ability to transmit at high data rates ($\geq$ 100Mbps) and consequently, would prefer lower CDMA spreading lengths so that we can make efficient use of the degrees of freedom of the spectrum.

Capitalizing on the environmental characteristic of a delay spread much less than the coherence bandwidth of the channel, and seeking to take advantage of frequency diversity available by partitioning a larger frequency selective band into smaller flat frequency channels (though typically not all independent in their channel fade), we choose the Orthogonal Frequency Division Multiplexing (OFDM) as the modulation scheme for the physical layer architecture. Our total bandwidth B is divided into K tones of bandwidth W ($W = \frac{B}{K}$). Bandwidth W

is chosen much less than the coherence bandwidth of the channel, which is proportional to the reciprocal of the delay spread of the channel. This is to ensure that the channels on each tone can be represented by a single (complex) filter tap. OFDM is implemented by applying an N-point Inverse Discrete Fourier Transform (IDFT) on each block of N symbols and then either pre-pending the last N_{cp} codewords as a cyclic prefix or N_{cp} zeros, where N_{cp} is greater than the length of the delay spread to prevent inter-symbol interference. The block of length $N + N_{cp}$ is then transmitted, and at the receiver the cyclic is discarded, and an N-point Discrete Fourier Transform (DFT) is used to recover the transmitted symbols.

The drawbacks of OFDM include the lost transmission time which equals the duration of the cyclic prefix, as well as the computational complexity of computing the IDFT and the DFT. The latter is greatly reduced when the number of symbols is a power of two, and the Fast Fourier Transform (FFT) algorithm can be employed. OFDM also has a heightened sensitivity to frequency offsets, which causes inter-carrier interference in OFDM. Another drawback of OFDM systems is the high peak to mean envelope power fluctuation (also called the crest factor) which is often present in systems in which transmit symbols are composed of trigonometric series. To combat this problem, advanced linear power amplifiers with a high dynamic range are needed to reduce the non-linear distortion of the signals at the receiver. This problem worsens as the number of OFDM tones increases [46].

The basic idea of OFDM[5] is to transform a wideband channel of width W used to transmit a length N serial input sequence into several narrow band overlapping and orthogonal channels of width W/N over which the input sequence is transmitted in parallel by modulating each of the N symbols onto one of the N carriers. The resulting OFDM symbols is then the sum of the modulated carriers. At the receiver the N symbols are demodulated, and a parallel-to-serial converter is used to reconstruct the original input sequence. This narrowband transmission feature of OFDM makes it resistant to narrow band fading and

[5]The original idea behind OFDM was introduced by R.W. Chang of Bell Systems in 1966, but was not widely implemented until recently due to the complexity of the modulation and demodulation procedures.

interference, which in an OFDM system, affects a subset of carriers and not an entire symbol or series of symbols in the case of a bursty channel. The duration of the OFDM symbol is N/W, which is N times the duration of the non-OFDM symbol $1/W$ over the same bandwidth. The longer symbol duration can provide some increased resistance to the effects of multipath / delay spread. The longer symbol duration, and the lower sampling frequency, also reduce the likelihood of errors in the sampling procedure. Another benefit of OFDM compared to a wideband transmission procedure occurs in the demodulation procedure. To demodulate a signal transmitted over a wideband requires a channel equalizer to undo the effect of the frequency selective channel on the input signal. A key benefit of OFDM is that the system does not require the use of a channel equalizer, as the tones in OFDM can be chosen such that the tones are flat in frequency and represented by a single tap. For a more complete exposition of OFDM, see [47].

If we let $B = \frac{W}{N} = \frac{1}{T}$ be the bandwidth of an OFDM tone where T is the symbol time, and let $\omega_o = 2\pi B = \frac{2\pi}{T}$ be the modulation frequency in radians of the first tone, $\omega_n = n\omega_o$ where $n \in \{1, \ldots, N\}$ describes the modulation frequency of each of the N tones of our frequency architecture. Let the sequence $\{x_{1k}, x_{2k}, \ldots, x_{nk}\}$ be the N quadrature amplitude modulation (QAM) input signals at time t_k. The transmit duration of each OFDM symbol is T, and we model that transmission time with a rectangular transmission pulse $r(t - Tk)$ where k is the signaling interval index.[6] Our OFDM transmit symbol is thus:

$$s(t) = \Re\left\{\sum_{k=-\infty}^{\infty}\sum_{n=0}^{N-1} x_{nk} r(t - kT) e^{jw_n t}\right\}$$

If we consider the Fourier transform of $s(t)$ into the frequency domain over a single transmission interval, $s(t_o)$ is the sum of N convolutions between a sinc pulse $\text{sinc}(\omega_n T))$ and the dirac delta functions $\delta(\omega_n)$:

[6]The raised cosine window is a more typically used transmission pulse [48], but for simplicity, we use a rectangular pulse.

$$S(j\omega) = \Re\left\{\sum_{n=0}^{N-1} x_{nt_o}\text{sinc}(\omega_n T)\delta(\omega_n)\right\}$$

The sinc functions ($\text{sinc}(\omega_n T) = \frac{\sin(\omega_n T)}{\omega_n T}$ are zero at all frequencies that are a multiple of $\frac{2\pi}{T}$ and consequently, all have their maximum value at $\omega_n T$, and zero crossings at integer multiples of $\frac{2\pi}{T}$. An OFDM receiver decodes a received signal by estimating the value of the spectrum at these peaks. Since these zero crossings are at the peak of all of the other OFDM symbol pulse's maximum values, inter-carrier interference is avoided and the OFDM symbols are essentially orthogonal.

If we consider only the 0th signaling index, and rewrite $s_o(t)$ equivalently:

$$s_o(t) = \sum_{n=1}^{N} x_{n0} e^{j2\pi\omega_n t}$$

If we consider now sampling $s(t)$ at a rate $\frac{1}{T_s}$, where $T_s = \frac{T}{M}$ and $M = 2(N-1)$ so that the Nyquist criterion is met,

$$s[m] = s_0(mT_s) = \sum_{n=0}^{N-1} x_{n0} e^{j\frac{2\pi}{N}nm} \quad m = 0, \ldots, N-1 \tag{2.50}$$

Equation 2.50 corresponds to the N-point Inverse Discrete Fourier Transform (IDFT) of the input symbols.[7] Here we have shown the method used in OFDM to eliminate the need for separate modulation and demodulation oscillators in hardware for each carrier. Instead, an IDFT is computed, and the resulting OFDM symbol is transmitted. This method becomes even more computationally efficient when the Fast Fourier Transform Algorithms are used at both the transmitter and receiver for modulation and de-modulation respectively.

The N-point Discrete Fourier Transform (DFT) decomposes a discrete time signal into to a sequence which is the sum of the N harmonically related complex and periodic exponen-

[7]The synthesis equation of the Discrete Fourier Transform (DFT) is given by $x[n] = \frac{1}{N}\sum_{n=0}^{N-1} X[k]e^{[\frac{2\pi}{N}nk}$. [49]

tials. Because of its inherent periodicity, the DFT and the IDFT assume a periodic input. Consequently, when the DFT of the input signal is passed through the channel, a cyclic convolution between the input signal and the channel is performed.

$$y_{i,k} = \sum_{j=0}^{N_{ch}} h_j s_{i(n-j \bmod N)} + w_{i,k} \qquad n = 0, \ldots, N-1$$

In order to prevent aliasing, a periodicly replicated version of the (finite) input signal can be used, whose total length N_{OFDM} of the signal N_s plus the length of the channel N_{ch} ($N_{OFDM} = N_s + N_{ch}$). Typically the last N_{ch} samples of the signal are used to prefix the transmit symbol, and are called the cyclic prefix. Then at the receiver, the first N_{ch} samples are discarded and the remaining portion of OFDM symbol is processed using the DFT:

$$\begin{aligned} \hat{x}_{i,k} &= \sum_{n=0}^{N-1} y_{i,n} e^{-j\frac{2\pi}{N}nk} \\ &= x_{i,k} \sum_{n=0}^{N-1} \check{h}_{i,n} e^{-j\frac{2\pi}{N}nk} \\ &= x_{i,k} h_{i,k} \end{aligned}$$

where $\check{h}_{i,n}$ is the nth sample of the channel response at time i, $s_{i,k} = \sum_{n=0}^{N-1} x_{i,n} e^{-j\frac{2\pi}{N}nk}$, $h_{i,k}$ is the DFT of the channel response at time i and on tone k. When $h_{i,k}$ is known, $x_{i,k}$, as we've shown above that $x_{i,k}$ can be retrieved without inter-symbol interference or inter-carrier interference. Alternatively, the IFFT of the information symbols can be padded with zeros instead of the cyclic prefix.

The length of the cyclic prefix, which is the guard time between symbols to prevent inter-symbol interference, is governed by the tolerance of the modulation type to interference. It is typically suggested that for coding levels up to 64 QAM that the guard time be 2 - 4 times the root-mean-squared delay spread of the channel. The symbol duration T, which is the inverse of the tone bandwidth $B = \frac{1}{T}$, is a tradeoff between making T large, which

minimizes the fraction of time lost to guard time and power lost to the cyclic prefix, and making T so large that the tone bandwidth B becomes small, worsening the peak-to-average power ratio and making the system more sensitive to frequency offsets. Since $T > T_{ch}$, the tone bandwidth B is less than the coherence bandwidth of the channel.[8] The range of data rates the system can support can then be chosen by setting the total bandwidth of the system (number of tones), as well as the modulation types, error-control coding rates, and the number of transmit and receive antennas.

To facilitate comparisons to 802.11 protocols in our preliminary work, we use the 802.11(a, n) architectures where 48 tones, each of bandwidth 312.5kHz, are used for data transmissions. The symbol duration is 3.2 μs, and there is a 800 ns guard time. The guard time interval can be shortened, as in 802.11(n), for indoor environments where there are typically much shorter delay spreads.

2.13 Multi-Carrier Code-Division-Multiple-Access (MC-CDMA)

In this work we will make use of MC-CDMA for the underlying spectrum usage architecture. Here we briefly explain MC-CDMA, and summarize its benefits.

Multi-Carrier Code-Division-Multiple-Access (MC-CDMA) is a modulation scheme that divides a large bandwidth into flat, narrow-band tones to be used for Orthogonal-Frequency-Division-Multiplexing (OFDM); and instead of modulating different symbols onto each tone as is typically the case in OFDM, the MC-CDMA scheme modulates the same symbol on multiple tones and scales each symbol by a chip in a known pseudo-random spreading code. An illustration of the MC-CDMA architecture is given in figure 2-6. OFDM systems, and

[8]The coherence bandwidth of the channel is the reciprocal of the delay spread of the channel.

thus MC-CDMA systems, are particularly useful in frequency-selective channel environments that are converted into flat-fading channels on each tone, simplifying equalization by limiting inter-symbol interference. This scheme is effective in environments with a low delay spread where the duration of an OFDM symbol can be chosen to be much larger than the delay spread. Since the delay spread is much less than the symbol duration, several tones will also be contained within one coherence bandwidth, limiting frequency diversity. MC-CDMA is a technique to spread the signal energy over a larger bandwidth, gaining back frequency diversity but retaining the immunity to inter-symbol interference relative to other wide band techniques such as Spread-Spectrum CDMA. The main advantage of MC-CDMA is that the receiver can always use all the received signal energy scattered in the frequency domain, whereas in the time domain, Rake receivers attempt to collect the signal energy, but are not as successful as MC-CDMA techniques. [50, 51]

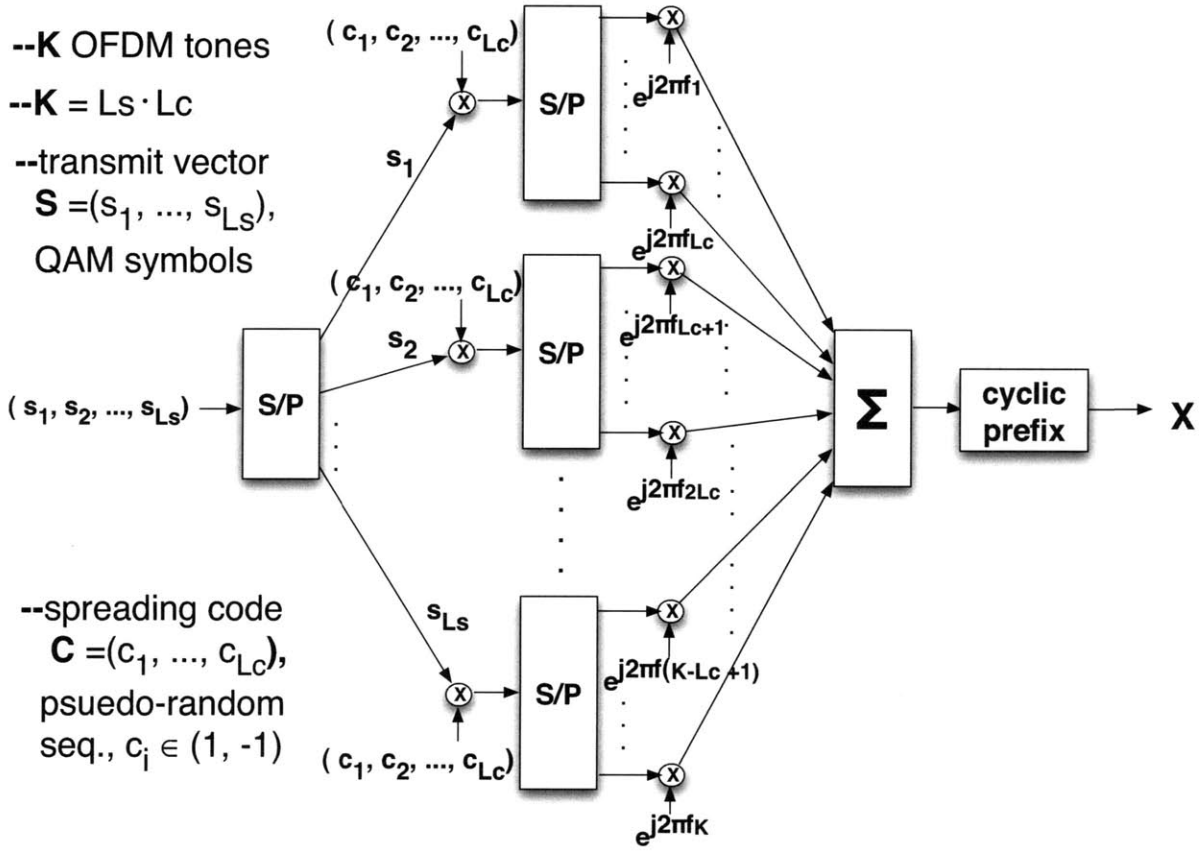

Figure 2-6: MC-CDMA

Chapter 3

Prior Work

3.1 Introduction

Wireless network protocols can be characterized by three fundamental components: (1) the engineering architecture by which bits are transmitted over the physical medium; (2) the space in which either contention-based or reservation-based medium access control takes place; and (3) the nature of the division of resources between data transmissions. This partition of the protocol space by the physical layer (PHY) scheme, the medium-access-control layer scheme (MAC), and the (non) orthogonality of the control versus data transmissions is illustrated in figure 3-1.

The vast majority of prior work has been focused in the area of orthogonal transmissions between individual users in the network. The research described in this thesis is situated in the space of non-orthogonal transmissions, and explores that space with three different ways to organize the control mechanism of the joint MAC-PHY layer architecture. In this section we discuss the prior work in the area of wireless protocol design within the taxonomy of protocols described in figure 3-1. We begin by summarizing the many MAC layer variants developed in the literature in both the single antenna and multiple antenna space. Next we discuss the IEEE 802 family of protocols. We focus on the 802.11 protocols which will

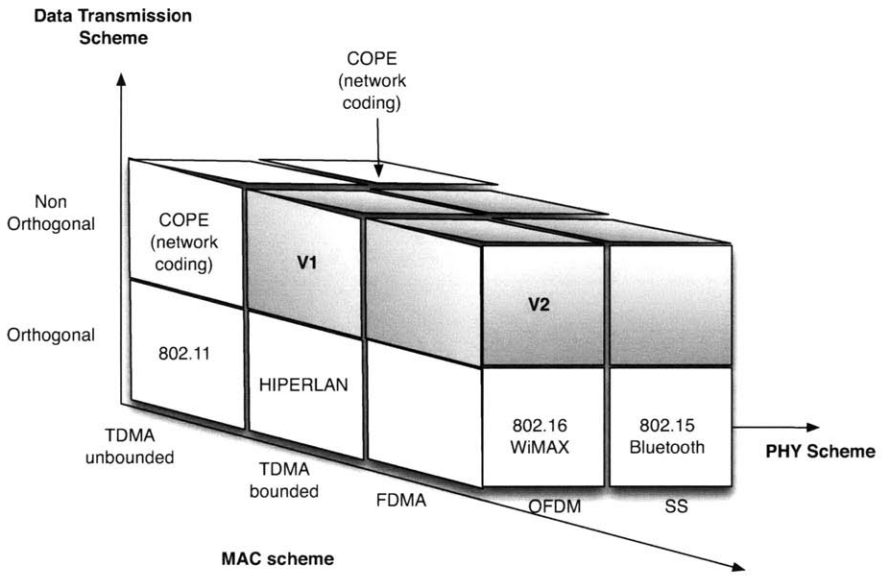

Figure 3-1: Taxonomy of Ad Hoc Wireless Networking Protocols

be a key basis for comparison with our work. We also discuss the 802.15 protocols (MESH networking). We then discuss the protocols in the non-orthogonal data-transmissions space including Network Coding and other work that makes use of Zero-Forcing beamformers.

3.2 MAC Layer Protocols in the Literature

Research in ad hoc network protocols can be partitioned into two sets based on their access scheme: random access schemes, and time scheduled/reservation schemes. Random access schemes began with ALOHA schemes, where nodes transmit at random times, and yields a maximum throughput of 0.18 and 0.36 in the slotted case relative to the maximum utilization of 1 [4]. To reduced the number of collisions, Carrier Sense Multiple Access with Collision Avoidance (CSMA/CA) was developed, where nodes sense the medium and transmit with some probability derived from its collision avoidance scheme only if no other

transmission in sensed. But as the Hidden and Exposed Terminal Problems developed[1], the MACA schemes and its multiple variants with the RTS-CTS schemes were developed to reduced the likelihood of these events. Other schemes like Floor Acquisition Multiple Access schemes (FAMA), and the Busy Tone Multiple Access (BTMA) schemes (described below) were also designed to combat the Hidden and Exposed Terminal problems. Time Scheduling/Reservation ideas follow from TDMA scheduling in centralized systems for their strict collision avoidance property. The reservation of slots becomes a distributed problem which, in the Five-Phase Reservation Protocol (FPRP), is approached using a random access scheme. In SEEDEX, the approach is more of a hybrid between a reservation and a contention-based random access scheme in that users have knowledge on when others may transmit, and based on its estimate of other possible users, will transmit in a given slot with a probability that is a function of its estimate. Reservation schemes still must contend with the hidden and exposed terminal problems as they seek maximum throughput and spatial reuse. In the sub-sections that follow, we will outline the features of each of the protocols, and the throughput researchers report either by analytic or experimental methods.

CSMA/CA

Carrier Sense Multiple Access with Collision Avoidance, introduced by Colvin in 1983, is a multiple access scheme in which before transmitting, nodes listen to the wireless medium, and transmit with some probability derived from their collision avoidance scheme only if no other nearby node is transmitting. In CSMA/CA, when a node seeks to transmit, it first senses the medium and transmits only if the no other transmission is sensed on the medium. CSMA/CA is implemented via baseband processing that determines the amount of received energy. Among the most common ways of detecting the transmission of another user are:

[1]The Hidden Terminal Problem describes the event where two nodes out of communication range of each other seek to communicate with a common receiver, resulting in outage at the common receiver and dis-enabling both nodes from establishing communication with the common receiver. The Exposed terminal problem refers to an event where a transmitting node seeks to communicate with another node, but senses the medium to be busy and consequently doesn't transmit, even though it could transmit and not cause outage to the other Tx-Rx pair transmission currently in progress.

- Preamble detection: received signals are correlated with known preambles to determine if a signal is being transmitted.

- Energy Detect: receivers measure received signals, and report the presence of a signal if the received power measurement exceeds that of the noise floor.

The theoretical analysis of CSMA have shown throughput ranging from 0.5 to 0.84 for slotted 1-persistent CSMA and optimum p-persistent CSMA respectively,[2] and throughput versus delay curves which outperform pure and slotted ALOHA [52]. These results are relative to a perfect utilization equal to 1.

Experimental analysis of CSMA/CA have demonstrated that the fundamental weakness of CSMA/CA is that it relies on measurements of the channel made at transmitters to determine the likelihood of collisions at receivers. This is a problem is often consequent of differing environmental conditions at transmitter and receivers caused by exposed terminals [53]. Its also not uncommon for simultaneous transmissions to be received and decodeable, an effect sometimes referred to as the 'capture effect' [54]. Researchers have also note unfairness in CSMA/CA protocols particularly when the Binary exponential back-off algorithm is used for collision avoidance [55].

MACA Family of Protocols

The Multiple Access with Collision Avoidance (MACA) protocol was designed in 1990 to address the hidden and exposed terminal problems inherent to CSMA protocols [56]. It assumes that nodes have comparable transmitter powers and receiver noise levels, and link reciprocity. Hidden Terminal problem describes the situation where two or more nodes out of detectable range from each other simultaneously attempt to communicate with a node

[2] p-persistent CSMA schemes transmit after an idle slot with probability p. 1-persistent CSMA is p-persistent CSMA with $p = 1$.

within the communication range of all of them, causing a collision at the receiver. The Exposed Terminal problem describes the situation where a node is within the range of a transmitting node, and thus does not try to transmit. There are nodes with which it can transmit that would not cause excessive interference at the already transmitting node. Both of these problems, if left unaccounted for, lead to a decrease in the throughput of the network. It functions by the well known Request-to-Send (RTS) Clear-to-Send (CTS) dialogue between nodes that would like to reserve the medium in order to communicate. When the sender X wants to transmit to a receiver Y, it first sends an RTS packet to Y. Included in that RTS packet is the amount of data it plans to send. If Y responds with a CTS package within a specified time window, sender X will then send its packet(s) to receiver Y. All users must refrain from transmitting for a given time window after an RTS message has been sent. Echoed in the CTS packet is the amount of data X intends to send. If X does not receive a CTS packet within a specified time window, then sender X will wait for a time τ before retransmitting the RTS. Other users that overhear a CTS message are required to refrain from transmitting for a duration that is a function of the amount of data X intends to send. Thus, users must decode the CTS message in order to estimate the wait time. When collisions occur, nodes use a randomized binary exponential back-off algorithm to determine the time at which they will next transmit, in which the back-off is doubled after a collision and reduced to its minimum value after a successful RTS-CTS dialogue.

Bharghavan, et al. [57] modified MACA to include a data sending (DS) packet following the CTS packet, and ACK packet following the transmission of the data packets from sender X to receiver Y, and added a universal back-off timer to the system in order to address fairness concerns with the RTS-CTS dialogue and the back-off algorithm. MACAs backoff algorithm allowed users that had not had RTS collisions in a given contention period an advantage in the next contention period as their back-off windows were still set to their minimum values. Only the node that eventually won the contention period, as well as those who had not had any collisions would begin the next contention period with minimum back-off times.

MACAW modifies the back-off algorithm so that after any successful transmission, all nodes reset their back-off time to the minimum. This is called a universal back-off timer, and is implemented with a packet field that has the current value of the back-off timer. When a node has control of the medium, all users will decode that packet field, and use the specified value as the seed for their own back-off algorithms. To the RTS-CTS exchange, MACAW adds an ACK packet. This allows a retransmission procedure to commence without an additional contention period as MACA would require. It also marks the beginning of a contention period, without relying on other users to estimate the start time from RTS packet fields. To alleviate interference at the transmitter, MACAW adds a DS packet so that terminals within range of a sender, but out of range of the corresponding receiver refrain from transmission though they have not heard the CTS message from the receiver Y.

MACA-BI is another variant of MACA that aims to reduce the overhead time for the sending and receiving control packets [58]. Talucci and Gerla design a receiver driven single control packet protocol, where a receiver sends Ready to Receive (RTR) packet to a specific transmitter, and then the corresponding transmitter sends a data packet. Included in each data packet is information about the backlog in the transmitter, from which the receiver can estimate the average rate of packets and the future backlog. In this scheme, each data packet is effectively ACKd with the RTR packet. Other users refrain from transmitting when they hear an RTR message. By decoding the estimate of future packets echoed in the RTR messages, other users can estimate the next contention period, which is when they can gain control of the medium. While there can be no DATA packet collisions in this protocol, both the exposed and hidden terminal problems persist. While the efficiency of this protocol depends on the ability to predict when neighbors have packets to transmit, no algorithm for this procedure is given.

FAMA

The Floor Acquisition family of protocols [59, 60] pre-date the MACA protocols, but have very similar specification. The goal in FAMA is to acquire the floor, which is to acquire control of the medium. This achieved in this protocol by a dialogue which is equivalent to the RTS-CTS exchange. Where the family of protocols differ is in the use of CSMA/CA. FAMA protocols require the use CSMA/CA in order to prevent RTS and CTS collisions with data packets. The authors contend that this protocol solves the hidden terminal problem by making the duration of a CTS packet long enough to jam any hidden sender that did not hear the RTS being acknowledged. This protocol is designed specifically for transmissions where the duration of data packets is much greater than that of the RTS-CTS exchange.

BTMA

Busy tone Multiple Access schemes began in 1975 with the work of Kleinrock in centralized networks. The basic idea of the scheme is to have divide system bandwidth into two channels one of small bandwidth for control signals, and one of large bandwidth for data. The two most recent designs building on this work are Receiver Initiated Busy Tone Multiple Access (RI-BTMA) and Dual Busy Tone Multiple Access (DBTMA) , both described below.

In Receiver-Initiated BTMA (RI-BTMA), the channel is divided into a data channel and control channel, where the control channel is used to send busy tones and is subsequently also called the tone channel. Sessions are initiated with RTS packets sent on the data-channel. CTS packets are replaced with a receiver-busy tone that acknowledges both receipt and a positive response to an RTS packet, but it also is used to prevent other nodes from transmitting. Nodes can only send an RTS packet when the control channel is idle, and can only transmit data on the data channel when it has been acknowledged by a busy tone by the corresponding receiver.

The Dual Busy Tone Multiple Access protocol [61] is designed to address the hidden termi-

nal/exposed terminal problem. The protocol architecture defines two out of band control channels on which they broadcast receive-busy tones, and transmit -busy tones. The Btr is broadcast by the node that would like to transmit to a given receiver and is currently sending a RTS packet to that given receiver. If the receiver is able to receive the transmission, it responds by broadcasting a Btr signal. All users only initiate a transmission if there are currently no BT broadcasts on either of the side channels. Since the receiver maintains the broadcast of the Btr signal, terminals near those receivers know not to transmit (alleviating the hidden terminal problem). Similarly, nodes that cannot sense the Btr transmssion are out of range of the receiver, and thus can transmit (alleviating the exposed terminal problem). Simulations of the protocol with 200 bit control packets, and 4096 bit data packets in networks with 30 contiguous nodes, with busy tones bandwidth .1 10kHz in a 100MHz channel, gave a performance gain of 140% over FAMA and MACA protocols, and 20% over RI-BTMA.

Reservation-Based Schemes

Reservation-based schemes assume some degree of synchrony among network nodes, and typically assign some time slot to a specific user. In this assumption, they can attain much higher throughputs than contention-based schemes, but a method for attaining this level of synchrony and for assigning slots has not been reported.

TSMA

The Time-Spread Multiple Access (TSMA) protocol assigns[62] each node a unique code that deterministically specifies in which time slots the node is assigned to transmit. All nodes have a code of equal weight. Codes are binary and have N entries that correspond to a time slot within a period. A code bit 0 corresponds to idle, and 1 corresponds to transmit. In each time slot, nodes with bit 1 transmit, and nodes with bit 0 are idle. Collisions occur in a particular slot if (1) the intended recipient of a nodes transmission also has a bit 1 in

that slot; or (2) if nodes near a given recipient have a bit 1 and the transmissions interfere and prevent reliable decoding.

ADAPT

A Dynamically Adaptive Protocol for Transmission (ADAPT) MAC protocol [62] combines a synchronous TDMA reservation scheme with a CSMA/CA contention-based scheme. In ADAPT, each time slot within a frame is assigned to a particular user. Within each time slot is a short duration sensing period in which all nodes that would like an additional slot sense to determine whether or not the node assigned to that slot is using the assigned slot. If the assigned node does not transmit within this sensing period, other nodes can contend for this slot using the RTS-CTS dialogue. At low loads, this protocol performs similarly to a contention protocol. At high loads, it performs like a TDMA reservation scheme.

SEEDEX

The SEEDEX Protocol developed by Kumar and Rozovsky [63] is an 802.11 MAC collision avoidance protocol based on the idea of broadcasting nodes schedules. Schedules are binary sequences where a 1 corresponds to a slot in which the node might transmit, and a 0 corresponds to a slot in which the node will listen. Sequences are generated using a pseudo-random number generator, where each node has its own seed. Nodes broadcast the state of their pseudo-random number generator, and that of their neighbors. When a node T1 wants to transmit to node R1, T1 should be in the possibly transmit state and R1 in the listening state. R1 should then check the transmission schedules of the other nodes in its area that want to transmit. Where n is the number of nodes that want to transmit in a particular slot, the probability of exactly one transmission in that slot is maximized when each node transmits with probability $1/(n+1)$. As some of the n other nodes may not have a packet to transmit, this probability is scaled by a, where $a = 1.5$ was found experimentally

to result in the highest throughput.

The throughput and mean-delay are compared to 802.11 using the ns2 simulator. [63] results a 10% average increase in throughput over 802.11, and a 40% average decrease in mean delay, and the mean jitter is reduced by a factor of 5.

Cooperative Diversity Protocols

Laneman at al [64] develop several protocol strategies that aim to exploit spatial diversity using a collection of nodes and their antennas to work together as a virtual antenna array to relay messages to neighboring nodes. They develop a protocol strategy called amplify-and-forward in which the relay nodes amplifies the signal that it receives, and then forwards that message to its intended recipient. They also develop a protocol strategy called decode-and-forward in which the relay nodes decodes, then re-encodes, and then forwards the message to its intended recipient. They develop an adaptive protocol called selection relaying in which nodes employ a threshold test to determine the channel quality, and then choose the strategy with the best performance. They also develop another adaptive protocol called incremental relaying in which nodes have limited feedback from the intended recipient, such as a single bit indicating the success or failure of the message transmitted directly to the intended recipient, and retransmit only if a negative acknowledgment packet is received. Each of the schemes uses either orthogonal direct transmission or an orthogonal cooperative diversity scheme using TDMA. They show that, with the exception of the fixed decode and forward scheme, these schemes can achieve the full gains of spatial diversity (reduction in the probability of outage). They also show that at fixed low rates, amplify-and-forward and selection decode-and-forward are at most 1.5 dB from optimal and can has an increased received SNR over transmission without the relay.

SUO SAS

The Small Unit Operations Situation Awareness System (SUO SAS) was a DARPA-funded communications program that provides individual soldiers with situation awareness information including voice, video, and data communications [65, 66]. The SUO SAS network is ad hoc, self-organizing, and designed to be robust, reliable, and to assure connectivity for up to 10,000 nodes. The architecture of the SUO SAS network has three tiers. Tier one is a self-contained multi-hop network called an island. Within each island, a node is elected the island head and serves as the gateway to other tier-1 islands. The second tier consists of 2 or more tier-1 islands connected through their island heads/gateways. The third tier is virtual, and is the connection between nodes within the tier 2 network. The tiered structure is to simplify the process of obtaining link state information, route determination, and packet forwarding [66]. Tier 1 networks are formed and maintained through nodes periodically broadcasting neighborhood discovery messages. When an island is identified, subject to island size limits, and throughput requirements a new node can become a member by registering with island head [65]. At the network and application layers, the SUO SAS network is compatible with Internet protocols.

3.3 Multiple Antenna Protocols

NULLHOC

NULLHOC [6] is a multi-antenna MAC protocol which uses transmitter and receiver beamforming to achieve spatial reuse and energy savings. Beamformers are designed with weight vectors, which steer the antenna beam toward the receiver (or transmitter) for beamforming, and away from neighboring receivers to null with some of the remaining degrees of freedom, where there are available degrees of freedom (at most N-1). The protocol divides the frequency space into two channels: the data channel and the control channel. On the control channel, nodes use CSMA/CA and MACAW signaling to gain access to the Data Channel.

Included in the RTS-CTS and DS messaging are the weights that will be used. Other users learn the weight vectors of other users by listening to the control channel. Also included in RTS-CTS messages are training symbols by which any user can estimate the channel to that transmitting users. Simulation results compare NULLHOC to 802.11 in 100 nodes in 750m x 750m grid show a doubling of throughput over 802.11, but throughput levels off as the number of antennas increase because of the increased control overhead. This protocol also reports substantial energy savings. This protocol differs from the protocol we design here in its control channel mechanisms, and in the processing carried out at the receiver, and in the use of informed transmitters.

SPACE-MAC

SPACE-MAC [7] is a multi-antenna protocol which uses channel information from the antenna arrays at each transmitter and receiver pair to implement transmit and receive antenna beamforming that achieves offers a power gain for the intended receiver, while nulling a subset of local receivers. The main advantage of SPACE-MAC over 802.11 type protocols is that it allows multiple data streams to coexist in the same physical space, and the same frequency space. Instead of having a channel separate from the data channel where CSI is exchanged, all protocol functionality takes place on a single channel. The traditional RTS-CTS packets carry training symbols so that the channel matrix can be estimated. Tx-Rx pairs then compute a weight vector that corresponds to antenna configurations so that it can beamform to the corresponding user. In order to null out a coexisting node, other nodes just need to know the channel matrix between itself and the interfering node, and that interfering users weight vector. Simulations of SPACE-MAC report a 30% increase in throughput as a function of number of antennas over NULL-HOC for simulations of 20 nodes of random topology, all within range of each other.

MIMA-MAC

MIMA-MAC [67] (Mitigating Interference using Multiple Antennas) is a joint physical and MAC layer transceiver design for ad hoc wireless networks. The transceiver uses MIMO technology to allow simultaneous transmissions by performing synchronization and channel estimation techniques to effectively null co-channel interference. The transceiver simulations (ns-2)of this system in the 2.4GHz band use a network with 2 Tx-Rx pairs at a fixed distance apart, and examine the BER for SINRs ranging between 2 and 16 dB, the throughput for each pair, and the relative throughput as a measure of fairness. Simulations show a slight increase in total throughput over 802.11 and that MIMA-MAC allows simultaneous transmissions with ranges of fairness depending on the distance between the node pairs.

3.4 802.11 Family of Protocols

3.4.1 802.11(a), (b), & (g)

The 802.11 protocol, commonly known as Wi-Fi, is an IEEE standard for the physical (PHY) and medium access control (MAC) layers of a wireless local area network (WLAN). In its various versions (summarized below in table 3.1), it aims to provide between 1 and 100 Mbps over a 30 to 60 m radius while operating in 20MHz channels in the UNII or the ISM frequency bands. In this section we begin with a summary of the network architecture. Here we describe the Medium Access Control (MAC) Layer protocol and timing , the Physical Layer (PHY) protocol, and the 802.11 packet structure.

Network Architecture

The basic architecture of the system is as follows. A Mobile Station (STA) is any wireless

Table 3.1: Summary of 802.11 Protocol Versions

Version	Year	New features
802.11	development 1990 −1999	Original
802.11a	1999; products shipped, 2001	Increased data rate over (b);new PHY 5 Ghz (UNII Band)
802.11b	1999	Increased data rate over original
802.11c	2001	Bridge operation procedures;
802.11d	2001	International roaming features
802.11e	2005	QoS support for multimedia; various ACK schemes
802.11g	2003	Increased data rate; backward compatible with (b)
802.11h	2004	Dynamic frequency selection and transmitter power control
802.11i	2004	Security enhancements
802.11n	2008	Higher throughput; multiple antennas

terminal/device/node in the network. The Basic service set (BSS) is composed of two or more STAs. The region over which they communicate is called the Basic Service Area (BSA). A network in which nodes within a BSS communicate directly is called an Independent BSS, and more generally is called an ad hoc network. More typically, 802.11 networks operate as an Infrastructure network where a node called an Access Point (AP) serves as a central node through which STAs communicate. Communication between BSS in an infrastructure network occurs between APs via a set of services called the distribution system (DS). It is also through the DS, through a logical architectural component called a portal, that 802.11 packets can access the wired network. A collection of BSSs and the DS by which they communicate make up an Extended Service Set (ESS) network.

Medium Access Control (MAC) Layer

The 802.11 protocol offers two types of coordination for accessing the medium. The first, and most commonly used type of coordination is a distributed coordination function (DCF) in which all nodes in the network operate according to the same access method. The second type of coordination is a point coordination function (PCF) in which one node coordinates

all access to the medium. The DCF access method is carrier sense multiple access with collision avoidance (CSMA/CA). This access method is used in both IBSS and Infrastructure networks, and is the most commonly used access scheme. In an Infrastructure network, the PCF access method is implemented using a polling protocol. For more information on the PCF, see [68].

Carrier-sense-multiple-access with collision-avoidance (CSMA/CA) works as follows. For a STA to transmit, it must first sense the medium. If the medium is idle for a specified duration, the STA can transmit. If the medium is busy, the STA must defer until the end of the current transmission. Once the current transmission is complete, the STA must select a random backoff interval, uniformly and randomly distributed between its current contention-window-minimum value and its contention-window-maximum value. While the medium remains idle, the backoff interval is decremented. When the end of the backoff interval is reached, the STA can transmit. If another transmission occurs during the backoff interval, the decrementing pauses, and resumes when the medium is again idle. To further minimize the likelihood of a collision, the STA can transmit a RTS and wait for a CTS control packet before transmitting. The duration field of the RTS-CTS hand shake is used by other transmitting nodes to determine the time at which the upcoming packet and ACK packet transmissions will be complete.

In addition to the basic CSMA/CA access method, there is a secondary level of control implemented via timing delays. The time interval between transmissions is called an interframe space (IFS). Different types of packets have different interframe spacing requirements which allows for priority access to the medium. The shortest interframe spacing (SIFS) is used for ACKs, a CTS, the subsequent packets that have resulted when a larger MAC packet is fragmented and transmitted as shorter packets, and management packets in which a STA is responding to a polling request by the PCF. Packet transmissions that require only the SIFS are prioritized packet transmissions. The next shortest IFS is the PIFS, which is used as the interframe space between packets whose transmit order has been scheduled by the PCF. The spacing longer that the SIFS allows for ACKs and packet fragments to be transmitted

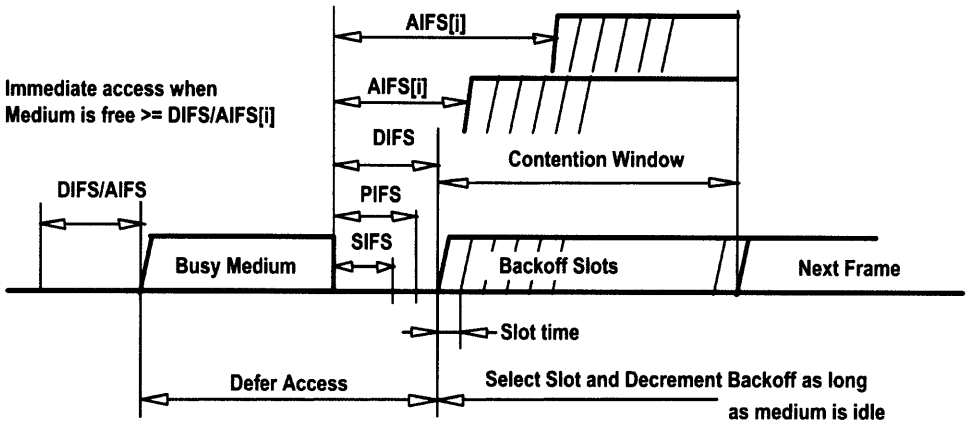

Figure 3-2: 802.11 (a, g) Interframe Spacing

before the next transmitter in a poll. The third shortest IFS is the interframe space used with the DCF. The DIFS is the duration of the idle slot after which deferred nodes can begin a backoff interval, and after which a node that has just arrived to the medium can transmit.

When a packet (data or RTS) transmission is not acknowledged within the SIFS duration with either the ACK or CTS, the transmitting node increments the long-retry-count or short-retry-count respectively. The transmitter then defers retransmission by first incrementing the contention window maximum length, and the choosing a retransmission time within the new larger contention window. The minimum-contention window size is seven slots, and the maximum contention-window-sizes are $\{7, 15, 31, 63, 127, 255, 255\}$. When either the long-retry-count or short-retry-count reaches its maximum value, the current packet is dropped. After the reception of an ACK, the long-retry-count is reset to zero. After the reception of a CTS, the short-retry-count is reset to zero.

Physical Layer (PHY)

Table 3.2 gives the specification for the PHY layer of 802.11 family of protocols:

The 802.11(a), (g), and (n) protocols use an orthogonal frequency divisions multiplexing (OFDM) modulation scheme. In 802.11(a) and (g), the channel of bandwidth of 20 MHz is

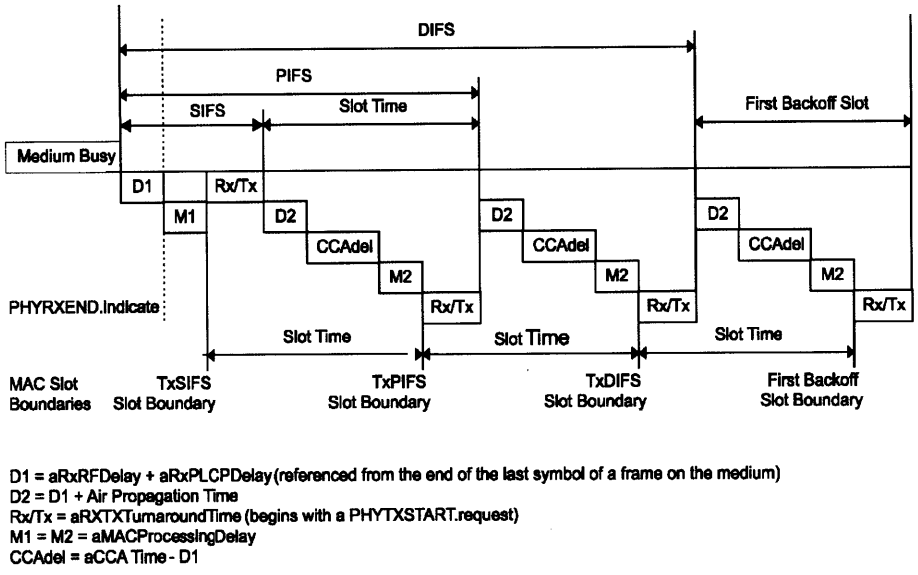

Figure 3-3: 802.11 (a, g)Timing

Table 3.2: 802.11 Physical Layer Description

Protocol	Rates (Mb/s)	Spectrum	Channel width	Multi-Access Scheme
802.11	1 or 2	2402-2480 MHz	1 MHz (79 total)	FH-SS,DS-SS and Infrared
802.11(b)	5.5 or 11	2402 2480 MHz	3 X 22 MHz	DS-SS
802.11(a)	54	5.47 5.725 GHz	12 X 20MHz;	OFDM
802.11(g)	54	2402 2480 MHz	3 X 22 MHz	OFDM
802.11(n)	> 100	5.47-5.725	20, 40 MHz	OFDM, SDM(MIMO)

divided into 52, 312.5kHz tones. In 802.11(a) and (g), 48 of these tones are used for data, 4 tones are used for pilot tones for estimation and synchronization. OFDM symbols are transmitted with symbol duration 3.2 μs, and with an $800ns$ guard time. 802.11(a) and (g) support BPSK, QPSK, 16 QAM and 64 QAM modulation scheme, and convolutional coding rates 1/2, 2/3, and 3/4, yielding data rates: 1, 2, 6, 9, 12, 18, 24, 36, 48 and 54 Mbps.
The physical layer of 802.11 is divided into two functional parts:

1. Physical Medium Dependent (PMD) Sublayer: a system that defines the characteristics and method of transmitting and receiving data through a wireless medium. This

includes the electrical and RT characteristics required to interoperability of implementations of the 802.11 specification. The PMD defines the modulation scheme, the power constraints, the spectral masks, and lists the specific channels in which 802.11 transmissions take place. For the details of these components, see [68], chapter 17.

2. Physical Layer Convergence Protocol (PLCP): defines a method for mapping the PSDU into a framing format suitable for sending and receiving between to STAs. This includes methods for source encoding, interleaving, modulation, de-interleaving, and decoding as well as prepending a header, preamble and check sum to the packet. The output of this sublayer is a PLCP protocol data unit (PPDU).

The PLCP functions include:

1. Prepending the preamble which consist of 10 repetitions of a short training sequence for detection, timing acquisition and coarse frequency acquisition and which contains BPSK symbols sent on the pilot tones; And 2 repetitions of a long training sequence for channel estimation and fine frequency acquisition containing BPSK symbols sent on all tones.
2. Producing the PLCP header
3. Encoding, interleaving the data bits and puncturing the bit stream.
4. Modulating the data bits into data symbols
5. Converting the sequence of data symbols into OFDM symbols
6. Inserting pilot subcarriers
7. prepending the cyclic prefix to each symbol
8. upconverting the complex baseband signal to an RF frequency
9. Carrier sensing is handled by the PLCP through a protocol called Clear Channel Assessment (CCA). CCA is carried out by checking the received signal strength and

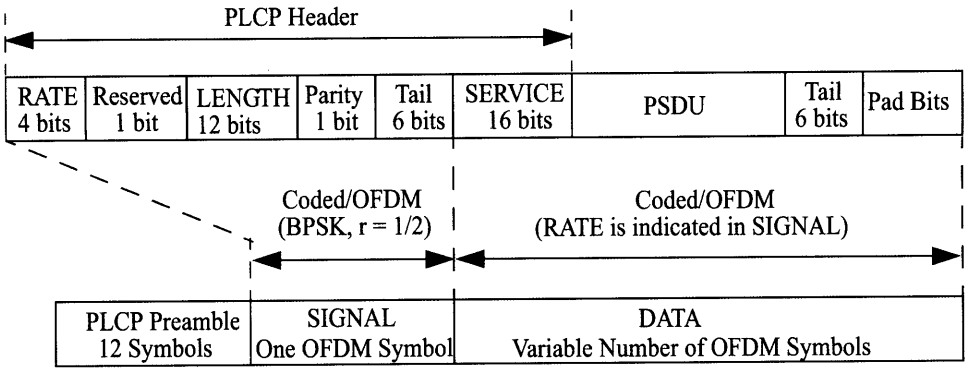

Figure 3-4: 802.11 (a, g) Physical Layer Convergence Protocol Packet

comparing it to a prescribed threshold. In 802.11(a, g, n), the medium is sensed to be busy when the received power is greater than -95 dBm. Protocol specifications assume the noise floor is at -100 dBm.

10. undoing each of the steps below when a packet is received

During transmission, the PSDU is processed (i.e., scrambled and coded) and appended to the PLCP preamble to create the PPDU. At the receiver, the PLCP preamble is processed to aid in demodulation and delivery of the PSDU. For the detailed implementation specifications for each of these functions, see [68], chapter 17.

Packet Types and Structure

There are 3 types of packets transmitted on 802.11 networks:

1. Data Packets: The transmission of data over the network requires a MAC layer header, a PHY header and a preamble for the PHY processing. Each of these three functions are described in more detail below.

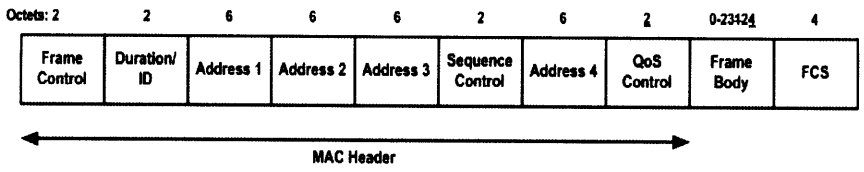

Figure 3-5: 802.11 (a, g) Data Packets

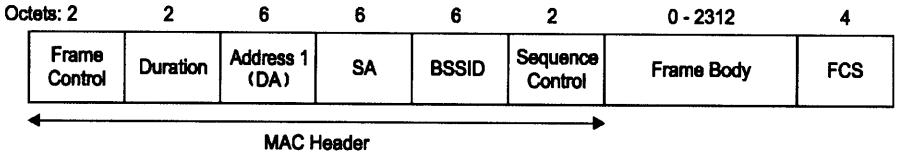

Figure 3-6: 802.11 (a, g) Management Packets

2. Management Packets: In an infrastructure network, these packets facilitate the association, disassociation, and reassociation of a STA with an AP. The authentication procedure is considered a management function, and is managed by packets sent between the STAs and the AP. Lastly, timing functions and packets sent to discover and then join a BSS are classified as management Beacon and Probe packets.

3. Control Packets: There is an optional Request-to-Send (RTS) and Clear-to-send (CTS) hand shake between an transmitting node and a receiving node that have gained control of the medium that is intends to protect the upcoming transmission by providing packet duration information so that other nodes in the area will not transmit. Acknowledgment packets (ACK) are transmitted from the receiving node to the transmitting node to verify that the packet was received. If an ACK is not received, the transmitter will attempt to retransmit the packet

Analysis of 802.11 in the Literature

Analytical and simulation-based analysis of 802.11 protocols have shown that 802.11 protocols are tremendously inefficient in terms of throughput and delay. That inefficiency

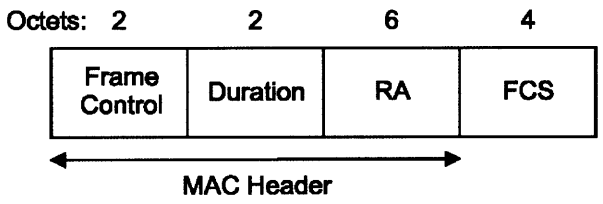

Figure 3-7: 802.11 (a, g) Acknowledgement Packets

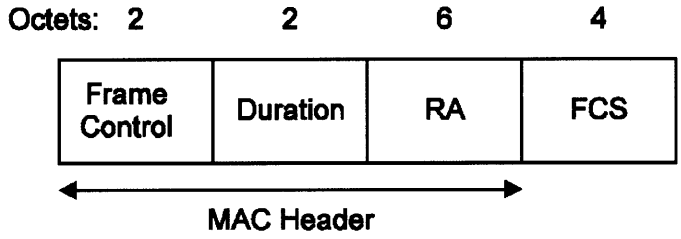

Figure 3-8: 802.11 (a, g) Clear-to-Send Packets

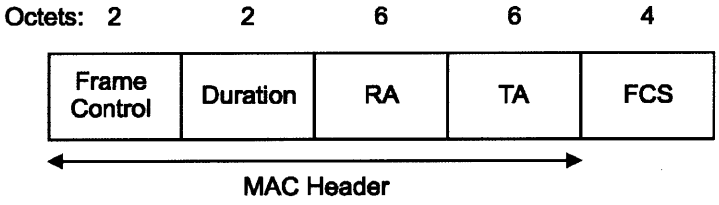

Figure 3-9: 802.11 (a, g) Request-to-Send Packets

is caused primarily by the back-off procedure during contention periods, the inter-frame spacings required by the MAC, packet overhead (headers), and the requirement for an acknowledgment packet after each packet is received [69, 70, 71, 72]. Xiao et al. demonstrated that even in the best of channel and network conditions, the throughput of 802.11 networks was fundamentally bounded, and the delay is lower-bounded by MAC overhead, and yielded bandwidth efficiencies $< 60\%$ [73, 69, 71]. Via the dependence on the contention window, the throughput of 802.11 networks is highly dependent on the number of nodes in the network. Bianchi [70] and Chatzimisios et al. [72] have developed a Markov based analytical model of the protocol and network where each node in the network always has a queued packet (saturated), and show that 802.11 throughput efficiency drops steeply with the number of nodes in the network, and delay increases with the number of nodes in the network. Bianchi et al. has showed by simulation that this dependence on the number of mobile stations can be controlled by an adaptive-contention-window mechanism that dynamically selects the optimal backoff window according to the estimated of the number of contending stations [74].

Experimental studies of the 802.11 protocols have demonstrated that MAC inefficiency is also a a function of interference [75]. There are many causes of interference to 802.11 networks. Since 802.11 operates in unlicensed frequency bands[3], there are many interference sources including Bluetooth devices, microwave ovens, cordless phones, etc., many of which do not operate according to the CSMA/CA protocol used in 802.11 networks, resulting in degraded performance at receivers, an increase in the number of packet errors, and ultimately, a reduction in the network throughput and increased latency and jitter. Mitigating this interference required changing channels, increasing Tx power, or transmitting at a lower rate to decrease the error rate, or trying to identify the interfering device and reducing its transmit power. Many of these proposed interference mitigation techniques introduce techniques to orthogonalize communications, which further reduce system throughput.

[3]802.11(b) operates in the 3-channel 2.4 GHz Industrial Scientific and Medical (ISM) Band. 802.11(a) operates in the 8-channel 5GHz Unlicensed National Information Infrastructure (U-NII) band

3.4.2 802.11-2007

In 2007, the IEEE standards body released a version of the 802.11 standard that combines the original 802.11(a) standard, the 801.22(b) standard and amendments to the standard introduced in versions (g), (d), (e), (h), (i), (j). Versions (d), (h), (i), and (j) include provisions for country specific regulations, transmit power regulations to limit interference with satellites and radar in the 5GHz band, and security provisions. 802.11(e) contains provisions relevant to our implementation and we discuss the amendment below.

802.11(e)

The 802.11(e) amendment was approved in 2005, and introduces provisions for Quality of Service QoS control into 802.11. The amendment defines a new mobile station type called a Quality-of-Service (QoS STA) that implement a set of functions that facilitate the exchange of QoS requirements, including frame formats, frame exchange rules, and the coordination function. There are 2 standard mechanisms for QoS support in 802.11(n). The first is the Enhanced Distribution Channel Access (EDCA) mode allows for a priority access scheme by varying the duration of interframe spacing, allowing nodes to send multiple packets with block acknowledgments, and varying the duration of the contention window when collisions occur. And the second is the Hybrid Coordination Function (HCF) which allows nodes to reserve the medium for high throughput transmissions or longer duration transmissions.
The hybrid coordinator (HC) is co-located with the access-point (AP), and provides for contention-free (scheduled) transmissions. Using the HCF, a non-access point (non-AP) STA, based on its quality-of-service requirements, is able to send a request to the hybrid coordinator (HC) for a transmit opportunity (TXOP) for both for its own transmissions as well as for transmissions from the AP to itself. The HC either accepts or rejects the request based on an admission control policy. If the request is accepted, the HC schedules TXOPs for both the AP and the non-AP STA. For transmissions from the non-AP STA, the HC polls the non-AP STA based on the parameters supplied by the non-AP STA at the time of its request. For transmissions to the non-AP STA, the AP directly obtains TXOPs from the collocated

HC and delivers the queued frames to the non-AP STA, again based on the parameters supplied by the non-AP STA. The HCF uses both contention based channel access methods, and control channel access methods. The former are called enhanced distributed channel access (EDCA), and the latter is called HCF controlled channel access. In EDCA, the HCF implements both a user priority mechanism that categorizes users by the level of quality of service they require (ranked 0 through 7, with the highest priority being voice, followed by video, and lowest being best effort), and corresponding to the way the protocol handles its transmissions; and an access category that relates to the duration and frequency of packet transmissions (background, best effort, video, voice). Associated with each user priority is a set of parameter values that control the duration of idle slots, the size of contention windows, the length of block ACKs and the number of packets that can be sent without returning to the medium for contention. The QoS AP announces the EDCA parameters in selected Beacon frames and in all Probe Response and (Re)Association Response frames by the inclusion of the EDCA Parameter Set information element.

The HCCA operates similarly to the PCF, typically issuing a QoS poll to associated non-AP STAs.

Block Acknowledgements (ACKs)

The Block ACK mechanism improves channel efficiency by aggregating several acknowledgments into one frame. There are two types of Block ACK mechanisms: immediate and delayed. Immediate Block ACK is suitable for high-bandwidth, low-latency traffic while the delayed Block ACK is suitable for applications that tolerate moderate latency. The Block ACK mechanism is initialized by an exchange of Add-Block-ACKs request response (ADDBA Request/Response) frames. After initialization, blocks of QoS data frames can be transmitted from the originator to the recipient. A block may be started within a polled TXOP or by winning EDCA contention. The number of frames in the block is limited, and the amount of state that is to be kept by the recipient is bounded. The MPDUs within the block of frames are acknowledged by a Block ACK control frame, which is requested by a Block ACK Request (BlockAckReq) control frame.

3.4.3 802.11(n)

This the latest version of the 802.11 protocol was released in April of 2008 [9]. It boasts data rates greater than 100Mbps, a max rate of 600 Mbps (four spatial streams with 40MHz channels), and 50 meters of indoor coverage. The MIMO technology extensions allow the use of up to 4 transmit and receive antennas used either for receiver beamforming for diversity and to increase the receive range; and / or for multiplexing to increase the data rate by sending multiple transmit streams. 802.11(n) extends (a) and (g) with MIMO technology to increase data rates with enhancements to the MAC to increase efficiency, and optional extensions of the PHY layer that include increasing the total bandwidth to 40MHz, a shorter cyclic prefix, and more robust source coding techniques including spatial multiplexing, space-time block coding, and low-density parity check (LDPC) encoding. For a short summary of 802.11(n) PHY enhancements, see [76].

Additions to the 802.11(n) Network Architecture

The 802.11(n) protocol defines a high throughput station (HT STA) and a high-throughput access point (HT AP) that modifies aspects of the MAC and PHY to allow for data rates up to 600 Mbps. HT STAs are an extension to the Quality-of-Service stations (QoS STA) that is also capable of MIMO transmissions.

802.11(n) Medium Access Control (MAC)

Key modifications to the MAC for use with the HCF and for increasing throughput include:

1. MIMO operations (MIMO)
2. Spatial Multiplexing (SM)
3. Antenna Selection (ASEL)

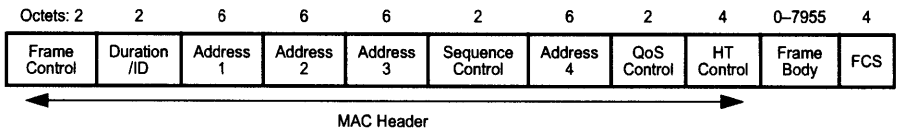

Figure 3-10: 802.11 (n) Data Packets

The procedures for initiating a high-throughput packet transmission involves the exchange of sounding packets and acknowledgements that can occur either just before the packet is transmitted, or within the maximum delay that is set for each method. For the precise procedures, see [77]. In chapter 7, we will discuss the details of the MIMO operations which serve as our benchmark.

These changes in capabilities are represented in the MAC packet header and PLCP protocol data unit (PPDU) formats, and several PHY parameters that we describe below.

The MAC header in 802.11(n) is modified in the following 3 ways:

1. The maximum size of the MSDU moves from 2304 octets to the maximum A-MSDU size 3839 or 7935 octets, depending on the STA's capability, plus any overhead from security encapsulation. Data packets in 802.11(n) can contain several MSDU fragments that are joined together into one packet whose total payload is at most 7955 octets.

2. The QoS control field, which contains information on the ACK policy

3. and the HT Control field contains information on the current transmit strategy: the modulation and coding scheme, if calibration has occurred and a calibration sequence, if antenna selection is being used and the number of additional sounding PPDUs that are required.

Management frames used for association with an access point expand to contain fields regarding HT Capabilities of the STAs and the APs that will be used in later packet trans-

missions and information on the size of the channel. The HT information exchanged included:

1. MIMO control: how channel state information or transmit beamforming feedback information will be exchanged (compressed/non-compressed; implicit vs explicit)
2. The size of the channel matrix and the coefficients
3. The CSI report which contains channel coefficients, and the SNR on each channel
4. ASEL: the index of the transmit antenna preferred by the receiver
5. Supported modulation and coding schemes and cyclic prefix duration

The 802.11(n) MAC adds two additional interframe space (IFS) durations. The first is called the reduced interframe space (RIFS). The RIFS can be used to separate multiple transmissions from a single transmitter to a single receiver when know SIFS-separated response transmission is expected. The SIFS is still required before an ACK and a CTS. The second is called the arbitration IFS (AIFS) and is used only by the QoS facility. It is longer than the DIFS and is used by the QoS STA to transmit all data frames, management frames, and RTS, CTS and Block ACKs. When the wireless medium is won during an EDCA contention (after an AIFS), the transmission that results is called a transmit opportunity (TXOP).

802.11(n) Physical Layer (PHY)

In 802.11(a,g) only 48 tones are used for data and 4 for pilot signals, but in 802.11(n) 52 tones are used for data, and 4 for pilot tones, increasing the total bandwidth used for data from 15 MHz to 16.25 MHz (the remaining portion of the 20MHz is used for training and guard bands between 802.11 channels). The optional PHY extensions include optional short guard interval of 400 ns for indoor transmissions where the delay spread is shorter. 802.11(n) also includes provisions to use 40 MHz channels (104 tones). Additional coding options include a 5/6 convolutional code rate, low density parity check (LDPC) error correction coding which

require lower SNRs than the equivalent convolutional coding rate, and Space Time Block Coding for robustness, and transmission of multiple transmit streams.

The essential structure of the physical layer is unchanged in the high-throughput enhancement. The packet preambles are modified to facilitate more channel estimation for the use of multiple transmit antennas, and the packet header is modified to include parameters required for MIMO, spatial multiplexing, antenna selection and the HT modulation and coding schemes (additional convolutional code rates, LDPC codes). An illustration of the packet headers is given in figure 3-11. 802.11 accommodates three types of packet headers so that nodes incapable of the 802.11(n) throughput can co-exist with nodes sending 802.11(n) packets. Only in networks with all 802.11(n) STAs are HT-greenfield preambles used. For details on the legacy and high-throughput Short-training-fields (L-STF, HT-STF) and the legacy and high-throughput long-training-fields (HT-LTF, L-LTF), see [77].

The HT-STF is used to facilitate AGC. The composition of HT-STF is composed of one OFDM symbol in which 12 (equally spaced) of 52 tones contain QPSK symbols.
The HT-GF-STF includes the transmission of multiple BPSK streams one each tone, and has a period of $.8\mu s$, and includes 10 periods to make up the HT-GF-STF (p285). The mapping matrix is given by:

$$P = \begin{bmatrix} 1 & -1 & 1 & 1 \\ 1 & 1 & -1 & 1 \\ 1 & 1 & 1 & -1 \\ -1 & 1 & 1 & 1 \end{bmatrix} \tag{3.1}$$

Steering matrix $\mathbf{Q}$ is multiplied by P, where steering matrix $\mathbf{Q}$ accounts for the number of transmit chains and space-time streams for a given Tx-Rx pair ($\mathbf{Q}$ is size $N_{TX} \times N_{STS}$). When there are independent streams on each transmit chain, then $\mathbf{Q} = \mathbf{I}$. When the transmitter and receiver are beamforming, $\mathbf{Q}$ is composed of the preprocessing required for spatial multiplexing.

The HT-LTF provides a means for the receiver to estimate the MIMO channel between the set of QAM mapper outputs (or, if STBC is applied, the STBC encoder outputs) and the receive chains. If the transmitter is providing training for exactly the space-time streams (spatial mapper inputs) used for the transmission of the PSDU, the number of training symbols, N_{LTF}, is equal to the number of space-time streams, N_{STS}, except that for three space-time streams, four training symbols are required. The HT-LTF portion has one or two parts. The first part consists of one, two, or four HT-LTFs that are necessary for demodulation of the HT-Data portion of the PPDU. These HT-LTFs are referred to as HT-DLTFs. The optional second part consists of zero, one, two, or four HT-LTFs that may be used to sound extra spatial dimensions of the MIMO channel that are not utilized by the HT-Data portion of the PPDU. These HT-LTFs are referred to as HT-ELTFs, and are used primarily in sounding packets. HT-LTFs are of duration 4 μs, and use the same matrix P in equation (3.1), and the steering matrix Q corresponding to N_{STS} and N_{TX}.

The packet duration:

$$TXTIME = T_{GF-PREAMBLE} + T_{HT-SIG} + T_{SYM} \cdot N_{SYM} \tag{3.2}$$

where:

$$T_{HT-GF-STF} + T_{HT-LTF1} + (N_{LTF} - 1)T_{HT-LTFs} \tag{3.3}$$

and where:

$$N_{SYM} = m_{STBC} \times \text{ceil}\left(\frac{8 \cdot LENGTH + 16 + 6}{m_{STBC} \cdot N_{DBPS}}\right) \tag{3.4}$$

The PHY supports the beamforming, spatial multiplexing and antenna selection in MIMO environments during a TXOP. To attain the channel state information required for these techniques, 802.11(n) offers the following techniques:

1. Implicit feedback beamforming: When STA A is beamforming to STA B, STA A and

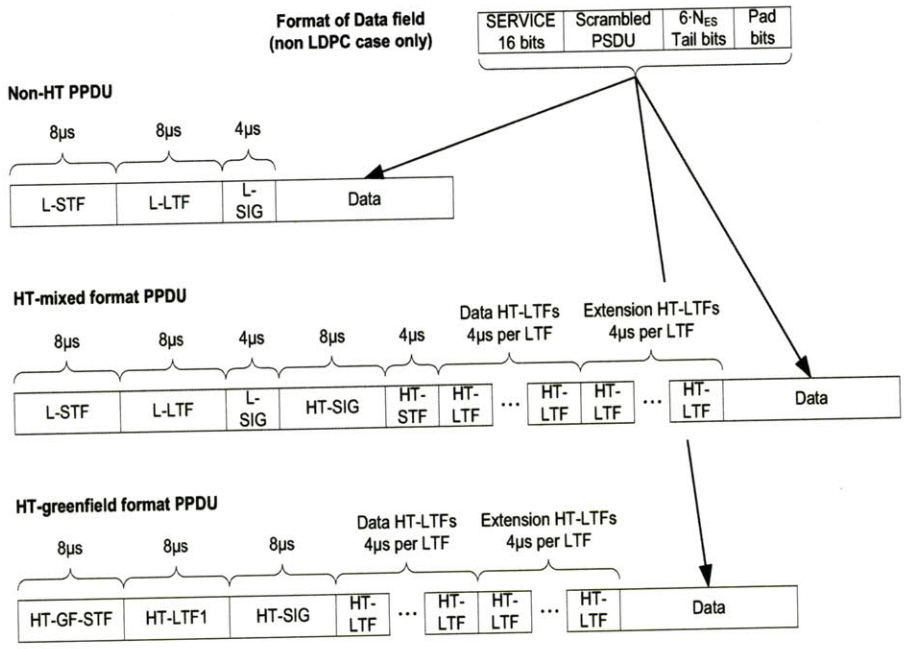

Figure 3-11: 802.11 (n) Preambles Packets

STA B must be pre-calibrated. STA A requests for STA B to transmit the known preamble which STA uses to estimate the channel. STA A can then choose modulation and coding scheme parameters that can be supported by the channel. STA A can then send a packet to the STA B. The modulation and coding scheme are included in the header. Additional training that may be required follows the high throughput header. For details of the callibration procedure, see [77]

2. Explicit feedback beamforming: When STA A intends to beamform to STA B, STA sends a sounding packet to STA B. STA B measures the channel, and sends STA A either the beamforming vector(s), or the channel matrix. The real and imaginary parts of each element in the matrix are quantized to N_b bits with twos complement encoding, where N_b is defined in the protocol.

Table 3.3: 802.11(n) Timing Parameters

Parameter	Value
Total Transmit Bandwidth	16.6MHz or 33.2 MHz
Subcarrier Spacing	312.5kHz Δ_F
Number Transmit Tones	48 or 104
Number of Pilot Tones	4 or 6
Slot Time	$9\mu s$
RIFS	2 μs
SIFS	16 μs
IDFT/DFT Period	3.2 μs
Long Guard Interval	0.8 μs
Short Guard Interval	0.4 μs
Preamble	16 μs
LTF	8 μs
STF	4 μs
PLCP Header	8 μs
Max Packet Duration	10 ms
CWmin	15
CWmax	1023

3.4.4 802.11(s)

IEEE 802.11(s) is the 802.11 draft amendment[4] to enable wireless devices operating according to an 802.11(a), (b) or (n) protocol to interconnect, creating a mesh network. 802.11 networks are primarily used in infrastructure mode, where Access Points (AP) govern the WLAN as part of an ESS, and act as the gateway to other networks (i.e. the Internet). The mesh networking standard allows nodes to cooperate in forwarding each other's unicast, multicast or broadcast packets over self-configuring multi-hop paths between AP and/ or STA devices. This decrease the required density of AP's connected to a wired infrastructure, effectively creating a more inexpensive and more robust wireless back haul, and enables nodes over a broader area to share more cost-effective access to the Internet.

[4]The most recent draft of the standard was released in January 2006, and the task force is scheduled to meet July 2008. The standard is scheduled for completion in August 2009

A Mesh Point (MP) is a device that supports the forwarding of frames within the mesh network, and mesh network in 802.11(s) is defined as a network comprised of two or more Mesh Points (MPs). The mesh network has a mesh establishment mechanism akin to the mechanism by which an STA associates with an AP in which association request and responses messages are exchanged. The forwarding capabilities of MPs operate according to the same Enhanced Distributed channel Access (EDCA) specification of 802.11(a, b, n). To facilitate its relay function, MPs passively listen for beacon frames that other MPs uses to associate with a mesh network; and actively transmit probe request frames seeking other MPs. Once a mesh link (ML) is established, the MPs calculates the airtime cost. The airtime cost is stored in a table relating neighboring nodes and the time cost of a path, and is later used in typology learning and dynamic path selection algorithms. When a packet requiring a relay is received, the MP decrements the packet's time-to-live field by the airtime cost for the packet's destination node and adds the airtime cost to the current path method field contained in the packet.

Like its predecessors, 802.11(s) suffers from the exposed terminal problem which leads to reductions in throughput when nodes sense the transmissions of a neighboring Tx-Rx pair and choose to not transmit although they could have transmitted to another node without causing excessive interference to the neighboring Tx-Rx pair. Several have noted [78, 79, 80] that this problem is more acute in 802.11(s) where the density of MPs is increased over traditional 802.11 networks not using mesh. This reduction in throughput is further exacerbated by the priority mechanisms of the EDCA, which increases the duration of interframe spacings as well as by network congestion caused by the transmission of MP probe requests.

3.5 Multiple-Beam Adaptive Arrays

In [81, 82] Ward et al develop a protocol called Multiple Beam Adaptive Array (MBAA) which presents a method for successfully receiving and decoding multiple packets that are transmitted in a slotted-ALOHA (S-ALOHA) random access channel with a separate channel for acknowledgment packets. The physical layer architecture of the protocol is described as

follows:

1. Narrow frequency bandwidth (relative to CDMA bandwidths)
2. Separate channel for acknowledgment packets
3. Slot width is the duration of one packet plus an uncertainty interval T_u over which packet transmission times are randomized so that each packet arrives at a slightly different time.

In [82], three periods of a known pseudo-noise sequence is used as a preamble. To acquire decoding weights, a matched filter is constructed using one period of the known preamble. The second and third period of the pseudo-noise sequence in the received signal is used to create the sample interference covariance matrix. This same process is performed with multiple pseudo-random sequences in order to detect and decode multiple transmitted packets.

Ward categorizes the performance of the system in terms of two main parameters: (1) the number of antenna degrees of freedom (N-1); and (2) the resolution capability of the adaptive array, which depends primarily on the array aperture size and less so on the element patterns and the number of elements. The resolution width θ_r is defined as the minimum angular separation between a desired and interfering packet at which the array can maintain an output SINR as large as the output SNR for a packet received by an omni-directional antenna. In Monte-Carlo simulations, Ward et al. model systems with M transmitting nodes, N antennas, where r is the period of the pseudo-noise preamble, T_b is the bit duration, and where the uncertainty interval $T_u = (r-1)T_b$. They assume that packet arrival angles are random variables independent of the arrival times and uniformly distributed between angles $[0, 2\pi]$ about the receiver. Transmitting nodes transmit a new packet with probability p_n, and when a transmission fails, a packet is retransmitted with probability $p_r > p_n$. No fading or pathloss is contained in the model. When $N = 8$, $M = 50$, $p_r = 0.2$, and $p_n = 0.02$, and angular resolution $\theta_r = 5°$, $r = 63$, Ward reports that the number of packets that are decodable per slot is approximately equal to $N-2$, which is the number of degrees of freedom

available for nulling interferers.

3.6 Protocols with Non-Orthogonal Data Transmission

3.6.1 Network Coding

The theory of Network Coding was introduced in 2000 in a paper by Ahlswede et al.[83], which showed how bottleneck nodes in a network could increase throughput and achieve the broadcast capacity of that network by combining the transmissions from different nodes. There have been many important theoretical results on encoding and decoding algorithms obtained for network coding in lossless (wired) directed networks, and particularly in multicast and broadcast scenarios [84, 85, 86], which show that substantial throughput gains can be achieved by employing network coding under several network topologies. Under less contrived topologies and with undirectional links, some authors have reported that gains in throughput are at most a factor of two [87, 88]. In unicast transmissions, however, results have shown that there is no coding gain [87]. In lossy environments (wireless networks), results have shown that there is both an increased, and capacity approaching, throughput as well as an increased robustness (or energy savings) offered by network coding in multicast transmissions [89, 90].

Network coding has been proposed as a very attractive solutionto the routing problem in ad hoc wireless networks due to the broadcast nature of transmissions and because packets are often forwarded along several hops before reaching its intended recipient [91, 89]. Practical concerns of a non-stationary environment, interactions with other network layers, and the primarily unicast and bursty traffic make the challenges even more substantial. The wireless networking protocol COPE, described below, is designed so that nodes take advantage of network coding opportunities to increase throughput in a mesh network, where unicast transmissions predominate.

COPE

COPE [92, 93] is a forwarding architecture for wireless mesh networks which implements network coding based on an opportunistic coding and forwarding scheme. In [92], COPE is integrated into the current network stack between the MAC and IP layers, sitting ontop of the 802.11(a) MAC and PHY architecture. The opportunistic approach driving the protocol design is that nodes listen to transmissions on the medium, store copies of the packet transmissions and the nodes that receive them. Nodes then seek out opportunities to send multiple packets simultaneously with coding in a manor that the receiving nodes can extract the packet that they need since they also have copies of the other packets in the XOR'd transmission. COPE uses extended and variable length packet headers which include a reception report that informs neighbors which packets it has stored. Nodes that have no data packets to transmit periodically send the reception reports in control packets. COPE headers also include the ID numbers of all the 'native' packets contained in a given packet transmission, since each packet transmission be the XOR of many 'native' packets. Nodes also keep a hash table of packet information which stores the probability that each neighbor has a given packet. The performance of COPE was evaluated in a 20 node test bed, under both the TCP and UDP protocols, and evaluated according to two metrics. The first metric, coding gain, is defined as the ratio of the number of transmissions required by the current non-coding approach to the minimum number of transmissions used by COPE to deliver the same set of packets. The second metric, coding-plus-MAC gain, results from a reduction in the queues at bottlenecks and the reduced number of dropped packets that follows the reduction in congestion that is a consequence of network coding. In Ad-hoc network simulations with a TCP test bed, the authors report a 2 - 3% coding gain. These results are a consequence of a high number of collisions. But when collisions are eliminated by compressing the topology of the testbed, asa congestion increased the throughput increased to offer a 38% increase in throughput over the case when no coding is used. When simulations were run with a

UDP testbed, the authors report that COPE increases the throughput of the testbed by 300 - 400% on average. The throughput results are presented as a function of the offered load. The throughput peaks when demand is approximately 5.6 Mb/s, corresponding to the coding and transmission of ~3 'native' packets.

Analog Network Coding

In [94], Katti et al.introduce an analog network coding protocol that seeks to strategically exploit interference by allowing nodes to transmit simultaneously when the receiver knows the content of the packet that interfered with the packet it seeks to receive. The authors implement a proof of concept experimental test bed which contains 3 - 5 software defined radios under various topologies, and develop synchronization and estimation algorithms required to separate the known signal from the unknown signal intended for the receiver. In the proof of concept work in [94], the MAC is centrally scheduled for the evaluation of the successive interference cancelation functionality. The authors report a 70% average throughput gain over the traditional approach.

3.6.2 Conflict Maps (CMAP)

The CMAP protocol [95] is a link-layer channel access scheme that aims to increase throughput by limiting the susceptibility of networks that use CSMA/CA to the exposed terminal problem. The exposed terminal problem is a side effect of transmitters making transmit decisions without information about the interference environment at neighboring receivers. CSMA assumes channel reciprocity, and limits transmitters from transmitting if their measure of their own interference environment would mandate back-off because the new transmission would cause outage at the already active receivers and would not allow their transmission to be received. As has been widely reported in the literature, this is overly cautious. In the CMAP protocol, nodes initially make the alternate assumption: that their transmission and the transmission in progress would be successful. CMAP then observes the presence

or absence of acknowledgements, and dynamically creates a 'map' of its local environment that captures which nodes can transmit simultaneously. Before a node chooses to transmit, it consults the 'map' to determine whether to transmit or to differ. To address the hidden terminal problem where two nodes out of hearing range of each other both send a packet to a given node simultaneously, CMAP also implements a loss-based backoff mechanism that reduces the packet transmission rate in response to receiver feedback about packet loss. The CMAP protocol was implemented in a 50-node testbed operating the 802.11(a) protocol. The authors demonstrate improvements in throughput between 21% and 47% in access point based topologies, where the medial per-source throughput is 1.8X better than CSMA. CMAP also achieves a 52% improvement in aggregate throughput over CSMA in content dissemination mesh networks.

3.6.3 Frequency-Aware Rate Adaptation (FARA) MAC Protocol

Frequency-Aware Rate Adaption Protocol [96] is a MAC layer protocol that enables transmitter-receiver pairs to exploit frequency diversity by choosing frequency bands that are far from each other in the frequency spectrum, and that have significantly different SNRs, and to assign different bit rates to different frequency bands. A FARA receiver makes measurements of the SNR in each subband, and maps it into an optimal bit rate using characterization tables for the receiver hardware, and periodically reports the optimal bit rate for each subband to the transmitter. They also implement a frequency aware MAC scheme in which once a transmitter acquires control of the medium and has packets for several receivers, it can simultaneously transmit packets to each of these receivers by allocating frequencies to the different receivers in a way that maximizes the overall throughput across these receivers. FARA's rate adaptation mechanisms are facilitated at the receiver. Transmitters initially send at the most conservative data rates. Receivers use the transmitted packets to estimate the SNR in each tone. Feedback on the received SNRs is fed back to the transmitter in sequenced acknowledgment packets which is augmented with a feedback field. The feed-

back is sent with 2-bits per tone, telling the transmitter to implement one of the following three options: (1) maintain the same bit rate, (2) reduce the bit rate, or (3) increase the bit rate to the next highest bit rate supported by the protocol. The feedback is also compressed using run length coding. When the channel coherence is long, FARA is more efficient.

This protocol was implemented using the WiGLAN radio platform and compared to 802.11. The research showed an SNR spread of approximately 20 dB across OFDM tones. They also showed a channel stability for periods of up to 5 seconds. Using the FARA scheme yielded gains of up to 3.1X in their testbed. They showed that 70% of gains are due to the frequency-aware rate adaption, and 30% are due to the frequency-aware MAC.

3.6.4 MIMO MAC

Redi et al [97] present a design and simulation of a MAC scheme for MIMO communications that attempts to take full advantage of the capabilities of MIMO systems, and to account for the required training, feedback and coding delays inherent to high-dimension MIMO schemes. The aim is to achieve hundreds of Mbps links with 8 to 10 antennae at each node. The MAC protocol uses a CSMA/CA access scheme with BLAST transceivers with out RTS/CTS or acknowledgement frames. Instead of acknowledgements, this protocol implements a retransmission module that detects when packet segments appear to require retransmission and initiates the retransmission of these segments. The protocol also implements a link adaptation module where once a receiver receives a message from its target transmitter, it sends a MAC message to notify the transmitter what data rate should be used in future communications. Simulations of this protocol scheme are conducted with 5 nodes, with 5 W transmit power with 10 receive antennas and up to 8 transmit antennas. 80% of packets were received with only 10% of the traffic exceeding 2s end-to-end latency.

Chapter 4

Simultaneous Transmissions in Interference (STI-MAC) Protocols

The key idea behind this work is to develop simple protocols that take advantage of more sophisticated signal processing techniques and multiple antennas in order to allow simultaneous transmissions in interference environments. The aim of the joint PHY-MAC design that makes use of of these signal processing techniques is to ultimately increase network throughput, reduce delay, and that have a side effect of improved fairness across network nodes. In this chapter we discuss the challenges posed for protocols in interference, formulate the design problem, and discuss designs for protocols in interference. In the next chapters we optimize parameters related to these designs, and validate these designs through simulation and analysis.

4.1 Problem Formulation

There are three key problems that must be accounted for when transmitter-receiver pairs communicate in mutually interfering environments. The first problem is to determine at what data rate the communication from transmitter to receiver can occur. This requires estimating the SINR at the receiver. For use of the MMSE receiver, the covariance matrix of

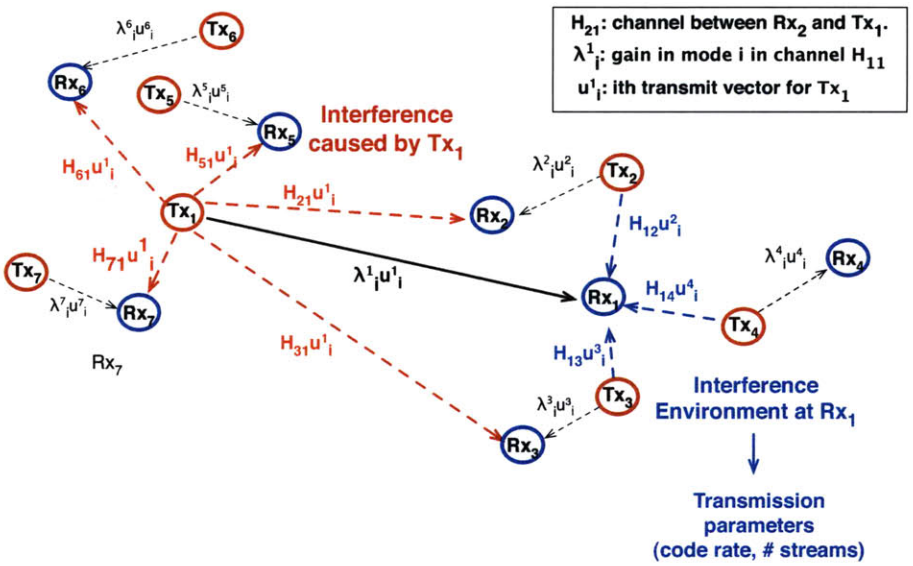

Figure 4-1: Diagram of Problem

the interference environment and an estimate of the target channel is required both for determining the received SINR and for decoding. A procedure for determining the interference covariance matrix is described below. An estimate of the target channel can be obtained at the receiver using the transmission of a known sequence from the transmitter.

The second key problem arises when transmitters intend to beamform to their target receivers. In order for this to take place, the transmitter must have the modes of the channel as observed at the receiver. Due to the effects of transmitter and receiver processing chains, the channel between the transmit signal at baseband at the transmitter and the received signal at baseband at the primary receiver is typically not identical to the channel between the transmit signal at baseband at the primary receiver and the received signal at baseband at the primary transmitter. If the channel has been calibrated to remove the effects of the processing chains, then the channel can be considered reciprocal and channel state information can be obtained by sending training signals from transmitter to receiver and from receiver to transmitter. In the absence of calibration, the transmitter can send training data to the receiver. Then the receiver can send channel measurements back to the transmitter.

The third key problem deals more directly with the protocol mechanisms. It is the problem of initiating a session in interference without causing too much interference at neighboring receivers that are receiving a transmission. The three options for effects at the receiver are (1) the transmission causes no change in the SINR at the neighboring interferer; (2) the transmission causes changes in the SINR that cause the packet to be received in error; or (3) the transmission causes changes in the SINR, but the receiver is able to adapt in real time to interferer and prevent packet errors. In a highly loaded system, while adapting the interference nulling capabilities of decoding weights is possible, as more degrees of freedom are used for nulling, the received SINR would drop. SINR levels would, with large probability, vary to such a degree that modulation and coding schemes for non-trivial data rates could not be maintained. This would cause packet errors in the data packets being actively transmitted, reduce the sum data rate across the network and increase delay caused by the required retransmissions.

To facilitate the distributed control functionality required in an ad hoc network, we propose the use of a broadcast control channel where sessions are initiated, and where nodes can obtain low mean-squared-error frequency offset estimates and target channel estimates. In each of the designs below, a fraction of the degrees of freedom are assigned for control functionality. The details of these procedures are described below.

4.2 Physical Layer Architecture

As discussed in chapter 2, WLANs for high data rate communications typically operate in frequency selective channels that can be characterized by a pathloss exponent and by their delay spread. Following steep improvements in the performance of digital signal processing chips, and aided by the efficiency of the Fast-Fourier Transform algorithm, OFDM provides a simpler means of channel equalization relative to equalization schemes required for schemes that spread the signal energy for a single symbol across a larger frequency band. Conse-

quently, in this work we will use a MC-CDMA scheme.

4.3 Protocol Overview

The STI-MAC protocols are designed to increase sum data rates over known protocol schemes, while aiming to minimize delay. While Information theoretic results on the multiple-access channel in noise-limited environments have guided cellular system design, in the interference-limited regime, there are no known theoretical limits. And though delay caused by the MAC layer protocol is important in our case, we have seen very little work that investigates the parameter and design space in consideration of delay. We take as our starting point a given network, which is the collection of M transmit-receive node pairs, and the radii and the channel parameters between each pair of nodes. To consider the set of achievable rates in a given network in which all nodes have n_t transmit antennas and n_r receive antennas, a computationally intensive means to an answer would search over the sum rates in the $2^{M \min(n_t, n_r)}$ possible combinations of transmitting and receiving node pairs schemes[1]. A few authors have investigated the expected SINR for transmit schemes for multiple antennas in wireless networks [11, 42]. If we consider an infinite network of a given density, and where the average number of transmitters closer to a receiver than its target transmitter is A, Govindasamy [11] showed that the optimal transmit-covariance-rank for a given density of interferers is given by:

$N_t^* \approx \max(1, N_a)$ where

$$N_a = \underset{N_t \in \left\{\text{floor}\left(\frac{N}{3A}\right), \text{ceil}\left(\frac{N}{3A}\right)\right\}}{\text{argmax}} N_t \log_2 \left(1 + G_\alpha \left(\frac{N}{N_t A}\right)^{\alpha/2}\right) \tag{4.1}$$

Consistent with this result, Blum [42] showed that as the number of interferers goes to infinity, each user should transmit solely in their strongest mode.

[1]Here we have made the simplifying assumption that transmit nodes use all data tones for transmissions.

These analyses provide a bounding rate under the particular transmit-receive scheme using MMSE receivers and eigenmode transmissions in an OFDM based-architecture with MC-CDMA. In an ad hoc network, however, the contention for access to the medium provides an ordered (first-come-first-served) subset of nodes that will transmit simultaneously, and choose their own data subject to their own quality-of-service needs and according to whatever local information is available. The duration and reliability of the information exchanged during the initiation of a session affects both the total sum rates and the average delay. The control channel scheme we propose below provides a means for a contention based access to the data channel that has three rules that aim to force sum rates towards the bounding rates described above:

1. Session initiation that, with high probability, initiates a transmission in an (interference) channel with a high probability of success

2. The selection of a data rate and a number of streams amenable to the interference environment and the quality-of-service request

3. Delayed access by a user that would cause an unsatisfactory SINR for an already transmitting node

The key mechanisms by which these rules are implemented are:

- Initiation procedure: Described in greater detail below, the initiation procedure allows nodes to choose a transmission scheme (coding, eigenmodes, spreading) that has a low probability of outage; that allows for target channel estimation in a low probability of outage environment to further reduce the probability of outage, and that allows other receiving nodes to guard against outage.

- Multi-Antenna slotted-ALOHA on the control channel. Nodes that have arrived to the medium during a control channel slot can contend in the next data channel slot in order to reserve a transmission for the following data channel slot. For a system

that has a control channel in time, nodes arriving during a data channel slot must wait until the next control channel slot to contend.

- Protest Scheme. Following the initiation procedures, transmissions on the data channel are delayed to allow previously queued receivers in the next slot to 'protest,' requesting that the target transmitter in question delay transmission.

- An upper bound on the duration of packets. This ensures that no transmit-receive pair is denied access to the medium caused by a strong interferer that remains on the data channel.

4.3.1 Fairness

The protocol structure gives nodes equal opportunities for access to the medium, and protects already reserved transmitters with the protest mechanism. In order that nodes do not dominate the medium, the number of data channel slots that can be used without returning to the side channel for contention is limited. The maximum spectral efficiency at which a node can transmit is given in the protocol specifications. The disparities between channel quality and the disparities in data rates that can result is not addressed by the protocol. Instead, we rely on the inherent variability of the channel to introduce a range of data rate opportunities for all node pairs. Interference environments will change in time on the order of data channel slots. The target channel itself will also change with the coherence time.

4.3.2 Link Transmit and Receive Strategies

Transmissions on the network are done either with or without channel state information (informed and uninformed transmitter respectively), and are done with a transmit covariance of rank less than or equal to the number of transmit antennas n_t. In the case of uninformed transmissions, we consider the case of a single transmit antenna; and a transmit-covariance-rank of 2. Uninformed transmission schemes add interference components to neighboring

receivers that equal the transmitter-covariance rank.

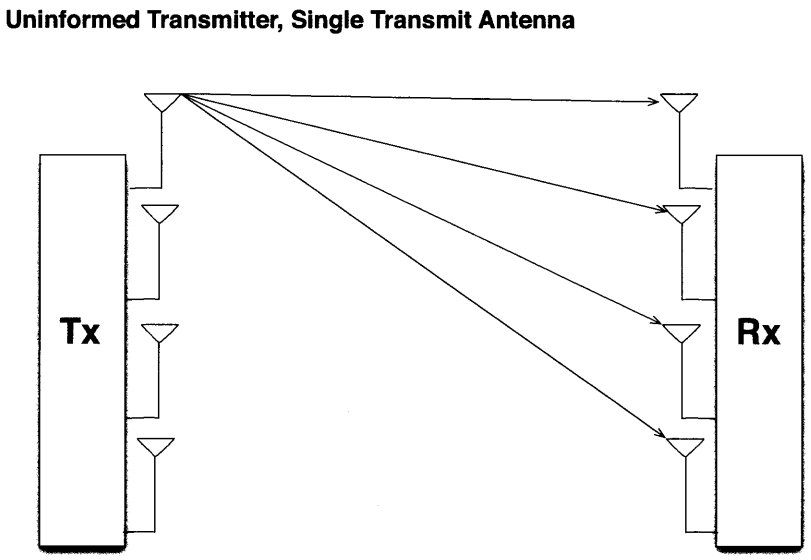

Figure 4-2: Single Transmitter

Uninformed transmitter strategies require that the receiver estimate the channel between itself and the transmit antennas, but does not require the transmitter to have channel state information, and thus the transmitters transmit omni-directionally. From the perspective of the protocol, fewer packet exchanges are required on the control channel which means that more nodes are capable of initiating transmissions for a given data channel slot. From the perspective of the network, each transmit antenna behaves like a separate interference mode, and the density of interferers behaves like the number of interfering nodes $\times$ the rank of the transmit covariance matrix. The use of uninformed transmitters will allow the data channel to become packeted more quickly, and will do so with fewer numbers of users.

Uninf ransmitter, Multiple Transmit Antennas

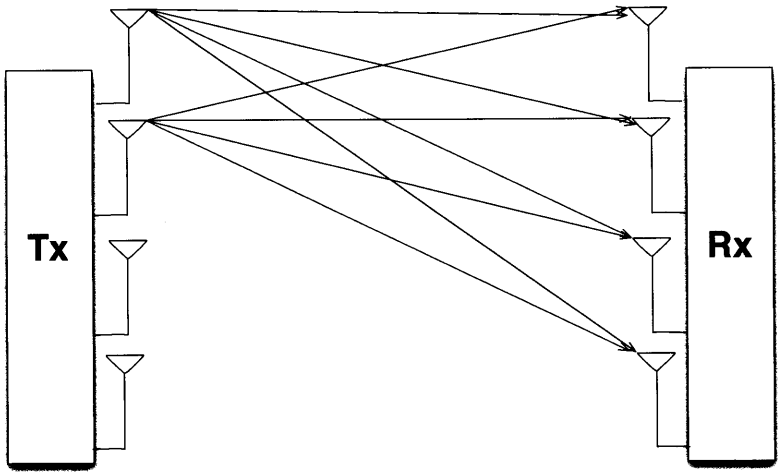

Figure 4-3: Uninformed Transmitter

In the case of informed transmissions, we consider only the use of target-channel-state-information (CSI) at the transmitter, and not the use of the interference covariance matrix seen by the receiver. This is suboptimal to the case where the transmitter has perfect knowledge of $\mathbf{K}^{-1/2}\mathbf{H}$. We consider the use of the strongest mode; and we briefly consider using a transmitter-covariance-rank of 2. Informed transmission schemes add number of interference components to neighboring receivers that is equal to the transmitter covariance rank. From the perspective of the protocol, the use of informed transmitters is expensive relative to the use of uninformed transmitters requiring additional control channel packet transmissions. There are gains in average achieved data rate, but those gains decrease as the interference environment becomes more dense. Still, the density of interferers behaves like the number of interfering nodes $\times$ the rank of the transmit covariance matrix. The utility of the use of informed transmitters depends on the size of the channel matrix, and the increase in the spectral efficiency provided by the transmit beamforming.

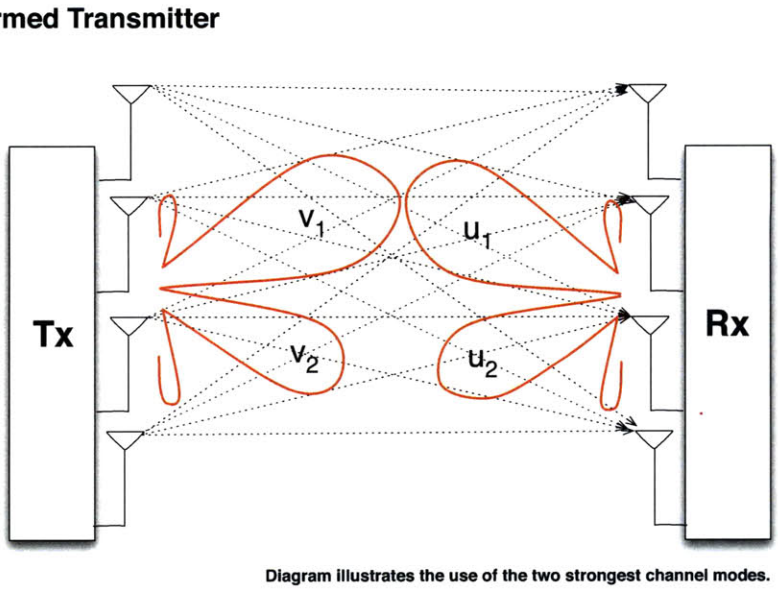

Figure 4-4: Informed Transmitter

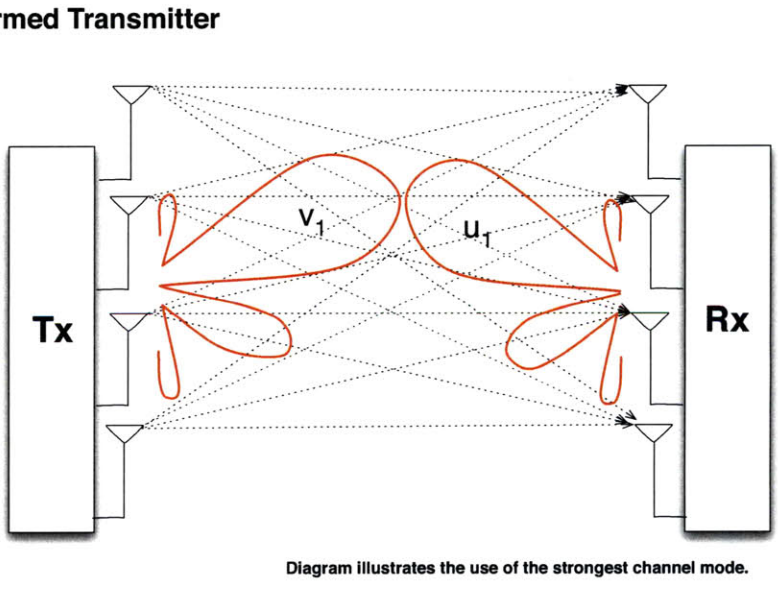

Figure 4-5: Informed Transmitter, Strongest Mode

4.4 Control Channel Procedures

4.4.1 Initiation Procedure

When the chosen strategy uses uninformed transmissions, the initiation procedure consists of the exchange of two initiation packets. When the chosen transmit-receive strategy uses informed transmissions, the initiation procedure consists of the exchange of three initiation packets. These packets are designed to be sent back-to-back, are of short duration, and sessions are initiated by the node that will be sending the data packet (the primary transmitter). This initiation takes place on the control channel during the scheduling period prior to the slot in which the transmitter would like to send the data channel packet. In order that all nodes being queued for the proceeding data channel slot can hear the reservations of all others being queued for the same slot, transmitting nodes must be receiving control channel packets from the beginning of the scheduling slot immediately prior to the data channel slot in which they intend to transmit. Each primary transmitter that wishes to contend for the next data channel slot then choose a uniformly and randomly selected slot from the $N_{cc} - 3$ control channel slots.

Each node randomly chooses from the N_{spread} control channel pseudo-noise spreading code seeds for its preamble. During each control channel slot where a packet is present, receiving nodes correlate the received signal with each of the N_{spread} spreading codes. Upon successful reception of the first initiation message, a given Tx-Rx pair continues to use the same code. Other receiving nodes then choose to use a different code for its next two packet transmissions to prevent interfering. The exchange of control packets is as follows:

1. Session Initiation: $Tx \rightarrow Rx$. This packet also functions as the receiver channel acquisition packet. In addition to the header, this messages contains the quality-of-service requirements of the proposed transmission, a data channel detection-preamble seed, and a multiple antenna training block so that the Rx can have an initial channel estimate. The receiver also uses this message to estimate the frequency offset relative to its

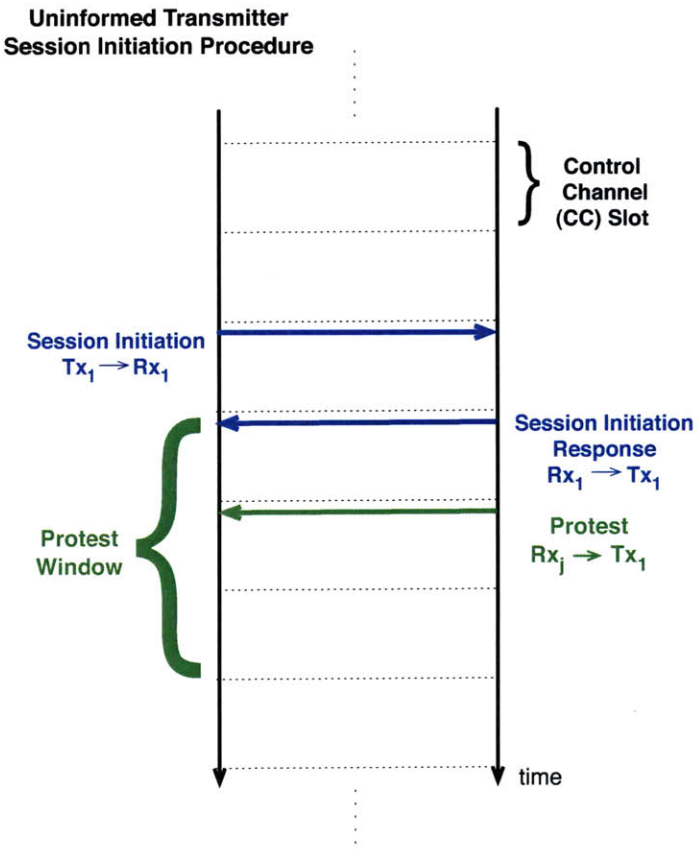

Figure 4-6: Uninformed Transmitter Timing Diagram

target transmitter. If the transmitter is proposing the use of an informed transmitter transmit scheme, this packet contains a training period during which the primary transmitter transmits equal power from each of its transmitting antennas. The data-channel preamble seed in this case corresponds to an index for multiple transmit streams, an these multiple transmit streams are also used in the training portion of this control channel packet. In both cases, the primary receiver uses this packet to estimate the target channel. Other primary receivers that receive this message use this to estimate the interference channel, and to determine if a protest packet will be required.

2. Session Response: $Tx \leftarrow Rx$.

   (a) An initiation-accepting response to the session initiation request packet would

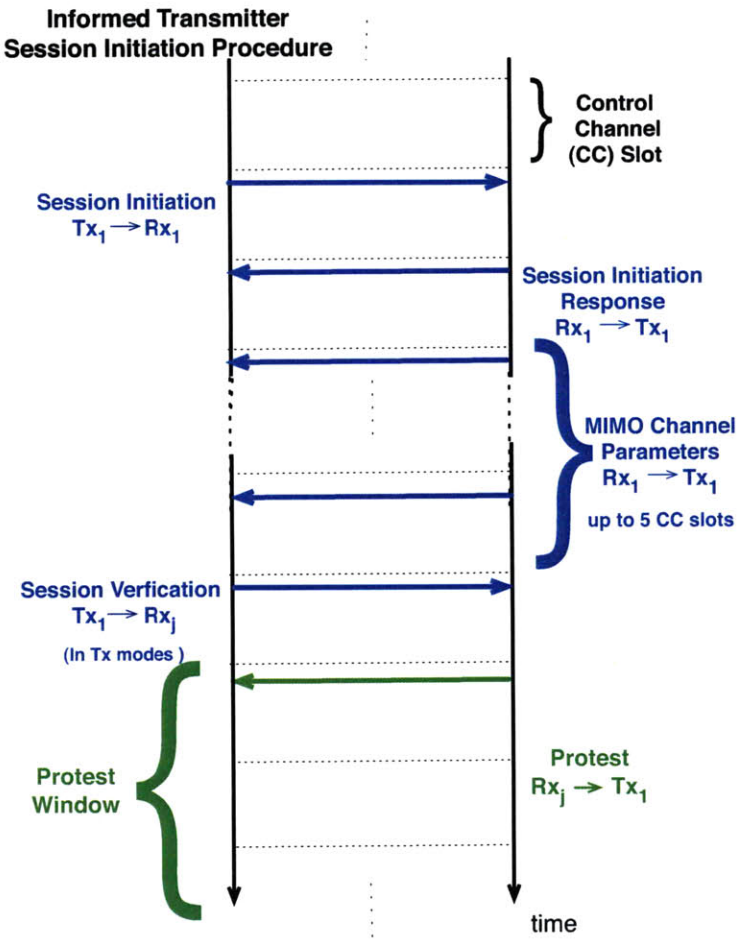

Figure 4-7: Informed Transmitter Timing Diagram

contain a suggested number of streams to fulfill the QoS requirement, and would echo the detection-preamble seed for verification. This packet also broadcasts the nodes estimate of its rank. If this session will use an informed transmitter transmit scheme, the target receiver sends quantized versions of the steering vector back to the transmitter. Since the channel may not be reciprocal after passing through the transmit and receive chains, this allows the transmitter to transmit in the eigenmodes of the receiver. The receiver chooses the eigenmodes on which it has the strongest SINR (which may not correspond to the mode with the largest eigenvalue).

(b) A initiation-declining response to the session initiation request packet would be a short packet with the header containing the initiation-decline message.

This exchange is illustrated in figures 4-8 and 4-6.

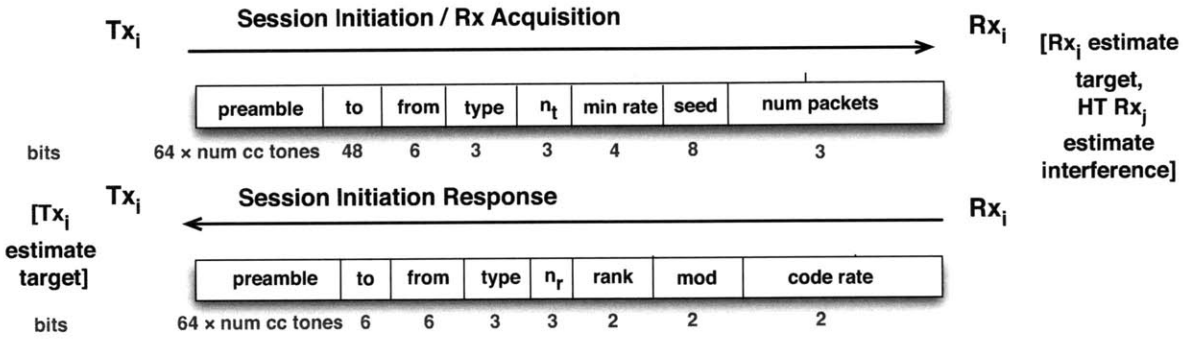

Figure 4-8: Session Initiation Packets

If the primary transmitter is using an uninformed transmitter scheme, then the control channel initiation scheme is finished, including only the two packets described above. In the case of informed transmissions , then a third packet is required:

3. $Tx \rightarrow Rx$ This last short, beamforming transmission is sent from the primary transmitter and is intended to alert other receivers as to the modes and power allocation that the transmitter will transmit on the data channel. The previous transmission of the transmit vectors came from the primary receiver. But there may be receivers out of receiving distance of the primary receiver, but in the interference environment of the primary transmitter that were not able to receive transmission of the eignmodes to determine if a protest packet is required. When this packet is transmitted by the primary transmitter in the prescribed transmit directions, nodes in the interference environment of the primary transmitter are notified of the reservation and of the interference it will cause.

This exchange is illustrated in figures 4-9 and 4-7.

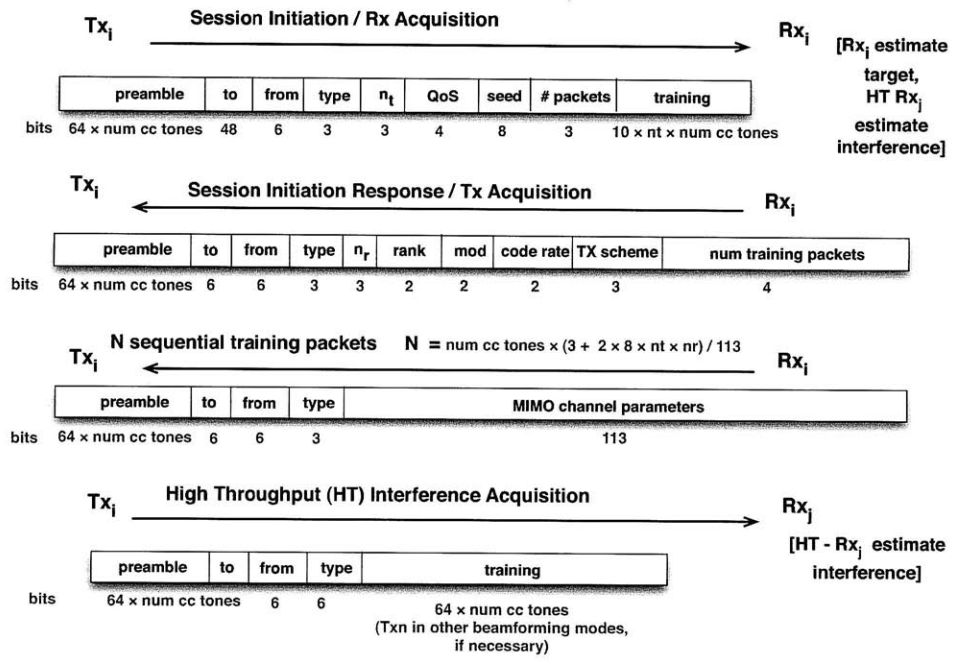

Figure 4-9: Informed Transmitter Session Initation Packets

Should a protest message be received, the proposed transmission is scraped and a re-initiation can be attempted after an amount of time equal to the maximum packet duration.

4.4.2 Protest Message

The objective of the protest message is to prevent a transmit-receive node pair seeking to initiate a session from lowering the SINR at the receiver of currently or previously-initiated session below what that receiver requires to maintain the rate it agreed upon with its target transmitter. A protest message can be initiated after receiving the message from the target transmitter in which the transmitter is transmitting in the eigenmodes of its target channel. The interference from this transmission can be received, and its outer product can be added to the sample interference covariance matrix. Using the new decoding weights, the received SINR at a given receiver can be computed. If this is less than the SINR required to support the data rate requirements for its own transmission, then that node transmits a protest message on the control channel. As stated above, this message must be transmitted within 3

time slots from the end of the session initiation response message. The format of the Protest packet is shown in figure 4-10

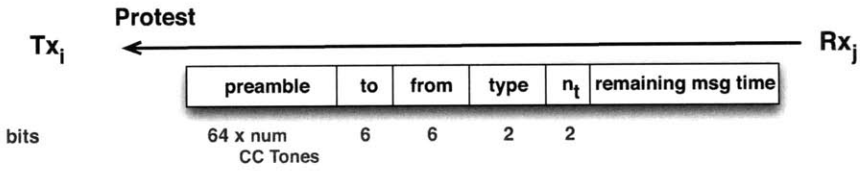

Figure 4-10: Protest Packets

4.4.3 Multiple Data Packet Transmissions: Transmission Continuing Message

Transmitter and receiver pairs can transmit some fixed number of packets before returning to the control channel to contend in order to reserve additional slots on the data channel. In order to continue transmitting, the target transmitter must broadcast a Transmission continuing packet to the control channel. This packet is transmitted by the primary transmitter in the channel modes that are used for transmissions. This packet contains the seed used for detection and the number of packets remaining in the multiple-packet-transmissions sequence. These messages can not be protested since the target transmitter will not receive the message before the next data channel slot.[2]

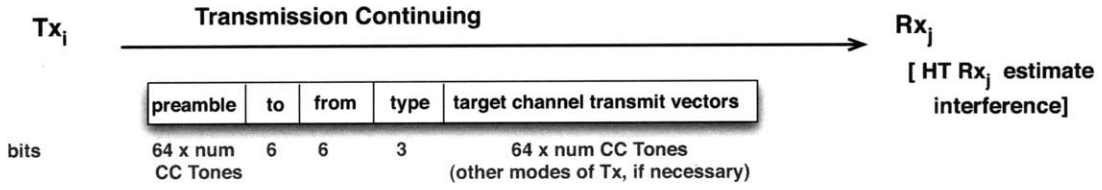

Figure 4-11: Transmission Continuing Packet

[2]We assume the wireless terminals cannot simultaneously transmit and receive.

4.4.4 Rate-Adjustment Message

A rate adjustment message is sent by the primary receiver, and is used to change the transmission parameters for a transmission that was scheduled earlier in the current contention period just before the next data channel packet slot. This packet is most often used when a receiving node receives a multiple data packet transmission packet that causes a change in its interference environment. This packet includes the new transmit parameters (modulation and coding scheme) and also reaffirms the detection coding preamble.

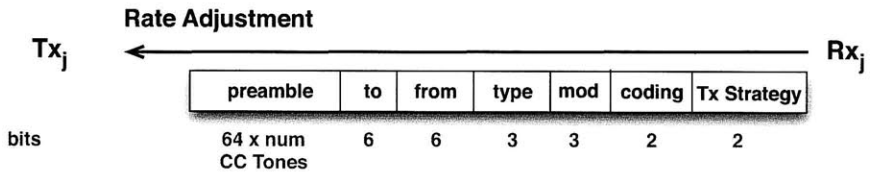

Figure 4-12: Rate Adjustment Packet

4.4.5 Acknowledgments

Positive acknowledgment messages are not used in this protocol scheme. If a packet is not received on the data channel, then either the level of interference or noise was too high, or the target interference channel changed. Since a packet not being received would require another reservation during the previous side channel period, the negative acknowledgement (N-ACK) procedure is a re-initiation procedure on the control channel, initiated by the primary receiver in the missed packet. In the header for the initiation, the receiver can specify the packet number to the transmitter to ensure that the packet is present. This procedure goes as follows:

1. Session Re-Initiation: $Rx \rightarrow Tx$. In addition to the header, this message contains the requested quality-of-service, a detection-preamble seed, and a multiple antenna training block so that the Tx can estimate the target channel. The target transmitter also uses this message to estimate the frequency offset relative to its target transmitter.

2. Session Re-Initiation Response: $Rx \leftarrow Tx$.

   (a) An initiation-accepting response message echos the detection-preamble, and broadcasts the rank estimate. The transmitter then sends equal power from each transmit antenna using a shortened version of the detection preamble to be used on the data channel so that the receiver can estimate the MIMO channel.

   (b) A re-initiation-declining response to the session initiation request packet would be a short packet with the header containing the initiation-decline message.

3. Session Re-Initiation Response 2: $Rx \rightarrow Tx$. In this packet, the receiver sends the quantized MIMO channel to the transmitter. In this message the receiver also verifies the quality-of-service parameters, and modifies them if its current interference environment requires that the parameters be changed.

If the session will use an informed transmitter transmit scheme, the following packet is required to inform receivers in the interference environment of the target transmitter of the interference channel strength:

4. Session verification: $Rx \leftarrow Tx$. In this brief message on the control channel, the transmitter broadcasts a packet, transmitting in the modes in which it will transmit on the data channel. The nodes that receive this message will then determine the modes on each tone, and using its previous measure of the interference channel, will find the interference caused by the impending transmission to determine if a protest message is needed.

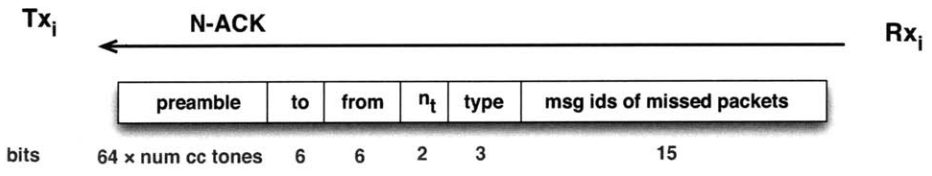

Figure 4-13: Negative Acknowledgment

The N-ACK packet can support a variable number of bits in the portion of the packet used for the message-IDs of missed packets (denoted 'msg ids of missed packets in figure 4-13).

4.5 Data Packets

Data packets in the STI-MAC protocol consist of a preamble that is used for detection, synchronization and estimation, followed by a header containing information about the modulation scheme, coding scheme, the transmit-covariance-rank, the number of bits contains in the packet and a packet number which is used by the transmitter and receiver as a packet identifier. The data packet is illustrated in figure 4-14.

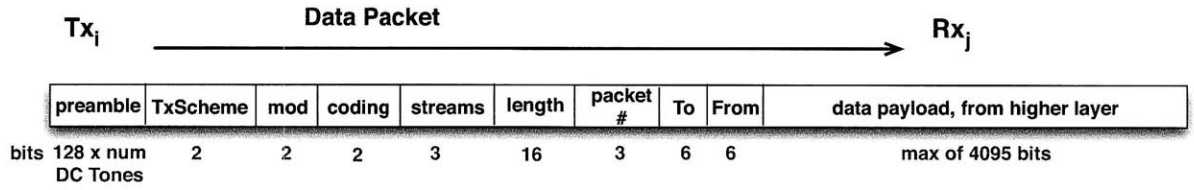

Figure 4-14: Data Packets

4.6 Protest Scheme Implementation

The protest scheme employed in this protocol is a mechanism designed specifically for communication in interference environments where interference mitigation techniques are used. Let link 1 be an already reserved or functioning transmit-receive link. If the transmitter in a new link 2 (Tx_2) begins to transmit, and interferes with the receiver in link 1 (Rx_1), then the interference from Tx_2 has the potential to drive the SINR received at Rx_1 below the SINR it requires to successfully decode the transmission from transmitter 1 (Tx_1). To prevent this post-emption by link 2, we introduce the protest scheme.

The protest scheme is a protocol mechanism that takes place on the control channel and

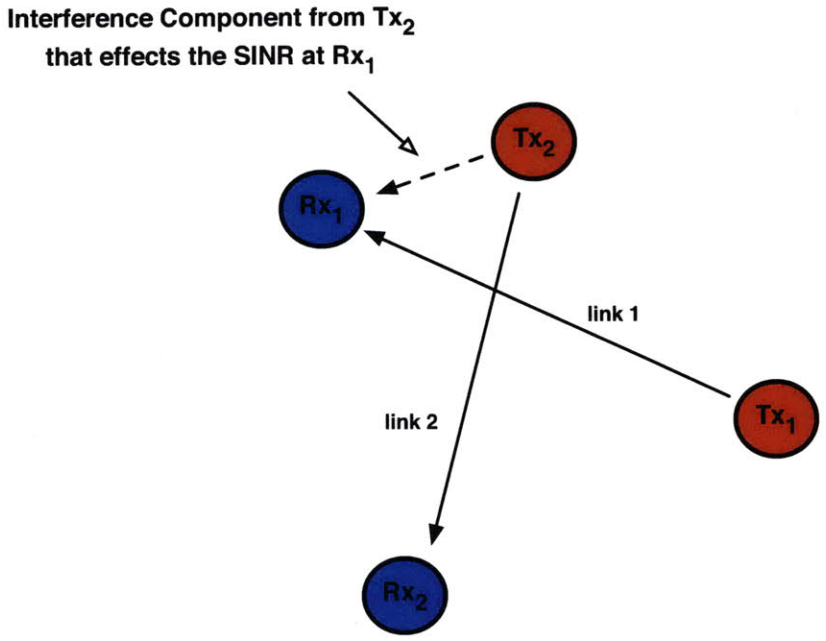

Figure 4-15: Illustration to Motivate Protest Scheme

that effects the scheduling of transmissions in the next data channel slot. The purpose of the protest scheme is for a given receiver a, that is already scheduled to receive a transmission from transmitter a in the next data channel slot, to estimate its own received SINR should transmitter b also transmit in the next data channel slot. Consider a network where all nodes operate with n_r receive antennas and a single transmit antenna. When a receiver has perfect knowledge of its own target channel $\mathbf{h}$, perfect knowledge of the interference channels of all of its interferers in the columns of $\mathbf{H}$, and the variance of the additive white Gaussian noise N_o, then its received SINR is given by:

$$SINR = \mathbf{h}^{\dagger}\mathbf{K}^{-1}\mathbf{h} \tag{4.2}$$

where $\mathbf{K} = \mathbf{H}\mathbf{H}^{\dagger} + N_o\mathbf{I}$. When a receiver is able to collect estimates of the target and interference channels on the control channel, the SINR in equation (4.2) can be estimated. The quality of the estimate of the SINR will depend on the quality of the estimates of the individual interference and target channels. Estimates of the interference channels are achieved in

interference environments. If we let matrix $\mathbf{A}$ describe the correlation between the sequences used to estimate channel $\mathbf{h}$ and interference channels $\mathbf{h_j}$, then the estimate $\hat{\mathbf{h}} = \mathbf{h} + \mathbf{n}$ is the sum of the actual channel $\mathbf{h}$ plus an additive noise component $\mathbf{n} \sim CN(0, (N_o/n)\mathbf{A})$ where N_o is the noise power, and n is the length of the estimation sequence. Using these estimate, the SINR estimate for the protest mechanism becomes:

$$\hat{\mathbf{h}}^{\dagger}\hat{\mathbf{K}}^{-1}\hat{\mathbf{h}} = (\mathbf{h}+\mathbf{n})^{\dagger}\left(\sum_j (\mathbf{h_j}+\mathbf{n_j})(\mathbf{h_j}+\mathbf{n_j})^{\dagger}\right)^{-1}(\mathbf{h}+\mathbf{n}) \tag{4.3}$$

$$= \mathbf{h}^{\dagger}\left(\sum_j (\mathbf{h_j}\mathbf{h_j}^{\dagger}+\mathbf{n_j}\mathbf{n_j}^{\dagger})\right)^{-1}\mathbf{h} + \mathbf{n}^{\dagger}\left(\sum_j (\mathbf{h_j}\mathbf{h_j}^{\dagger}+\mathbf{n_j}\mathbf{n_j}^{\dagger})\right)^{-1}\mathbf{n} + 2\Re\left\{\mathbf{h}^{\dagger}\left(\sum_j (\mathbf{h_j}\mathbf{h_j}^{\dagger}+\mathbf{n_j}\mathbf{n_j}^{\dagger})\right)^{-1}\mathbf{n}\right\} \tag{4.4}$$

where $\mathbf{h_i}$ and $\mathbf{n_i}$ are uncorrelated for all i. The similarity of the interference structure defined by $\hat{\mathbf{K}}$ depends on the relative power of the noise components versus the interference channel components. It should be noted that this interference channel can be entirely different from $\mathbf{K}$ when the power of the noise components approaches that of $\mathbf{h}$. If we consider each term of equation (4.4), the first term dominates, has a maximum value of $\frac{P}{N_o}$ and is the closest to the actual SINR. The magnitude of the second term relative to that of the first term depends on the power of the noise components, and has a maximum value of unity. Since $\mathbf{K}$ is Hermitian, the first two terms are always positive. When $\mathbf{n}$ and $\mathbf{h}$ are Gaussian, the third term has a maximum value $\sqrt{PN_o}/N_o$, and can be positive or negative. The accuracy of the SINR estimate should increase as the variance in the noise components approaches 0. This occurs when when interference channels are estimated in as low interference as possible, and when estimation sequences are sufficiently long. Since the protest scheme will operate best in minimal interference, this introduces a design trade off into the protocol. The protest scheme takes place on the control channel, where the control channel is designed so

that with high probability, the packets are transmitted in low-interference and are received with high reliability. This ensures that the variance of $\mathbf{n}$ is low relative to the transmit power.

In figure 4.6 we consider the mean spectral efficiency in a network where the spectral efficiency is generated in three ways:

1. The Asmyptotic Rate is generated using perfect target channel and interference covariance matrix (labeled asymptotic)

2. The Estimated Rate by which the receiver beamforming weights are generated. These beamforming weights are constructed using n snapshots of the received signal

$$\mathbf{w} = \left(\frac{\mathbf{1}}{\mathbf{n}}\mathbf{Y}\mathbf{Y}^{\dagger}\right)^{\dagger}\mathbf{Y}\mathbf{X}_{\mathbf{1}}^{\dagger}(\mathbf{X}_{\mathbf{1}}\mathbf{X}_{\mathbf{1}}^{\dagger})^{-\mathbf{1}}$$

   and then the SINR is computed $SINR = \frac{||\mathbf{w}^{\dagger}\mathbf{h}||^{\dagger}}{\mathbf{w}^{\dagger}\mathbf{K}\mathbf{w}}$. The sample interference-covariance-matrix contains the target channel. (labeled sample ICM with target, target estimated)

3. The Estimated Rate via the Protest Scheme: the target and each interference channel is estimated separately in the presence of $nr - 1$ interferers. These estimates are then used in the formula $\mathbf{h}^{\dagger}\mathbf{K}^{-\mathbf{1}}\mathbf{h}$ to estimate the SINR. (labeled protest)

The similarity in the behavior of the mean in the estimate of the rate using beamforming weights and the estimate of the mean using the protest function suggests that the noise power in the separate estimates of the interference channels is low enough that the SINR estimate and the asymptotic SINR have a significant correlation. This correlation is verified in a scatter plot of the estimated rate versus the asymptotic rate shown in figure 4-17. In figure 4-17 the asymptotic rate and an estimate of the rate generated using length n estimation sequences are shown.

As we would expect, as the length of the estimation sequence increases, the power of the noise decreases and the rate estimate becomes more highly correlated with the asymptotic rate.

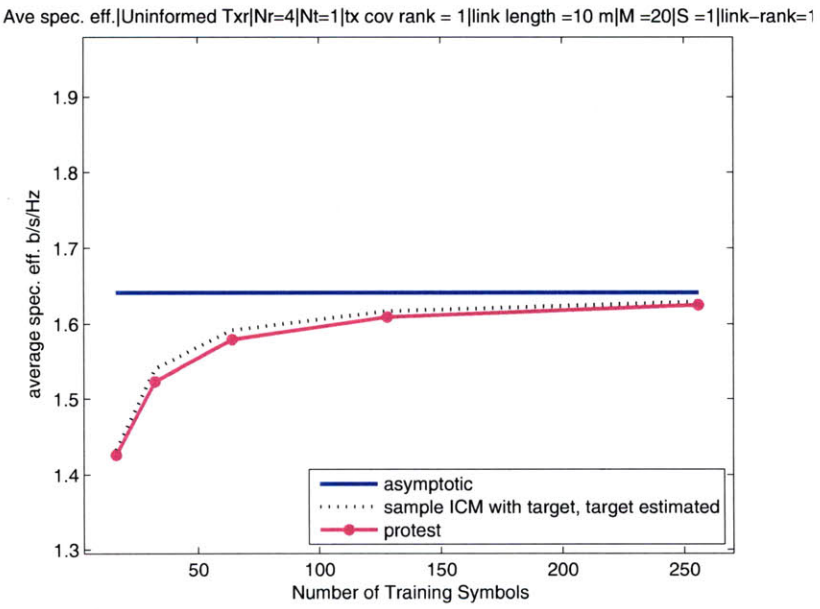

Figure 4-16: Mean Asymptotic Rate, Mean Estimated Rate using Receiver Beamforming weights, and Mean Estimated Rate using Protest Function as a function of the Estimation Sequence Lengths in Networks with M = 20 links, Link-Rank = 1, 4 Receive Antennas and a single Transmit Antenna and Link-Length = 10 m

Figure 4-17: Scatter Plot of Estimated Rate versus Asymptotic Rate

4.6.1 Prediction of Achievable SINR using $\hat{\mathbf{h}}^{\dagger}\hat{\mathbf{K}}^{-1}\hat{\mathbf{h}}$

Since the distribution of the estimate of the SINR, $SINR_{est}$, is unknown but certainly not independent of the asymptotic SINR, $SINR_{asy}$, we instead characterize the joint distribution of the $SINR_{asy}$ and $SINR_{est}$ through Monte Carlo simulation. To account for instances when we consider the use of a transmit-covariance-rank that is greater than 1, we will consider random variables that are a function of SINR, the maximum achieveable rate associated with a given SINR:

$$r_{asy} = \sum_{j} \log_2(1 + (SINR_{asy})_j) \tag{4.5}$$

$$r_{est} = \sum_{j} \log_2(1 + (SINR_{est})_j) \tag{4.6}$$

where $(SINR_{asy})_j$ is the asymptotic SINR of stream j. Let R_{asy} be the random variable describing the asymptotic data rate, $R_{est}(n)$, is the random variable describing the estimated data rate when the estimation of each (target and interference) channel using a pseudo-random estimation sequence of length n. R_{asy} and $R_{est}(n)$ are both random variables that are generated from the underlying random variables in a network with M links, n_r receive antennas, n_t transmit antennas, length n training sequences and random variables $H, H_1, ..., H_j$ describing the target and interference channels, $X, X_1, \ldots X_j$ transmit data and additive white Gaussian noise W.

The strong correlation between the asymptotic rate and the estimated rate evidences that the estimated rate can be used to predict the asymptotic rate. In figures 4-18(a) and 4-18(b), we plot the joint density on $R_{est}(n)$ and R_{asy} for $n = 32$ and $n = 64$.

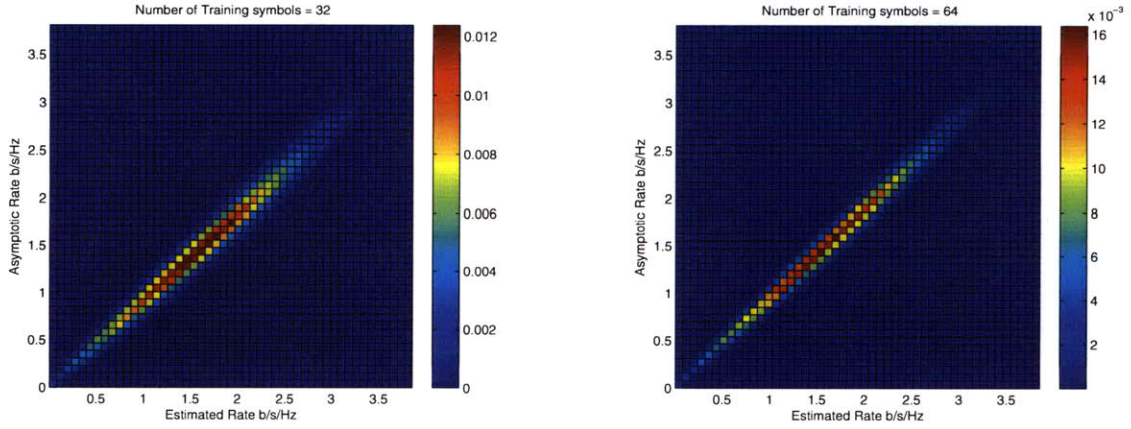

(a) Joint PDF $R_{est}(32)$ versus R_{asy}

(b) Joint PDF $R_{est}(64)$ versus R_{asy}

Figure 4-18: Joint Probability Density Function (PDF) on Asymptotic Rate versus Estimated Rate for Estimation Sequence Lengths $n = 32$ and $n = 64$ in Networks with M = 20 links, Link-Rank = 1, 4 Receive Antennas and a single Transmit Antenna and Link-Length = 10 m

The utility of the rate estimate will be in its ability to predict, based on some estimated value y, that the asymptotic rate is greater than some value x with high probabilty:

$$P(R_{asy} > x | R_{est}(n) = y) \tag{4.7}$$

The probability density function defined by is generate from the joint distribution on R_{asy} and $R_{est}(n)$. It allows one to take an estimate y of the rate, and predict the likelihood that R_{asy} is greater than some value x.

Using data generated via Monte Carlo simulations, in figure 4-19 we generate the conditional complementary distribution functions defined in equation (4.6.1) for networks with M = 20 links, Link-Rank = 1, 4 Receive Antennas, a single Transmit Antenna and Link-Length = 10 m.

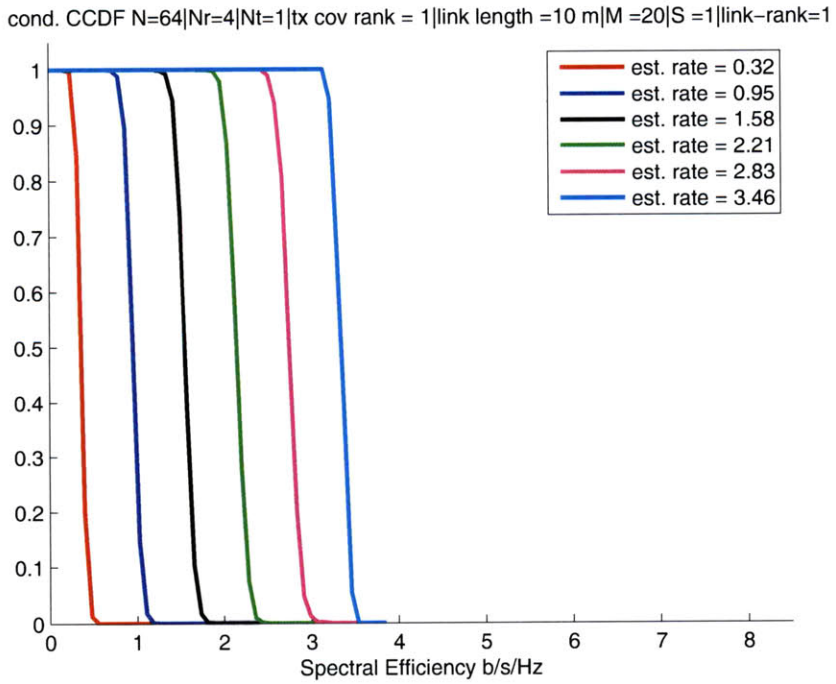

Figure 4-19: Conditional Complementary Distribution Function

To achieve 90% accuracy, we use the protest estimation function shown in figure 4-20 which relates the estimated SINR value on the x-axis to the corresponding 90 %-accuracy asymptotic rate on the y-axis. This corresponds to a 10% probability that a protest should have been sent, but was not (probability of a miss), which is the upper bound on the probability that a data channel packet is in outage when the target and interference channels are static.

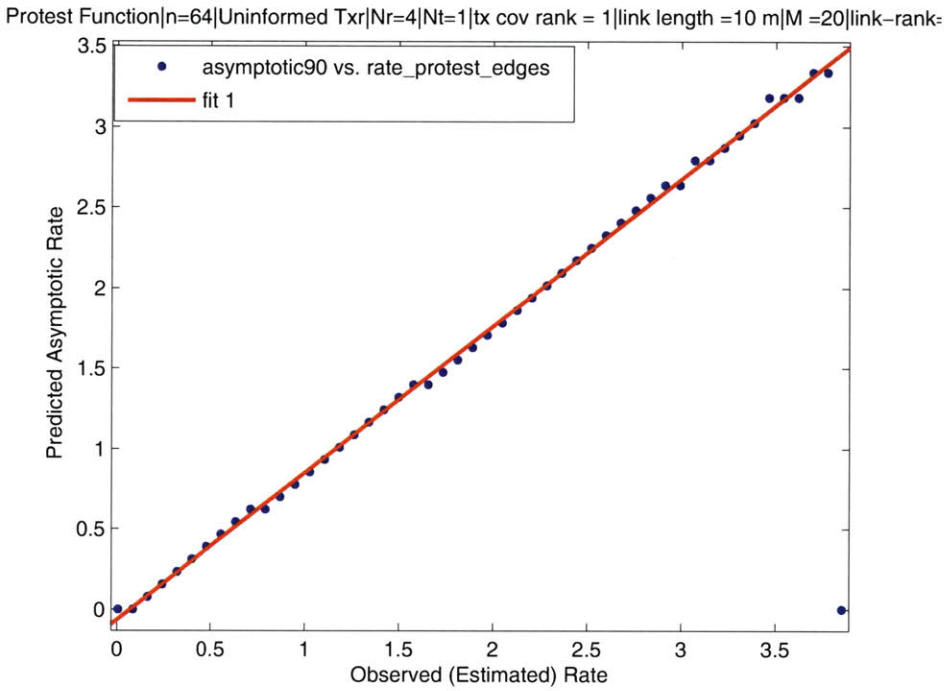

Figure 4-20: Protest Prediction Function

An estimate of the protest prediction function is generated for each element of our parameter space.

4.7 Modulation and Coding Schemes

In this work we will consider the use of a convolutional error correction code of rate 1/2, and source coding rates: BPSK, QPSK, QAM16, and QAM64. These schemes are used in 802.11 protocols, and were chosen for the sake of comparison with 802.11 protocols. The measure

$\frac{E_b}{N_o}$ relates to the SINR that is measured at the receiver through the following relationship:

$$SINR = \frac{E[||\mathbf{w}^\dagger \mathbf{h}||^2]}{E[\mathbf{w}^\dagger \mathbf{K} \mathbf{w}]} = \frac{E_s}{E_I + \sigma^2} = \frac{E_b}{N_o} \cdot \log_2(M)\frac{k}{n} \tag{4.8}$$

where $\frac{k}{n}$ is a function of the error correction coding scheme. Variable k is the number of information bits corresponding to n coding bits; and where $\log_2 M$ is the number of bits per modulation symbol where the modulation scheme consists of M alternative symbols. The expectation in equation (4.8) is taken over the noise and the transmit symbols; and the target and interference channels are static over the duration of a frame. The effective energy-per-bit-over-N_o (E_b/N_o) as a function of the received SINR and source coding rates is given in table 4.7.

Table 4.1: Relationship between energy-per-bit-over-N_o, the received SINR, and the Modulation and Coding Schemes used in STIMAC Protocols

Code	$\frac{E_b}{N_o}$
BPSK	$2 \cdot SINR$
QPSK	$SINR$
QAM16	$\frac{SINR}{2}$
QAM64	$\frac{SINR}{3}$

To determine the approximate $\frac{E_b}{N_o}$ required to achieve a bit-error-probability of less than 10^{-6}, we consider the coding gain of the convolutional coding rate that is most often used in 802.11 networks, which is a rate 1/2 length with constraint length $L = 7$ with generator polynomials $g_0 = 133$ and $g_1 = 171$ in octal mode. These 1/2 rate codes have a minimum-free distance of 5, yielding a coding gain of $10 \log_{10}\left(\frac{5}{2}\right) = 3.98\ dB$. If we consider the performance of an uncoded 2-Pulse-Amplitude-Modulation (2-PAM) system in additive-white-Gaussian-Noise (AWGN) in the low SNR regime(as shown in figure 4-21), to achieve a bit-error-probability of less than 10^{-6} requires an $\frac{E_b}{N_o}$ approximately $10.6\ dB$ [98]. Thus, the $\frac{E_b}{N_o}$ required for rate

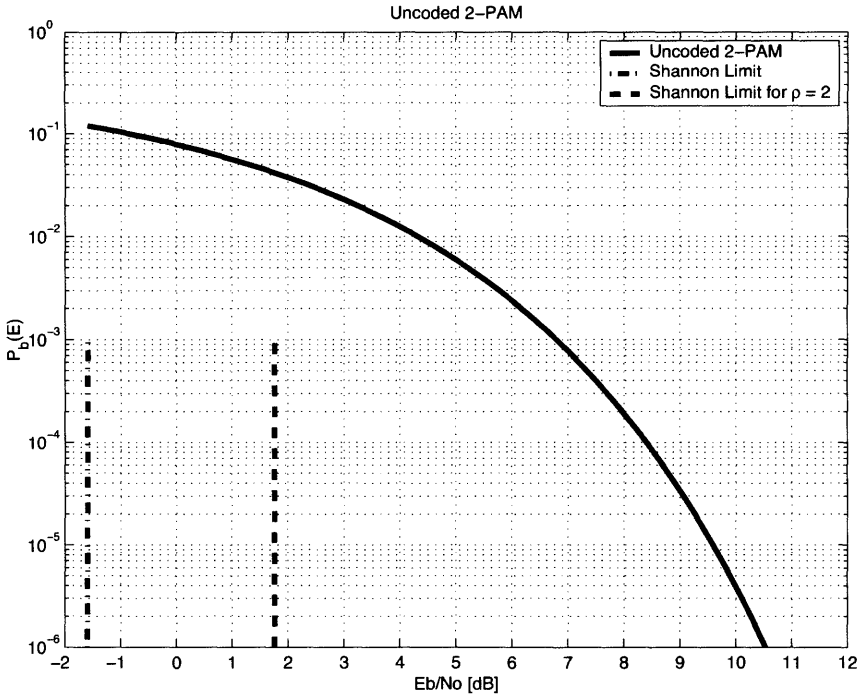

Figure 4-21: Bit Error Rate Curve for Uncoded 2-Pulse-Amplitude Modulation

1/2 convolutional codes with constraint length $L = 7$ is approximately 6.6 dB[3].

When nodes use a transmit-covariance-rank = 2, we will assume that they can double whatever data rate they seek, provided that they have enough received SINR.

[3]In real systems, $\frac{E_b}{N_o}$ tends to vary between $5 - 10$ dB, where ~ 10 dB is more realistic for the weaker convolutional codes.

Table 4.2: Relationship between the received SINR, and the Modulation and Coding Schemes used in STIMAC Protocols

Code	$SINR\ (dB)$
BPSK	3.3
QPSK	6.6
QAM16	13.2
QAM64	19.8

These codes are widely used, but are relatively weak relative to the strongest codes that approximate the Shannon limit for the minimum Eb/No, a limit found by taking $\rho \rightarrow 0$:

$$E_b/N_o > \frac{2^\rho - 1}{\rho} \tag{4.9}$$

$$= \ln 2 \tag{4.10}$$

$$\approx -1.59\, dB \tag{4.11}$$

4.8 STI-MAC Designs

In these STI-MAC designs, the means by which the orthogonality between the control channel and the data channel is achieved varies, but mechanisms of the MAC for session initiation and protest remain the same. We first describe the control channel in frequency which uses a subset of tones for control and the rest for data. We then describe the control channel in time which alternates between using the entire frequency band for transmitting control packets and using the entire frequency band for transmitting data packets. Lastly, we briefly outline a design for a control channel in code which reserves as subset of code space for control packets, and uses the rest of code space for data packets.

4.8.1 Control Channel in Frequency, Synchronous Data Transmissions

The total bandwidth W is broken up into K tones of width $B = W/K$, where B is less than the coherence bandwidth. A fraction K_{cc}/K of tones is used for the control channel.
The number of tones K_{cc} is lower bounded by the delay spread of the channel L. Estimation of the control channel tones is achieved with known transmit symbols. In order to estimate the channel on the tones not used for control, the following technique is used. Recall the Discrete Fourier Transform relating the channel impulse response in time to the channel impulse response in the frequency domain:

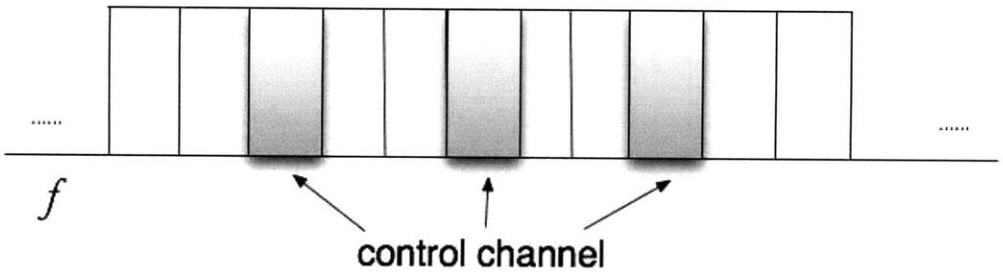

Figure 4-22: Control Channel in Frequency

$$H_k = \frac{1}{\sqrt{K}} \sum_{n=0}^{L-1} h_n e^{-j2\pi kn/K} \tag{4.12}$$

where L is the channel length, K is the number of tones. If we let $\mathbf{H} = (H_0, H_1, \ldots, H_{K-1})^T$ This is also represented in matrix form as:

$$\mathbf{H} = \frac{1}{\sqrt{K}} \begin{pmatrix} 1 & 1 & 1 & \ldots & 1 \\ 1 & W_K^{1\cdot 1} & W_K^{2\cdot 1} & \ldots & W_K^{(L-1)\cdot 1} \\ 1 & W_K^{1\cdot 2} & W_K^{2\cdot 2} & \ldots & W_K^{(L-1)\cdot 2} \\ \ldots & \ldots & \ldots & \ldots & \ldots \\ 1 & W_K^{K-1} & W_K^{2(K-1)} & \ldots & W_K^{(L-1)(K-1)} \end{pmatrix} \mathbf{h} \tag{4.13}$$

When the channel length L is short relative the total number of tones K, it is more computationally efficiency to determine the response of the channel in time (L taps) than to determine the response of the channel in frequency (K taps). Since the linear equations represented by the matrix in equation (4.13) are dependent, we only require L rows to determine h. This corresponds to estimating the channel parameters in frequency on L tones. If we let $\mathbf{H_{cc}}$ be the vector of L pilot tones frequency response measurements $\mathbf{H_{cc}} = (H_{k_1}, \ldots, H_{k_L})^T$, and $\mathbf{h}$ be the length L channel response, and where $W_N = e^{-j2\pi/N}$ then:

$$\mathbf{H_{cc}} = \frac{1}{\sqrt{K}} \begin{pmatrix} 1 & W_K^{k_1} & W_K^{2k_1} & \dots & W_K^{(L-1)k_1} \\ \dots & \dots & \dots & \dots & \dots \\ 1 & W_K^{k_L} & W_K^{2k_L} & \dots & W_K^{(L-1)k_L} \end{pmatrix} \mathbf{h} \tag{4.14}$$

Since the DFT matrix above is invertible, the channel impulse response in the time domain $\mathbf{h}$ can be found by estimating $\mathbf{H}$ on at least L tones. In [17], the author show that equally spaced tones minimizes the estimation error over all possible placement of tones in the mean square sense, and with estimation error given by:

$$E[|\hat{\mathbf{h}} - \mathbf{h}|^2] = \sigma^2 K \tag{4.15}$$

where σ^2 is the noise power per tone $N_o W$ (which is also the the AWGN per time sample), and assuming a transmit power per tone of unity. By Parseval's Theorem:

$$E[|\hat{H}_k - H_k|^2] = \sigma^2 K \tag{4.16}$$

Comparing this noise power level to that obtained by match filter in the frequency domain (or equivalently in the time domain):

$$\hat{\mathbf{h}} = \mathbf{h} + \mathbf{w} \quad \text{or} \quad (\hat{H}_k = H_k + W_k) \tag{4.17}$$

where $w \sim N(0, \sigma^2)$. The average error is given by:

$$E[|\hat{\mathbf{h}} - \mathbf{h}|^2] = E[|W_k|^2] = E[|w|^2] \tag{4.18}$$

$$= \sigma^2 L \tag{4.19}$$

When there are multiple antennas at the receiver (n_r), these calculations can be performed for each of the n_r channels $H = (\mathbf{h_1}, \dots, \mathbf{h_{n_r}})$.

The timing ..

A timing diagram for the control channel in frequency is shown in figure 4-23. For the control

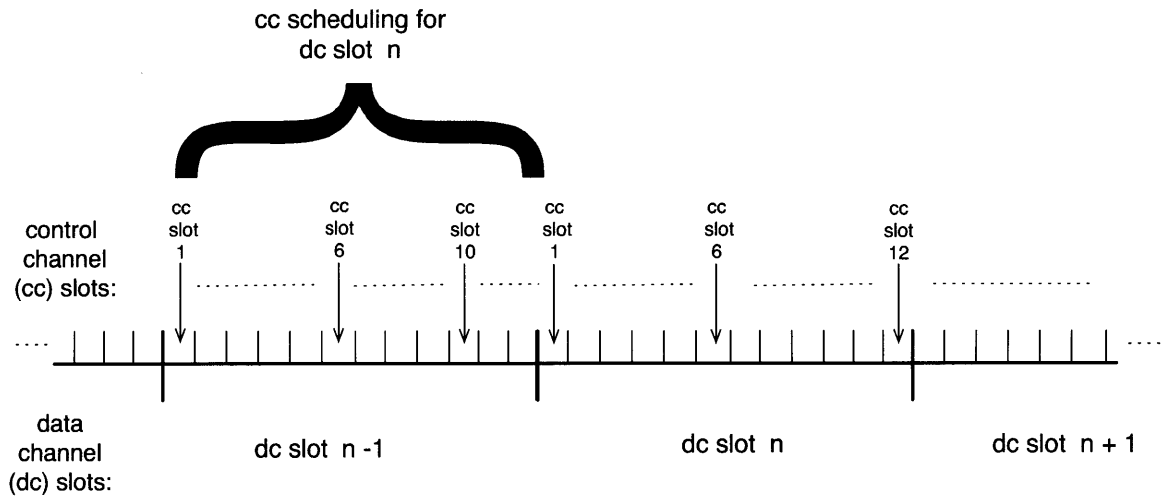

Figure 4-23: Timing Diagram for Control Channel in Frequency

channel in frequency, a node with a packet to transmit can send a session initiation packet to the control channel at any time. A successful session initiation packet will reserve for the following data channel slot. If a session initiation packet is sent within the last 3 slots of the control channel before the next data channel slot, then it is not able to reserve for the immediate next data channel slot since there would be no time for a protest message. It is therefore reserving a slot for the following data channel slot.

In figure 4-24 we give a diagram of a time series of the control channel in frequency.

4.8.2 Control Channel in Time, Synchronous Data Transmissions

The control channel in time formulation corresponds more directly to the traditional reservation based protocol. Time is broken up into alternating control and data slots where T_{cc} is the duration of the control channel, and T_{dc} is the duration of the data channel which is the duration of a packet. The fraction of degrees of freedom used for control can be chosen to support the expected offered load, and the data rates the protocol would like to support. A key difference between the functionality of the protocol with a control channel in time

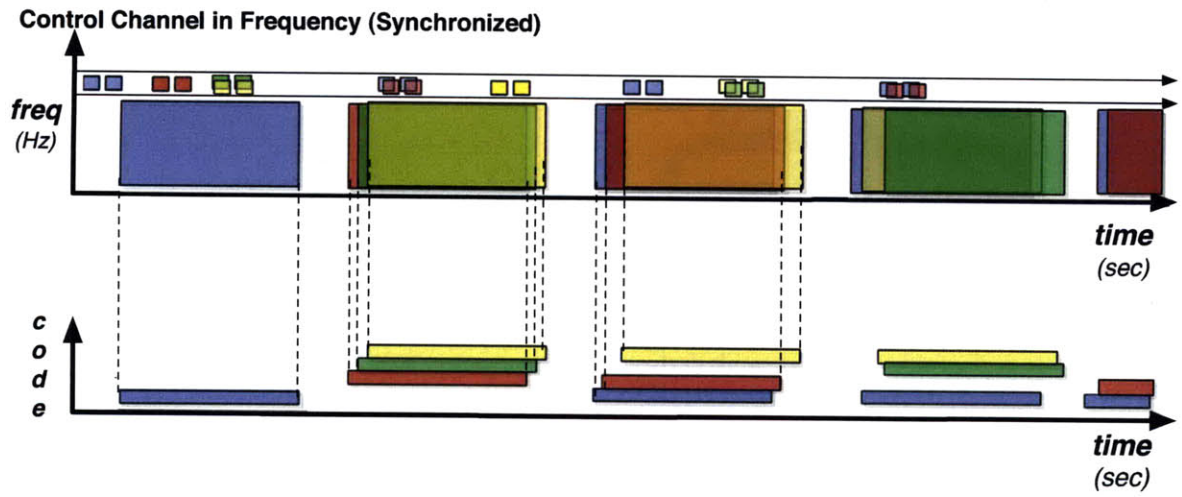

Figure 4-24: STI-MAC Protocol, Control Channel in Frequency

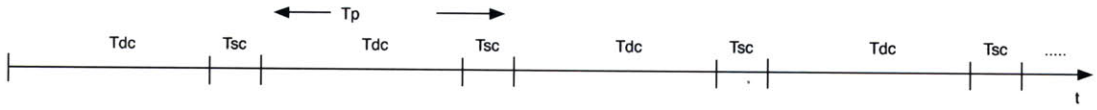

Figure 4-25: Illustration of the Side Channel and data-channel periodicity in Time

versus the control channel in frequency is that in the protocol with the control channel in frequency, a node that arrives during a data channel period must wait until a control channel period in order to contend for the next data channel period. All transmissions take place on all tones, reducing the duration of control channel packets and data channel packets relative to those durations in the control channel in frequency case. Channel estimation can be of shorter duration when the fade on more tones are estimated directly instead of via interpolation. The control channel in time is also usable over environments with more of a range on the delay spread. A diagram of a time series of the control channel in time is given in figure 4-24 .

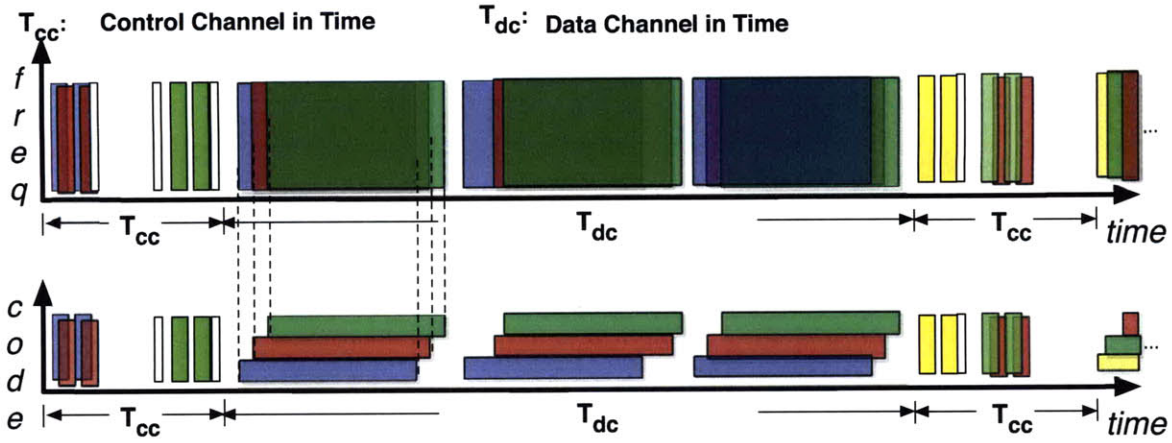

Figure 4-26: STI-MAC Protocol, Side Channel in Time

4.8.3 Control Channel in Code, Synchronous Data Transmissions

The design of a control channel in code was conceptualized, but not explored. Such a protocol include reserving a subset of codes for control, and using remaining codes for the transmission of data. In order to model random process describing the received symbols as stationary, and for the interference covariance matrix to be well behaved, nodes would need to use spreading codes of the same length. An illustration of a control channel in code is shown in figure 4-27.

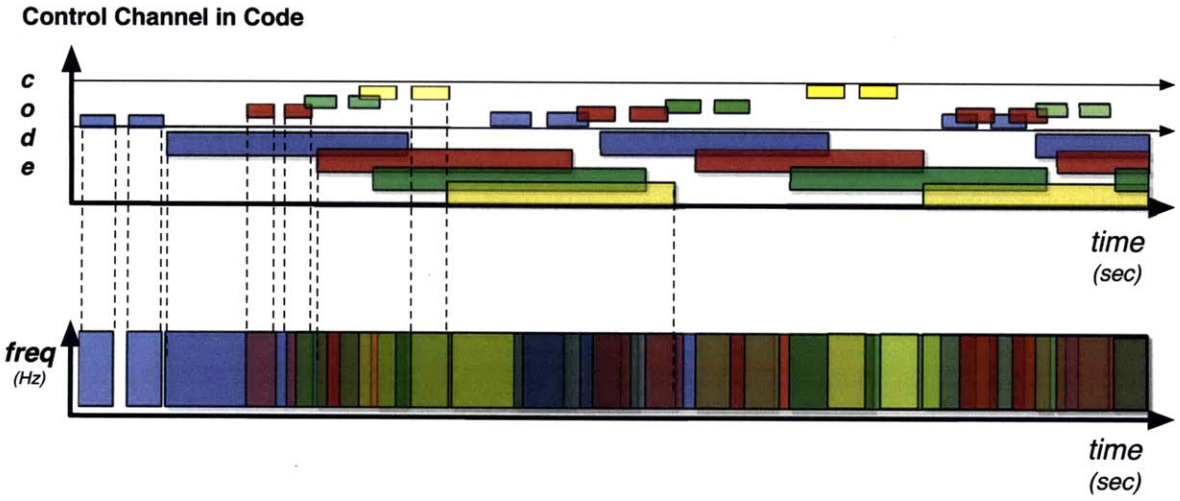

Figure 4-27: STI-MAC Protocol, Side Channel in Code

Chapter 5

Parameter Space

In this chapter we will first discuss the key parameters that characterize our parameter space for ad hoc wireless networks in interference environments. These parameters are link-length, link-rank, number of transmit receiver pairs, and the number of receive antennas. Then we will discuss a fifth importation dimension of the parameter space: the transmit-receive scheme which will include using an informed or an uninformed transmitter, and a transmitter covariance rank of either one or two.

5.1 Characterization of Ad Hoc Networks with Single-Input-Multiple-Output Links

Networks of wireless nodes that communicate simultaneously while interfering with each other can be of arbitrary shape, have an arbitrary number of transmit-receive pairs, and consequently exhibit widely varying performance in terms of average sum spectral efficiency and average delay per transmission. In [11], the author demonstrated that in an infinite network of nodes communicating in interference in which nodes are uniformly and randomly distributed on a plane with density $\rho \left[\frac{1}{m^2}\right]$; when the distance between transmitters and their respective receivers is fixed throughout the network, then the average spectral efficiency of receive nodes can be characterized by a variable called the link-rank. The link-rank is defined

as the average number of interfering transmitters that are closer to a given receiver than its target transmitter. If we let r_1 be the link length in meters, then the link-rank is defined as:

$$\text{Link–rank } (A) = \pi r_1^2 \rho \tag{5.1}$$

Govindasamy then shows that in the interference-limited regime that the mean spectral efficiency is primarily a function of link rank rather than the specific value of link length or interferer density. He demonstrates this by showing that the mean spectral efficiency of links with constant length but varying interferer density are nearly identical to the mean spectral efficiency of links with constant interferer density by varying link length as long as the rank remains constant. In order to determine a set of network parameters where networks in interference environments perform substantially better than networks requiring orthogonal transmissions, we compare the mean sum spectral efficiency achieved in two basic protocol schemes in Monte Carlo simulations. We consider networks where we condition on a given number of transmitter-receiver pairs M, with a given link-rank A, where each node-pair has a link-length r_1, n_t and n_r receive antennas, and transmit power P operating over bandwidth B with pathf-loss exponent α. We then consider the average sum spectral efficiency measured at the receiver nodes under two different protocol schemes operating over a duration T where the expectation is taken over node location and realizations of the Rayleigh fading target and interference channels. The two protocol schemes we compare are:

1. Perfectly Scheduled TDMA with zero Interference: In the perfectly scheduled TDMA network, we assume that each node occupies $1/M$th of the duration T. The network radius, link length and link-rank make all nodes are mutually interfering with a high probability. Since the transmission takes place in a noise limited environment, a matched-filter is use for the decoding weights. An illustration of this protocol scheme is given in figure 5-1.

   Since the total power constraint per user over the duration T is power P, in the perfectly scheduled TDMA case, this corresponds to a transmit power PM. For a single transmit-receive pair, the maximum achievable rate is given by:

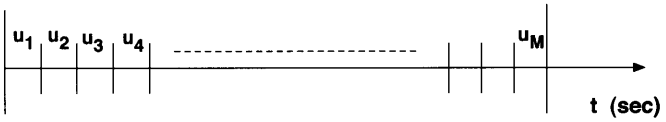

Figure 5-1: Perfectly Scheduled TDMA

$$\frac{1}{M}\log_2\left(1+\frac{PM||\mathbf{h}||^2}{r^\alpha NoB}\right) \tag{5.2}$$

where $\mathbf{h}$ is the $(n_r \times 1)$ channel signature between the transmitter and receiver, and r is the distance between them. Summing over the spectral efficiency of all receive nodes i $\{i|1,\ldots,M\}$ in the network gives:

$$\sum_{i=1}^{M}\frac{1}{M}\log_2\left(1+\frac{PM||\mathbf{h}_i||^2}{r_i^\alpha NoB}\right) \tag{5.3}$$

2. Simultaneous transmissions using MMSE receivers for interference mitigation: In networks where all nodes use MMSE receivers simultaneously while mutually-interfering, all nodes transmit over the entire duration T. An illustration of this protocol scheme is given in figure 5-2.

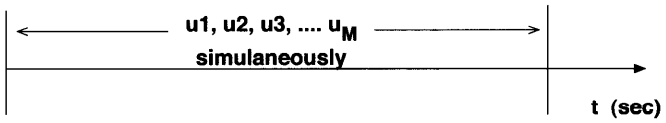

Figure 5-2: MMSE Transmissions

In order to increase degrees of freedom, we consider the use of multiple receive antennas paired with a spread code to be used in a Multi-Carrier CDMA architecture as described in chapter 2. This architecture is used to increase the number of degrees of freedom available to the MMSE receiver which is $n_r \cdot N$ where n_r is the number of receive antennas and N is the length of the spread code. We first consider the use of a single

transmit antenna and n_r receive antennas so that $\mathbf{h}$ is an $(n_r \cdot N \times 1)$ length vector describing the channel between the transmitter and receiver that are separated by a distance r; and K^{-1} is the $(n_r \cdot N \times n_r \cdot N)$ matrix which is the inverse of the interference covariance matrix.For a single transmit-receive pair, the maximum achievable rate is given by:

$$\frac{1}{N}\log_2\left(1+\frac{P}{r^{\alpha}}\mathbf{h}^{\dagger}\mathbf{K}^{-1}\mathbf{h}\right) \tag{5.4}$$

Summing over the spectral efficiency of all receive nodes in the network gives:

$$\sum_{i=1}^{M}\frac{1}{N}\log_2\left(1+\frac{P}{r_i^{\alpha}}\mathbf{h_i}^{\dagger}\mathbf{K}^{-1}\mathbf{h_i}\right) \tag{5.5}$$

This comparison between simultaneous transmissions using MMSE receivers for interference mitigation and perfectly scheduled TDMA mimics optimal performance of our protocol scheme and our benchmark, 802.11, respectively in networks where all nodes are mutually-interfering. Protocols like 802.11 that aim for orthogonal transmissions – where orthogonality requires that any interfering signal be beneath the clear channel assessment (CCA) threshold – the actual sum rate over a particular duration of time in which each of the M nodes is able to receive is on average less than the perfectly schedule rate. Experimental evaluation of 802.11 networks in the literature find that these networks generally spend approximately 1/2 of the time sending actual data, and the rest of the time contending for the medium and carrying out various management functions. Also, a fraction of degrees of freedom in 802.11 are reserved for pilot signals which is an additional cost to the protocol. In addition, any modulation and coding scheme used to send data that uses a spectral efficiency less than the capacity is another protocol loss. There will be similar losses in the networks that we propose, and those losses will be evaluated in later chapters.

In the figures below, we simulate a networks with M = 20 transmit-receive pairs where transmit nodes are uniformly and randomly located in a plane such that when their target

transmitters are placed at a distance of 10 m (link-length $r_1 = 10m$), the link-rank is 3 ($\text{link} - \text{rank} = \pi r_1^2$). Each transmitter node has a single transmit antenna. Each receiver node has 4 receive antennas $n_r = 4$. In figure 5-3(a) we plot the mean spectral efficiency for the receiver nodes averaged over 10,000 networks, as a function of spreading length. As shown in figure 5-3(a), the mean spectral efficiency generated when nodes operate according to a protocol using MMSE receivers to mitigate interference substantially exceeds the mean rate when network nodes use the perfectly scheduled TDMA protocol scheme. In [11], Govindasamy showed that in infinite networks, the optimal spreading length N^* occurs where $N^* \approx \frac{3 \cdot A}{Nr}$, where A is the link-rank. Heuristically, this corresponds to placing nulls on interferers closer that the target transmitter, and using remaining degrees of freedom for beamforming on the target transmitter. Since these peaks are just a function of the rank and Nr, S^* corresponds to an opportune operating point for networks with a given link-rank A and Nr receive antennas. In finite networks, the optimal spreading length N_{opt} is typically less than that predicted in infinite networks $N_{opt} < N^* \approx \frac{3 \cdot A}{Nr}$ since there is typically less total interference seen at a given receiver in a finite network relative to the total interference seen by that same receiver when the distribution of interferers extends to infinity. In figure 5-3(a), the optimal spreading length occurs at $N_{opt} = 2$.

When the link-rank is 1, as shown in figure 5-4(a), the optimal spreading length is 1 (no spreading). Relative to the mean spectral efficiencies in link-rank 3 networks in figure 5-3(a), the link-rank 1 networks have a higher mean spectral efficiency since fewer degrees of freedom are required to null nearby interferers in the link-rank 1 networks.

In all figures where we compare to the perfectly scheduled TDMA rate, as stated earlier, it should be noted that the interference is zero because all nodes are mutually interfering. This is a simulation of perfectly scheduled TDMA, not a simulation of 802.11. Perfectly scheduled TDMA is an upper bound on the performance of 802.11 when all nodes are mutually interfering.

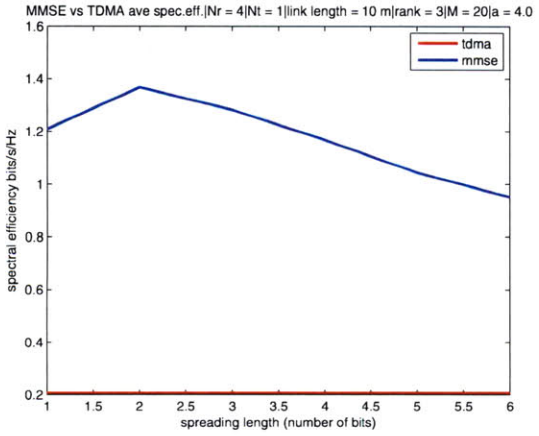

(a) Average Spectral Efficiency per node in Network with MMSE Beamformers

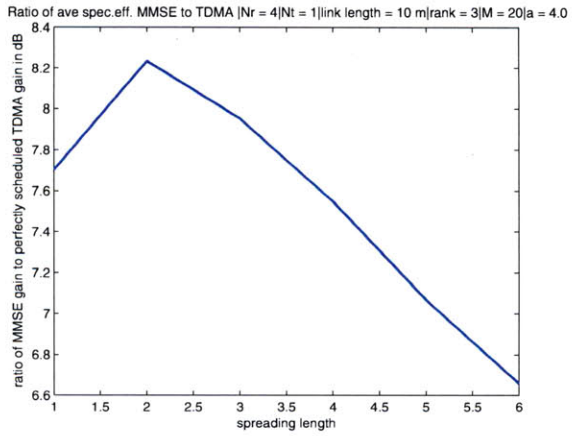

(b) Ratio of Average Spectral Efficiency in MMSE vs Perfectly Scheduled TDMA Network

Figure 5-3: Average Spectral Efficiency in MMSE vs Perfectly Scheduled TDMA Network with 20 Transmit-Receive pairs with 4 Receive Antennas and 1 Transmit Antenna, Link-Rank = 3, and Link Length = 10m

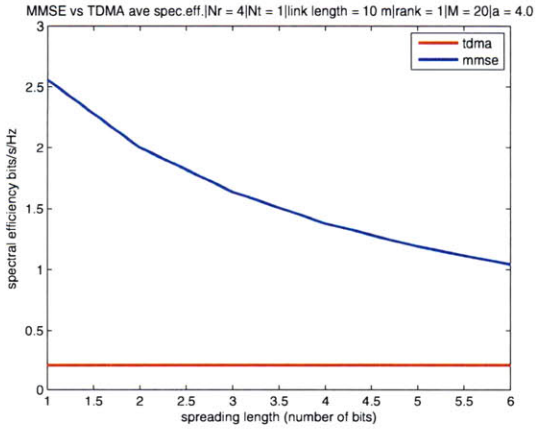

(a) Average Spectral Efficiency per Node in Network with MMSE Beamformers

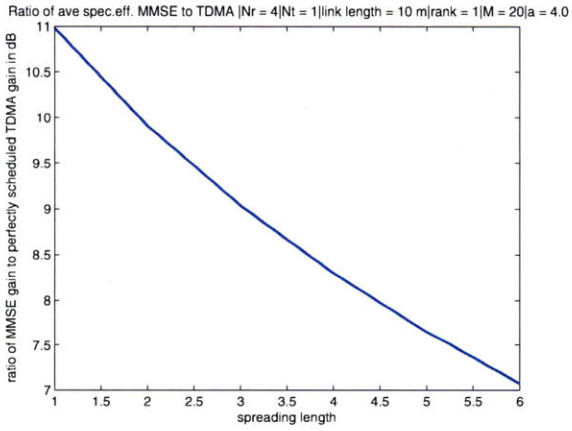

(b) Ratio of Average Spectral Efficiency in MMSE vs Perfectly Scheduled TDMA Network

Figure 5-4: Average Spectral Efficiency in MMSE vs Perfectly Scheduled TDMA Network with 20 Transmit-Receive pairs with 4 Receive Antennas and 1 Transmit Antenna, Link-Rank = 1, and Link Length = 10m

A question a network designer may ask is to understand the value of increasing the number of receive antennas per node in an ad hoc network. In figure 5-5(a) as a function of the number of receive antennas, we consider the performance of networks with 20 transmit-

receive pairs with a fixed link-rank 1. As shown in 5-5(a) the mean spectral efficiency grows linearly with the number of receive antennas per node. Since the link-rank is immaterial in perfectly scheduled TDMA networks, the ratio of the gains in the MMSE case to the gains in the TDMA case are the largest in link-rank 1 networks where the MMSE gains are the largest.

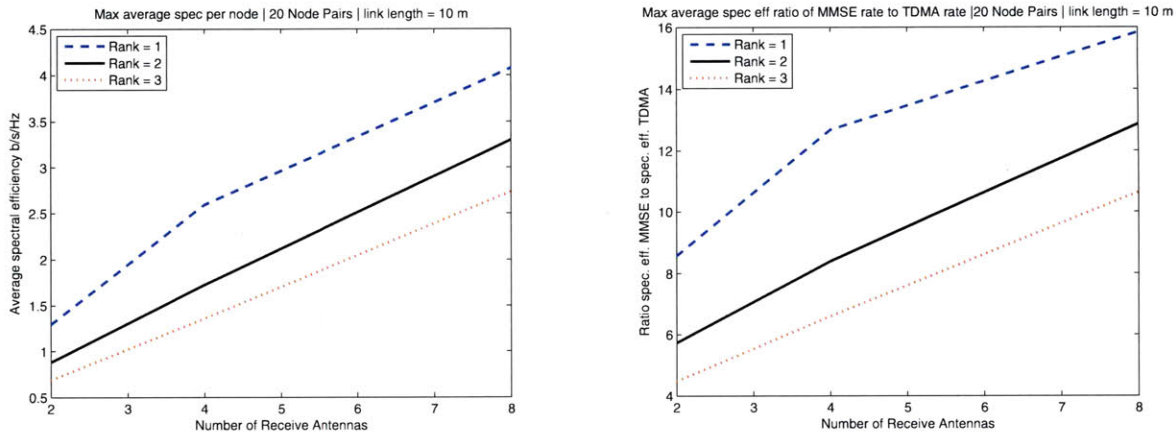

(a) Average Spectral Efficiency in MMSE vs Number of Receive Antennas

(b) Ratio of Average Spectral Efficiency in MMSE vs Number of Receive Antennas

Figure 5-5: Average Spectral Efficiency in MMSE vs Perfectly Scheduled TDMA Network with 20 Transmit-Receive pairs with 1 Transmit Antenna, Link-Rank = 1, varied Number of Receive Antennas and Link Length

A designer might also be concerned with the question of packing nodes into a smaller space, while keeping the link-length fixed. This corresponds to varying the link-rank. If we consider the performance networks with 20 transmit-receive pairs as a function of the link-rank, while keeping the link-length fixed at 10m, as shown in 5-6(a) the mean spectral efficiency also grows linearly with the link-rank. When we fix the link-length and increase the link-rank, this corresponds to decreasing the density of nodes in the network. As the density of nodes increases, the average spectral efficiency per node also increases when the number of transmitter-receiver pairs is kept fixed.

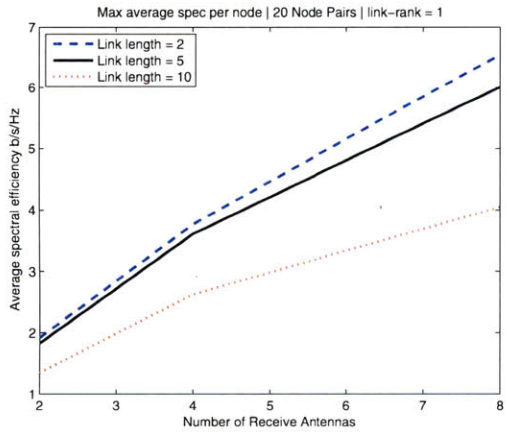

(a) Average Spectral Efficiency in MMSE vs Link-Rank

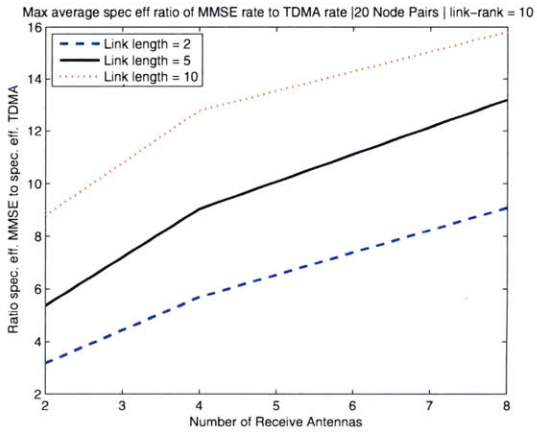

(b) Ratio of Average Spectral Efficiency in MMSE vs Link-Rank

Figure 5-6: Average Spectral Efficiency in MMSE vs Perfectly Scheduled TDMA Network with 20 Transmit-Receive pairs with 4 Receive Antennas and 1 Transmit Antenna and Link Length = 10m, variable Link-Rank

In this work we choose parameters that reflect typical sizes of today's networks, and some other networks of interest that reflect common research areas, and network sizes where our schemes perform particularly well. In the first area of our parameter space we consider a simple network that could correspond to a home environment in which multiple wireless terminals such as laptops are used in a shared space. In this network, we let the number of transmitter and receiver pairs $M = 4$. We vary the link-rank over { 1, 2, 3 }. We vary the link-length over { 2m, 10m}. We vary the number of receive antennas { 2, 4, 8 }. We also consider networks with $M = 4$ transmit and receive pairs and link lengths of $50\,m$ and link-rank = 1 in order to evaluate the performance of a network where nodes are operating in near noise limited environments. We also consider link lengths of $50\,m$ with link-rank = 3 in order to explore use of this protocol when links are transmitting over longer distances, conceivably performing as backbone. We always choose the spreading length that corresponds to the optimal N^*. As shown in figure 5-7(a), for a given link-rank, a given link-length, and a fixed number of node-pairs, as the number of receive antennas increases, the average sum spectral efficiency increases. Since there is less interference in these networks with far fewer transmit-receive pairs, the average spectral efficiencies per node are much higher. And since

the degrees of freedom are shared with fewer other transmit-receive pairs in the perfectly scheduled TDMA scheme, the ratio of the MMSE scheme mean spectral efficiency to the TDMA scheme mean spectral efficiency is lower.

As shown in figure 5-7(a), the spectral efficiency in networks with M=4 transmitter-receiver pairs grows linearly as a function of the number of receive antennas. For a given number of receive antennas and a fixed link length, if we increase the link-rank, the average spectral efficiency per node decreases. This is shown in figure 5-8(b). And for a fixed link-rank, if we increase the link length, then the mean spectral efficiency decreases as shown in figure 5-8(a).

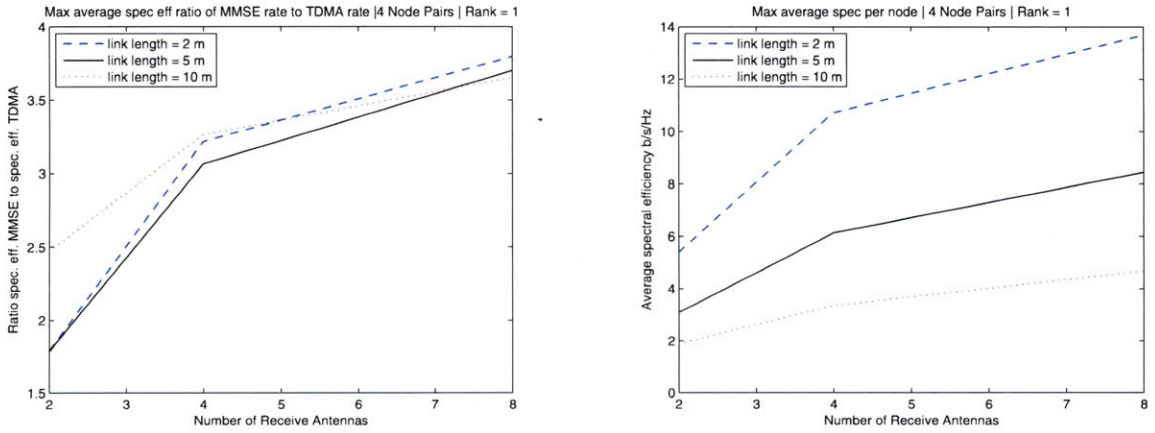

(a) Ratio of Average Spectral Efficiency in MMSE vs number of Receive Antennas

(b) Average Spectral Efficiency per Node

Figure 5-7: 4 Node Pairs (M = 4) & Link-Length = 10m & Rank = 1, Variable number of Receive Antennas

These same relationships between link-rank, link-length and the number of receive antennas is represented in the third area of our parameter space where we consider networks with a larger number of nodes. In these networks, we let the number of transmitter and receiver pairs $M = 40$. We vary the link-rank over { 1, 2, 3 }. We vary the link-length over { 2m, 10m}. We vary the number of receive antennas { 2, 4, 8 }. If we consider the mean spectral efficiency performance of nodes in a network with link-rank 1 and vary the number of receive

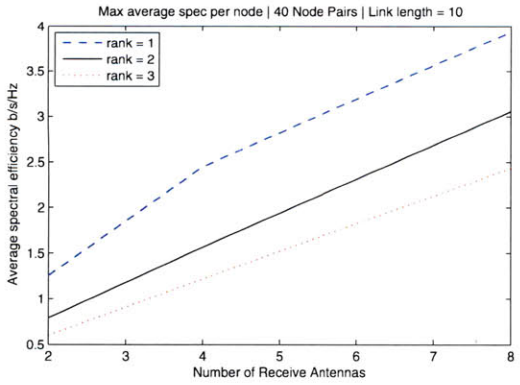

(a) Ratio of Average Spectral Efficiency in MMSE to Perfectly Scheduled TDMA Network versus Link-Rank

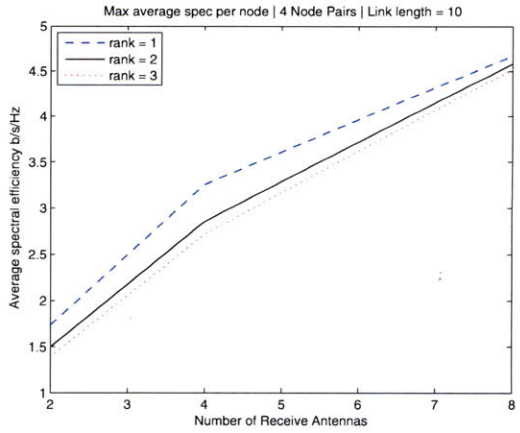

(b) Average Spectral Efficiency per Node

Figure 5-8: 4 Node Pairs (M = 4) & Link Length = 10, 4 Receive Antennas, Variable Link-Rank

antennas, as shown in figure 5-9(a), the spectral efficiency grows linearly with the number of receive antennas; and the gain over perfectly scheduled TDMA is substantial as shown in figure 5-9(b).

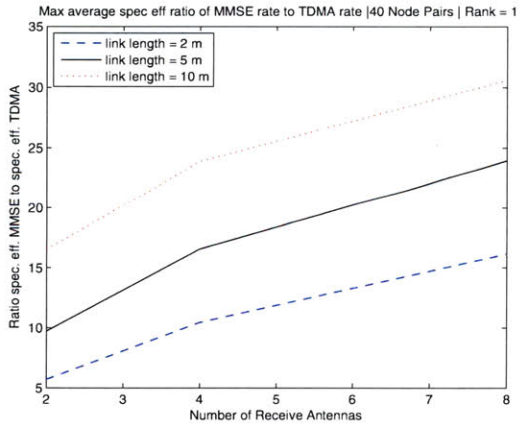

(a) Ratio of Average Spectral Efficiency in MMSE to Perfectly Scheduled TDMA Network

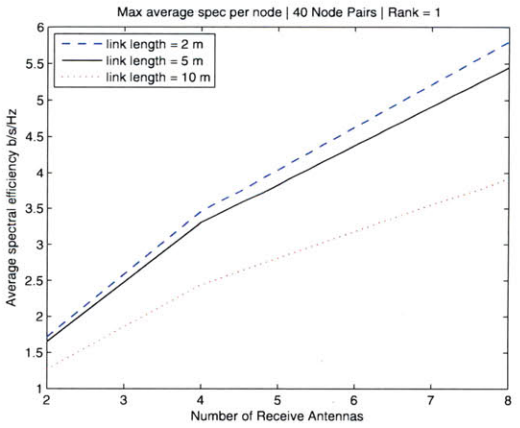

(b) Average Spectral Efficiency per Node

Figure 5-9: 40 Node Pairs (M = 40) & Rank = 1

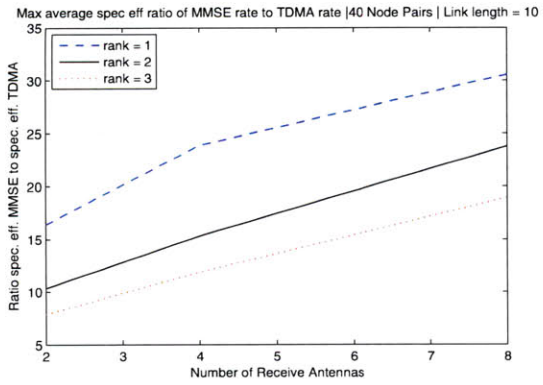

(a) Ratio of Average Spectral Efficiency in MMSE to Perfectly Scheduled TDMA Network

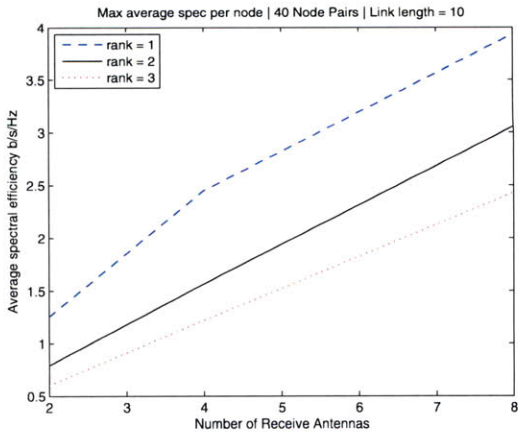

(b) Average Spectral Efficiency per Node

Figure 5-10: 40 Node Pairs (M = 40) & Link Length = 10

As can be seen from the figures above, increasing the number of transmit receive pairs in a network while keeping the link length, number of receive antennas, and link rank fixed serves to decrease the spectral efficiency per node. This relationship is shown more succinctly in figure 5-12(b). While the mean spectral efficiency per node decreases with increasing transmit-receive pairs, the ratio of mean spectral efficiency in the MMSE scheme to the TDMA scheme grows linearly with the number of transmit receive pairs.

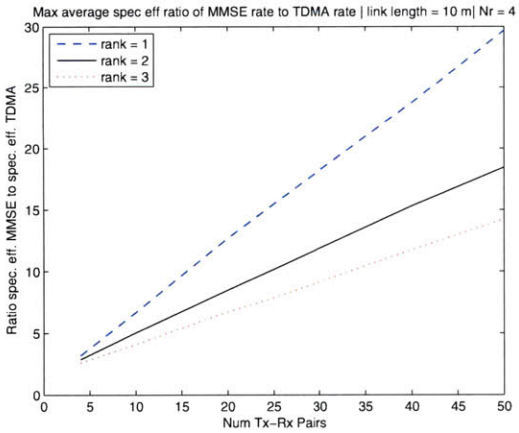

(a) Ratio of Average Spectral Efficiency in MMSE to Perfectly Scheduled TDMA Network

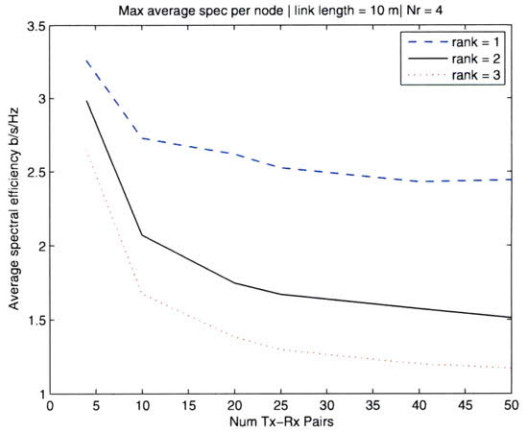

(b) Average Spectral Efficiency per Node

Figure 5-11: Average Spectral Efficiency versus Number of Transmit-Receive Node Pairs versus Rank

Similarly, if we fix the link-length at 10m, the number of receive antennas at 4, and if we vary the number of transmit-receiver pairs M, the same relationship between the number of transmit-receive pairs and the mean spectral efficiency per node for link-length = 2m.

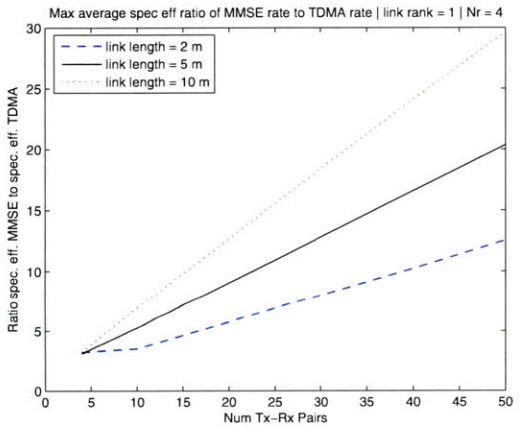

(a) Ratio of Average Spectral Efficiency in MMSE to Perfectly Scheduled TDMA Network

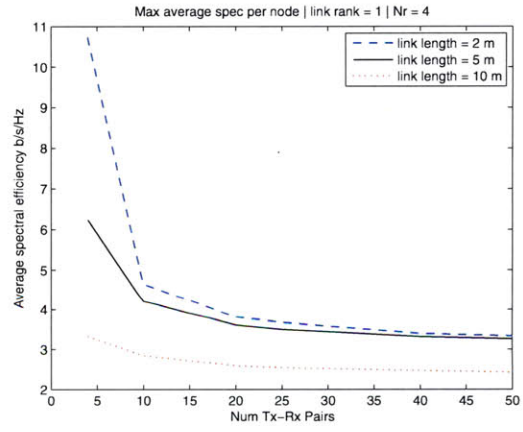

(b) Average Spectral Efficiency per Node

Figure 5-12: Average Spectral Efficiency versus Number of Transmit-Receive Node Pairs versus Link Length

5.2 Characterization of Ad Hoc Networks with varying Transmit Schemes

In the networks considered in this work, we will employ uninformed transmissions with transmit covariance matrix rank of 1 and 2; and we will employ informed transmissions with transmit covariance matrix rank of 1 and 2. The analytic relationship between the peak mean spectral efficiency, link-rank, and number of transmit antennas n_t, receive antennas and the spreading length is not clear for $n_t > 1$. It is consistently the case, however, that for strongest mode transmissions, the spreading length at which the peak occurs is less than $\frac{3 \cdot A \cdot n_{t-\text{rank}}}{n_r}$. In the figures below we first compare the mean spectral efficiency, as a function of the spreading length, for the transmit schemes we consider in this work. We will then determine the peak mean spectral efficiency and the spreading length at which the peak occurs as a function of the number of transmit and receive antennas, the link-rank, and the link length.

First considering networks with M = 20 transmit-receive pairs, the maximum sum spectral efficiency is achieved when each node in the network uses an informed transmitter transmit-scheme using its strongest transmit mode with no spreading (spreading length = 1). As shown in figure 5-13, for M=20, all nodes using their strongest mode to transmit just exceeds using the two strongest modes to transmit. When nodes use the two strongest modes to transmit, there is double the interference relative to strongest mode transmissions which lowers the SINR for each stream. That average decrease in SINR in the 2 strongest modes is apparently more substantive than the gain in spectral efficiency of receiving two streams relative to strongest mode transmission. Comparing strongest mode transmission to transmissions with a single transmit antenna produces gains that are consistently approximately 30 %. Using an uninformed transmitter with transmit covariance rank equal to 2 always under performs using the 2 strongest modes with an informed transmitter, as expected.

In networks with M=4 transmit-receive pairs where there is less total interference, the peak

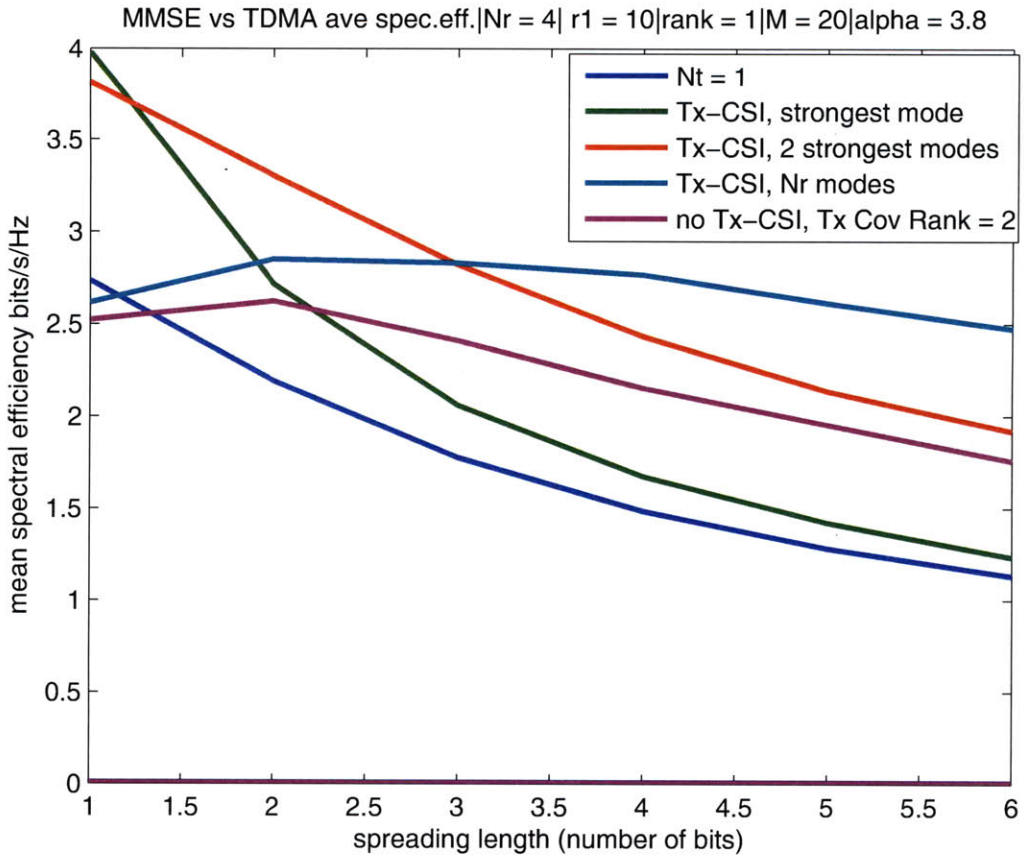

Figure 5-13: Comparison of Mean Spectral Efficiency as a function of Spreading Length for 5 Transmit Schemes in a Network with 20 Transmit-Receive Pairs, 4 Receive Antennas, Link Length = 10m, and Link-Rank = 1

of the average sum spectral efficiency (as shown in figure 5-14) is achieved when there is no spreading (spreading length = 1), and is achieved when the transmit strategy in use is an informed transmitter with the strongest 2 modes (when the rank of the transmit covariance matrix is 2). In this small network with a link-rank equal to one, the signal power is strong enough, and the interference low enough, that when 2 degrees of freedom are used for interference nulling, the remaining degrees of freedom on the target transmitter still exceeds the sum rate when just one degree of freedom is used for interference nulling and the transmit covariance rank is 1. However, in networks with M=40 transmit-receive pairs (figure 5-15), the results parallel those of networks with M = 20 transmit-receive pairs. The peak of the

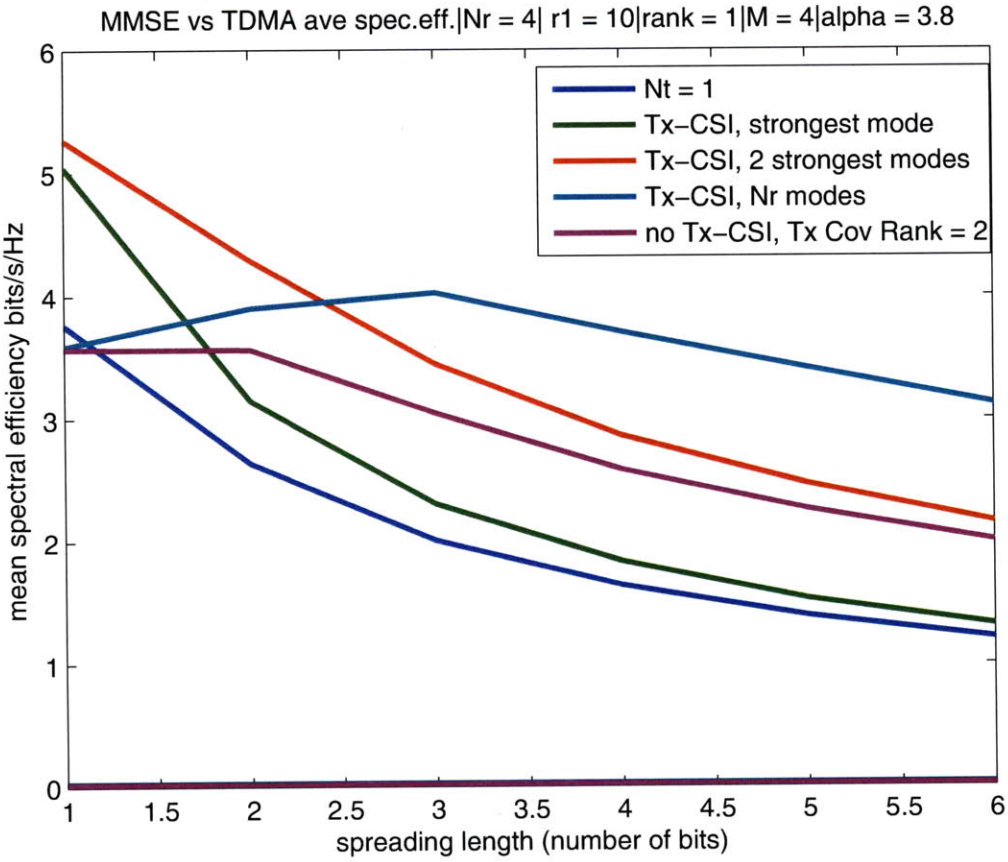

Figure 5-14: Comparison of Mean Spectral Efficiency as a function of Spreading Length for 5 Transmit Schemes in a Network with 4 Transmit-Receive Pairs, 4 Receive Antennas, Link Length = 10m, and Link-Rank = 1

average spectral efficiency is achieved with strongest mode transmission with no spreading (spreading length = 1). In the case of M = 40, as in the case of M=20, the additional interference drives SINR lower and produces data rates that are lower than the rates when just the strongest mode is used. If we decrease the link length in networks with M=4 transmit-receive pairs, this effectively increases the level of interference. As shown in figure 5-16, the peak of mean spectral efficiency is then obtained using the strongest mode transmit strategy.

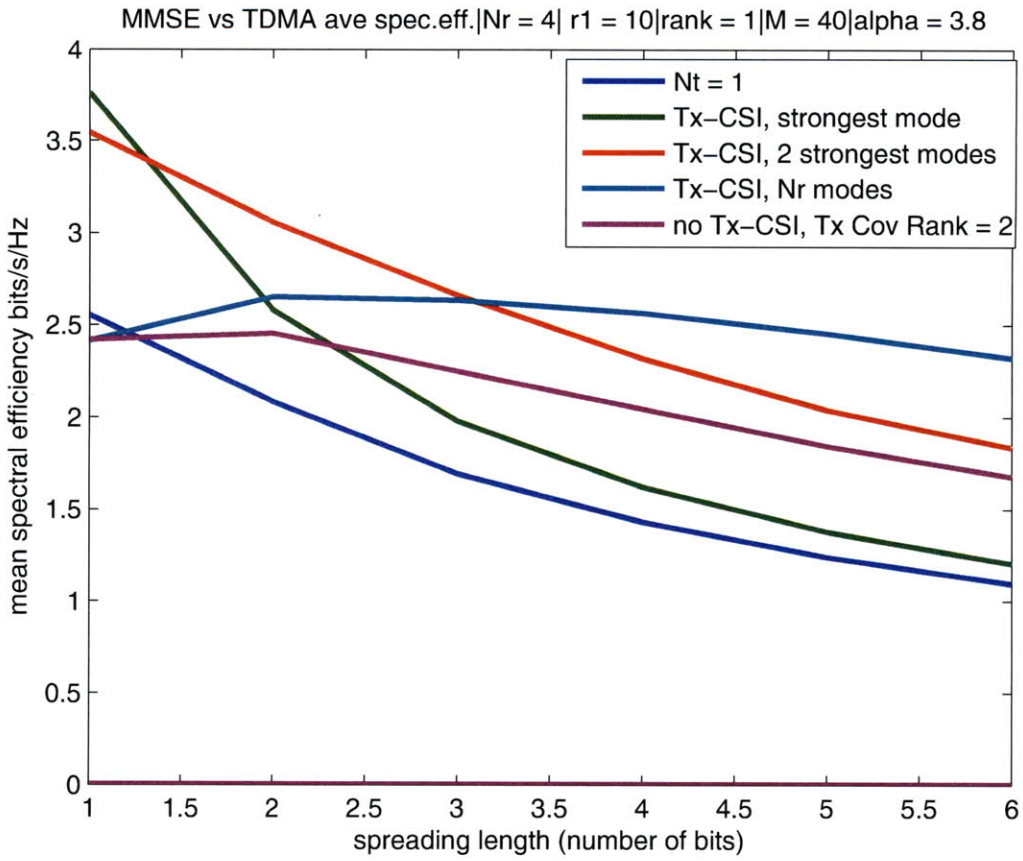

Figure 5-15: Comparison of Mean Spectral Efficiency as a function of Spreading Length for 5 Transmit Schemes in a Network with 40 Transmit-Receive Pairs, 4 Receive Antennas, Link Length = 10m, and Link-Rank = 1

If we now consider how the peak of the mean spectral efficiency varies as a function of the number of receive antennas, in figures 5-17(a) and 5-17(a), we see that using the two strongest transmit modes in networks with M=4 and M=20 link-rank 1 and 10m link length networks achieve the highest sum spectral efficiencies. But relative to perfectly scheduled TDMA networks – as shown in figures 5-17(b) and 5-18(b) – all transmitters using the single strongest mode achieves the highest gain.

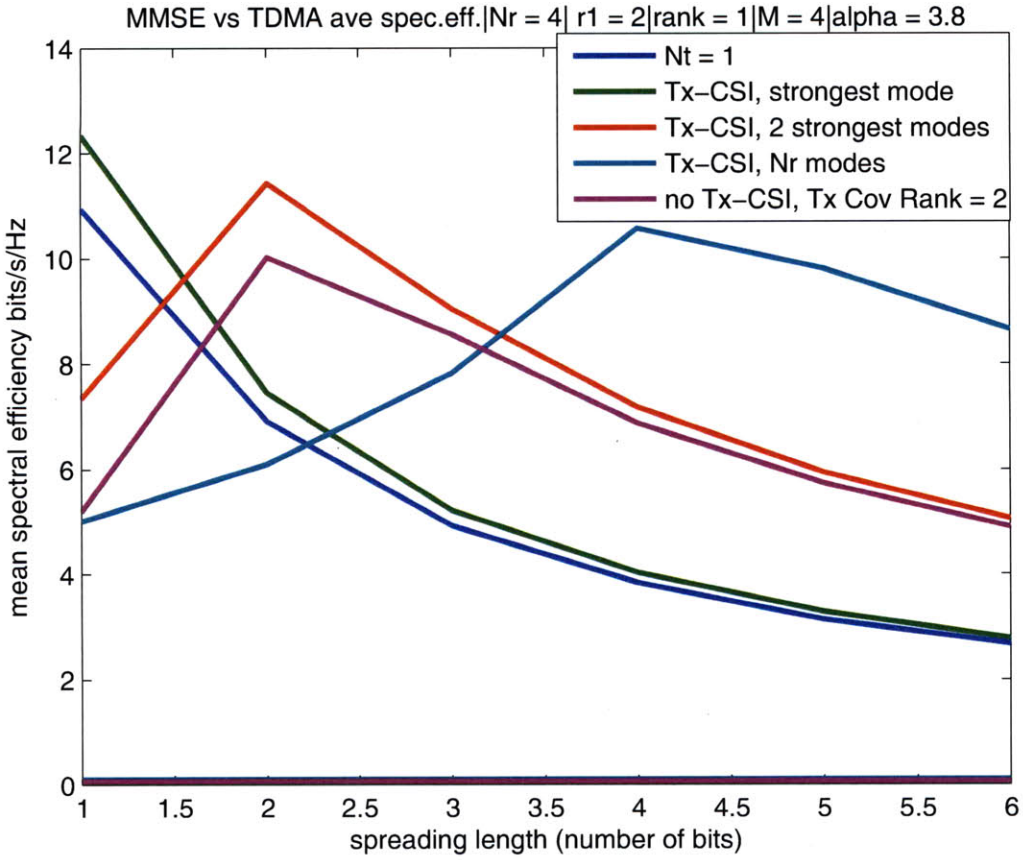

Figure 5-16: Comparison of Mean Spectral Efficiency as a function of Spreading Length for 5 Transmit Schemes in a Network with 4 Transmit-Receive Pairs, 4 Receive Antennas, Link Length = 2m, and Link-Rank = 1

If we now consider how the peak of the mean spectral efficiency varies as a function of the link-length, as shown in figures 5-20(a) and 5-19(a), with increasing link length, the spectral efficiency decreases. Figure 5-20(b) also demonstrates the relative benefit in the mean spectral efficiency of informed transmitters over uninformed transmitters. Again, when the transmit covariance rank is 2, the mean spectral efficiency per transmitter increases due to the additional stream; and the interference environment has approximately twice the interference. From figure 5-20(b), the net effect leaves the mean rate equivalent to strongest mode transmissions in environments where each interferer has a transmit-covariance-rank of 1.

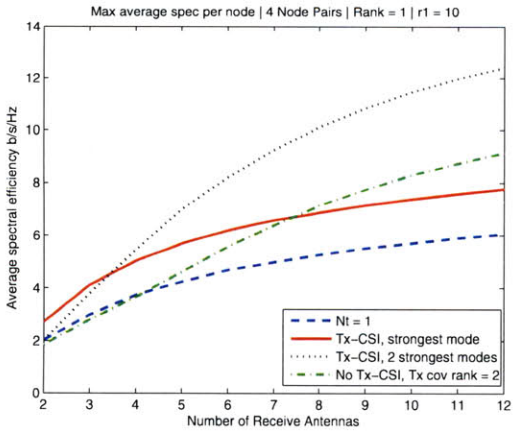

(a) Average Spectral Efficiency per Node

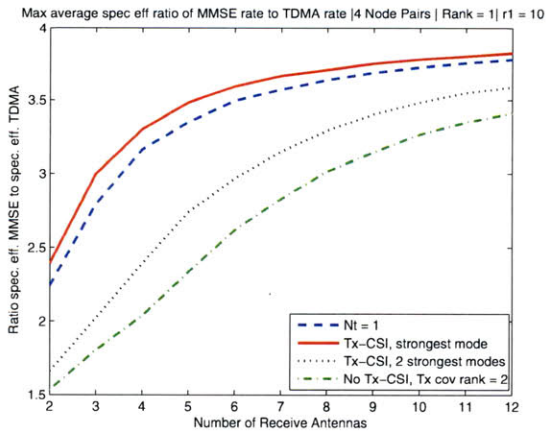

(b) Ratio of Average Spectral Efficiency in MMSE to Perfectly Scheduled TDMA Network

Figure 5-17: Average Spectral Efficiency versus Number of Receive Antennas by Transmit Scheme for M=4

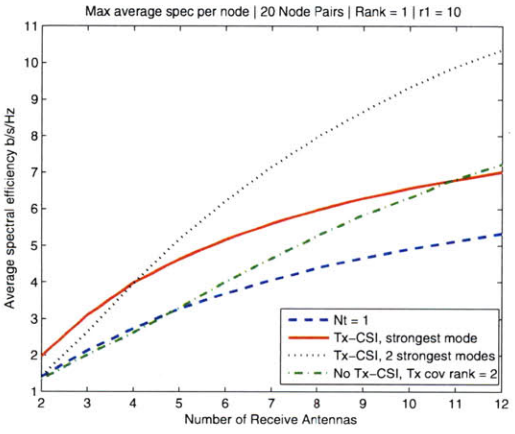

(a) Ratio of Average Spectral Efficiency in MMSE to Perfectly Scheduled TDMA Network

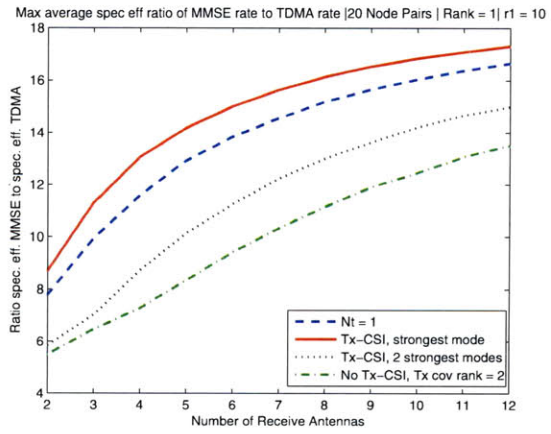

(b) Average Spectral Efficiency per Node

Figure 5-18: Average Spectral Efficiency versus Number of Receive Antennas by Transmit Scheme for M=20

If we now consider how the peak of the mean spectral efficiency varies as a function of the link-rank, for the cases where the number of transmit-receiver pairs are 20 and 40, strongest mode transmission dominates for all link-ranks as shown in figures 5-22(b) and 5-23(b). However, for M=4, transmitting in the two strongest modes yields the highest mean spectral efficiency for link-rank = 1. Relative to the cases with M=20 and M=40, each receiver

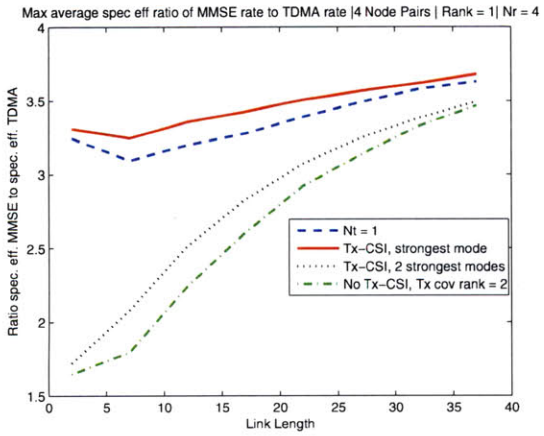

(a) Ratio of Average Spectral Efficiency in MMSE to Perfectly Scheduled TDMA Network

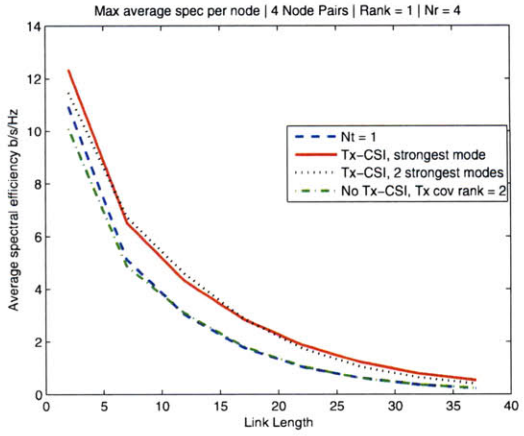

(b) Average Spectral Efficiency per Node

Figure 5-19: Average Spectral Efficiency versus Link-Length by Transmit Scheme for M=4

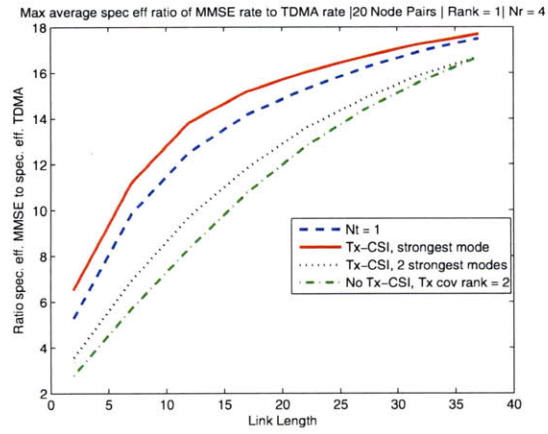

(a) Ratio of Average Spectral Efficiency in MMSE to Perfectly Scheduled TDMA Network

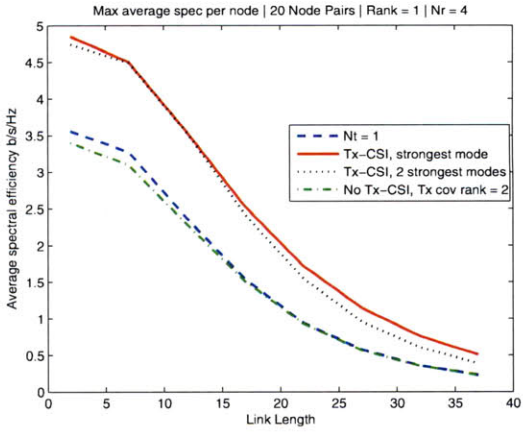

(b) Average Spectral Efficiency per Node

Figure 5-20: Average Spectral Efficiency versus Link-Length by Transmit Scheme for M=20

in the M=4 case experiences a lower interference level which allows the additional stream in the transmit-covariance-rank=2 case to surpass the strongest mode case for rank =1 links.

To summarize, the mean spectral efficiency when using strongest mode transmission relative to single transmit antenna is typically approximately 30 % at the spreading length corresponding to the peak spectral efficiency. When using multiple transmit modes, peak spectral

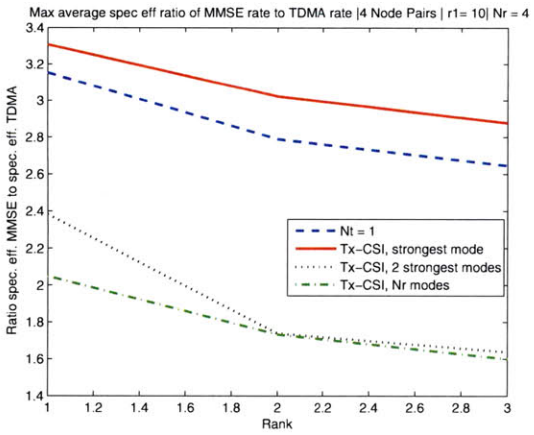

(a) Ratio of Average Spectral Efficiency in MMSE to Perfectly Scheduled TDMA Network

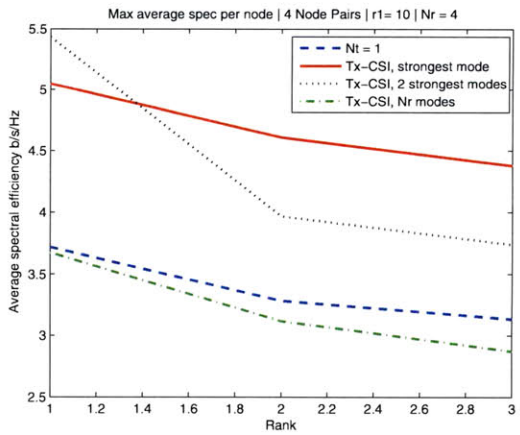

(b) Average Spectral Efficiency per Node

Figure 5-21: Average Spectral Efficiency versus Link-Rank by Transmit Scheme for M=4

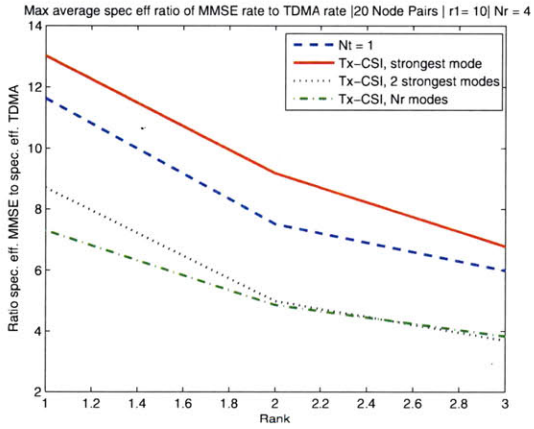

(a) Ratio of Average Spectral Efficiency in MMSE to Perfectly Scheduled TDMA Network

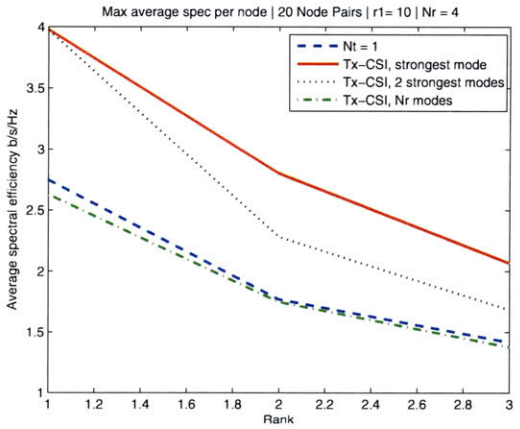

(b) Average Spectral Efficiency per Node

Figure 5-22: Average Spectral Efficiency versus Link-Rank by Transmit Scheme for M=20

efficiencies require a higher level of spreading. The gains per node are strongest in networks that are less dense.

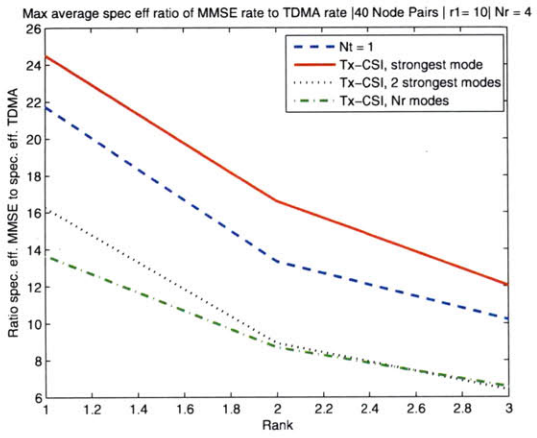

(a) Ratio of Average Spectral Efficiency in MMSE to Perfectly Scheduled TDMA Network

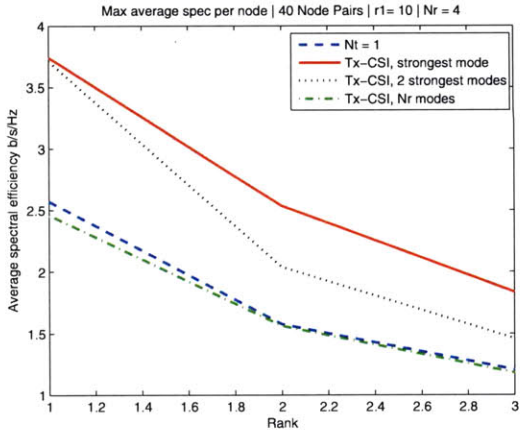

(b) Average Spectral Efficiency per Node

Figure 5-23: Average Spectral Efficiency versus Link-Rank by Transmit Scheme for M=40

5.3 Protocol Specific Variables

Packet length and the degrees of freedom reserved for control are two important variables affecting achievable data rates and delays. The short control channel packets allow the protocol to spend fewer resources on control. Long data packets increase the fractional time nodes spend transmitting data in the coherence bandwidth exceeds the packet duration; and longer packets reduce the amount of time a given transmitter-receiver node pair spends contending for the channel.

5.3.1 Packet Length

The packet length has clear and direct effects on sum rates and delays. Longer data packets are beneficial in stable channels. Shorter data packets are beneficial in less-stable channels. For this work we use the same parameters as the 802.11(n) benchmark.

5.3.2 Number of Degrees of Freedom Alloted for Control

When there is a fixed total bandwidth B separated into K orthogonal tones of bandwidth $B/K = \tau_s$, where K_{cc} tones will be used for the control channel, there is a tradeoff between

the total number of degrees of freedom reserved for the control channel and the achievable sum rates and delays seen on the data channel. If we let $K_{dc} = K - K_{cc}$ be the number of data channel tones, τ_s is the duration of an OFDM symbol, b_{dc} be the number of bits in a data channel packet, d_{dc} be the number of bits used on each tone for training and detection for data packets, and let a be the total number of bits per symbol, then the duration of a data channel packet T_{dc} is given by:

$$T_{dc} = \left(\frac{\frac{b_{dc}}{a}}{K_{dc}} + d_{dc} \right) K\tau_s \tag{5.6}$$

And if we let b_{cc} be the number of bits in a control channel packet and let d_{cc} be the number of bits used on each tone for training and detection on the control channel, then the duration of a control channel packet T_{cc} is given by:

$$T_{cc} = \left(\frac{b_{cc}}{K_{dc}} + d_{dc} \right) K\tau_s \tag{5.7}$$

If there are N_{cc} control channel slots, the total duration of the control channel is given by $N_{cc}T_{cc}$. Then the maximum bandwidth used for the transmission of data B_d is given by:

$$B_d = \frac{T_{dc}K_{dc}}{T_{cc}N_{cc} + T_{dc}(K_{dc} + K_{cc})}B \tag{5.8}$$

For the control channel in frequency, the number of control channel slots is given by:

$$N_{cc} = T_{dc}/T_{cc} \tag{5.9}$$

For the control channel in time, N_{cc} is more flexibly defined.

5.3.3 Simulation Parameters

In the following simulations we investigate the performance of the STI-MAC protocols as a function of several key parameters:

- Number of Transmit-Receive Pairs
- Number of Receive Antennas
- Transmit Scheme
- Link-Length
- Link-Rank
- Offered Load
- Requested Load

The performance of the protocols is measured according to the distribution of the achievable rates, sum rates, delays, observed probability of outage and fairness. We hope to show the sensitivity of the protocol to these parameters to support network designers in determining what parameter values to select in building real networks.

There are 3 key areas that we explore in our parameter space. The first corresponds to a 'typical network.' This is a network with 20 transmit-receive pairs is intended to model a typical office environment or coffee shop where multiple users are accessing wireless service. Using 4 receive antennas is typical of 802.11(n) users, and is feasible for a variety of devices.[1] We benchmark these results relative to simulations of the 802.11(n) network. From there we pivot to the second area of our parameter space where we examine a key question for the designers of these networks: the value of multiple antennas. In SIM2 and SIM3 we use 8 and 2 receive antennas respectively and consider network performance along these key metrics. Finally, the third key area of our parameter space models networks where our protocol does particularly well. This also corresponds to the future networks we forsee, in which many users will interact to share the medium, and have multiple antennas given the gains that multiple antennas offer. In this area of our parameter space, nodes have 8

[1] An inter-element antenna spacing of $1/2$ wavelength corresponds to approximately 3 cm for transmissions in the 5GHz range. This inter-element spacing is feasible for devices including current iPod-minis, cell phones, net-books, and laptops.

transmit and receive antennas, have a link-length of 10m, a link-rank = 3, and use channel state information at the transmitter. We benchmark these results relative to the 802.11(n) protocol.

Chapter 6

Parameter Optimization

In the last section we discussed network operating points as a function of link length, link-rank, the number of transmit and receive antennas and the transmit scheme. In this section we discuss the optimization of parameters that allow networks to achieve the average data rates associated with these operating points. The key parameters that will influence performance are the channel estimation scheme and the ratio of the control channel degrees of freedom to the data channel degrees of freedom. Following the parameter optimization carried out in this chapter, in the next chapter we will discuss simulation results.

6.1 Channel Estimation

In order for nodes to decode transmitted packets, receiver nodes require receiver beamforming weights that mitigate the effects of the channel on transmitted symbols. As described in chapter 2, the effects of the channel include a multiplicative component which results from the constructive and destructive interference of the multiple refracted signal components that arrive at the receiver, and which in this work we model as Rayleigh fading. The effects of the channel also include an additive component of white Gaussian noise, and interference from other transmitting nodes.

The optimal receiver beamforming weights are composed of a whitening filter $\mathbf{K}^{-1/2}$ that mitigates the additive interference and noise, and the projection of the received signal $\mathbf{Y}$ onto the product of target channel and the whitening filter $\left(\mathbf{K}^{-1/2}\mathbf{H}\right)^{\dagger}\mathbf{K}^{-1/2}\mathbf{Y}$. We define $\mathbf{K}$ as the asymptotic interference channel and H as the asymptotic target channel, and the optimal beamforming weights are thus $\mathbf{K}^{-1}\mathbf{H}$. To estimate these optimal weights, a known pseudo-random signal $\mathbf{X}$ of length N is sent from the transmitter to the receiver. When there are n_t transmit antennas, $\mathbf{X}$ is a $(n_t \times N)$-size matrix. At the receiver, a least-squares estimator is used to gain an estimate of the target channel $\mathbf{H}$. The least squares estimator, which is widely used in practice, is the maximum-likelihood estimator of a unknown signal in interference [99]:

$$\hat{\mathbf{H}} = \mathbf{Y}\mathbf{X}^{\dagger}(\mathbf{X}\mathbf{X}^{\dagger})^{-1} \tag{6.1}$$

To estimate the interference covariance matrix, the same $(n_r \times N)$ received matrix Y used to estimate the target channel is used to construct the sample interference covariance matrix:

$$\hat{\mathbf{K}} = \frac{1}{N}\mathbf{Y}\mathbf{Y}^{\dagger} \tag{6.2}$$

When the transmitted estimation sequence $\mathbf{X}$ is Gaussian, the sample interference covariance matrix $\hat{\mathbf{K}}$ is the maximum-likelihood estimator of the asymptotic interference covariance matrix $\mathbf{K}$ [100]. When the distribution on $\mathbf{X}$ is non-Gaussian, the distribution is unknown. But as shown below via simulation, the convergence properties are similar.

As the length of the training sequence increases, the performance of the estimated beamforming weights $\hat{\mathbf{w}} = \left(\frac{1}{N}\mathbf{Y}\mathbf{Y}^{\dagger}\right)^{-1}\hat{\mathbf{H}}$ approaches the performance of the asymptotic weights $\mathbf{w} = \mathbf{K}^{-1}\mathbf{H}$, where the performance measure is mean squared error of the average-SINR as a function of the length of the training length N and the number of degrees of freedom at the receiver n_r:

$$E\left[\left(SINR_{asyp}(n_r) - \hat{SINR}(N, n_r)\right)^2\right] \tag{6.3}$$

where we define the average-SINR $E[SINR_{asyp}(n_r)]$ to be:

$$E[SINR_{asyp}(n_r)] = \frac{E\left[\mathbf{w}^\dagger \mathbf{H}\mathbf{X}\mathbf{X}^\dagger \mathbf{H}^\dagger \mathbf{w}\right]}{E\left[\mathbf{w}^\dagger \left(\sum \mathbf{H_j}\mathbf{X_j} + \mathbf{W}\right)\left(\sum \mathbf{H_j}\mathbf{X_j} + \mathbf{W}\right)^\dagger \mathbf{w}\right]} \tag{6.4}$$

where $\mathbf{w}$ is the $(n_r \times 1)$ asymptotic beamforming weights vector, $\mathbf{H}$ is the target channel and $\mathbf{K}$ is the interference covariance matrix. The expectations in equation 6.4 are taken over channel realizations { target channel: $\mathbf{H}$, interference channels: $\mathbf{H_1}, \ldots, \mathbf{H_j}$ }, transmit matrices { target transmissions: $\mathbf{X}$, interference transmissions: $\mathbf{X_1}, \ldots, \mathbf{X_j}$ }, and additive white Gaussian noise matrices $\mathbf{W}$. The average-estimated-SINR $E[\hat{SINR}(N, n_r)]$ is defined identically except the estimated weights $\hat{\mathbf{w}}$ defined in equation 6.5 are substituted for the asymptotic weight $\mathbf{w}$:

$$\hat{\mathbf{w}} = \left(\frac{1}{N}\mathbf{Y}\mathbf{Y}^\dagger\right)^{-1} \hat{\mathbf{H}} \tag{6.5}$$

where $\hat{\mathbf{w}}$ is the $(n_r \times 1)$ estimated beamforming weights vector, $\mathbf{H}$ is the target channel and $\mathbf{K}$ is the interference covariance matrix. In this work, we will use the random variable $SINR$ to mean the Signal-to-Interference-plus-Noise-Ratio given a particular (target and interference) channel realization $\mathbf{H}, \mathbf{H_1}, ..., \mathbf{H_j}$:

$$SINR = \frac{E\left[\mathbf{w}^\dagger \mathbf{H}\mathbf{X}\mathbf{X}^\dagger \mathbf{H}^\dagger \mathbf{w} \middle| \mathbf{H}, \mathbf{H_1}, ..., \mathbf{H_j}\right]}{E\left[\mathbf{w}^\dagger \left(\sum \mathbf{H_j}\mathbf{X_j} + \mathbf{W}\right)\left(\sum \mathbf{H_j}\mathbf{X_j} + \mathbf{W}\right)^\dagger \mathbf{w} \middle| \mathbf{H}, \mathbf{H_1}, ..., \mathbf{H_j}\right]} \tag{6.6}$$

The expectations in 6.6 are taken over transmit vectors $\mathbf{X}, \mathbf{X_1}, \mathbf{X_2}, ..., \mathbf{X_j}$ and noise vectors $\mathbf{W}$.

A few authors have considered this problem analytically when the transmit signals are Gaussian. In Reed, Mallett and Brennan [101], the authors derive a statistical relationship on the ratio of the SINR obtained when the sample interference covariance matrix is used to

construct MMSE beamforming weights, and the SINR obtained when the asymptotic beamforming weights are used. They assume that the noise and interference have a complex Gaussian distribution. This statistical relationship is a function of the number of snapshots S used to construct the sample interference covariance matrix, and N, the number of degrees of freedom of the MMSE beamforming weights. Letting ρ be the expectation ratio of the sampled-ICM-SINR to the asymptotic-ICM-SINR, where $0 \leq \rho \leq 1$:

$$f(\rho(K,N)) = \frac{S+2-N}{S+1} \tag{6.7}$$

In order for the probability that the sample-ICM-SINR diverges from the asymptotic SINR by more than 3dB to be less that 0.3 % ($P(\rho(S,N) < 1/2) \leq .003$), then $S > 4N$ samples are required. Boronson et al [102] extended this result to consider the case when the target channel is not known exactly and when the sample interference covariance matrix contains the target channel and when the target channel estimate also contains some error. His essential conclusion is that additional snapshots are required over the Reed result.

In practical use of the sample-matrix-inversion algorithm (SMI), several have showed that the algorithm generates a pattern with distorted mainbeams and high sidelobes [103]. In [104], Carlson explains the distortion of the beams as resulting from distortions in the eigenvectors of the interference covariance matrix that are misaligned from the interference plane waves they seek to null. This misalignment behaves like other interferers at relatively low power levels, and distracts the nulling from the strong (and actual) interferers. This effect can be countered by diagonal loading the covariance matrix. This raises the noise level beyond that of the distortions in the interference covariance matrix but lower than the strong interferers (leaving the eigenvectors unchanged), desensitizing the interference covariance matrix from the (false) weak interferers.

In practice, discrete, zero-mean random variables which are signal constellations for a phase-shift-keying or quadrature-amplitude-modulation (QAM) scheme will be used. Though in-

tractable analytically, we determine via simulation the training lengths required for the average achieved spectral efficiency to be within some threshold of the mean of the asymptotic results. We consider the performance as a function of training length by simulation in each area of our parameters space: number of transmit-receive pairs $\{M|4, 20, 40\}$, number of receive antennas $\{Nr|4, 20, 40\}$, transmit schemes { TxS — Uninformed transmitter with Tx-covariance rank = 1, Uninformed transmitter with Tx-covariance rank = 2, Informed transmitter with Tx-covariance rank = 1, Informed transmitter with Tx-covariance rank = 2 }. As described in chapter 2, when the interference covariance matrix contains the target channel, the MMSE weights are simply multiplied by a scale factor which is less than 1, and which cancels out in the SINR computation. In the simulations described below, we separately compute the average SINR when the sample interference covariance matrix contains the target channel and when the sample interference matrix does not contain the target channel in order to verify the performance in each case.

6.2 Estimation of Receiver Beamforming Weights, Mean Signal-to-Interference-plus-Noise Ratio(SINR) and Mean Spectral Efficiency

Here we briefly describe the algorithms used to compute the mean SINRs and mean spectral efficiencies, where the mean SINRs and spectral efficiencies are computed as a function of the training length used to estimate the beamforming weights. A given network is generated by randomly placing M transmitting nodes uniformly and randomly in a circular area of size $\sqrt{\frac{Mr_1^2}{A}}$ where A is the link-rank and r_1 is the link-length. Receiver nodes are then placed a distance r_1 from their target transmitter nodes. Target channels and interference channels are then generated between all $2M$ nodes. Size $(n_t \times N)$ BPSK transmit data is generated pseudo-randomly for all transmit nodes, and is used for the least-squares estimation of the target channel and for the construction of the interference covariance matrix.

The receiver-beamforming-weights can be jointly estimated using known transmit signals sent from the target transmitter, used to construct the interference covariance matrix, and used to estimate the target channel. As noted in chapter 2, when the target channel is contained in the interference covariance matrix, MMSE receiver beamforming weights constructed using that interference-covariance-matrix are equal to the original beamforming weights times a scale factor less than 1. This simplifies the training process, which can be carried out using a preamble of sufficient length for the case of the uninformed transmitter. For the case of the informed transmitter, we choose a suboptimal approach using where the transmit beamforming weights are constructed using only the target channel, not the target channel times the receiver's interference whitening filter. This leads to a reduction in mean spectral efficiency, but simplifies the protocol.

Let $\mathbf{K}$ be the covariance matrix of the interference and noise. Let $\mathbf{K_t}$ be the covariance matrix of the interference and noise, and including the target channel. Below we consider the computation of these beamforming weights under the four transmit schemes considered in this work: Uninformed transmitters with transmit covariance rank 1 and 2, and Informed transmitters with transmit covariance rank 1 and 2.

6.2.1 Uninformed Transmitter, Transmit Covariance Rank = 1, Multiple Receive Antennas

When the transmit scheme consists of a single uninformed transmitter and n_r receive antennas, the asymptotic rate for a given node and in a given network is computed for as:

$$R_i = \log_2(1 + \mathbf{h}^\dagger \mathbf{K}^{-1} \mathbf{h}) \tag{6.8}$$

When the interference covariance matrix contains the target channel, the asymptotic rate is

given by:

$$R_i^t = \log_2\left(1 + \frac{||\mathbf{h}^\dagger \mathbf{K_t}^{-1}\mathbf{h}||^2}{\mathbf{h}^\dagger \mathbf{K_t}^{-1}\mathbf{K}\mathbf{K_t}^{-1}\mathbf{h}}\right) \quad b/s/Hz \tag{6.9}$$

As shown in chapter 2, these rates are identical. Then the average of the asymptotic rates is computed by averaging over many networks:

$$E[R] = E[\log_2(1 + SINR_{asy}(n_r))] = \frac{1}{n}\sum_{i=1}^{num-iters} R_i \quad b/s/Hz \tag{6.10}$$

$$E[R^t] = E[\log_2(1 + SINR^t_{asy}(n_r))] = \frac{1}{n}\sum_{i=1}^{num-iters} R_i^t \quad b/s/Hz \tag{6.11}$$

The average estimated rate as a function of the training length is computed by find $SINR(n_r, N)$ using estimated weights using N snapshots:

$$\hat{\mathbf{w}} = \left(\frac{1}{N}\sum \mathbf{Y_{intf}}\mathbf{Y_{intf}}^\dagger\right)^{-1} \mathbf{Y}\mathbf{X}^\dagger(\mathbf{X}\mathbf{X}^\dagger)^{-1} \tag{6.12}$$

where $\mathbf{Y}$ and $\mathbf{Y_{intf}}$ are $(n_r \times N)$ matrix, and $\mathbf{X}$ is a $(1 \times N)$ vector. The rate is computed:

$$\hat{R}_i = \log_2\left(1 + \frac{||\hat{\mathbf{h}}^\dagger \hat{\mathbf{K}}^{-1}\hat{\mathbf{h}}||^2}{|\hat{\mathbf{h}}^\dagger \hat{\mathbf{K}}^{-1}\mathbf{K}\hat{\mathbf{K}}^{-1}\hat{\mathbf{h}}|}\right) \quad b/s/Hz \tag{6.13}$$

When the beamforming weights contain the target channel, the beamforming weights are given by:

$$\hat{\mathbf{w}}_\mathbf{t} = \left(\frac{1}{N}\sum \mathbf{Y}\mathbf{Y}^\dagger\right)^{-1} \mathbf{Y}\mathbf{X}^\dagger(\mathbf{X}\mathbf{X}^\dagger)^{-1} \tag{6.14}$$

And where the corresponding rate is given by:

$$\hat{R}_i^t = \log_2\left(1 + \frac{||\hat{\mathbf{h}}^\dagger \hat{\mathbf{K}_t}^{-1}\hat{\mathbf{h}}||^2}{|\hat{\mathbf{h}}^\dagger \hat{\mathbf{K}_t}^{-1}\mathbf{K}\hat{\mathbf{K}_t}^{-1}\hat{\mathbf{h}}|}\right) \quad b/s/Hz \tag{6.15}$$

6.2.2 Uninformed Transmitter, Transmit Covariance Rank = 2, Multiple Transmit and Receive Antennas

When the transmit scheme consists of a uninformed transmitter with a transmit covariance rank of 2, at the transmitter 2 transmit antennas are chosen. The receiver uses n_r receive antennas. Since the target transmitter has no knowledge of the channel, both antennas are used isotropically, each with transmit power $P/2$. In the computation of the asymptotic rate using MMSE receivers, when decoding the transmission from antenna 1 $\mathbf{h_1} = \mathbf{H}(:, \mathbf{1})$ ($\mathbf{h_2} = \mathbf{H}(:, \mathbf{2})$), the transmission from antenna 2 $\mathbf{h_2}$ ($\mathbf{h_1}$) is contained the interference covariance matrix $\mathbf{K_1} = \frac{P}{2}\mathbf{h_2}\mathbf{h_2^\dagger} + \mathbf{K}$ ($\mathbf{K_2} = \frac{P}{2}\mathbf{h_1}\mathbf{h_1^\dagger} + \mathbf{K}$). The total rate is given by:

$$R_i = \log_2(1 + \mathbf{h_1^\dagger}\mathbf{K_1^{-1}}\mathbf{h_1}) + \log_2(1 + \mathbf{h_2^\dagger}\mathbf{K_2^{-1}}\mathbf{h_2}) \quad b/s/Hz \tag{6.16}$$

When the the asymptotic beamforming weights contain are computed from interference covariance matrix that contains the target channels $\mathbf{K_t} = \frac{P}{2}\mathbf{h_2}\mathbf{h_2^\dagger} + \frac{P}{2}\mathbf{h_1}\mathbf{h_1^\dagger} + \mathbf{K}$, the identical rates are given by:

$$R_i^t = \log_2(1 + \mathbf{h_1^\dagger}\mathbf{K_t^{-1}}\mathbf{h_1}) + \log_2(1 + \mathbf{h_2^\dagger}\mathbf{K_t^{-1}}\mathbf{h_2}) \quad b/s/Hz \tag{6.17}$$

When estimated-weights are used, the beamforming weights are computed when two known transmit sequences, each of length N are sent on each antenna with power $P/2$. We represent this transmission as matrix X of size $(2 \times N)$. Again using the least-squares estimator for H, the target channel vectors are given by $\hat{\mathbf{h}}_\mathbf{1} = \hat{\mathbf{H}}(:, \mathbf{1})$ and $\hat{\mathbf{h}}_\mathbf{2} = \hat{\mathbf{H}}(:, \mathbf{2})$. The estimated rate is given by:

$$\hat{R}_i = \log_2\left(1 + \frac{||\hat{\mathbf{h}}_\mathbf{1}^\dagger \hat{\mathbf{K}}_\mathbf{1}^{-1} \hat{\mathbf{h}}_\mathbf{1}||^2}{|\hat{\mathbf{h}}_\mathbf{1}^\dagger \hat{\mathbf{K}}_\mathbf{1}^{-1} \mathbf{K} \hat{\mathbf{K}}_\mathbf{1}^{-1} \hat{\mathbf{h}}_\mathbf{1}|}\right) + \log_2\left(1 + \frac{||\hat{\mathbf{h}}_\mathbf{2}^\dagger \hat{\mathbf{K}}_\mathbf{2}^{-1} \hat{\mathbf{h}}_\mathbf{2}||^2}{|\hat{\mathbf{h}}_\mathbf{2}^\dagger \hat{\mathbf{K}}_\mathbf{2}^{-1} \mathbf{K} \hat{\mathbf{K}}_\mathbf{2}^{-1} \hat{\mathbf{h}}_\mathbf{2}|}\right) \quad b/s/Hz \tag{6.18}$$

When the interference channel estimate contains the target channel, the estimated rate is

given by:

$$\hat{R}_i^t = \log_2\left(1 + \frac{||\hat{\mathbf{h}}_1^\dagger \hat{\mathbf{K}}_t^{-1} \hat{\mathbf{h}}_1||^2}{|\hat{\mathbf{h}}_1^\dagger \hat{\mathbf{K}}_t^{-1} \mathbf{K} \hat{\mathbf{K}}_t^{-1} \hat{\mathbf{h}}_1|}\right) + \log_2\left(1 + \frac{||\hat{\mathbf{h}}_2^\dagger \hat{\mathbf{K}}_t^{-1} \hat{\mathbf{h}}_2||^2}{|\hat{\mathbf{h}}_2^\dagger \hat{\mathbf{K}}_t^{-1} \mathbf{K} \hat{\mathbf{K}}_t^{-1} \hat{\mathbf{h}}_2|}\right) \quad b/s/Hz \quad (6.19)$$

In practice, it is simpler to estimate the weights when the target channels are contained within the interference channel.

6.2.3 Informed Transmitter, Transmit Covariance Rank = 1, Multiple Transmit and Receive Antennas

There are three steps required for an informed transmission from a primary transmitter to its target primary receiver. First, the primary transmitter must obtain an estimate of the whitened channel seen by the receiver.

$$\mathbf{K}^{-1/2}\mathbf{Y} = \mathbf{K}^{-1/2}\mathbf{H}\mathbf{X} + \mathbf{K}^{-1/2}(\sum_{\mathbf{j}} \mathbf{H_j X_j} + \mathbf{W}) \quad (6.20)$$

where $\mathbf{K} = \sum_j P\mathbf{H_j H_j^\dagger} + N_o\mathbf{I}$. To obtain this estimate, the primary transmitter can send training to the primary receiver. The whitened channel is then estimated by the receiver. Then the channel coefficients are fed back to the target transmitter.

In step two, the transmitter performs a singular value decomposition on the channel estimate it received from the target receiver:

$$\text{svd}(\mathbf{K}^{-1/2}\mathbf{H}) = \mathbf{U}\mathbf{\Lambda}\mathbf{V}^\dagger \quad (6.21)$$

For strongest mode transmissions, the transmitter then transmits in the direction $\mathbf{v} = \mathbf{V}(:, \mathbf{1})$ corresponding to the strongest eigenvalue in Λ.

$$\mathbf{Y} = \mathbf{Hvx} + \sum_{\mathbf{j}} \mathbf{H_j X_j} + \mathbf{W} \tag{6.22}$$

$$\tag{6.23}$$

When the beamforming weights $\mathbf{K^{-1/2}u}$, where $\mathbf{u} = \mathbf{U}(:, \mathbf{1})$, are applied, this simplifies to:

$$\mathbf{Y} = \mathbf{Hvx} + \sum_{\mathbf{j}} \mathbf{H_j X_j} + \mathbf{W} \tag{6.24}$$

$$= \mathbf{u^\dagger K^{-1/2} H} v x + \mathbf{K^{-1/2}} \left(\sum_{\mathbf{j}} \mathbf{H_j X_j} + \mathbf{W} \right) \tag{6.25}$$

$$= \lambda_i x + \mathbf{u^\dagger \tilde{w}} \tag{6.26}$$

where $\tilde{\mathbf{w}} \sim CN(0, \mathbf{I})$ In this asymptotic case, the achieved spectral efficiency is:

$$R_i = \log_2 \left(1 + \lambda_1^2 P\right) \quad b/s/Hz \tag{6.27}$$

When the receiver then uses estimated weights, the transmitter then transmits a known pseudo-random sequence $\mathbf{s}$ in the direction $\mathbf{v} = \mathbf{V}(:, \mathbf{1})$.

$$\mathbf{Y} = \mathbf{H}v x + \sum \mathbf{H_j X_j} + \mathbf{W} \tag{6.28}$$

The receiver uses known transmit vector $\mathbf{X}$ to perform a least squares estimate of the target channel $\mathbf{g} = \mathbf{Hv}$, $\hat{\mathbf{g}} = \mathbf{YX^\dagger (XX^\dagger)^{-1}}$. The same received vector $\mathbf{Y}$ is then used to construct the interference covariance matrix. When the target channel is included, the beamforming weights are given by $\hat{\mathbf{K}}_\mathbf{t}^{-\mathbf{1}} \hat{\mathbf{g}}$, and the received spectral efficiency is given by:

$$R_i = \log_2 \left(1 + \frac{P || \hat{\mathbf{g}}^\dagger \hat{\mathbf{K}_\mathbf{t}}^{-\mathbf{1}} \mathbf{Hv} ||^2}{| \hat{\mathbf{g}}^\dagger \hat{\mathbf{K}_\mathbf{t}}^{-\mathbf{1}} \mathbf{K} \hat{\mathbf{K}_\mathbf{t}}^{-\mathbf{1}} \hat{\mathbf{g}} |} \right) \quad b/s/Hz \tag{6.29}$$

6.2.4 Informed Transmitter, Transmit Covariance Rank = 2, Multiple Transmit and Receive Antennas

When using an informed transmitter with a transmit covariance rank of two, identical steps are follow to estimate the channel as in the case of the Informed transmitter with transmit covariance rank one. When the the transmit covariance matrix rank is two, the two strongest transmit modes $\mathbf{V}(:,\mathbf{1}), \mathbf{V}(:,\mathbf{2})$ are used to transmit data. Let $\bar{\mathbf{V}}$ be the first 2 columns of $\mathbf{V}$:

$$\mathbf{Y} = \mathbf{H}\bar{\mathbf{V}}\mathbf{X} + \sum \mathbf{H_j X_j} + \mathbf{W} \tag{6.30}$$

In the asymptotic case, the spectral efficiency is given by:

$$R_i = \log_2\left(1+\lambda_1^2 P\right) + \log_2\left(1+\lambda_2^2 P\right) \quad b/s/Hz \tag{6.31}$$

Let $\mathbf{g_1} = \mathbf{Hv_1}$, and $\mathbf{g_2} = \mathbf{Hv_2}$. When the estimated weights are used, and the interference covariance matrix contains the target channel:

$$R_i = \log_2\left(1+\frac{P||\hat{\mathbf{g}}_\mathbf{1}^\dagger \hat{\mathbf{K}}_\mathbf{t}^{-1}\mathbf{Hv}||^2}{|\hat{\mathbf{g}}_\mathbf{1}^\dagger \hat{\mathbf{K}}_\mathbf{t}^{-1}\mathbf{K}\hat{\mathbf{K}}_\mathbf{t}^{-1}\hat{\mathbf{g}}_\mathbf{1}|}\right) + \log_2\left(1+\frac{P||\hat{\mathbf{g}}_\mathbf{2}^\dagger \hat{\mathbf{K}}_\mathbf{t}^{-1}\mathbf{Hv}||^2}{|\hat{\mathbf{g}}_\mathbf{2}^\dagger \hat{\mathbf{K}}_\mathbf{t}^{-1}\mathbf{K}\hat{\mathbf{K}}_\mathbf{t}^{-1}\hat{\mathbf{g}}_\mathbf{2}|}\right) \quad b/s/Hz \tag{6.32}$$

6.3 Simulation Results

For networks with M=20 transmit-receive pairs, we show simulation results in figures 6-1(a) - 6-1(d) with 4 receive antennas and a variable number of transmit antennas and transmit schemes. The transmit symbols in these simulations are BPSK, which correspond to the modulation scheme used on the control channel, and to packet preambles.

For the case of 4 degrees of freedom at the receiver (4 receive antennas figures), after approximately 80 samples, the rate at which the estimated rate approaches the asymptotic rate decreases substantially. In figures 6-2(a) - 6-2(d), we demonstrate the same four trans-

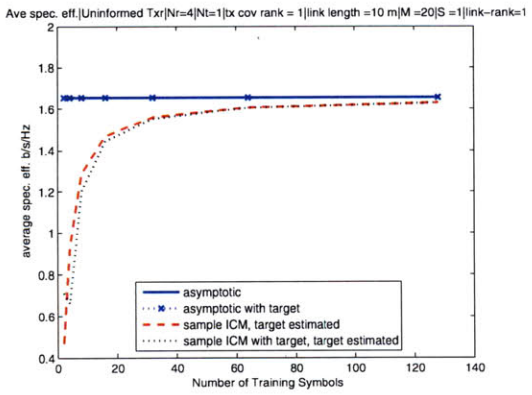

(a) Uninformed Transmitter, Nr=4, Nt=1, Transmit-Covariance-Rank = 1

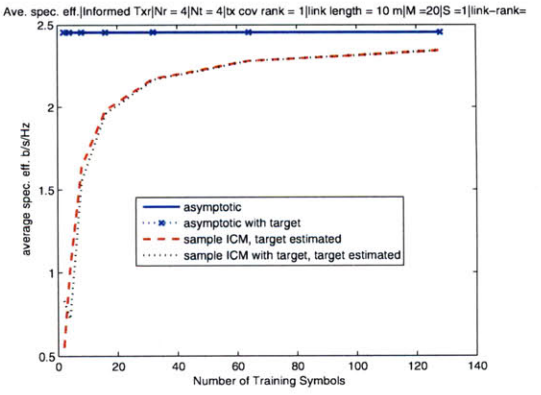

(b) Informed Transmitter, Nr=4, Nt=4, Strongest Mode (Tx-Covariance-Rank=1)

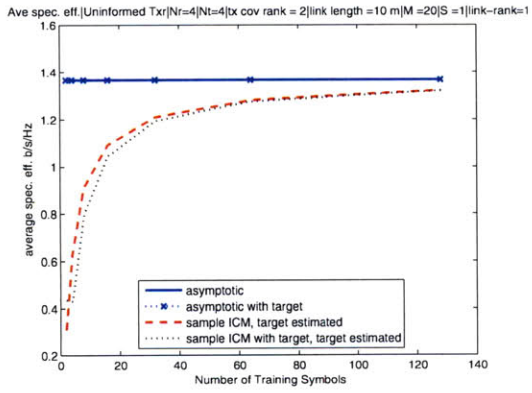

(c) Uninformed Transmitter, Nr=4, Nt=4, Transmit-Covariance-Rank = 2

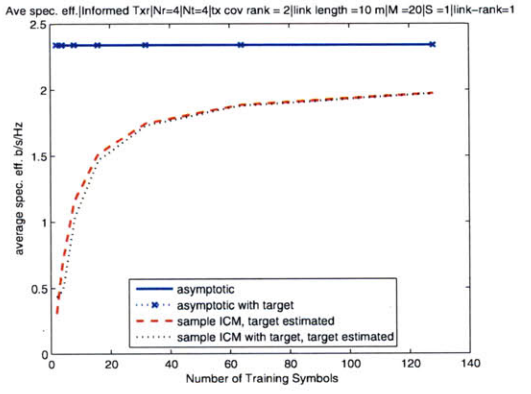

(d) Informed Transmitter, Nr=4, Nt=4, 2 Strongest modes, Transmit-Covariance-Rank = 2

Figure 6-1: Average Rate as a function of the training length and transmit scheme for networks with M = 20 Transmit-Receive Pairs, 4 Receive Antennas, Link-length = 10m, Link-Rank = 1

mit schemes, but with 8 degrees of freedom at the receiver. When Nr = 8, we see that approximately x samples are required to be within .2 bits/sec/Hz of the asymptotic rates.

When Nr = 2 as shown in figures 6-3(a) - 6-3(d), the convergence is much faster. Only 40 samples are required to come within .1 bits/sec/Hz of the asymptotic rate.

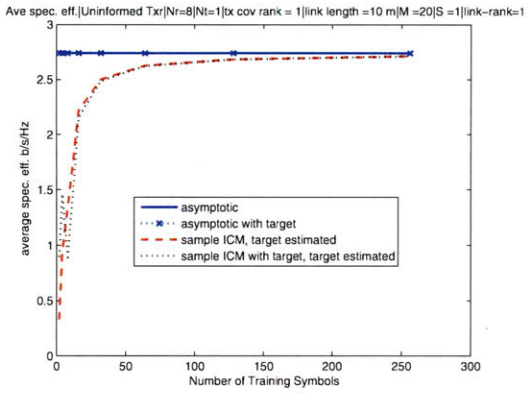

(a) Uninformed Transmitter, Nr=8, Nt=1, Transmit-Covariance-Rank = 1

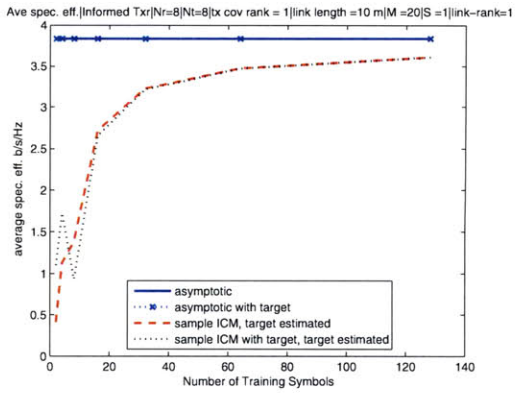

(b) Informed Transmitter, Nr=8, Nt=8, Strongest Mode (Tx-Covariance-Rank=1)

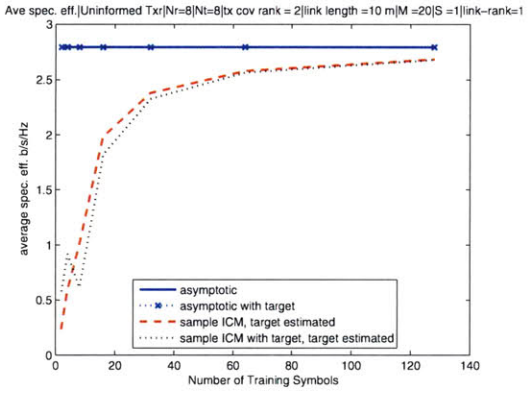

(c) Uninformed Transmitter, Nr=8, Nt=8, Transmit-Covariance-Rank = 2

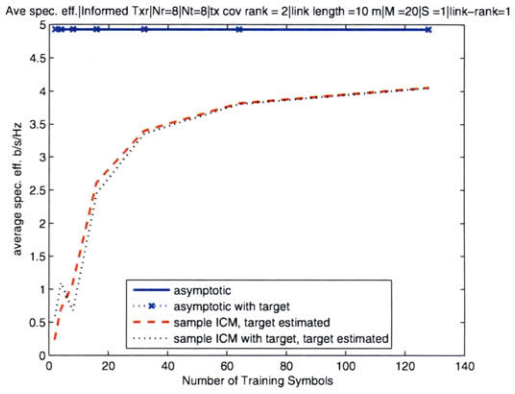

(d) Informed Transmitter, Nr=8, Nt=8, 2 Strongest modes, Transmit-Covariance-Rank = 2

Figure 6-2: Average Rate as a function of the training length and transmit scheme for networks with M = 20 Transmit-Receive Pairs, 8 Receive Antennas, Link-length = 10m, Link-Rank = 1

6.3.1 Receiver Beamforming Weights for the Informed Transmitter

Recall that for the informed transmitter, we seek to determine transmitter and receiver beamforming weights in the system defined by equation (6.33). Let equation 6.33 define the received signal $\mathbf{Y}$ at a given receiver from its target transmitter that sends signal $\mathbf{X}$, through channel $\mathbf{H}$; and where the receiver also receives signals from interferers $\mathbf{X_j}$ and corresponding interference channels $\mathbf{H_j}$. And let $\mathbf{W}$ be additive white gaussian noise.

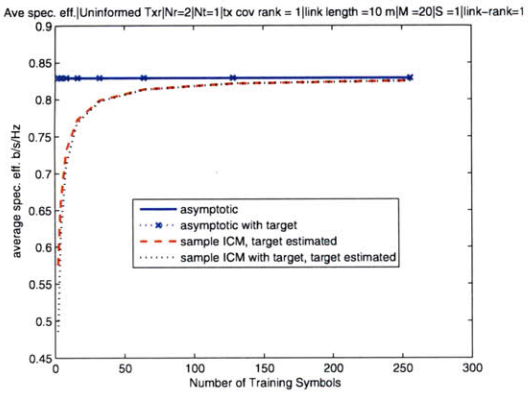

(a) Uninformed Transmitter, Nr=2, Nt=1, Transmit-Covariance-Rank = 1

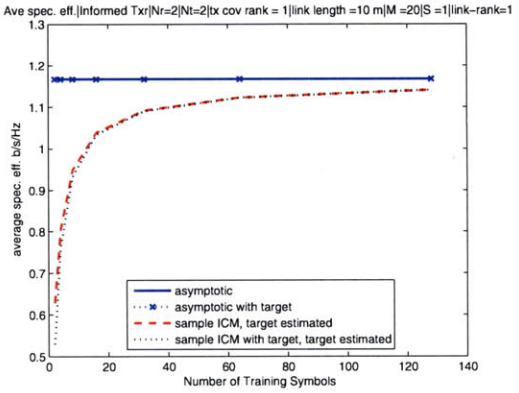

(b) Informed Transmitter, Nr=2, Nt=2, Strongest Mode (Tx-Covariance-Rank=1)

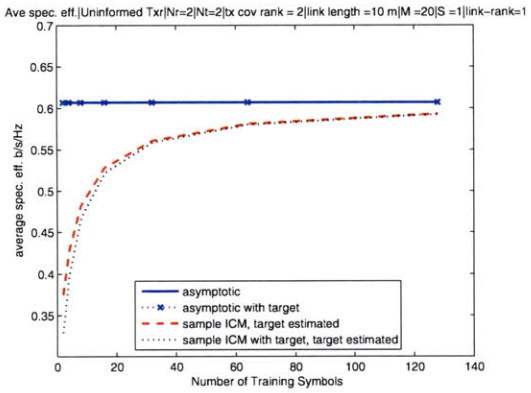

(c) Uninformed Transmitter, Nr=2, Nt=2, Transmit-Covariance-Rank = 2

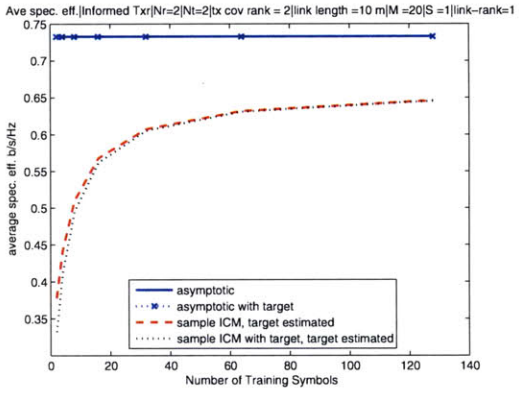

(d) Informed Transmitter, Nr=2, Nt=2, 2 Strongest modes, Transmit-Covariance-Rank = 2

Figure 6-3: Average Rate as a function of the training length and transmit scheme for networks with M = 20 Transmit-Receive Pairs, 2 Receive Antennas, Link-length = 10m, Link-Rank = 1

$$\mathbf{Y} = \mathbf{HX} + \sum \mathbf{H_j X_j} + \mathbf{W} \tag{6.33}$$

Let a transmit receive pair with transmit covariance rank I be defined by the receive array response $\mathbf{g_i}$,

$$\mathbf{Y} = \sum_{i=1}^{I} \mathbf{g_i} x + \sum \mathbf{H_j X_j} + \mathbf{W} \tag{6.34}$$

The MMSE-receive-beamforming-weights are given by:

$$\mathbf{w_i} = \mathbf{K_i^{-1}} \mathbf{g_i} \tag{6.35}$$

where $\mathbf{K_i}$ is the covariance matrix of the interference seen by the receiver with respect to transmit-vector i:

$$\mathbf{K_i} = P\mathbf{g_i}\mathbf{g_i^\dagger} + \sum P\mathbf{H_j}\mathbf{H_j^\dagger} + N_o\mathbf{I} \tag{6.36}$$

The received data rate is given by:

$$r = \log_2\left(1 + \frac{||\mathbf{w}^\dagger \mathbf{g_i}||^2}{\mathbf{w_i^\dagger} \mathbf{K_i} \mathbf{w_i}}\right) \tag{6.37}$$

$$= \log_2\left(1 + \frac{\mathbf{w}^\dagger \mathbf{g_i}\mathbf{g_i^\dagger}\mathbf{w}}{\mathbf{w_i^\dagger} \mathbf{K_i} \mathbf{w_i}}\right) \quad b/s/Hz \tag{6.38}$$

$$\tag{6.39}$$

When the interference covariance matrix contains the target channel $\mathbf{g_i}$, as shown in chapter 2, the receiver-beamforming-weights $\mathbf{w_t}$ are equal to $\beta\mathbf{w}$, where β is some scale factor less than 1. We will refer to the covariance matrix of $\mathbf{Y}$ as $\mathbf{K_y}$.

The optimal transmit and receive beamforming weights can be determined when the transmitter has knowledge the receiver's-interference-covariance-matrix (Tx-K_{R_x}-CSI) and knowledge of the target channel. In this case, the beamformer, SINR, and data rate are given by:

$$\text{svd}(\mathbf{K_1^{-1/2}}\mathbf{H}) = \bar{\mathbf{U}}\mathbf{\Lambda}\bar{\mathbf{V}}^\dagger \tag{6.40}$$

$$\mathbf{g_1} = \mathbf{H}\bar{\mathbf{v}}_\mathbf{1}, \bar{\mathbf{v}}_\mathbf{1} = \bar{\mathbf{V}}(:, \mathbf{1}) \tag{6.41}$$

$$\mathbf{w_1} = \mathbf{K^{-1}H\bar{v}_1} \tag{6.42}$$

$$= \mathbf{K^{-1/2}K^{-1/2}H\bar{v}_1} \tag{6.43}$$

$$= \lambda_1 \mathbf{K^{-1/2}\bar{u}_1} \tag{6.44}$$

$$K_1 = \sum P\mathbf{H_j H_j^\dagger} + N_o\mathbf{I} \tag{6.45}$$

$$R = \log_2\left(1 + \frac{||\mathbf{w_1^\dagger g_i}||^2}{\mathbf{w_1^\dagger K_1 w_1}}\right) \tag{6.46}$$

$$= \log_2\left(1 + \frac{||\lambda_1 \mathbf{\bar{u}_1^\dagger K^{-1/2} H\bar{v}_1}||^2}{\lambda_1^2 \mathbf{\bar{u}_1^\dagger K_1^{-1/2} K_1 K_1^{-1/2} \bar{u}_1}}\right) \tag{6.47}$$

$$= \log_2\left(1 + \frac{||\lambda_1 \mathbf{\bar{u}_1^\dagger K^{-1/2} H\bar{v}_1}||^2}{\lambda_1^2 \mathbf{\bar{u}_1^\dagger K_1^{-1/2} K_1^{1/2} K_1^{1/2} K_1^{-1/2} \bar{u}_1}}\right) \tag{6.48}$$

$$= \log_2\left(1 + \frac{||\lambda_1^2 \mathbf{\bar{u}_1^\dagger \bar{u}_1}||^2}{\lambda_1^2 \mathbf{\bar{u}_1^\dagger \bar{u}_1}}\right) \tag{6.49}$$

$$= \log_2(1 + \lambda_1^2) \tag{6.50}$$

Sub-optimal transmit and receive beamforming weights can be determined when the transmitter only has knowledge of the target channel. Though sub-optimal in terms of the mean rate, not requiring the receiver to feedback its interference covariance matrix simplifies the protocol, and allows the receiver to adapt to changes in its interference environment and still be matched to the transmit beamformer. In this case, the beamformer, SINR, and data rate are given by:

$$\text{svd}(\mathbf{H}) = \mathbf{U\Lambda V^\dagger} \tag{6.51}$$

$$\mathbf{g_1} = \mathbf{Hv_1} = \lambda_1 \mathbf{u_1}, \mathbf{v_1} = \mathbf{V}(:, \mathbf{1}) \tag{6.52}$$

$$\mathbf{K_1} = \sum P\mathbf{H_j}\mathbf{H_j^\dagger} + N_o\mathbf{I} \tag{6.53}$$

$$\begin{aligned} R &= \log_2\left(1 + \frac{||\mathbf{w_1^\dagger g_i}||^2}{\mathbf{w_1^\dagger K_1 w_1}}\right) && (6.54)\\ &= \log_2\left(1 + \frac{||\lambda_1^2\mathbf{u_1^\dagger K_1 u_1}||^2}{\lambda_1^2\mathbf{u_1^\dagger K_1 u_1}}\right) && (6.55)\\ &= \log_2\left(1 + \lambda_1^2\mathbf{u_1^\dagger K_1 u_1}\right) && (6.56) \end{aligned}$$

In the simulation results described below, we compare the mean SINR and mean data rate as a function of the training length achieved under both of these schemes.

In figure 6-4 we show the average spectral efficiency achieved when the transmit-receive scheme is an informed transmitter with transmit-covariance-rank =1 using the strongest mode as a function of the number of BPSK training symbols. We average over 10,000 network iterations in which 4 transmit-receive pairs each have 4 transmit and 4 receive antennas, are 10 m from their target transmitter, and where the average link rank is 1. If we first consider the case with no receiver-interference-covariance-matrix-CSI at the transmitter (Tx-K_{R_x}-CSI), average asymptotic rate in which the ICM does not contain the target channel and the average asymptotic rate when the ICM does contain the target channel are shown to be identical. The red and black curves, which are receive-beamforming weights computed using the number of training symbols specified on the x-axis, show the relatively quick convergence of the data rate to within approximately 10% of the asymptotic rate. When we consider the case of Tx-K_{R_x}-CSI at the transmitter, the asymptotic rate is, as we would expect, greater than the asymptotic rate when there is no Tx-K_{R_x}-CSI at the transmitter. When we consider reproducing the weights at the receiver via training, when the receiver is able to generate weights by estimating the target channel and computing the interference covariance matrix not including the target channel, the resulting data rate ap-

proaches approximately 10% of the asymptotic value. When the receiver generates weights using an interference covariance matrix that contains the target, the resulting rate is much lower. This result follows from the mismatch between the Tx-K_{R_x}-CSI channel state information at the transmitter, and the estimate of receiver's interference covariance matrix K_{R_x} at the receiver which contains the target transmitter. This result suggests that using the transmitter-beamforming that depends on the interference covariance matrix at the receiver may be less valuable, on average, in an ad hoc network setting relative to more traditional transmitter channel state information Tx-CSI containing just the target channel transmit-beamformer.

There are similar relationships between the mean spectral efficiencies with and without Tx-K_{R_x}-CSI in networks with M=20 (figure 6-5) and M=40 (figure 6-6) transmit-receive pairs, that mirror the relationships shown above with M=4 transmit-receive pairs. As the network increases in the number of interferers, which increases the richness of the interference environment, the effect of the mismatch between the covariance matrix at the receiver that contains the target channel and the covariance matrix used to create the transmit-beamformer decreases. This reduction in the effect of the mismatch reduces the gap between the spectral efficiency with the ICMat the transmitter and and the receiver are matched.

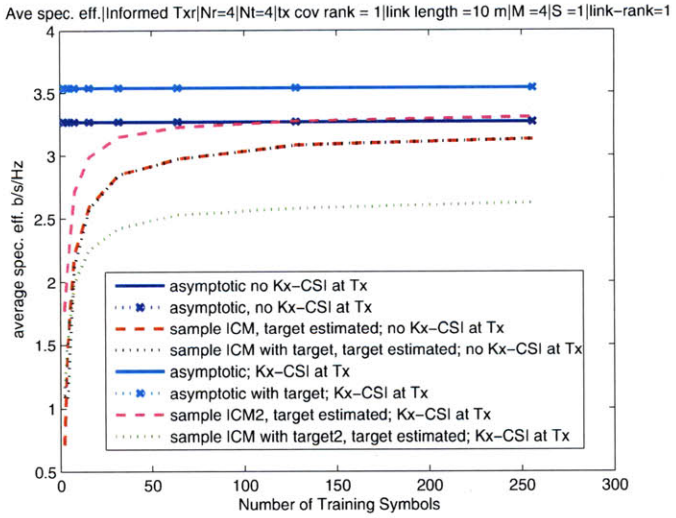

Figure 6-4: Mean Spectral Efficiency as a function of Number of Training Symbols, Informed Transmissions in networks with M=4 Tx-Rx pairs, 4 Receive Antennas, 4 Transmit Antennas, Link Length = 10m, Link-Rank = 1,Transmit Covariance Rank = 1 (Strongest Mode)

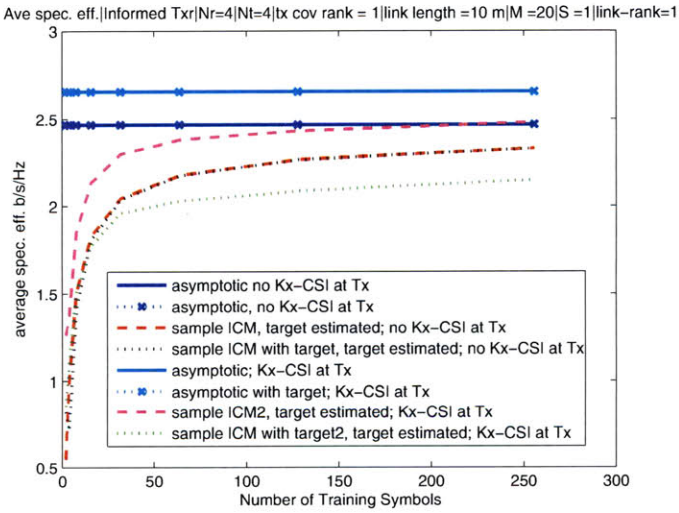

Figure 6-5: Mean Spectral Efficiency as a function of Number of Training Symbols, Informed Transmissions in networks with M=20 Tx-Rx pairs, 4 Receive Antennas, 4 Transmit Antennas, Link Length = 10m, Link-Rank = 1,Transmit Covariance Rank = 1 (Strongest Mode)

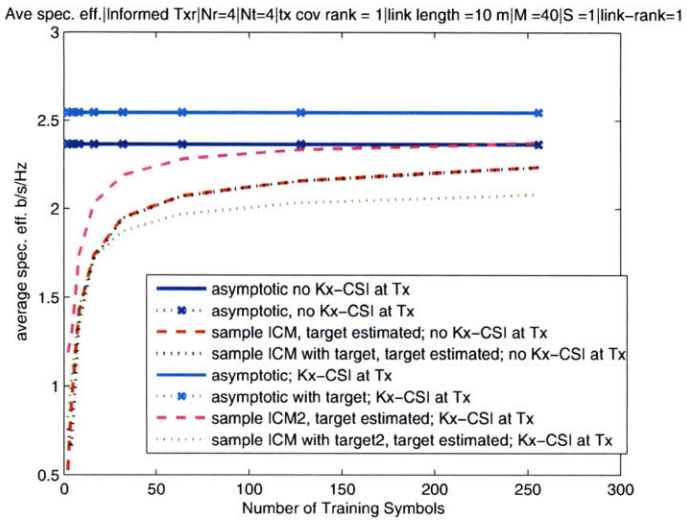

Figure 6-6: Mean Spectral Efficiency as a function of Number of Training Symbols, Informed Transmissions in networks with M=40 Tx-Rx pairs, 4 Receive Antennas, 4 Transmit Antennas, Link Length = 10m, Link-Rank = 1,Transmit Covariance Rank = 1 (Strongest Mode)

In figures 6-7 - 6-9, we consider the mean spectral efficiency of informed transmissions when the rank of the transmit-covariance-matrix is 2. First considering the case when M=4 with no receiver-interference-covariance-matrix-CSI at the transmitter (Tx-K_{R_x}-CSI), the gap between the average asymptotic rate and the rate as a function of the number of samples approaches approximately 80% of the asymptotic value, double that of transmission in the strongest single mode. A similar gap of approximately 80 % also is shown between the average asymptotic rate when there is Tx-K_{R_x}-CSI at the transmitter, and the asymptote approached by average rate as a function of the spreading length. Since in all nodes in this network have a transmit covariance rank of 2, the density of interference is double the density in networks where transmitters use strongest mode transmission (as shown in the figures above). As the number of nodes in a network increases, the gap between mean spectral efficiency in the matched Tx-K_{R_x}-CSI at the transmitter and receiver narrows, and the value of Tx-K_{R_x}-CSI decreases.

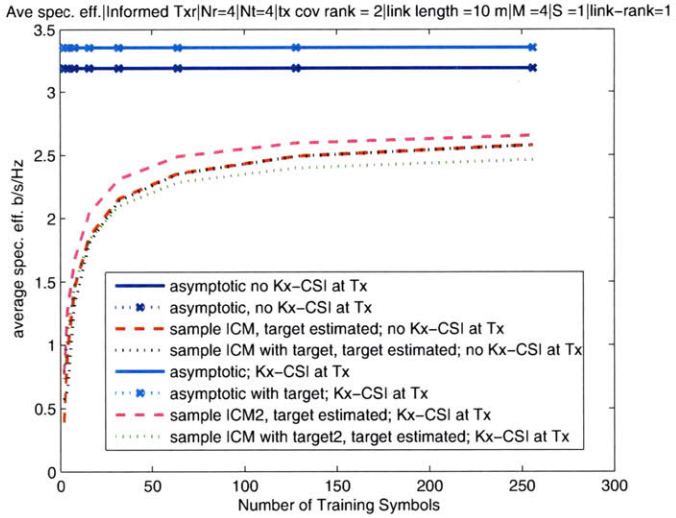

Figure 6-7: Mean Spectral Efficiency as a function of Number of Training Symbols, Informed Transmissions in networks with M=4 Tx-Rx pairs, 4 Receive Antennas, 4 Transmit Antennas, Link Length = 10m, Link-Rank = 1,Transmit Covariance Rank = 2 (2 Strongest Modes)

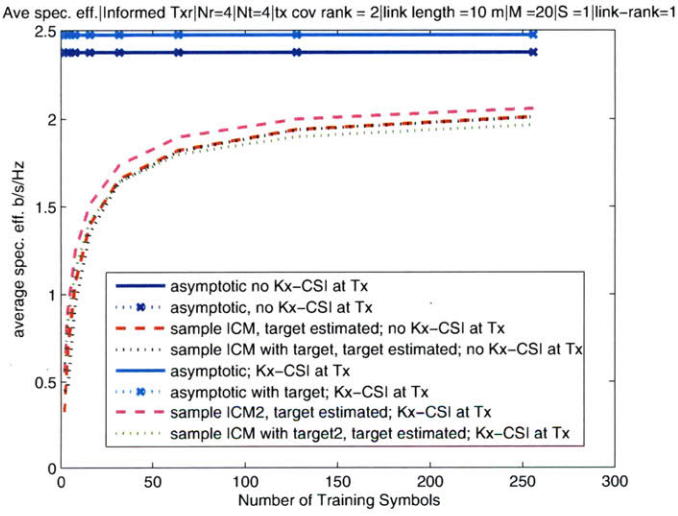

Figure 6-8: Mean Spectral Efficiency as a function of Number of Training Symbols, Informed Transmissions in networks with M=20 Tx-Rx pairs, 4 Receive Antennas, 4 Transmit Antennas, Link Length = 10m, Link-Rank = 1,Transmit Covariance Rank = 2 (2 Strongest Modes)

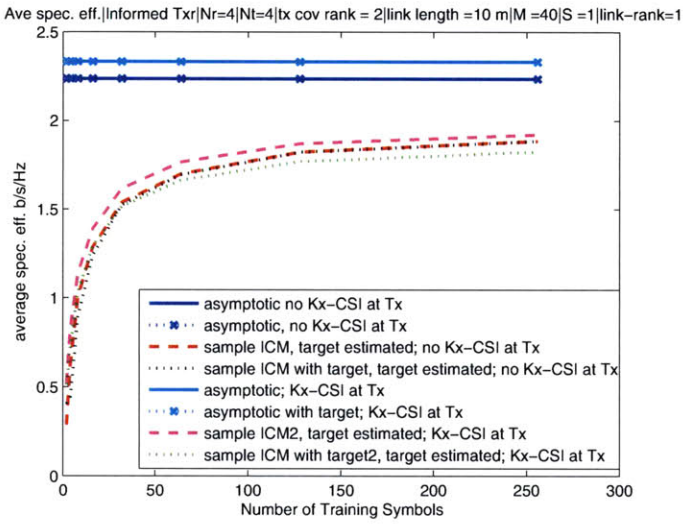

Figure 6-9: Mean Spectral Efficiency as a function of Number of Training Symbols, Informed Transmissions in networks with M=40 Tx-Rx pairs, 4 Receive Antennas, 4 Transmit Antennas, Link Length = 10m, Link-Rank = 1,Transmit Covariance Rank = 2 (2 Strongest Modes)

6.3.2 Receive-Beamforming Weight Adaptation

In the case of uninformed transmissions, when the receiver has knowledge of the training symbols, the weights can be adapted when the known sequence directly precedes the data that is sent. When there is no change in the target or interference channels, there is no loss in producing the weights in this fashion, provided that the training signal is long enough. Whether the change is in the interference environment, or in the target channel, this results in a fairly unpredictable change in the interference environment.

In the case of informed transmitters with no receiver interference covariance matrix channel state information (Tx-K_{R_x}-CSI), the weights can similarly adapt to a changing environment. A change in the interference environment is accounted for in the sample interference covariance matrix. A change in the target channel from H_o to H_1 will modify $\mathbf{g_i} = \mathbf{H_o v_i} = \lambda_i \mathbf{u}$ to $\mathbf{g_i} = \mathbf{H_1 v_i}$, where $\mathbf{g_i^\dagger K^{-1} g_i}$ is statistically likely to be less than $\lambda_i^2 \mathbf{u_i K^{-1} u_i}$.

In the case of informed transmissions with receiver-interference-covariance-matrix-channel-state-information at the transmitter (Tx-K_{R_x}-CSI), adaptation is still possible but the loss in spectral efficiency is likely to be the greatest. Similarly to the case of no Tx-Kx-CSI, a change in the target channel takes $\mathbf{g_i} = \mathbf{H_o v_i}$ to $\mathbf{g_i} = \mathbf{H_1 v_i}$, but the received SINR goes from λ_i^2 to $\mathbf{g_i^\dagger K^{-1} g_i}$, where the latter is likely to be much less than the former. This relationship and drop in the received SINR is also true in the case where the interference covariance matrix changes, and is unmatched to the estimate of $\mathbf{K}$ that was used to create the transmit-beamforming-vector that was sent to the transmitter. If in the latter case, the change in $\mathbf{K}$ was caused by the addition of an interferer, its likely that the transmit-beamforming still benefits in its avoidance of the signal space accounted for in the older version of $\mathbf{K_o}$ that produced the transmitter-beamforming weights.

In figure 6-10 we consider the number of training symbols required for the average data rate to be within 25% of the asymptotic rate for the informed transmitter with

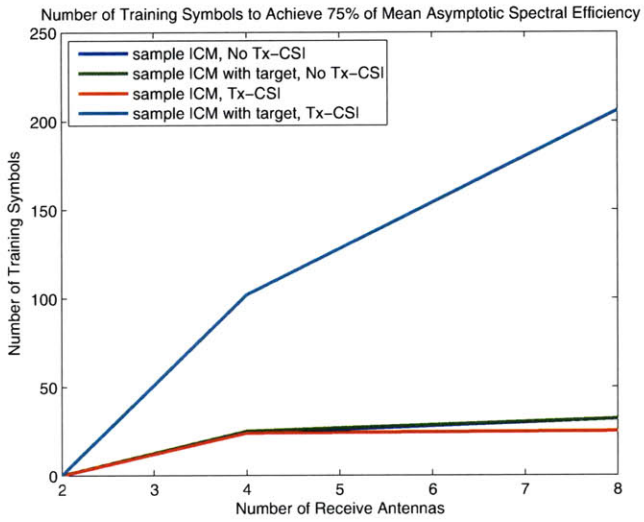

Figure 6-10: Number of Training symbols for Mean Spectral Efficiency to be within 25 % of Asymptotic Rate in networks with M=20 Tx-Rx pairs, Link Length = 10m, Link-Rank = 1,Transmit Covariance Rank = 1(1 Strongest Modes)

6.4 Computational Complexity

To form the sample covariance matrix requires $KN(N+1)/2$ complex multiplies. To invert the sample interference covariance matrix requires $N^3/2 + N^2$ complex multiplies. To form the beamforming weights then takes N^2 multiplies. When $K = 2N$, this is a total of $7/6N^3$ multiplies compared with N^2 multiplies required for the matched-filter beamforming weights (on the same amount of training data) [102].

6.5 Network Synchronization

A key problem in any decentralized network is the problem of synchronizing the clocks of all nodes in the network. In centralized networks, all nodes operate with the time and frequency referenced to the central terminal. For instance, in 802.11 infrastructure networks, the mobile stations synchronize their clocks to the access point at the time that they join the network (associate). In their independent basic service set (BSS) (i.e. ad hoc) mode, the node that initiates the network becomes its time reference. The key challenge in network synchronization arises when two separate networks with different time references begin to interact. The migration to a single clock reference from one or more is the key problem.

In this work, we will adopt a solution from the broad literature on the prior work in this area. We will assume that all nodes have a global-positioning-system (GPS) reference, and that the protocols described here mandate absolute times for the beginning of a data channel packet and its duration, and the duration of a side channel sub slot.

Chapter 7

Simulation Results

In this section we begin with a description of our simulation set up. We then describe the data collected in the simulations, and the metrics that we use to evaluate the network performance. Finally, we show and discuss the results of the simulation over the parameter space described in chapter 5, and compare the results to our benchmark.

7.1 Network Simulation Parameters and Simulation Set up

Recall the key parameters that we use to describe the physical layout of ad hoc networks considered in this research are:

- Link-Rank (A)
- Link-Length (r_1)
- Number of links (M)

The primary transmitters in each transmit-receive pair are uniformly and randomly distributed within a circle whose radius R is set so that $\rho = \frac{M}{\pi R^2}$, where the density of nodes ρ relates to the link rank A and the link-length r_1 such that $\rho = \frac{A}{r_1^2}$. The primary receivers

are placed at a fixed distance r_1 from their target transmitter, with an angle uniformly and randomly distributed around its target transmitter and within the network area πR^2. For each network realization, a Rayleigh channel is generated between each node and all other nodes in the network. This channel evolves in time according to a Gauss-Markov process assuming a channel coherence time of 500 *msec* or 1 *sec* as described in chapter 2, and its frequency response is derived from its time response and from the the delay spread parameter which we fix at 50 *ns* to model typical indoor wireless environments.

Associated with each transmit-receiver pair in a network is n_r receive antennas, n_t transmit antennas, and a transmit scheme which is one the following four options:

- $(n_r > 1, n_t = 1)$ Single Uninformed Transmitter with Multiple Receive Antennas (Transmit Covariance Rank = 1)
- $(n_r > 1, n_t = n_r)$ Uninformed Transmitters with Multiple Receive Antennas, Transmit Covariance Rank = 2
- $(n_r > 1, n_t = n_r)$ Informed Transmitters with Multiple Receive Antennas, Transmit Covariance Rank = 1
- $(n_r > 1, n_t = n_r)$ Informed Transmitters with Multiple Receive Antennas, Transmit Covariance Rank = 2

In this work, the number of receive antennas is $\{2, 4, 8\}$. Finally, the other key protocol parameters include:

- Offered Load (G) $\left[\frac{1}{sec}\right]$
- The set of rates network nodes require

The offered load (G) $\left[\frac{1}{sec}\right]$ is a measure of the rate at which nodes (that are not backed-off) arrive to the control channel to contend for a spot on the next data channel. We will express this rate as the average number of nodes arriving within the duration of a data channel

packet. In simulations with M transmit-receiver pairs, this arrival rate will range between .5 and M arrivals per data channel packet where we assume one packet per fixed slot, where a data channel slot might last 50 msec.

The set of rates that network nodes require describes the system loading. When the distribution minimum rate that a node requires mimics the distribution on asymptotic rates achievable when an MMSE receiver is used for interference mitigation, the mean rate on the data channel mimics earlier results on the mean spectral efficiency. When the distribution on required rates shifts towards higher rates, the mean rate increases, but the mean number of nodes on the network at any given time decreases, and the average delay per node increases. Similarly, when the distribution on required rates shifts towards lower rates, the mean rate decreases, and the mean number of nodes on the network at any given time increases, and the average delay per node decreases. In this work, we vary the distribution of required rates as follows:

1. Low: All nodes require only the lowest two data rates the protocol can support. This data rate is either 0.5 or 1 b/s/Hz.

2. Medium Loading: The requested rates are uniformly distributed over all rates the protocol can support: 0.5 or 1 or 2 or 3 b/s/Hz

3. High: All nodes require one of the two highest data rate the protocol can support that is within the distribution of rates a network with the given set of parameters can support. This data rate is 2 or 3 b/s/Hz for transmit covariance rank = 1. This data rate is 3.5 or 4 b/s/Hz for transmit covariance rank = 2.

7.2 Evaluative Metrics

In our Monte Carlo network simulations, the key network parameters

$$\{M, n_r, n_t, TxScheme, r_1, A, n_{sub-slot}, \frac{K_{cc}}{K_{dc}}, \{(r_{\min})_i, \ \forall\ 1 \leq i \leq M\}, \{G_i, \ \forall\ 1 \leq i \leq M\}\}$$

are initially specified, and then the simulation itself consists of multiple time-series which are an alternating sequence of data channel slots and control channel subslots. In each time-series there is a given network configuration consisting of the location of the transmit-receive pairs in a plane, and an initial channel realization that evolves in time in accordance with the Gauss-Markov model. The nodes arrive to the control channel with a probability that is a function of the offered load, and operate on the control and data channel according to the protocol specifications. In each time series there is a fixed number of recorded slots (num-recorded-slots) that are followed by an additional 10×num-recorded-slots which allow the outworking of any sessions which are begun during the num-recorded-slots period, but not completed within that period. For each offered load G many time-series are evaluated. The rate and delay of each transmission, associated with a given transmitter-receiver pair, that initiates a transmission on the control channel is recorded. We also record the throughput per slot which is the number of successful data channel transmissions per slot. We define random variables to capture these metrics, and in order to capture each distribution and its corresponding mean and variance:

- Let R_{ml} be the rate of the mth node that is successfully received in the lth slot, where $R_{ml} = \log_2(1 + SINR)$, where $SINR$ is the signal-to-interference-plus-noise seen at the intended receiver.

- Let D_{ml} be the delay of the mth node that completes its transmission in lth slot, and that was initially queued during a previous slot $l_o < l$. $D_{ml} = l - l_o$.

- for the rate: $1 \leq m \leq M$ and $1 \leq l \leq L_R$, where L_R is the number of recorded slots

- for the delay: $1 \leq m \leq M$ and $1 \leq l \leq L_T$, where L_T is the number of total slots

- $L_T >> L_R$ to account for the delays of nodes that are queued at slot $l_o < L_R$ that are not successfully transmitted till $L_R < l \leq L_T$. If node k is not successfully transmitted by slot L_T, then the node k's delay is $D_k = L_T - x$, where x is the maximum index l at which $Q_{kl} = 1$.

- Let I_{ml} be an indicator random variable such that:

$$I_{ml} = \begin{cases} 1 & R_{ml} > 0 \\ 0 & \text{otherwise} \end{cases} \tag{7.1}$$

The sum of random variable I_{ml} over m and l counts the total number of successful transmissions.

- Let Q_{ml} be an indicator random variable such that:

$$Q_{ml} = \begin{cases} 1 & \text{node } m \text{ is queued in slot } l \\ 0 & \text{otherwise} \end{cases} \tag{7.2}$$

The sum of random variable Q_{ml} over m and l counts the total number of queued transmissions.

- The average throughput $E[T]$, which is the average number of successful transmissions per slot is given by:

$$E[T] = \frac{\sum_{m=1}^{M} \sum_{l=1}^{L_R} I_{mj}}{L_R} \tag{7.3}$$

- The average sum rate per slot:

$$E[R_S] = \frac{\sum_{m=1}^{M} \sum_{l=1}^{L_R} R_{mj}}{L_R} \tag{7.4}$$

- The average rate per node:

$$E[R_i] = \frac{\sum_{m=1}^{M} \sum_{l=1}^{L_R} R_{mj}}{\sum_{m=1}^{M} \sum_{l=1}^{L_R} I_{mj}} \tag{7.5}$$

- The average delay per node $E[D]$:

$$E[D_i] = \frac{\sum_{m=1}^{M} \sum_{l=1}^{L_T} D_{mj}}{\sum_{m=1}^{M} \sum_{l=1}^{L_R} Q_{mj}} \tag{7.6}$$

- The variance of the rate per node σ^2_{rate}:

$$\sigma^2_{\text{rate}} = \frac{\sum_{m=1}^{M}\sum_{l=1}^{L_R} R_{mj}^2}{\sum_{m=1}^{M}\sum_{l=1}^{L_R} I_{mj}} - \frac{\sum_{m=1}^{M}\sum_{l=1}^{L_R} R_{mj}}{\sum_{m=1}^{M}\sum_{l=1}^{L_R} I_{mj}} \tag{7.7}$$

- The variance of the delay per node σ^2_{delay}:

$$\sigma^2_{\text{delay}} = \frac{\sum_{m=1}^{M}\sum_{l=1}^{L_T} D_{mj}^2}{\sum_{m=1}^{M}\sum_{l=1}^{L_R} Q_{mj}} - \frac{\sum_{m=1}^{M}\sum_{l=1}^{L_T} D_{mj}}{\sum_{m=1}^{M}\sum_{l=1}^{L_R} Q_{mj}} \tag{7.8}$$

In addition to capturing the asymptotic rate, we also capture the rate achieved using the imperfect decoding weights, and we also record the actual rate achieved which is equal to the rate specified by the modulation and coding scheme of the protocol.

From these statistics we also compute a measure of fairness which seeks to capture the width of the distribution in the rates that nodes can achieve in a network with a given set of parameters:

- fairness: $\frac{\sigma_{\text{delay}}}{\mu_{\text{delay}}}$, $\frac{\sigma_{\text{rate}}}{\mu_{\text{rate}}}$

The statistics on the number of packets in outage on the control channel, the data channel, and the number of protest packets transmitted are collected.

- ave num. control channel outages: $\frac{\#\text{ of cc. outage packets}}{\text{slots*num-sub-slots}}$
- ave num. data channel outages: $\frac{\#\text{ of dc. outage packets}}{\text{slots}}$
- ave num. protest packets: $\frac{\#\text{ of protest packets}}{\text{slots*num-sub-slots}}$

In each data channel slot we also compute an approximate bounding rate for a given data channel slot where m nodes contend for the data channel slot in the previous control channel period. We define this bounding rate to be the maximum achievable sum rate consisting of simultaneous transmissions by all transmitting nodes in that subset, where transmitting nodes maintain the same transmit scheme (informed or uninformed), and where nodes use

a transmit covariance rank less than or equal to that originally used by each node. To find the maximum bounding rate, we would need to consider the sum rate for each of the $2^{(m \times \text{tx}-\text{cov}-\text{rank})}$ subsets of the m node-pairs. In our simulations, we consider a subset of these subsets, find the maximum, and call this rate the approximate bounding rate[1].

7.2.1 Protocol Cost

As a metric to quantify the fractional loss in throughput caused by the protocols mechanisms to communicate the channel state and the transmit and receive parameters required for communication, as well as the mechanisms to restore the communication link when outage occurs, we define the instantaneous protocol cost to a Tx-Rx pair, the instantaneous protocol cost to a network, and the average protocol cost to a Tx-Rx pair and to the network.

The highest received rate between a transmitter and receiver is achieved when the transmitter has perfect knowledge of the channel, and transmits at a data rate less than the Shannon limit so that reliable communication can be achieved. Achieving this highest possible rate also requires that at each instant, the receiver has adequate knowledge of the channel for decoding, and knowledge of the transmitter's modulation and coding scheme. In a real system, however, packets are sent with preambles for channel estimation and synchronization. Header information is included to communicate the modulation and coding information of each packet. Redundancy is introduced into the packet to make each packet robust to channel fluctuations. Acknowledgment messages are sent to inform a user whether or not packets have been received in outage. Packets received in outage can be retransmitted. And in this protocol for the interference-limited regime, transmiter-receiver pairs must adapt as well to a changing interference environment which can make an outage event more likely. In addition,

[1]There is a superior bounding rate that could be computed in which transmitter nodes are sent the receiver's-interference-covariance (K_{R_x}-CSI) channel state information so that the interference channel could be whitened. This method would involve nodes repeatedly computing their transmit-beamformer, letting the receiver nodes train, then letting receiver nodes send K_{R_x}-CSI to its target transmitter. The convergence properties of this sort of algorithm has not been investigated, however, so this method is not used in our simulations.

degrees of freedom are allotted for the control channel to facilitate management functions.

- The **instantaneous cost of a protocol scheme to a transmit-receive pair** is defined as the difference between the maximum achievable rate when perfect knowledge of the Tx-Rx channel and the interference environment was present at both the transmitter and the receiver at that instant and the actual achieved rate at that instant under the protocol, divided by the instantaneous optimal rate.

- The **instantaneous cost of a protocol scheme to the network** is defined to be the difference of the sum of the maximum achievable rates for all transmit-receive pairs in the network and the sum of the achieved rates over all transmit-receive pairs in the network, divided by maximum achievable rates for all transmit-receive pairs in the network.

- The **average protocol cost to a transmit-receive pair** is the average instantaneous cost, where the instantaneous cost is computed over a sufficiently long duration including several side-channel and data-channel intervals.

- The **average protocol cost to the network** is the average instantaneous cost, where the instantaneous cost is computed over a sufficiently long duration including several side channel and data channel intervals.

To further characterize the aspects of the protocol that result in a divergence between the achieved rate and the maximum achieveable rate given a particular network and when all nodes have perfect knowledge of the channel we define:

- **Management Costs:** The spectral efficiency lost during the side-channel period when session initiation messages, and protest / backoff-request messages are broadcasted, and N-ACKs.

- **Session Maintenance Costs:** The efficiency lost during the reception of preambles for detection, estimation, synchronization, the use of pilot tones, and training fields

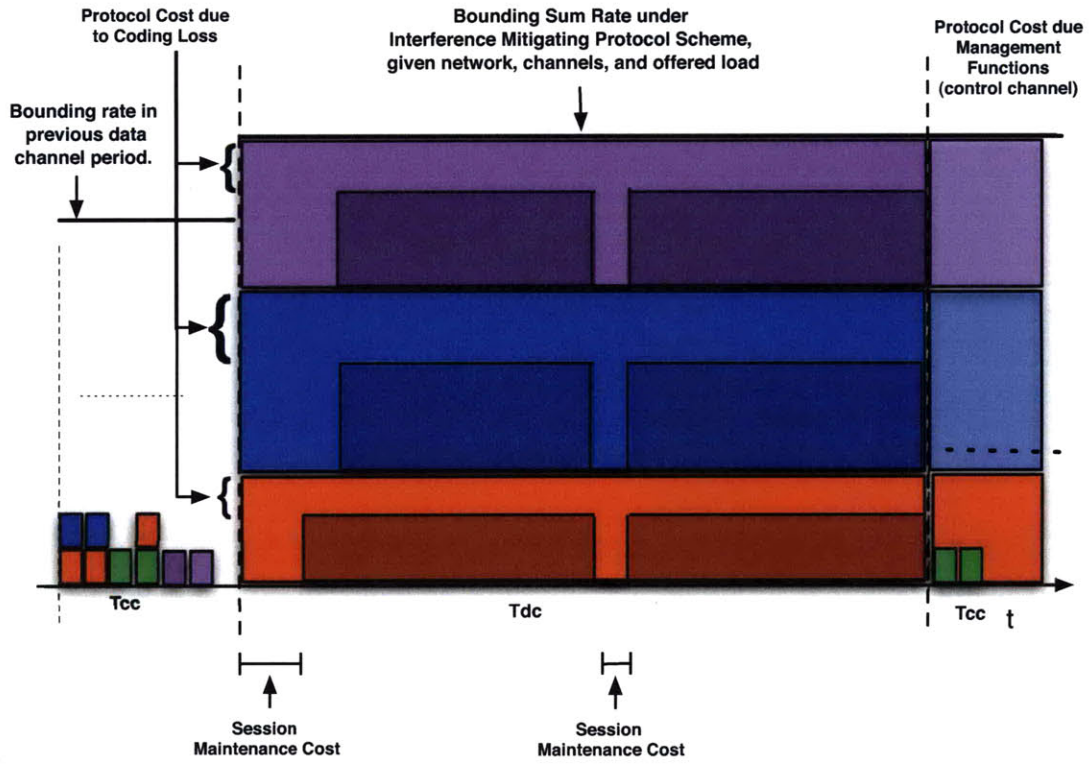

Figure 7-1: Protocol Cost

within data packets.

- **Protocol-Coding-Schemes Costs:** The modulation and error correction coding schemes that are used in typical network protocols have fairly minimal coding gains, leaving a large gap between achieved rates and capacity.

7.3 802.11(n) Benchmark

As described in chapter 2, the 802.11(n) standards provide many different modes of operation, many different transmit-receive schemes and specifies over 80 different data rates corresponding to these different transmit receive schemes. Throughout, the 802.11(n) network will operate according to the Hybrid Coordination Function's (HCF) Enhanced Distributed Channel Access scheme (EDCA) where nodes contend for 'transmit opportunities,' as described in chapter 3. These transmit receive schemes include transmitter beamforming, space-time-coding, error correction codes including convolutional coding and low density parity check codes, spatial division multiplexing with 2, 3 or 4 streams, two options for the OFDM guard time and 2 options for the total system bandwidth. For the purposes of comparison, we will compare our protocol against the following most basic operations of 802.11(n):

1. Receiver Beamforming: The 802.11 standard does not directly specify a method for receiver beamforming since receiver beamforming does not require any additional protocol functionality beyond the training preambles that are already provided. According to [105], many chip manufacturers are including the receiver beamforming capabilities in their chipsets.

2. Though 802.11 provides over 80 modulation and coding scheme mechanisms, we will consider only the use of 1/2 rate convolutional coding with BPSK, QPSK, 16-QAM

and 64-QAM modulation schemes; and the use of transmit-covariance-rank 2 matrices used with spatial division multiplexing that double the spectral efficiency.

3. Since we report mean spectral efficiencies and assume delay spreads circa 50 ns, our results can correspond to the use of 400 or 800 ns guard intervals

4. In the earliest 802.11 versions, packet sizes were limited to 1500 bytes. The 2007 revision of 802.11(a) extended packet sizes to 4095 bytes. With MAC aggregation in 802.11(n), the maximum packet size is 65535 bytes.

In place of the transmit beamforming mechanism that the 802.11(n) standard defines, we will implement a receiver beamforming in our WiFi simulations. Since this does not require CSI at the transmitter, the protocol operation with receiver beamforming will lead to higher average throughput. We will compare this scheme to our Uninformed Transmitter schemes. We will also implement 802.11(n)'s SDM scheme with explicit feedback to compare to our Informed Transmitter protocol schemes.

All nodes carrying out MIMO-communications will exchange CSI using explicit feedback (an exchange more efficient that implicit feedback when the channel is assumed to not be unchanging). Under this mode of operation, a node seeking a TXOP in 802.11(n) must wait the duration AIFS after the last transmission to begin the backoff counter. Nodes would then transmit a RTS packet (which are required in the EDCA mode as a mechanism to set other nodes' network allocation vector), would wait for a CTS packet from its target receiver, and then begin the training process.

To obtain Tx-CSI, the beamformer sends a sounding packet to the beamformee, requesting explicit feedback. The first sounding packet is referred to as a request for feedback sounding-PPDU, and is identified at the receiver by its CSI/Steering subfield which is set to zero, and its NDP Announcement subfield that is set to 0. The number of HT-LTFs is determined by the number of space-time streams transmitted, and additional dimensions are sounded using

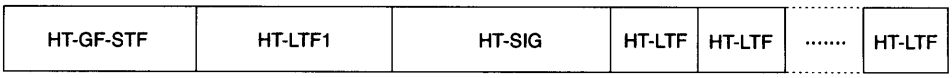

Figure 7-2: 802.11 (n) Sounding Packet

the HT-ELTFs where the latter are required for eigenbeamforming. A sounding PPDU may have any number of HT-LTFs ($N_LTFs \geq N_STS$. HT-ELTFs are used except where the number of spatial streams is 3 and N_LTF is 4. The format of sounding packets can be either staggered so that one transmit antenna transmits at a time; or sounding packets can use all transmit antennas simultaneously and then be decoded using space-time techniques. The duration of this packet we estimate to be 32 μs. The beamformee then sends the Explicit CSI feedback after a SIFS (16 μs) to the beamformer. The total number of bits returned to the transmitter when the receiver feedback CSI is $N_r \times 8 + 52 \times (3 + 2 \times N_b \times N_c \times N_r)$ where N_b is number of bits per coefficient, N_c is the number of columns in the CSI matrix and N_r is the number of receive chains[2]. This information encodes the SNR in each of the receive chains quantized to 8-bit twos complement value, where SNR_{ave} is the decibel representation of linearly averaged values over the tones represented. The remaining bits correspond to MIMO channel matrix on each of the 52 tones where N_b bits encode the real part, another N_b bits encode the imaginary part, and 3 bits are used to encode the amplitude. N_b can be 4, 5, 6 or 8 bits. N_c is the number of spatial streams. We estimate the duration of this packet exchange to be a total of 1240 μs for a system with 4 receive antennas and two transmit antennas, and using 8 bit quantization and 1/2 rate error correction coding and QPSK modulation. This corresponds to approximately 1/3 the duration of a data packet.

7.4 Simulations of STI-MAC in 'Typical' Networks

For this key area of our parameter space, we will discuss all the statistics collected from our simulations. The parameters of SIM1 correspond to a 'typical' multi-antenna wireless

[2]In simulations of Wi-Fi, we account for quantized feedback in the duration of packets; but we do not send bits to the transmitter.

network. In later sections, we will discuss the subset of these metrics that are most interesting in illuminating the benefits, or highlighting the weaknesses of the STI-MAC protocols. The parameters for SIM1:

- 20 Transmitter-Receiver Pairs
- Receive Antennas: 4
- Single Transmit Antenna
- Transmitter-Covariance-Rank: 1
- Link-Rank: 1
- Link-Length: 10 m
- Modulation and Coding scheme requested by Transmitter-Receiver pairs are Uniformly over { 0.5, 1, 2, 3 } bits/sec/Hz

In all of figures below, we let $'G'$ represent the offered load, which describes the probability that an individual node will try to transmit a new packet to the system when that node is not backed off due to outage or due to having received a protest packet. For instance, in a network with $M = 20$ users, an offered load $G = 8$ corresponds to each user that is not backed off transmitting a packet to the control channel with probability $G/M = 8/20$.
In figure 7-3(a), we illustrate the distribution on the asymptotic rates as a function of the offered load. These rates are bounding rates in the sense that they are achievable with optimal source and channel coding. They are a function of the asymptotic value of the SINR achieved by each node that transmits a packet on the data channel, and are a useful way to show the SINRs that are achieved independent of the rank of the transmit covariance matrix:

$$r_{asy} = \sum_{i=1}^{tx-cov-rank} \log_2(1 + SINR_i) \tag{7.9}$$

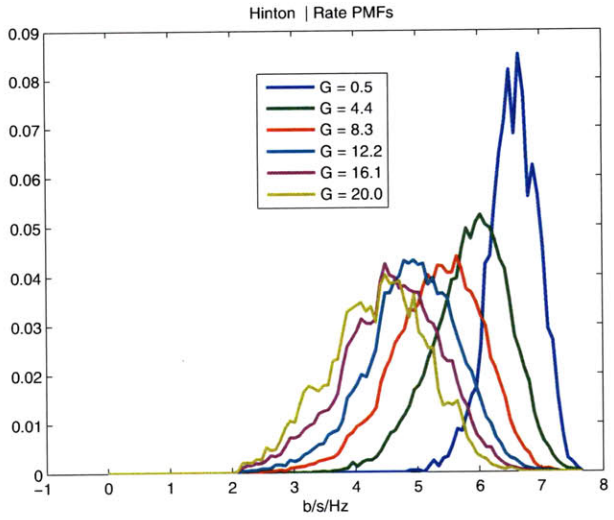

(a) SIM1 PDF on Asymptotic Rates

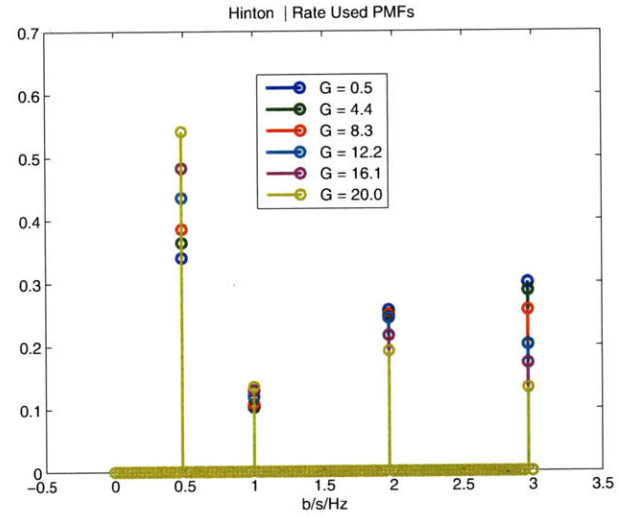

(b) SIM1 PMF on Actual Rates

Figure 7-3: Distribution on Asymptotic Rates and Actual Rates, Network with 20 Transmit-Receive pairs with 4 Receive Antennas and 1 Transmit Antenna, Link-Rank = 1, and Link Length = 10m

In figure 7-3(b), we illustrate the distribution on the actual rates that nodes use. These rates are in the set of rates offered by the protocol { 0.5, 1, 2, 3 } bits/sec/Hz. The requested rates are a function of the distribution on the requested load. Recall, these rates are lower than the asymptotic rates because the modulation and coding schemes used (taken from 802.11

protocols) code at efficiencies far below the Shannon limit. What is illuminating in these plots is the shift in the distribution on the asymptotic rate as the offered load increases. This results from the increased interference that is caused by more nodes transmitting simultaneously. In the distribution on the actual rates, there is a related change in the shape of the distribution. As the offered load increases, the nodes that access the medium tend to be the nodes that request the lowest data rate; whereas for the low offered loads, the distribution on the actual rates is more uniform. As we would expect, protocols in the interference regime will tend to favor data rates that require less SINR.

Observing the behavior of the mean as a function of the offered load is slightly more illuminating for this work. As shown in figure 7-4(a), the mean spectral efficiency per node declines as a function of the offered load. The mean actual rate, or the used rate (as it is labeled), declines with increasing offered load – consistent with the change in the distribution observed in figure 7-3(b). The observed behavior of the standard deviation of the per-user-rates is also consistent with the pdfs show in figure 7-3(a). When the interference is lower, receivers observe consistently high data rates with a low relative standard deviation. As the number of interferers increases, the variability of the target and interference channels leads to a wider variation in the observed SINRs and subsequent data rates. This results in a larger standard deviation of per user rates, and a decreasing mean.

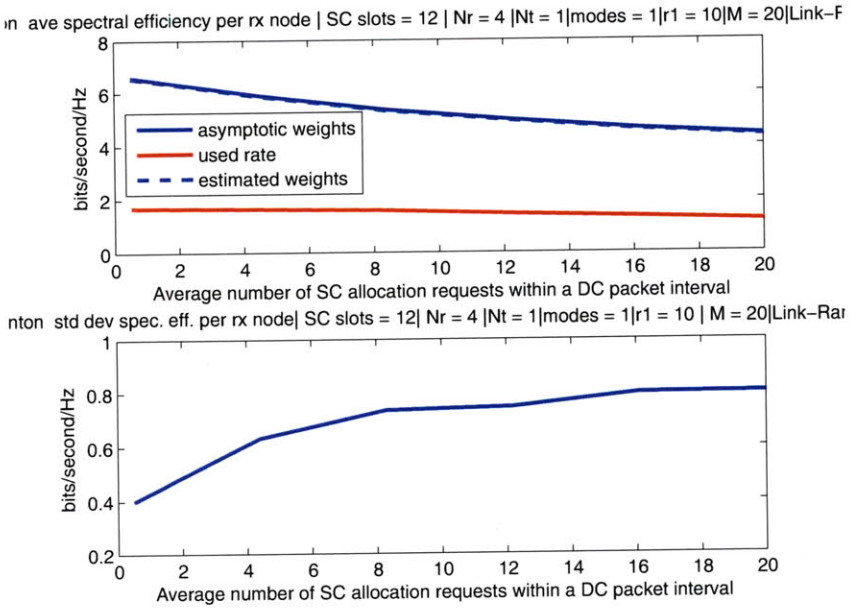

(a) Top graph: SIM1 Mean Rates per Node. Lower graph: SIM1 Standard Deviation of the Mean Rate per User

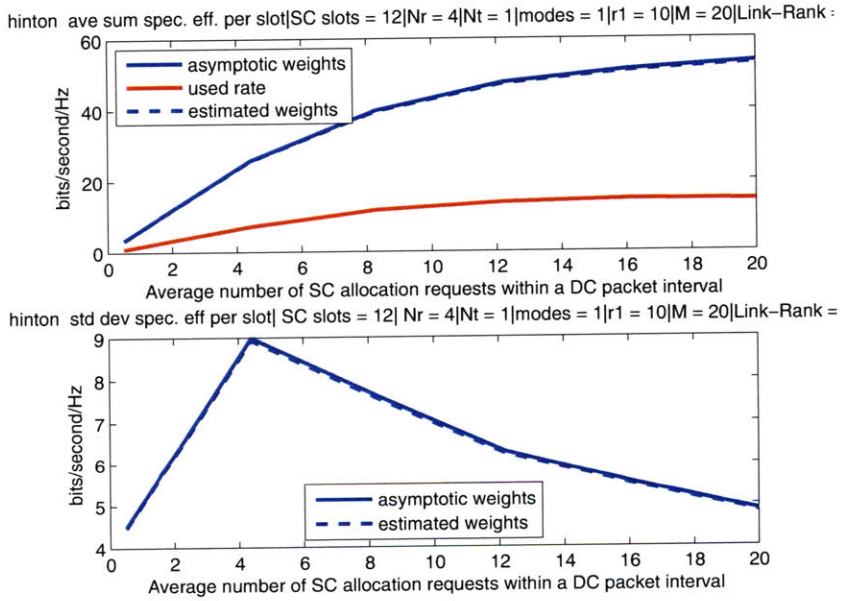

(b) Top graph: SIM1 Mean Sum Rates. Lower graph: SIM1 Standard Deviation of the Mean Sum Rate

Figure 7-4: Mean and Standard Deviation of Asymptotic Sum Rates; Mean and Standard Deviation of Asymptotic Per Node Rates, and Actual Rates, Network with 20 Transmit-Receive pairs with 4 Receive Antennas and 1 Transmit Antenna, Link-Rank = 1, and Link Length = 10m

The mean sum rate behaves quite differently from the per-node-rates. The mean sum rate shown in figure 7-4(b) increases with increasing offered load because an increasing number of nodes are contending, and gaining access to the medium. Because the distribution of rates is uniform, and as observed above in figure 7-3(b), the protocol begins selecting for the nodes that offer lower interference levels (allowing other nodes to maintain their rate), and that tend to have lower received SINRs. In order for the mean sum rate to decline consistently, over many data channel slots, the contention on the control channel – which results in first-come-first-come service – would need to be front loaded with nodes requesting higher data rates. Maintaining these rates would necessarily require lower SINR, which tends to reduce the number of interfering nodes. Because the offered load is uniformly distributed, it is equally likely that low-requested-rate users will be first to the control channel, allowing many users on the data channel simultaneously since they required less SINR. This would drive up the mean sum rate. Examining the mean sum rate, it appears that this latter effect dominates.

In figure 7-5(b), we observe the average delay as a function of the offered load. We normalize the delays by the duration of a data channel packet. As shown in figure 7-5(b), the average rate increases with increasing offered load. A delay of unity would correspond to transmitting immediately, and is achievable only in an ALOHA scheme. [3] The delay over unity in the STI-MAC protocols is characteristic of nodes that arrive to the medium during the previous data channel slot and must wait for the control channel slot (and its entire duration) to transmit a packet. In figure 7-5(a) we plot the logarithm of the tails of the distribution of of the delay, which as shown, have a low likelihood. Nodes are very likely to be successful on their first attempt at sending on the data channel. The tails of the distribution show that with higher offered load, nodes are more likely to have long delays, driving up the mean for higher offered loads. This likelihood decreases as the offered load increases.

[3] In CSMA/CA protocols, there would have to be an observed idle slot as well, making the delay slightly larger than the packet length.

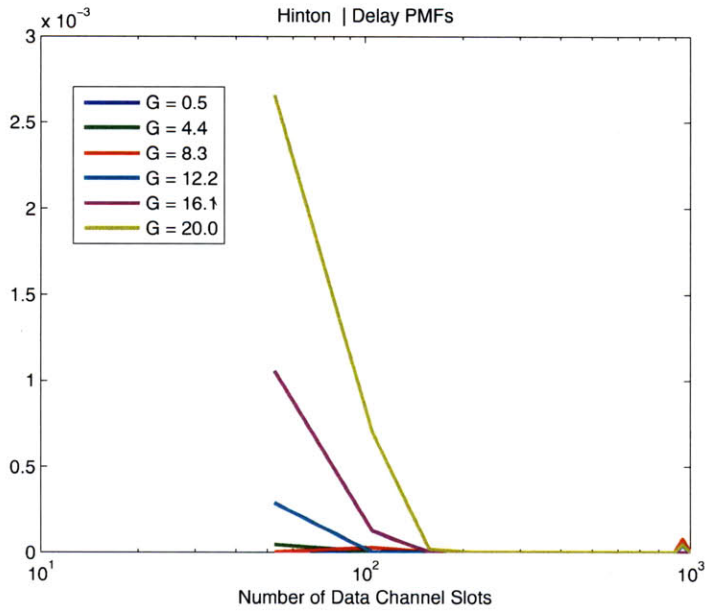

(a) SIM1 Delay PDF Tails

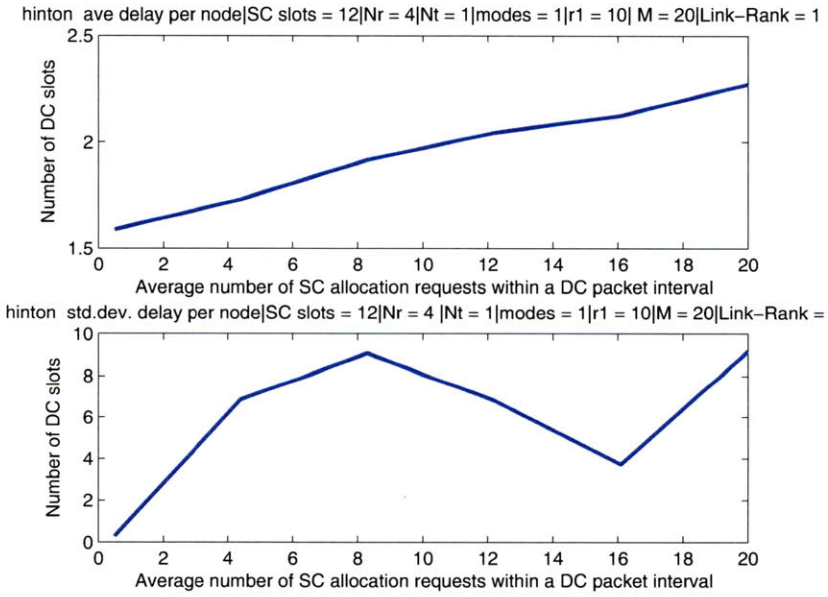

(b) SIM1 Mean Delay

Figure 7-5: (a) Distribution on Delay and (b) Mean Delay normalized by the duration of the data channel slot in upper graph of (b) subfigure and Standard Dev of delay in lower graph of (b) subfigure., Network with 20 Transmit-Receive pairs with 4 Receive Antennas and 1 Transmit Antenna, Link-Rank = 1, and Link Length = 10m

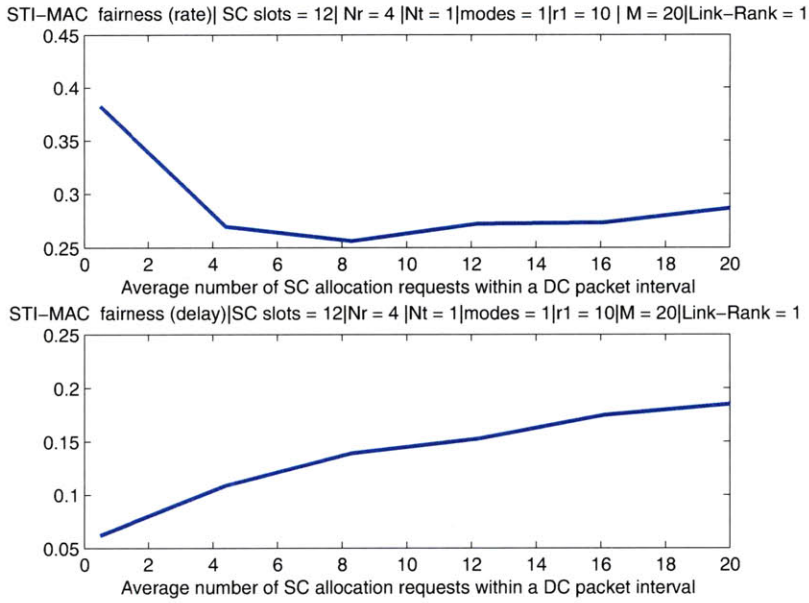

Figure 7-6: Fairness. Top graph a function of rate per node. Bottom graph a function of the delay normalized by the duration of a data channel slot. Network with 20 Transmit-Receive pairs with 4 Receive Antennas and 1 Transmit Antenna, Link-Rank = 1, and Link Length = 10m

In figure 7-6, we plot the fairness metric as a function of the offered load. In the upper graph in this figure, we plot the fairness in the per-node-rates. In the lower graph, we plot the fairness in the per-node-delays. Our fairness measures are equal to the standard deviation of the rate (delay) normalized by the mean rate (delay) as described in section 7.2, and thus is unitless. The decrease in the standard deviation of the rate is consistent with the distribution on the rate shown above. The increase in the standard deviation of the delay is consistent with many successful, near immediate transmissions, and more nodes taking a longer amount of time to successfully complete their transmission, evidenced by the mean delay.

In figures 7-7(a) and 7-7(b), we summarize the information from the above plots with scatter plots that show the mean per-node-asymptotic rates (or per-slot-sum rate) versus per-node-delays and versus the fairness metric for a collection of network iterations. Each point on

the plot corresponds to a particular network time series, showing the mean asymptotic rate and the mean delay.

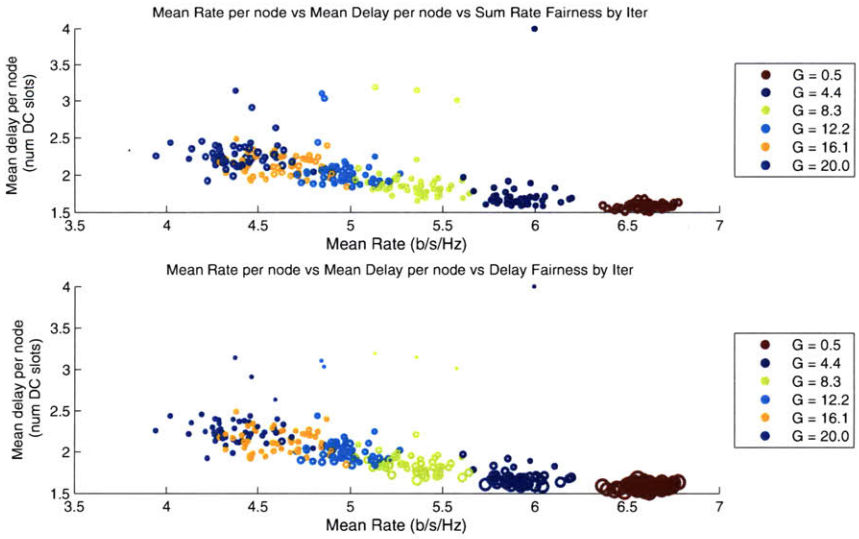

(a) SIM1 Scatter Plot of Ave Rate per Node versus Ave Delay

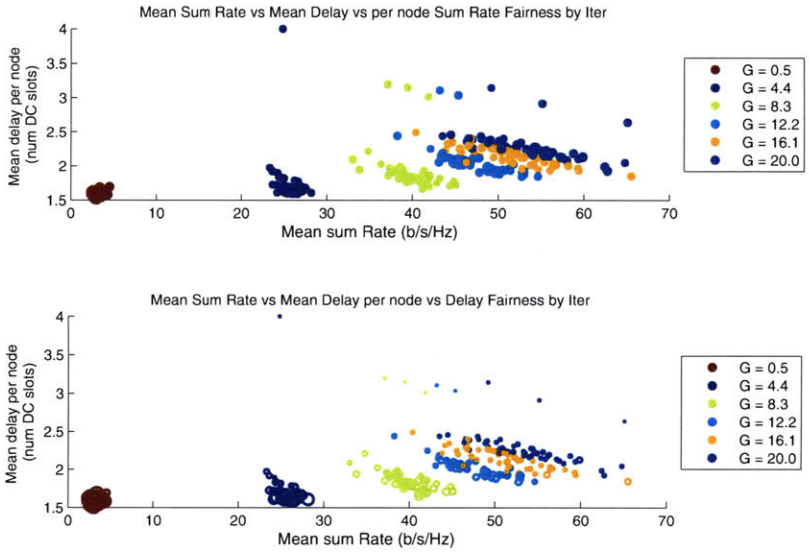

(b) SIM1 Scatter Plot of Ave Sum Rate per Data Channel Slot versus Ave Delay

Figure 7-7: (a) Scatter plots showing mean rate per node verses mean delay per node with the Fairness measure governing the radius of the data point. Top graph showing rate fairness. Bottom graph showing delay fairness. (b) Scatter plots showing mean rate per node verses mean delay per node with the Fairness measure governing the radius of the data point. Top graph showing rate fairness. Bottom graph showing delay fairness. . 20 Transmit-Receive pairs with 4 Receive Antennas and 1 Transmit Antenna, Link-Rank = 1, and Link Length = 10m

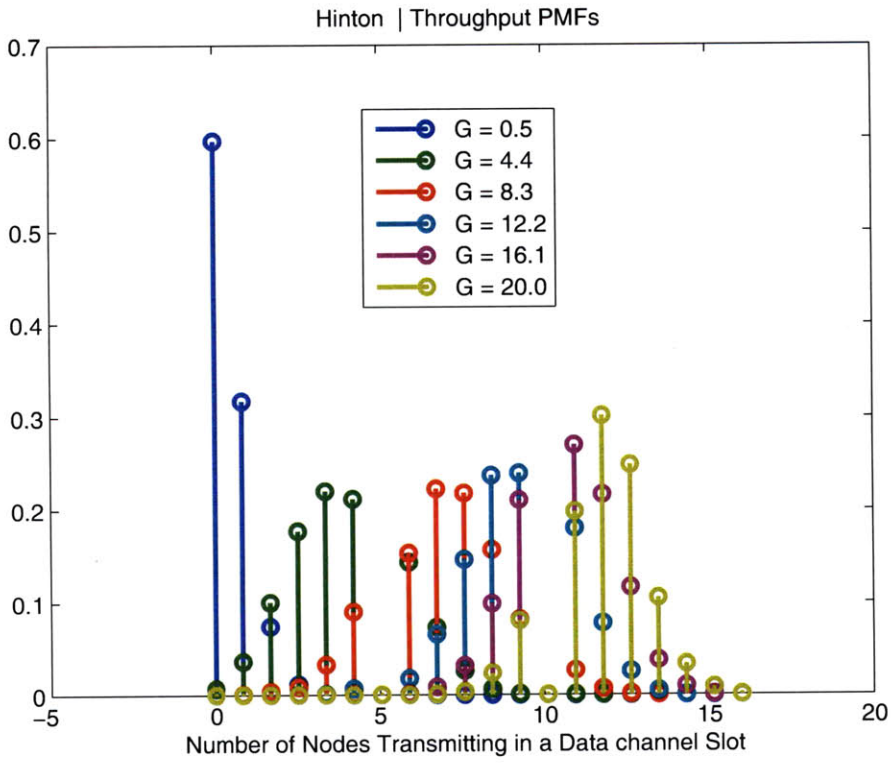

(a) SIM1 Throughput PMF

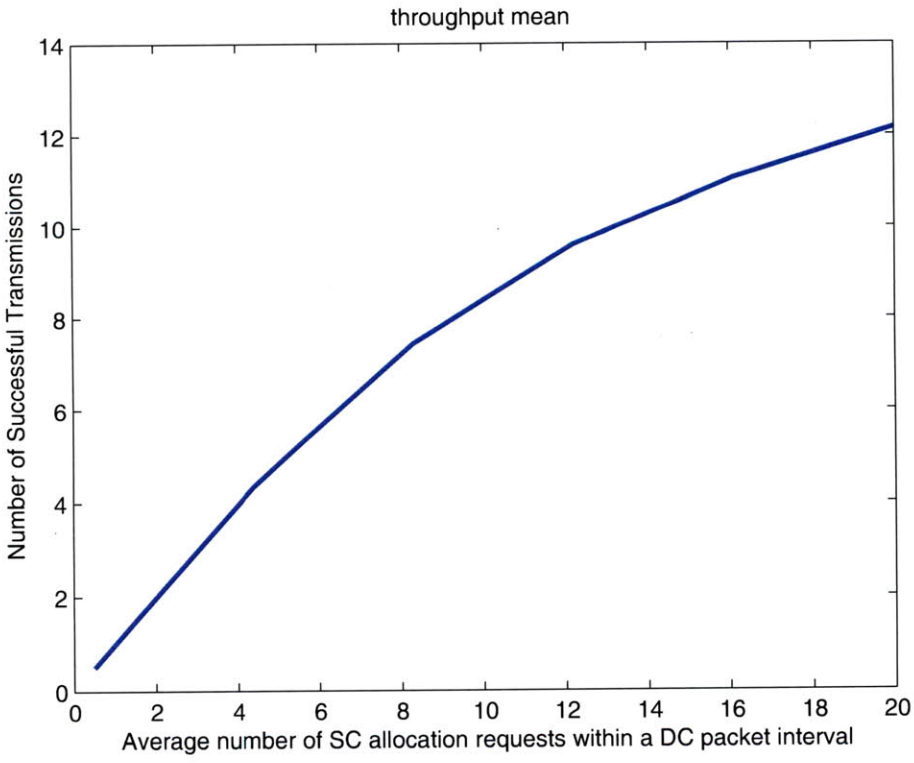

(b) SIM1 Mean Throughput

Figure 7-8: PMF and Mean Throughput, 20 Transmit-Receive pairs with 4 Receive Antennas and 1 Transmit Antenna, Link-Rank = 1, and Link Length = 10m

In figure 7-8(b) we plot the mean average number of nodes that transmit simultaneously in a data channel slot – the mean throughput – as a function of the offered load. As we determined above, the mean throughput increases with the offered load. In figure 7-8(a) we plot the distribution on the throughput as a function of offered load. As we will note in the next section, the mean throughput peaks at 12 transmissions per slot for this set of parameters.

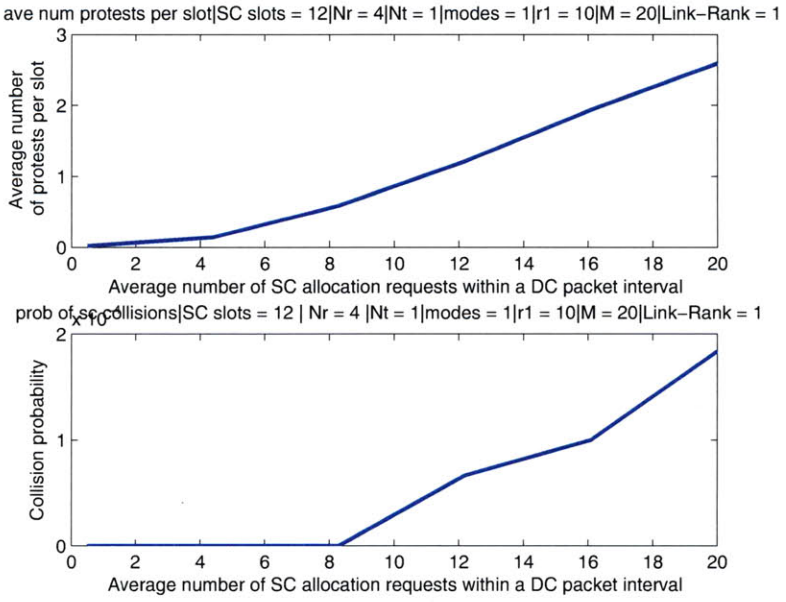

Figure 7-9: Average number of Protests per Slot (upper graph) and Probability of Control Channel Collisions (lower graph), Network with 20 Transmit-Receive pairs with 4 Receive Antennas and 1 Transmit Antenna, Link-Rank = 1, and Link Length = 10m

In figure 7-9, we plot the average number of protest packets sent on the medium as a function of the offered load. As we would expect, the number of protest packets increase as the number of nodes contending for the medium increases. In the lower plot of figure 7-9, we plot the average number of control channel outages per control channel period. As we would expect, the number of control channel packets in outage increases with the offered load since more nodes transmitting in the same slot increases the likelihood of outage.

7.4.1 Performance of STI-MAC in 'Typical Network' Simulations relative to 802.11(n) Benchmark

Here we summarize simulation results of a Wi-Fi network using the same set of parameters as those that are used above in the STI-MAC SIM1 simulations. These parameters correspond to 'typical' use of a multi-antenna network of nodes. First we consider the distribution on the asymptotic rates in figure 7-10. What is evident in this distribution of asymptotic rates is that for the lowest value of the offered load corresponding to an average of one new arrival in a duration equivalent to 10 data channel packets, the Wi-Fi nodes are essentially operating in a noise limited environment. As the offered load increases, however, more nodes are transmitting simultaneously, participating in spectral reuse, which accounts for the left-ward shift in the distribution of asymptotic rates.

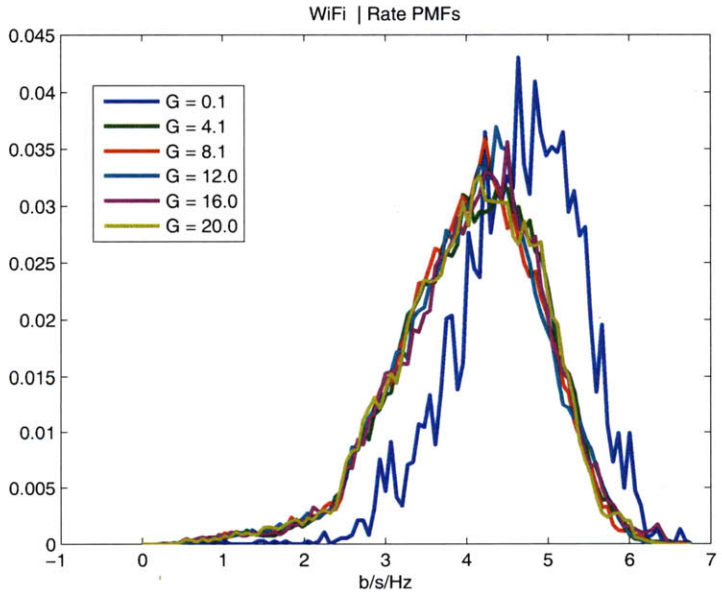

Figure 7-10: 802.11(n) Distribution on Asymptotic Rate, Networks with 20 Transmit-Receive pairs, 1 Transmit Antenna, 4 Receive Antennas, Link-Rank = 1, and Link Length = 10m

The presence of spectral reuse is illustrated in the mean throughput plot shown in figure 7-11. This shows that on average, there are effectively ~ 3 areas of the network which function as cells, allowing spectral reuse.

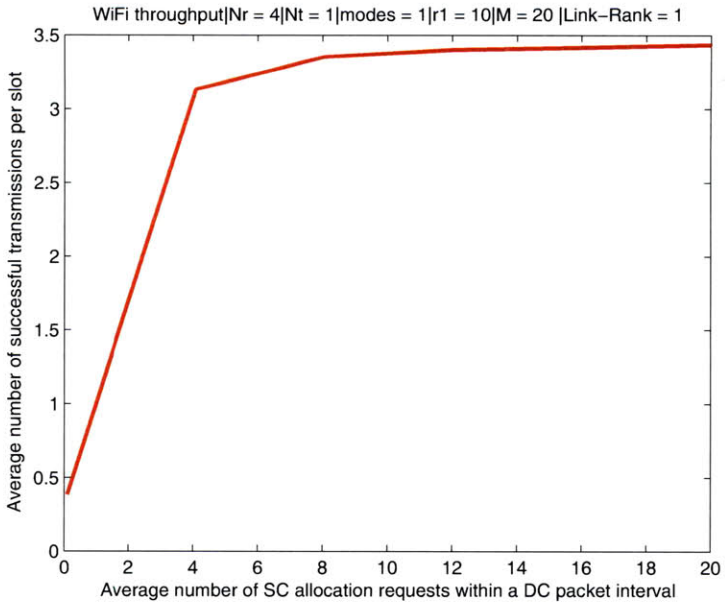

Figure 7-11: 802.11(n) Mean Throughput, Networks with 20 Transmit-Receive pairs, 1 Transmit Antenna, 4 Receive Antennas, Link-Rank = 1, and Link Length = 10m

Associated with this average throughput behavior is a mean sum rate that is approximately flat over the considered range of the offered load, and show in figure 7-12. The actual rate, or the used rate as it is labeled, is considerably less than the asymptotic rate due to the weakness of convolutional codes.

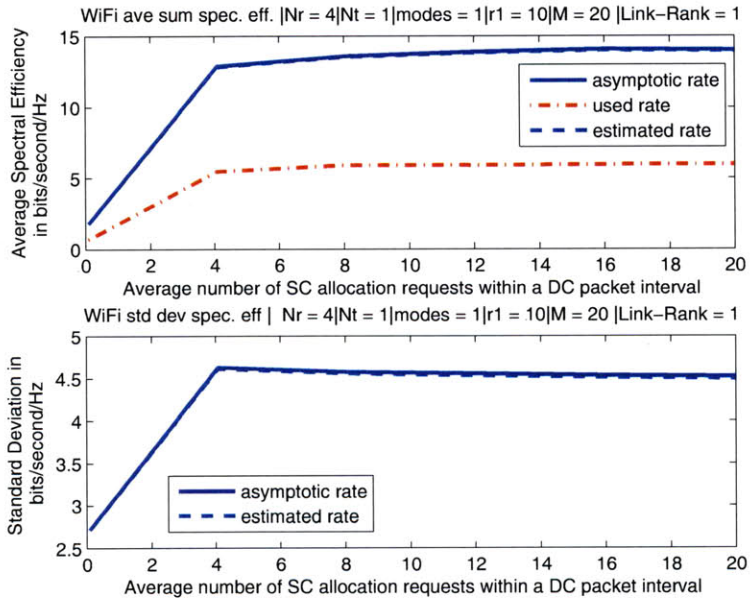

Figure 7-12: 802.11(n) Mean Sum Rate (upper graph), Standard Deviation of Sum Rate (lower graph) Networks with 20 Transmit-Receive pairs, 1 Transmit Antenna, 4 Receive Antennas, Link-Rank = 1, and Link Length = 10m

Similarly to the STI-MAC case, the mean rate per node decreases with increasing offered load, but to a lesser extent than in the STI-MAC case where more nodes are transmitting simultaneously. The mean rate per node is illustrated in figure 7-13.

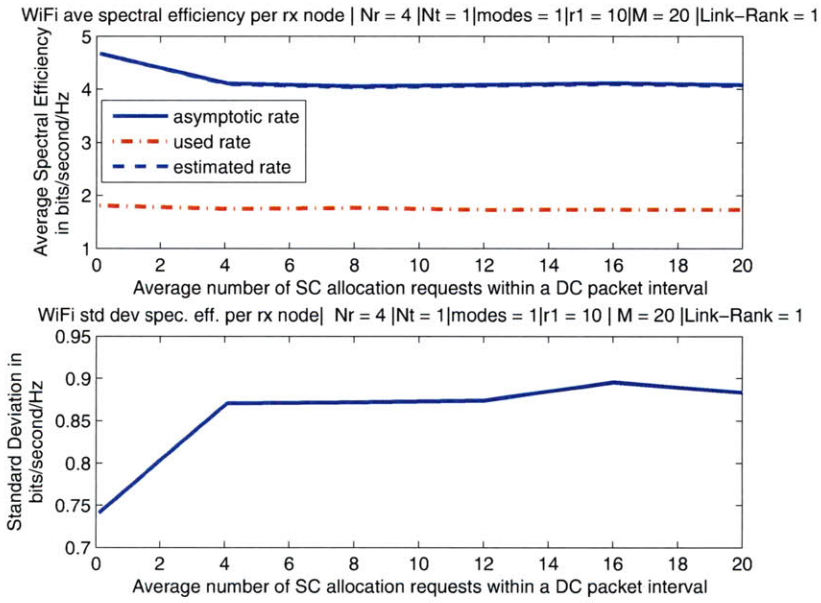

Figure 7-13: 802.11(n) Mean Rate Per Node (upper graph), Standard Deviation of rate per node (lower graph), Networks with 20 Transmit-Receive pairs, 1 Transmit Antenna, 4 Receive Antennas, Link-Rank = 1, and Link Length = 10m

If we consider the delay in these Wi-Fi networks, as expected, the delay is greater in this case than the delay in the STI-MAC protocols. This is shown in figure 7-14.

We also jointly plot the data from above in scatter plots that, in each data point in the plot, shows the mean statistics for a particular network time-series. In figure 7-15(a), we plot the per node rate versus the delay. In figure 7-15(b), we plot the mean sum rate versus the delay. Consistent with our results above, the mean asymptotic rates and mean delay are markedly different when operating in the noise limited regime (G = 0.1), versus when the network is exercising spectral reuse in the other cases of the offered load.

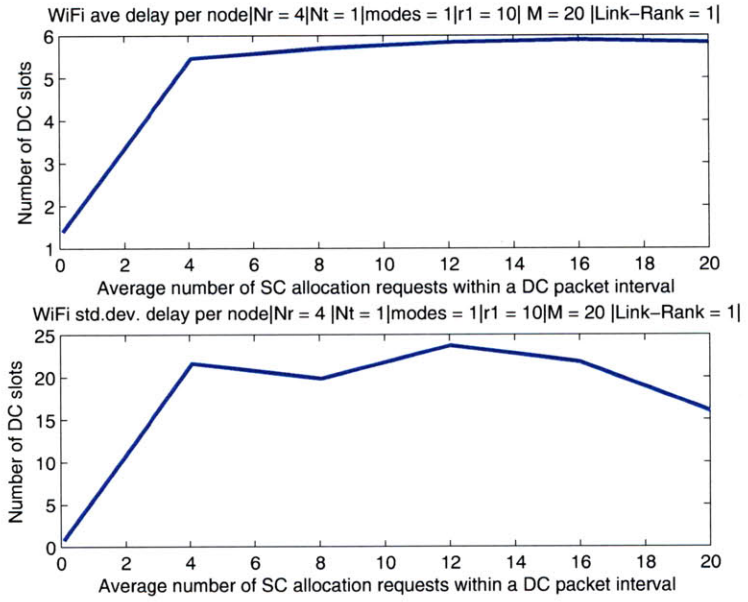

Figure 7-14: 802.11(n) (upper graph) Mean Delay normalized by the Duration of a Data Channel slot (Delay: from start of request to end of delivery) and (lower graph) Standard deviation of the normalized Delay, Networks with 20 Transmit-Receive pairs, 1 Transmit Antenna, 4 Receive Antennas, Link-Rank = 1, and Link Length = 10m

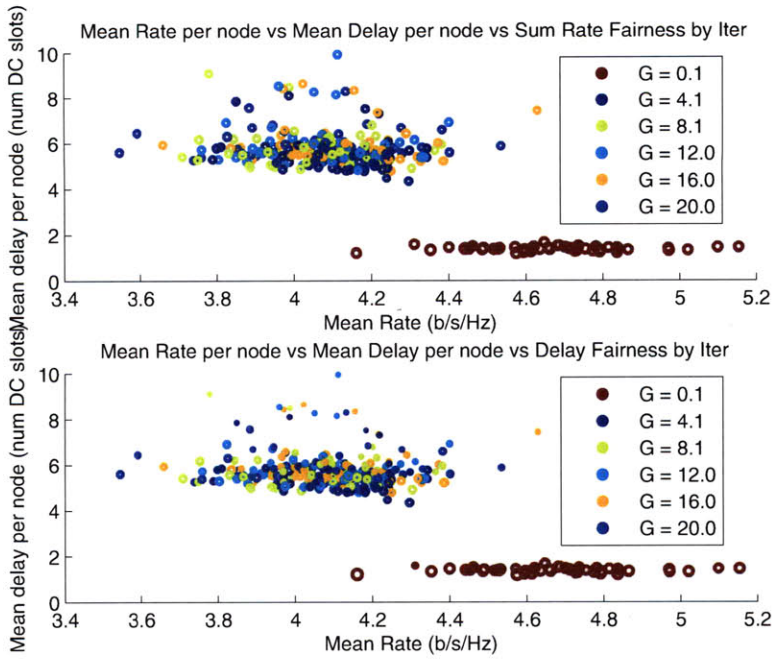

(a) SIM1 Wifi Scatter Plot of Ave Rate per Node versus Ave Delay

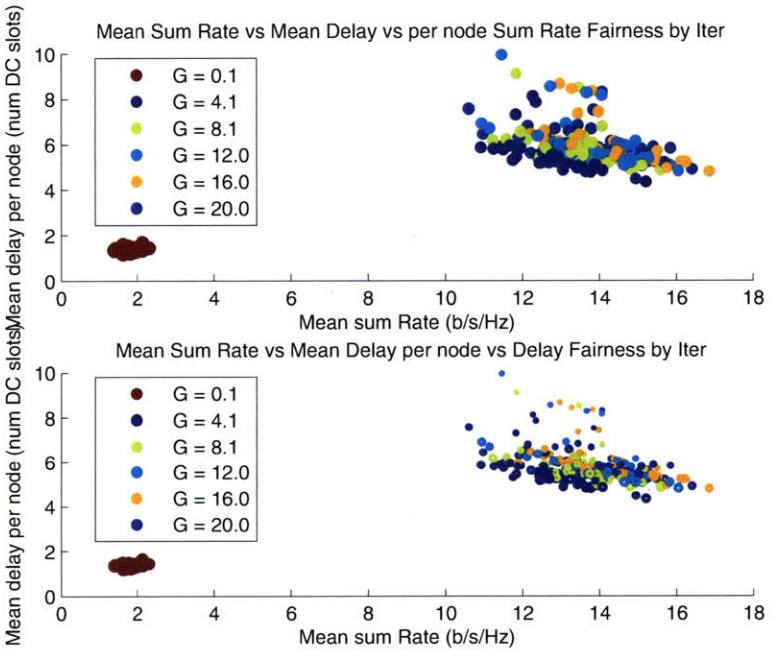

(b) SIM1 Wifi Scatter Plot of Ave Sum Rate per Data Channel Slot versus Ave Delay

Figure 7-15: 802.11(n) Scatter Plots – (a) avg rate per node vs. average delay. (b) avg sum rate vs. average delay. Fairness metric proportional to data point radius. Upper graph, fairness metric by rate. Lower graph, fairness metric by delay. Networks with 20 Transmit-Receive pairs, 1 Tx Antenna, 4 Rx Antennas, Link-Rank = 1, and Link Length = 10m

In figures 7-16 through 7-18, we look at head-to-head comparisons of the two protocols. In figure 7-16 we illustrate the throughput of the respective schemes as a function of the offered load. We see 3 - 4X improvements in throughput as the offered load and the number of people accessing the medium simultaneously rises.

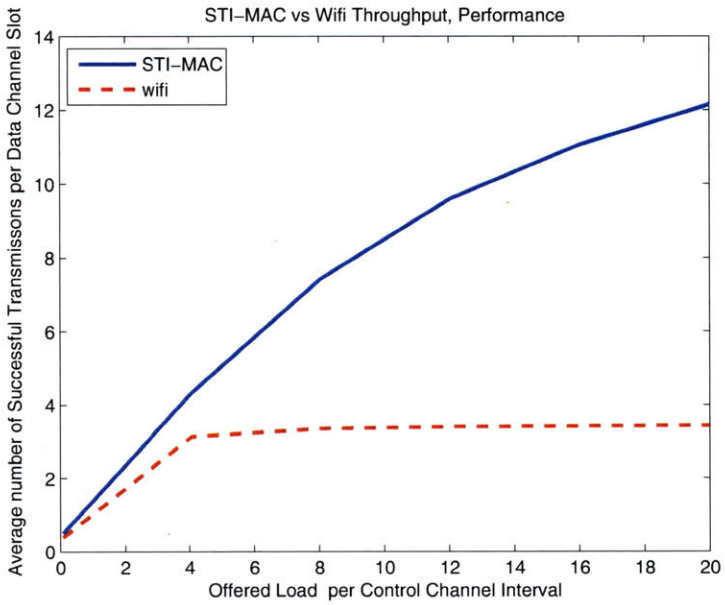

Figure 7-16: STI-MAC vs 802.11(n) Throughput Comparison, Networks with 20 Transmit-Receive pairs, 1 Transmit Antenna, 4 Receive Antennas, Link-Rank = 1, and Link Length = 10m

Commensurate with this rise in throughput is a rise in the total sum spectral efficiency as shown in figure 7-17. This shows that STI-MAC grows and seeks to make use of the entire pool of available resources. The growth in the total pie is not, however, independent. As show in figure 7-18, the per user asymptotic and actual rates decrease as the number of people using the medium grows. This occurs because transmissions are non-orthogonal, and are carried out in interference, bringing down the achievable rates.

In figure 7-19, we observe a much larger delay (factor of 3) in the Wi-Fi case relative to STI-MAC. As we would expect, when nodes are able to transmit simultaneously, most nodes incur lower delays.

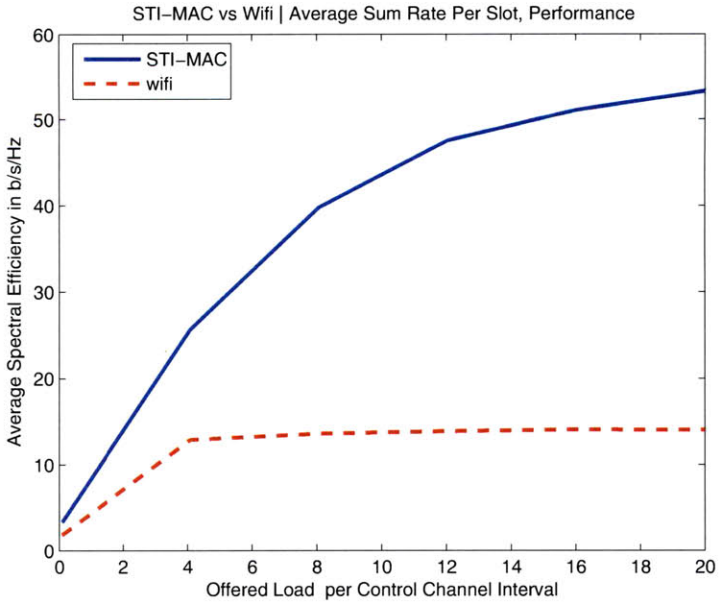

Figure 7-17: STI-MAC vs 802.11(n) Sum Rate Comparison, Networks with 20 Transmit-Receive pairs, 1 Transmit Antenna, 4 Receive Antennas, Link-Rank = 1, and Link Length = 10m

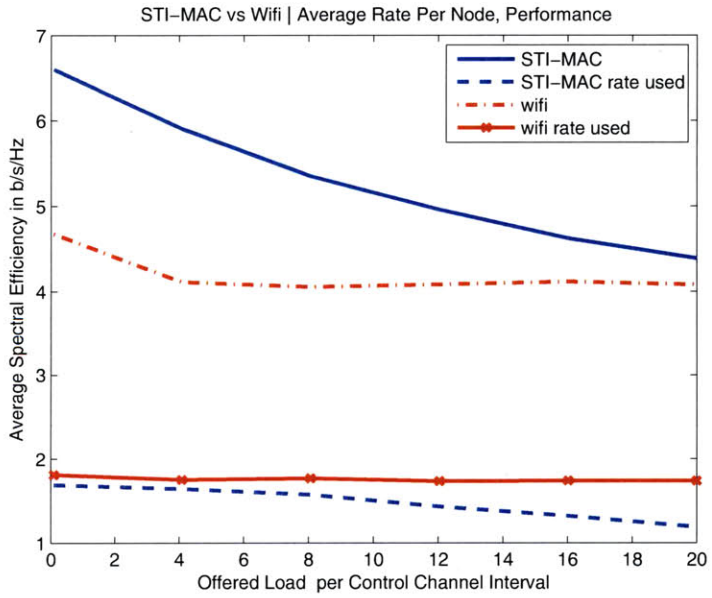

Figure 7-18: STI-MAC vs 802.11(n) Rate per Node, Networks with 20 Transmit-Receive pairs, 1 Transmit Antenna, 4 Receive Antennas, Link-Rank = 1, and Link Length = 10m

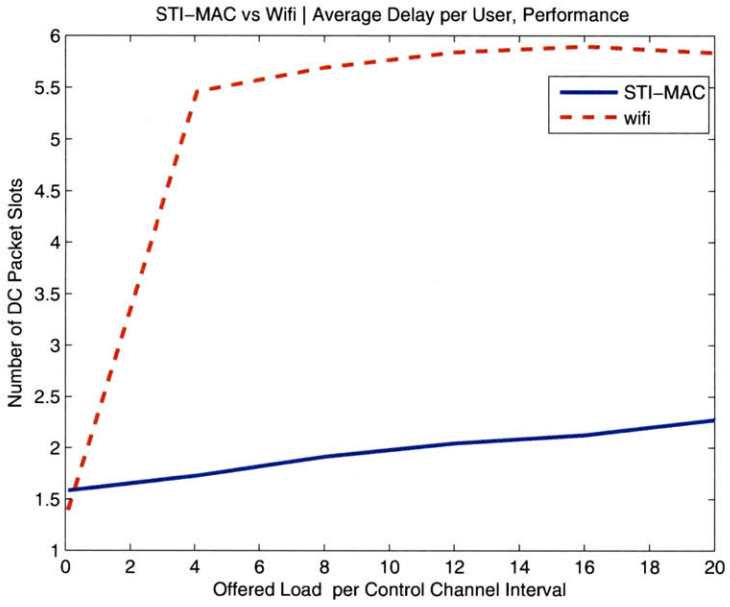

Figure 7-19: STI-MAC vs 802.11(n) Delay Comparison, Networks with 20 Transmit-Receive pairs, 1 Transmit Antenna, 4 Receive Antennas, Link-Rank = 1, and Link Length = 10m

7.5 Simulations to demonstrate the Effect of Receive Antennas on STI-MAC Protocols

In this area of our parameter space we are interested in understanding the value of increasing the number of receive antennas in the STI-MAC protocol with the control channel in time. **SIM2** operates with parameters:

- 20 Transmitter-Receiver Pairs
- Receive Antennas: 8
- Transmitter-Covariance-Rank: 1
- Uninformed Transmissions
- Link-Rank: 1
- Link-Length: 10m
- Modulation and Coding scheme requested by Transmitter-Receiver pairs are Uniformly over { 0.5, 1, 2, 3 } bits/sec/Hz

And **SIM3** operates with parameters:

- 20 Transmitter-Receiver Pairs
- Receive Antennas: 2
- Transmitter-Covariance-Rank: 1
- Uninformed Transmissions
- Link-Rank: 1
- Link-Length: 10m

- Modulation and Coding scheme requested by Transmitter-Receiver pairs are Uniformly over { 0.5, 1, 2, 3 } bits/sec/Hz

In figure 7-23, we compare the mean throughput as a function of the number of receive antennas. As we expected, the average throughput increases as a function of the number of receive antennas.

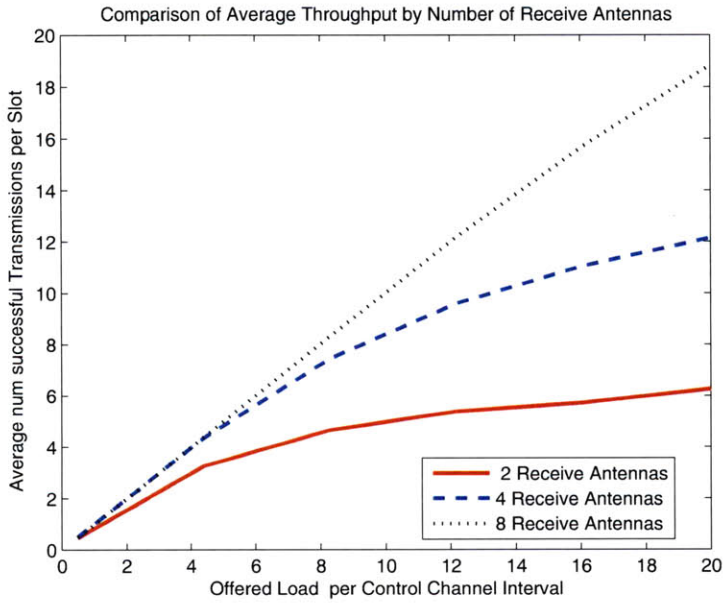

Figure 7-20: Average Throughput as a function of the number of Receive Antennas (Nr = 2, 4, 8), Networks with 20 Transmit-Receive pairs, 1 Transmit Antenna, Link-Rank = 1, and Link Length = 10m

Similarly, and as expected, average sum rate per slot and the average rate per node also grows with increasing number of receive antennas as shown in figures 7-21 and 7-22 respectively.

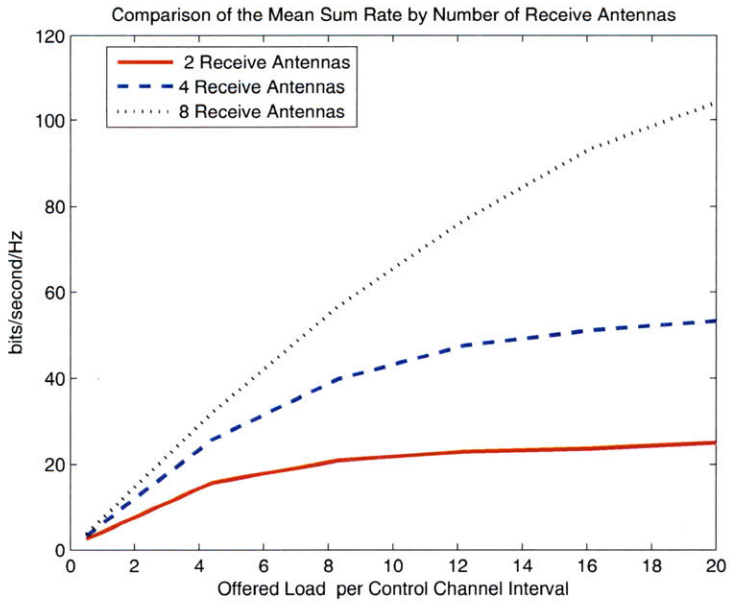

Figure 7-21: Average Sum Rate per Data Channel as a function of the number of Receive Antennas (Nr = 2, 4, 8), Networks with 20 Transmit-Receive pairs, 1 Transmit Antenna, Link-Rank = 1, and Link Length = 10m

Also as expected, the delay per node decreases as the number of receive antennas increases. This is a consequence of an increased likelihood of a collision on the control channel and more protest packets, sending more nodes to be backed off.

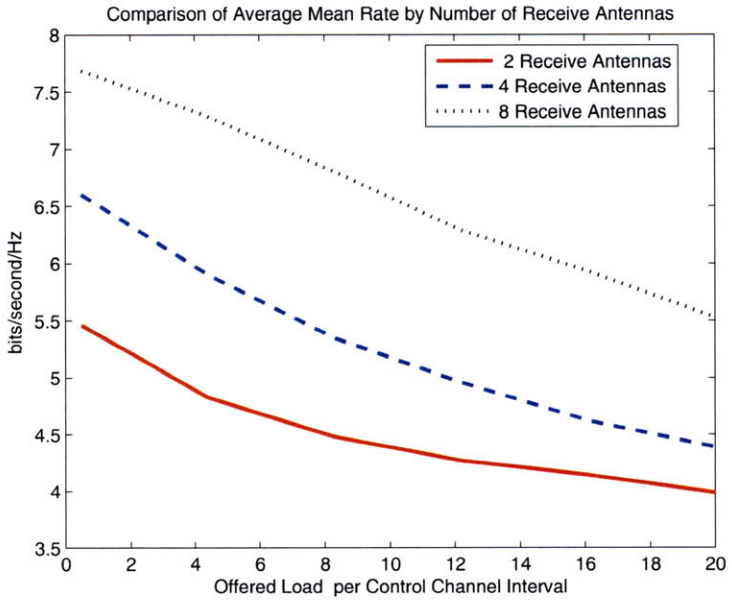

Figure 7-22: Average Rate per Node as a function of the number of Receive Antennas (Nr = 2, 4, 8), Networks with 20 Transmit-Receive pairs, 1 Transmit Antenna, Link-Rank = 1, and Link Length = 10m

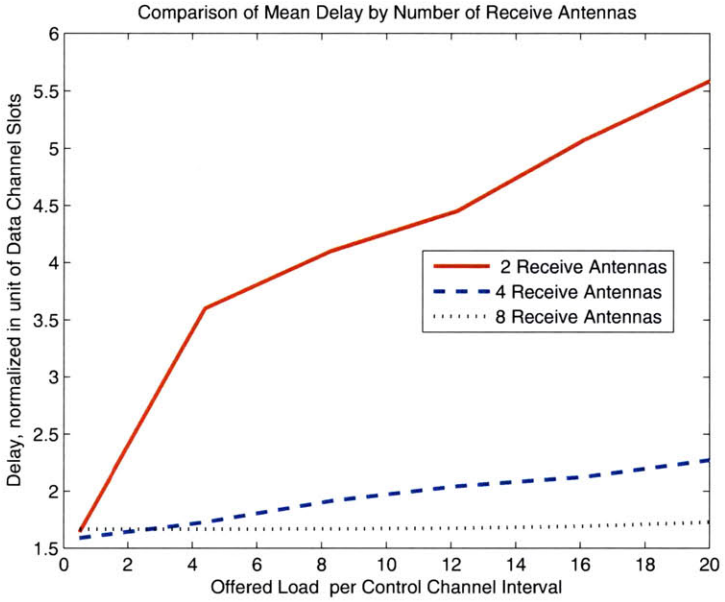

Figure 7-23: Average Delay as a function of the number of Receive Antennas (Nr = 2, 4, 8), Networks with 20 Transmit-Receive pairs, 1 Transmit Antenna, Link-Rank = 1, and Link Length = 10m

7.6 Simulations to Demonstrate Strong Performance of STI-MAC Relative to Wi-Fi

In this area of the parameter space, we observe the relative behavior of STI-MAC and Wi-Fi in an area where we expect STI-MAC to outperform Wi-Fi. We would expect STI-MAC to perform particularly well in situation where:

1. Many nodes compete for the medium
2. Transmitters delay transmitting because they sense neighboring transmissions.

We test this notion in these simulations of STI-MAC with 8 transmit and receive antennas with several antennas, and where interferers are closer to the receiver than its target transmitter, thus activating the back-off mechanism. This latter case corresponds to a high link rank of 3. Below we will add several individual plots on the performance of STI-MAC and Wi-Fi in this area of the parameter space.

- 40 Transmitter-Receiver Pairs
- Receive Antennas: 8
- 8 Transmit Antennas, Informed Transmitter using the Strongest Mode
- Transmitter-Covariance-Rank: 1
- Link-Rank: 3
- Link-Length: 10 m
- Modulation and Coding scheme requested by Transmitter-Receiver pairs are Uniformly over { 0.5, 1, 2, 3 } bits/sec/Hz

In figure 7-24, we see that in this area of our parameter space, there is a greater than 5X gain in throughput in STI-MAC over Wi-Fi. A key conclusion of our work is the influence

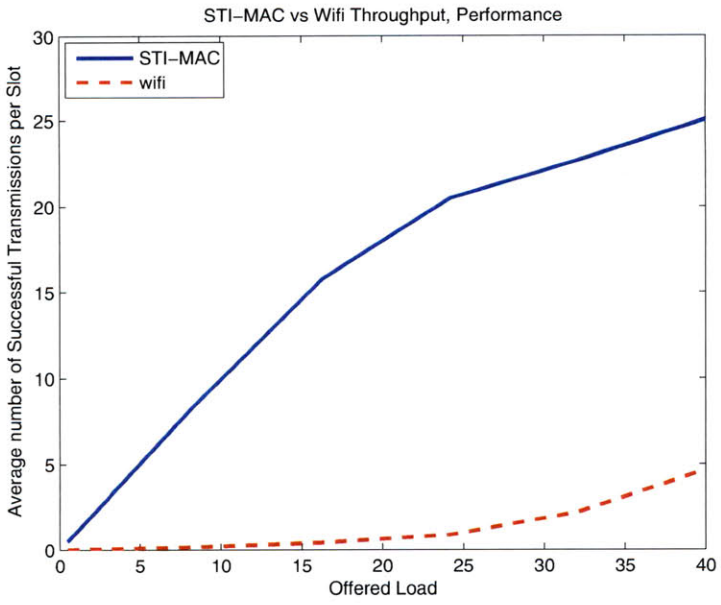

Figure 7-24: STI-MAC vs 802.11(n) Comparison of Average Throughput, Networks with 40 Transmit-Receive pairs, 8 Transmit Antenna, 8 Receive Antennas, Link-Rank = 3, Link Length = 10m, Informed Transmitter using Strongest Mode (Tx-covariance-Rank = 1)

of the link-rank on the performance of these protocols. Recall, the link-rank is the average number of nodes whose received power is higher at a given receiver than that receiver's target transmitter. For high link-rank networks with a many transmitter-receiver pairs, as shown in figure 7-24, Wi-Fi's throughput performance is largely muted. This is caused by the high likelihood that there is a neighboring node whose interference power is higher than the noise floor. In these high link-rank networks, STI-MAC uses its degrees of freedom to attenuate these interferers, and the STI-MAC throughput remains large. Consistent with earlier results and the behavior that we expect, as shown in figure 7-25, the per-node-rate decreases, on average, with the offered load while the total sum rate shown in 7-26 increases. Since more users are joining the network in the STI-MAC case, the SINRs seen at the receivers is lower, and so the modulation and coding scheme that can be supported offer a lower spectral efficiency. The total sum rate grows because more users are joining the network.

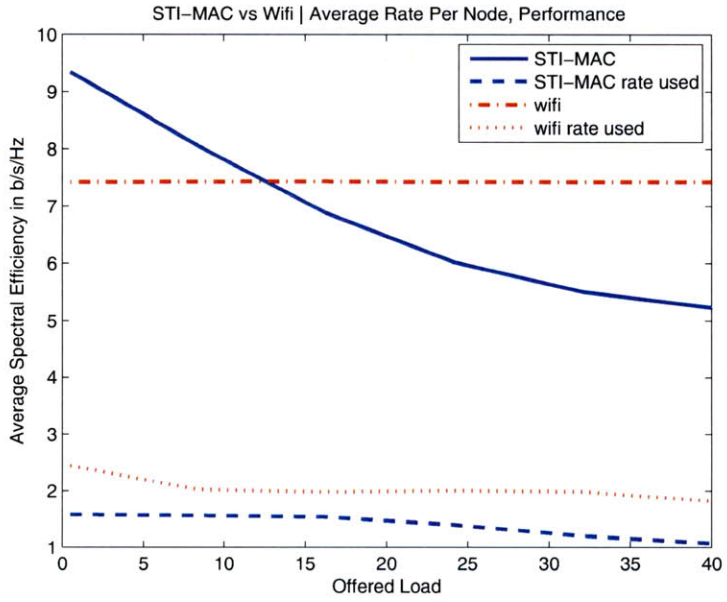

Figure 7-25: STI-MAC v 802.11(n) Comparison of Rate per Node, Networks with 40 Transmit-Receive pairs, 8 Transmit Antenna, 8 Receive Antennas, Link-Rank = 3, Link Length = 10m, Informed Transmitter using Strongest Mode (Tx-covariance-Rank = 1)

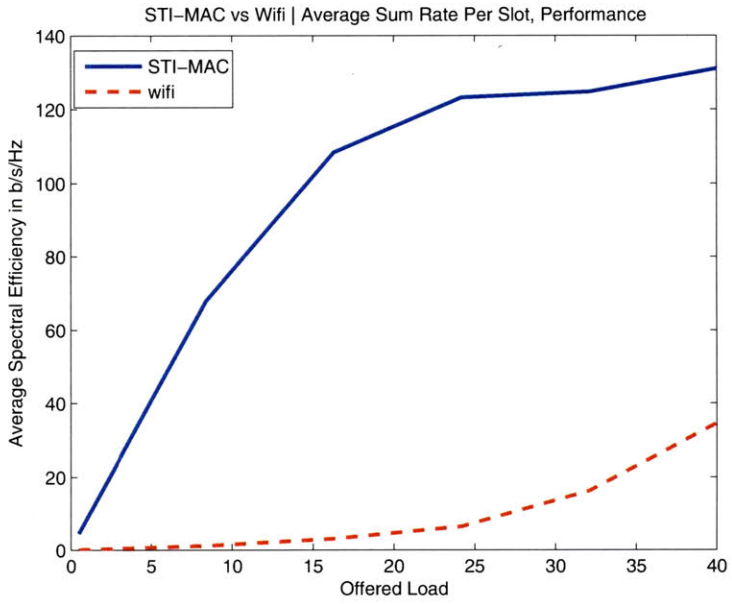

Figure 7-26: STI-MAC v 802.11(n) Comparison of Sum Rate, Networks with 40 Transmit-Receive pairs, 8 Transmit Antenna, 8 Receive Antennas, Link-Rank = 3, Link Length = 10m, Informed Transmitter using Strongest Mode (Tx-covariance-Rank = 1)

Chapter 8

Conclusions and Suggestions for Future Work

8.1 Summary and Conclusions

In this work we have presented the design of a new ad hoc wireless networking protocol scheme that offers a solution for network management in a Common's Model of spectrum management. The key idea behind the STI-MAC protocol is 'channel stuffing' in the spatial, time and frequency degrees of freedom of the channel. This is achieved in three key ways: First, through multiple antennas that are used at the receiver to mitigate interference using Minimum-Mean-Squared-Error (MMSE) receivers, allowing network nodes to transmit simultaneously in interference limited environments. The protocol also supports the use of multiple transmit antennas to beamform to the target receiver. Secondly, through the use of a control channel, that is orthogonal in time to the data channel, where nodes contend in order to participate on the data channel. And thirdly, through a protest scheme that prevents data channel overloading. This work presented designs for the STI-MAC protocol with the control in the time domain and, and the control channel in frequency domain. Simulation results are given for the control channel in time. The STI-MAC protocol is analyzed via simulation as a function of network parameters including the number of transmit and

receive antennas, the distance between a transmitter receiver pair (link-length), the average number of transmitters whose received signal is stronger at a given receiver than its transmitter (link-rank), number of transmitter and receiver pairs, the distribution on the requested rate, the offered load, and the transmit scheme.

The key conclusions of our work include that our protocol scheme increases the spectral efficiency of wireless LAN networks that use 802.11(n) schemes by at least 3X in 'typical' wireless networks, and reduces delay also by a factor of at least 2; and that our protocol scheme increases throughput by at least 5X in certain regimes tuned to take advantage of the STI-MAC benefits over the 802.11(n) scheme, particularly in 802.11(n)'s very inefficient requirement for interference levels to be at or below the noise floor threshold. This is due to our protocol strategy which uses degrees of freedom at the receiver to mitigate interference, and a protocol scheme that aims to 'stuff the channel' through the use of a control channel, and to prevent over stuffing via the protest scheme. A key parameter governing the performance of the networks is the link-rank parameter, which describes the average number of transmitters whose signal power is stronger at a given receiver than its target transmitter. We also demonstrated the value of increasing the number of receive antennas, which offered gains in throughput and also reduced the delay. In this work we also considered the performance of STI-MAC in an area of the parameter space where we expected performance to greatly surpass Wi-Fi. These networks have 40 transmitter-receiver pairs, eight transmit antennas and 8 receive antennas, transmitter beamforming through the strongest mode of the target channel, a link-length of 10 meters, and a link-rank of 3. Here we demonstrated more than 5X gains in throughput, and sometimes the gains are a result of high link-rank networks that cause back-off in Wi-Fi networks, whereas in STI-MAC networks, receive antennas are used to mitigate interference while maintaining high total network throughput.

8.2 Future Work

This work motivates several areas of future work. There are clear ways to improve the throughput, delay and overall performance of the network. These include the use of error-correction coding schemes that require lower ratios of energy-per-bit to spectral-noise-density such as those described in [106]. This also includes research into more robust and spectrally efficient space-time coding and decoding schemes such as space-time trellis coding. When more packets are received error-free, the control channel can be relieved of some of the load caused by N-ACKs and re-initiations and the data channel can be relieved of retransmissions improving both throughput and delay. Another way to potentially improve this work is to improve the adaptive schemes used to estimate and propagate the estimates of the link-rank so that nodes can choose the network-optimal spreading length; and ways to encourage users to modify their transmit schemes to allow for overall improvements in the sum spectral efficiency and delay characteristics of the network.

In order to further verify the utility of this work, a next step includes implementing this design in hardware, and testing this protocol in a WLAN by sending and receiving packets and collecting the statistics. Additional areas of research would include higher layer protocols that would leverage some of the information provided by the PHY and MAC that could be useful in routing packets in an ad-hoc network, and potentially higher up in the protocol stack. A problem common to all decentralized networks is that of network synchronization. While there is much prior work in this area, additional work in this area could provide solutions that converge faster and therefore improve the overall average throughput and lower the overall delay of the network.

Bibliography

[1] H A Roberts and T P Andrew, "Broadcom accelerates enterprise networks with industry's first end-to-end unified wlan solution," .

[2] Terrence P. McGarthy and Muriel Medard, "Wireless architectural alternatives: Current economic valuations versus broadband options, the gilder conjectures.," in *Telecommunications Policy Research Conference*, 1994.

[3] Andrew Lippman and DP Reed, "Viral communications," in *Internal White Paper, Media Laboratory MIT*, 203.

[4] Dimitri P. Bertsekas and Robert Gallager, *Data Networks*, Prentice-Hall, 1987.

[5] Siva C. Ram and B. S. Manoj, *Ad-Hoc Wireless Networks: Architectures and Protocols*, Prentice Hall Professional Technical Reference, 2004.

[6] J. C. Mundranath, P. Ramanathan, and B. D. Van Veen, "Nullhoc: a mac protocol for adaptive antenna array based wireless ad hoc networks in multipath environments.," in *Global Telecommunications Conference (Globecomm)*, Dec. 2005, pp. 2765–2769.

[7] J. Park, A. Nandan, M. Gerla, and H. Lee, "SPACE-MAC: Enabling spatial reuse using MIMO channel-aware mac," *Proc. ICC*, 2005.

[8] *IEEE Std 802.11a-1999, Part11: Wireless LAN Medium Access Control (MAC) and Physical Layer (PHY) specifications: High Speed Physical Layer in the 5GHz Band.*, 1999.

[9] *IEEE Draft Standard for Information Technology-Telecommunications and information exchange between systems-Local and metropolitan area networks-Specific requirements-Part 11: Wireless LAN Medium Access Control (MAC) and Physical Layer (PHY) specifications: Amendment 4: Enhancements for Higher Throughput*, Mar. 2008.

[10] S. Govindasamy, D. W. Bliss, and D. H. Staelin, "Spectral efficiency in single-hop ad-hoc wireless networks with interference using adaptive antenna arrays," *IEEE Journal on Selected Areas of Communications*, Sept. 2007.

[11] S. Govindasamy, *Multiple-antenna Systems in ad-hoc wireless networks*, PhD dissertation, Massachusetts Institute of Technology, Department of Electrical Engineering and Computer Science, 2008.

[12] K. Herring, *Propagation Models for Multiple-Antenna Systems: Methodology, Measurements, and Statistics*, PhD dissertation, Massachusetts Institute of Technology, Department of Electrical Engineering and Computer Science, 2008.

[13] G D Durgin, *Space-Time Wireless Channels*, Prentice-Hall, 2003.

[14] Nelson Costa and Simon Haykine, *Multiple Input Multiple Output Channel Models: Theory and Practice*, Wiley, 2010.

[15] D. W. Bliss, A. M. Chan, and N. B. Chang, "MIMO wireless communication channel phenomenology," *IEEE Transactions on Antennas and Propagation*, vol. 52, no. 8, pp. 2073–2082, Aug. 2004.

[16] D. Tse and P. Viswanath, *Fundamentals of Wireless Communications*, Cambridge University Press, 2005.

[17] R. Hegi and J. Cioffi, "Pilot tone selection for channel estimation in a mobile ofdm system," *IEEE Transactions on Consumer Electronics*, vol. 44, no. 3, pp. 1122–1128, August 1998.

[18] S Akin and M C Gursoy, "Training optimization for gauss-markov rayleigh fading channels," *IEEE Communications Society*, 2007.

[19] W C Jakes, *Microwave Mobile Communications*, Wiley, New York, 1974.

[20] W Turin, R Jana, C Martin, and J Winters, "Modeling wireless channel fading," in *Proceedings of the Vehicular Technology Conference*, 2001.

[21] M J Gans, "A power spectral theory of propagation in the mobile radio environment," *IEEE Transactions on Vehicular Technology*, vol. VT-21, pp. 27 – 38, 1972.

[22] R J Punnoose, P V Nikitin, and D D Stancil, "Efficient simulation of ricean fading within a packet simulator," *Proceedings of the Vehicular Technology Conference*, September 2002.

[23] Chen-Nee Chuah, D.N.C. Tse, J.M. Kahn, and R.A. Valenzuela, "Capacity scaling in mimo wireless systems under correlated fading," *IEEE Transactions on Information Theory*, vol. 48, no. 3, pp. 637–650, March 2002.

[24] Kai Yu and Bjorn Ottersten, "Models for mimo propagation channels, a review," *Wiley Journal on Wireless Communications and Mobile Computing Special Issue on Adaptive Antennas and MIMO Systems*, vol. 2, no. 7, pp. 653–666, 2002.

[25] M. Ozcelik, N. Czink, and E. Bonek, "What makes a good mimo channel model?," in *IEEE 61st Vehicular Technology Conference, 2005. VTC 2005-Spring*, June 2005, vol. 1, pp. 156–160.

[26] D. Shiu, G.J. Foschini, M.J. Gans, and J.M. Kahn, "Fading correlation and its effect on the capacity of multielement antenna systems.," *IEEE. Trans. Communications*, vol. 48, no. 3, pp. 502–13, Mar. 2000.

[27] Dmitry Chizhik, Jonathan Ling, Peter W. Wolniansky, Reinaldo A. Valenzuela, Nelson Costa, and Kris Huber, "Mutiple-input-multiple-output measurements and modeling

in manhattan," *IEEE Journal on Selected Areas in Communications*, vol. 21, no. 3, pp. 321–332, April 2003.

[28] Jean Philippe Kermoal, Laurent Schumacher adn Klaus Ingemann Pedersen, Preben Elgaard Mogensen, and Frank Frederiksen, "A stochastic mimo radio channel model with experimental validation," *IEEE Journal on Selected Areas in Communications*, vol. 20, no. 6, pp. 1211–1226, August 2002.

[29] E. Bonek, H. Özcelik, M. Herdin, W. Weichselberger, and J. Wallace, "Deficiencies of the 'kronecker' mimo radio channel model," in *in Proceeding of the 6th International Symposium on Wireless Personal Multimedia Communications (WPMC '03), Yokosuka, Japan,*, October 2003.

[30] Y C Eldar and A V Oppenheim, "MMSE Whitening and Subspace Whitening," *IEEE Transactions on Information Theory*, vol. 49, no. 7, pp. 1846 – 1851, 2003.

[31] Andrea Goldsmith, Syed Ali Jafar, Nihar Jindal, and Sriram Vishwanath, "Capacity limits of mimo channels," *IEEE Journal on Selected Areas in Communications*, vol. 21, no. 5, pp. 684 – 702, June 2003.

[32] Daniel W. Bliss, Keith W. Forsythe, and Amanda M. Chan, "MIMO wireless communication," *Lincoln Laboratory Journal*, vol. 15, pp. 97 – 126, November 2005.

[33] Lizhong Zheng and David N.C. Tse, "Diversity and multiplexing: A fundamental tradeoff in multiple-antenna channels," *IEEE Transactions on Information Theory*, vol. 49, no. 5, pp. 1073 –1096, May 2003.

[34] A.B. Carleial, "A case where interference does not reduce capacity," *IEEE Transactions on Information Theory*, vol. 21, pp. 569–70, 1975.

[35] R. Etkin, D. Tse, and H. Wang, "Gaussian interference channel capacity to within one bit," Pre-Print, In Review for IEEE IT Feb 2007.

[36] T.S. Han and K. Kobayashi, "A new achieveable rate region for the interference channel," *IEEE Transactions on Information Theory*, vol. IT-27, pp. 49–60, January 1981.

[37] P. Gupta and P. Kumar, "The capacity of wireless networks," *IEEE Transactions on Information Theory*, vol. 46, no. 2, pp. 388–404, Mar. 2000.

[38] Liang-Liang Xie and P.R. Kumar, "A network information theory for wireless communications: Scaling laws and optimal operations," *IEEE Transactions on Information Theory*, vol. 50, no. 5, pp. 748–768, May 2004.

[39] Massimo Fransecchetti, Olivier Dousse, David N.C. Tse, and Patrick Thiran, "Closing the gap in the capcity of wireless networks via percolation theory," *IEEE Transactions on Information Theory*, vol. 53, no. 3, pp. 1009–1018, 2007.

[40] Massimo Fransecchetti and Marco D. Migliore adn Paolo Minero, "The capacity of wireless networks: Information-theoretic and physical limits," Preprint available at: http://fleece.ucsd.edu/ massimo/Journal/Capacity-Ad-Hoc-Submisssion.pdf.

[41] A. Ozgur, O. Leveque, and D.N.C. Tse, "Hierarchical cooperation achieves optimal capacity scaling in ad hoc networks," *IEEE Transactions on Information Theory*, vol. 53, no. 10, pp. 3549–3572, October 2007.

[42] Rick S. Blum, "MIMO capacity with interference," *IEEE Journal on Selected Areas in Communications*, vol. 21, no. 5, pp. 793 – 801, June 2003.

[43] Biao Chen and Michael J. Gans, "MIMO communications in ad hoc networks," *IEEE Transactions on Signal Processing*, vol. 54, no. 7, pp. 2773–2783, 2006.

[44] Siddhartan Govindasamy, F. Antic, D.W. Bliss, and D.H. Staelin, "The performance of linear multiple-antenna receivers with interferers distributed on a plane," in *2005 IEEE 6th Workshop on Signal Processing Advances in Wireless Communications,*, June 2005, pp. 880–884.

[45] H.L. Van Trees, *Optimum Array Processing*, John Wiley & Sons, 2002.

[46] L. Hanzo, M. Munster, B.J. Choi, and T. Keller, *OFDM and MC-CDMA for Broadband Multi-User Communications, WLANs and Broadcasting*, John Wiley & Sons, 2003.

[47] T. Keller and L. Hanzo, "Adaptive multicarrier modulation: A convenient framework for time-frequency processing in wireless communications," *Proceedings of the IEEE*, vol. 88, no. 5, pp. 611–640, May 2003.

[48] Richard Van Nee and Ramjee Prasad, *OFDM for Wireless Multimedia Communication*, Universal Personal Communications. Artech House Publishers, 2000.

[49] Alan V. Oppenheim and Ronald W. Schafer, *Discrete-Time Signal Processing*, Prentice-Hall Signal Processing Series. Prentice-Hall Signal, 2nd edition, 1999.

[50] S Hara an R Prasad, "An oveview of multi-carrier cdma," in *IEEE 4th International Symposium on Spread Spectrum Technologies and Applicataions*, 1996, vol. 1, pp. 107–114.

[51] N Yee, J Linnartz, and G Fettweis, "Multi-carrier cdma in indoor wireless radio networks," in *Proc. IEEE International Symposium PIMRC*, 1993.

[52] Leonard Kleinrock and Fouad A. Tobagi, "Packet switching in radio channels: Part i – carrier sense multiple-access modes and their throughput delay characteristics," *IEEE Transactions on Communications*, vol. COM-23, no. 12, pp. 1400–1416, December 1975.

[53] K. Jamieson, Brett Jull, Allen Miu, and Hari Balakrishana, "Understanding the real-world performance of carrier sense," in *SIGCOMM '05 Workshop*, 2005.

[54] Jae Hyun Kim and Jong Kyu Lee, "Capture effects of wireless csma/ca protocols in rayleigh and shadown fading channels," *IEEE Transactions on Vehicular Technology*, vol. 48, no. 4, pp. 1277–1287, 1999.

[55] Xin Wang and Koushik Kar, "Throughput modelling and fairness issues in csma/ca based ad-hoc networks," in *Proceedings IEEE 24th Annual Joint Conference of the IEEE Computer and Communications Societies. INFOCOM*, March 2005, vol. 1, pp. 3– 34.

[56] P. Karn, "Maca: a new channel access method for packet radio.," in *9th Computer Networking Conference. ARRL/CRRL Amateur Radio*, 1990, pp. 134–140.

[57] Vaduvur Bharghavan, Alan Demers, Scott Schenker, and Lixia Zhang, "Macaw: A media access protocol for wireless lan," in *Proceedings on the conference on Communications Architectures, Protocols and Applications*, 1994, pp. 212–225.

[58] Fabrizio Talucci, Mario Gerla, and Luigi Fratta, "Maca-bi: A receiver oriented access protocol for wireless multihop networks," in *The 8th IEEE International Symposium on Personal, Indoor and Mobile Radio Communications, 1997. 'Waves of the Year 2000'. PIMRC '97.,*, September 1997, pp. 435–439.

[59] Chane L. Fullmer and J.J. Garcia-Luna-Aceves, "Floor acquisition multiple access (fama) for packet-radio networks," in *SIGCOMM*, 1995.

[60] Chane L. Fullmer and J.J. Garcia-Luna-Aceves, "Solution to hidden terminal problems in wireless networks," in *SIGCOMM*, 1997.

[61] Ztgmunt J. Hass and Jing Deng., "Dual busy tone multiple access (dbtma) – a multiple access control scheme for ad hoc networks," *IEEE Transactions on Communications*, vol. 50, no. 6, June 2002.

[62] Imrich Chalmtac, Adrias Farago, and Hongbiao Zhang, "Time-spread multiple-access (tsma) protocols for multihop mobile radio networks," *IEEE/ACM Transactions on Networking*, vol. 5, no. 6, December 1997.

[63] R. Rozovsky and P. R. Kumar, "Seedex: A mac protocol for ad hoc networks," in *SEEDEX: A MAC Protocol for ad hoc networks*, October 2001, pp. 65–75.

[64] J. Nicholas Laneman, David N.C. Tse, and Gregory W. Wornell, "Cooperataive diversity in wireless networks: Efficient protocols and outage behavior," *IEEE Transactions on Information Theory*, vol. 50, no. 12, pp. 3062–3080, December 2004.

[65] Larry J. Williams, "Technology advances from small unit operations situation awareness system development," *IEEE Personal Communication*, Feb 2001.

[66] Chris Li, C.J. Yoon, and J. Visvalder, "Suo sas radio intra-networking architecture," in *Military Communications Conference, 2001. MILCOM 2001. Communications for Network-Centric Operations: Creating the Information Force. IEEE*, 2001, vol. 1, pp. 235 - 239.

[67] Taiwen Tang, Minyoung Park, Jr. Robert W. Heath, and Scott M. Nettles, "A joint mimo-ofdm transceiver and mac design for mobile ad hoc networking," in *2004 International Workshop on Wireless Ad-Hoc Networks*, May 2004, pp. 315–319.

[68] LAN/MAN Standards Committee, *IEEE Standard for Information technology Telecommunications and information exchange between systems – Local and metropolitan area networks – Specific requirements. Part 11: Wireless LAN Medium Access Control (MAC) and Physical Layer (PHY) Specifications (802.11 - 2007)*, IEEE Computer Society, 3 Park Avenue, New York, NY 10016-5997, June 12 2007.

[69] Yang Xiao and Jon Roshdal, "Throughput and delay limists of ieee 802.11," *IEEE Communications Letters*, vol. 6, no. 8, pp. 355–357, August 2002.

[70] Giuseppe Bianchi, "Performance analysis of the ieee 802.11 distributed coordination function," *IEEE Journal on Selected Areas in Communications*, vol. 18, no. 3, pp. 535–547, Mar. 2000.

[71] Jangeun Jun and Pushkin Peddabachagari adn Mihail Sichitiu, "Theoretical maximum throughput of ieee 802.11 and its applications," in *Proceedings of the 2nd IEEE International Symposim on Network Computing and Applications*, 2003.

[72] P. Chatzimisios, A.C. Boucouvalas, and V. Vitsas, "Ieee 802.11 wireless lans: Performance analysis and protocol refinement," *EURASIP Journal on Wireless Communications and Networking*, vol. 2005, no. 1, pp. 67–78, Jan. 2005.

[73] Yang Xiao and Jon Roshdal, "Performance analysis and enhancments for hte current and future ieee 802.11 mac protocols," in *ACM SIGMOBILE Mobile Computing and Communications Review*, 2003.

[74] G. Bianchi, L Fratta, and M Oliveri, "Performance evaluation and enhancement of the csma/ca mac protocolfor 802.11 wireless lans," in *Seventh IEEE International Symposium on Personal, Indoor and Mobile Radio Communications, 1996. PIMRC'96.,*, October 1996, vol. 2, pp. 392–396.

[75] Ratish J. Punnoose, Richard S. Tsend, and Daniel D. Stancil, "Experimental results for interference between bluetooth and 802.11(b) dsss systems," in *IEEE VTS 54th Vehicular Technology Conference, 2001. VTC 2001 Fall.*, 2001, vol. 1, pp. 67– 71.

[76] A.M. Otefa, N.M. ElBoghdadly, and E.A. Sourour, "Performance analysis of 802.11n wireless lan physical layer," in *International Conference on Information and Communications Technology (ICICT)*, December 2007, pp. 279–288.

[77] LAN/MAN Standards Committee, *IEEE Standard for Information technology – Telecommunications and information exchange between systems Local and metropolitan area networks – Specific requirements Part 11: Wireless LAN Medium Access Control (MAC) and Physical Layer (PHY) Specifications Amendment 5: Enhancements for Higher Throughput (IEEE Std 801.11 n – 2009)*, IEEE Computer Society, 3 Park Avenue, New York, NY 10016-5997, October 29 2009.

[78] Guido R. Hiertz, Sebatian MAX, Yunpeng Zang, Thomas Junge, and Dee Denteneer, "Ieee 802.11s mac fundamentals," in *IEEE International Conference on Mobile Adhoc and Sensor Systems*, October 2007, pp. 1–8.

[79] S. H. Jeon, J.M. Lee, and J.K. Choi, "Performance evaluation of enhanced 802.11 in wireless mesh networks," in *Conference on Advanced Communication Technology (ICACT)*, Feb 2008, pp. 839–842.

[80] Stefano M. Faccin, Carl Wijting, Jarkko Kneckt, and Ameya Damle, "Mesh wlan networks: Concept and system design," *IEEE Wireless Communications*, vol. 13, no. 2, pp. 10–17, April 2006.

[81] J Ward and R T Compton, "Improving the performacne of a slotted aloha packet radio network with an adaptive array," *IEEE Transactions on Communications*, vol. 40, no. 2, pp. 292 – 300, February 1992.

[82] J Ward, "High throughput slotted aloha packet radio networks wit adaptive arrays," *IEEE Transactions on Communications*, vol. 41, no. 3, pp. 460 –470, March 1993.

[83] Rudolf Ahlswede, Ning Cai, Robert Li, and Raymond W. Yeung, "Network information flow," *IEEE Transactions on Information Theory*, vol. 46, no. 4, pp. 1204 –1216, 2000.

[84] R. Koetter and M. Medard, "An algebraic approach to network coding," *IEEE/ACM Transactions on Networking*, vol. 11, no. 5, pp. 782–795, October 2003.

[85] S. Li, R.W. Yeung, and Ning Cai, "Linear network coding," *IEEE Transactions on Information Theory*, vol. 49, no. 2, pp. 371–381, Februrary 2003.

[86] Tracey Ho, *Networking from a network coding perspective*, Ph.D. thesis, Massachusetts Institute of Technology, May 2004.

[87] Z. Li and B. Li, "Network coding in undirected networks," in *Proceedings of the 38th Annual Conference on Information Sciences*, 2004.

[88] Z. Li and B. Li, "Network coding: The case of multiple unicast sessions," in *Allerton Conference on Communications*, 2004.

[89] Desmond Lun, Muriel Medard, and Ralf Koetter, "Efficient operation of wireless packet networks using network coding," in *International Workshop on Convergent Technologies (IWCT)*, 2005.

[90] D.S. Lun, M. Medard, and M. Effros, "On coding for reliable communication over packet networks," in *Proc. 42nd Annu. Allerton Conf. Communication, Control, and Computing*, 2004.

[91] Christina Fragouli, Dina Katabi, Athina Markopoulou, Muriel Medard, and Hariharan Rahul, "Wireless network coding: Opportunities and challenges," in *IEEE Military Communications Conference (MILCOM)*, October 2007, pp. 1–8.

[92] Sachin Katti, Hariharan Rahul, Wejun Hu, Dina Katabi, and Muriel Medard adn Jon Crowcroft, "Xors in the air: Practical wireless network coding," *IEEE/ACM Transactions on Networking*, vol. 16, no. 3, pp. 497–510, June 2008.

[93] Sachin Katti, Dina Katabi, Wejun Hu, Hariharan Rahul, and Muriel Medard, "The importance of being opportunistic: Practical network coding for wireless environments," in *Allerton*, 2005.

[94] Sachin Katti, Shyamnath Gollakota, and Dina Katabi, "Embracing wireless interference: Analog network coding," in *SIGCOMM*, August 2007.

[95] M Vutukuru, K Jamieson, and K Balakrishnan, "Harnessing exposed terminals in wireless netorks," in *Proceedings of the 5th USENIX Symposium on Networked Systems Design and Implementation*, 2008, pp. p.59–72.

[96] H Rahul, F Edalat, D Katabi, and C Soding, "Frequency-aware rate adaptation and mac protocols," in *ACM MOBICOM*, 2009.

[97] J Redi, B Watson, R Ramanathan, P Basu, F Tchakountio, M Girone, and M Steenstrup, "Design and implementation of a mimo mac protocol for ad hoc networking," 2006.

[98] John G Proakis, *Digital Communication*, Mc Graw Hill Series in Electral and Computer Engineering, 3rd edition, 1995.

[99] Daniel W. Bliss and Peter A Parker, "Temporal synchronization of mimo wireless communications in the presence of interference," *IEEE Trans. on Signal Processing*, vol. 58, no. 3, pp. 1794 – 1806, March 2010.

[100] T. W. Anderson, *An Introduction to Multivariate Statistical Analysis*, Wiley-Interscience, 2003.

[101] I S Reed, J D Mallett, and L E Brennan, "Rapid convergence rate in adaptive arrays," *IEEE Transactions on Aerospace and Electronic Systems*, vol. AES-10, no. 6, pp. 853 – 863, Nov 1974.

[102] D M Boroson, "Sample size considerations for adaptive arrays," *IEEE Transactions on Aerospace and Electronic Systems*, vol. AES-16, no. 4, 1980.

[103] W R Gabriel, "Using spectral estimation techniques in adaptive array systems," in *Proceedings of the Phase Arrays 1985 Symposium*, August 1985, number August, p. 109.

[104] B D Carlson, "Covariance matrix estimationand diagonal loading in adaptive arrays," *IEEE Transactions on Aerospace and Electronic Systems*, vol. 24, no. 4, pp. 397 –401, 1988.

[105] Aruba Networks, "802.11n: The end of ethernet," .

[106] A Kothiyal, O Y Takeshita, W Jin, and M Fossorier, "Iterative reliability-based decoding of linear block codes with adaptive belief propagation," *IEEE Communications Letters*, vol. 9, no. 12, pp. 1067 – 1070, 2005.